

**Effect of Water on the Interfacial Mechanisms of the Tribofilms Formed by  
Zinc Dialkyl Dithiophosphate: Experimental and Analytical Study**

By

**Pourya Parsaeian**

Submitted in accordance with the requirements for the degree of  
**Doctor of Philosophy**

The University of Leeds  
School of Mechanical Engineering  
Leeds, UK

August, 2017

The candidate confirms that the work submitted is his own, except where work which has formed part of jointly-authored publications has been included. The candidate confirms that appropriate credit has been given within the thesis where reference has been made to the work of others.

In the following publications, the experimental and analysis of the results were performed by the author of this PhD thesis except the second publication in which the author contributed to the experimental part whereas the modelling part was performed by the main author:

1. **Parsaeian P**, Ghanbarzadeh A, Wilson M, Van Eijk MCP, Nedelcu I, Dowson D, Neville A, Morina A, An Experimental and Analytical Study of the Effect of Water and its Tribochemistry on the Tribocorrosive Wear of Boundary Lubricated Systems with ZDDP-Containing Oil. **Wear**, vol. **358-359**, pp.23-31. **2016**.
2. Ghanbarzadeh A, **Parsaeian P**, Morina A, Wilson MCT, Van Eijk MCP, Nedelcu I, Dowson D, Neville A, A Semi-deterministic Wear Model Considering the Effect of Zinc Dialkyl Dithiophosphate Tribofilm. **Tribology Letters**, vol. **61**, **2016**.
3. **Parsaeian P**, Van Eijk MCP, Nedelcu I, Morina A, Neville A, Study of the Interfacial Mechanism of ZDDP Tribofilm in Humid Environment and its Effect on Tribochemical Wear; Part I: Experimental. **Tribology International**. Volume **107**, March **2017**, Pages **135–143**.
4. **Parsaeian P**, Van Eijk MCP, Nedelcu I, Morina A, Neville A, Study of the Interfacial Mechanism of ZDDP Tribofilm in Humid Environment and its Effect on Tribochemical Wear; Part II: Numerical. **Tribology International**. Volume **107**, March **2017**, Pages **33–38**.
5. **Parsaeian P**, Van Eijk MCP, Nedelcu I, Morina A, Neville A, A new insight into the interfacial mechanisms of the tribofilm formed by zinc dialkyl Dithiophosphate **Journal of Applied Surface Science**. **Applied Surface Science** **403**, **472-486**. **2016**.

This copy has been supplied on the understanding that it is copyright material and that no quotation from the thesis may be published without proper acknowledgement.

*Assertion of moral rights:*

The right of Pourya Parsaeian to be identified as Author of this work has been asserted by him in accordance with the Copyright, Designs and Patents Act 1988.

© 2017 The University of Leeds Pourya Parsaeian

## Acknowledgements

First of all, I would like to express my sincere gratitude and special appreciation to my supervisors Professor Anne Neville and Professor Ardian Morina for their help, guidance and also being supportive and encouraging through my PhD. They have been tremendous mentors and this work would not have been possible without their support. I would also show my appreciation to FUTURE-BET consortium which gave a great opportunity to interact with experts in the field of tribology/tribochemistry.

I would like to thank Professor Duncan Dowson for the time he has put on sharing his knowledge, experience and passion on my PhD. His advice and guidance have been invaluable.

I am also thankful to the members of iFS research group, especially to Ali, Thibaut, Michael, Filippo, Erfan, Abdullah, Vishal, Fredrick, John, Fiona, Lukman, and Farnaz. I would also like to thank my friends, especially Ali, Abdel and Shahriar.

I especially thank my mom (Zahra Aryaeitabar), dad (Mohammad Naser), sister (Parisa), grandmother (Oliya) and my grandfathers (Mohsen and Hossein) for their continuous support, encouragement and love.

At the end, I would like to thank my lovely wife who supported me in all aspects of life and has been a great partner. Completion of my PhD would have not been possible without her support. Her constant support, love, motivation, encouragement and patience during my PhD is invaluable. Finally, but by no means least, I would like to dedicate this work to my son (Padra), my wife, my parents and my grandfather Mohsen who has passed away recently.

## **Abstract**

Understanding the true interfacial mechanisms of the growth of the tribofilms generated by Zinc Dialkyl Dithiophosphate (ZDDP) is important because it is the most widely used anti-wear additive and there is legislative pressure to find efficient environmentally-friendly replacements. The main focus of this study is to investigate the effect of water on the interfacial mechanisms involved in the formation of the ZDDP tribofilms and correlate it to the chemical properties of the glassy polyphosphates. The effect of different parameters such as temperature, humidity, mixed-water in oil, load and rubbing time on the tribofilm formation and its durability has been studied experimentally and analytically using a Mini Traction Machine (MTM) with the Spacer Layer Interferometry Method (SLIM) attachment. The role of additive depletion on the pre-formed tribofilm thickness under mechanical stress has also been studied. Results show that physical parameters such as temperature, humidity and pressure significantly influence the tribofilm. X-ray Photoelectron Spectroscopy (XPS) analysis was carried out to assess the evolution of the chemical structure of the tribofilm during the test. The chemical analysis suggests that there are different chemical properties across the thickness of the tribofilm and these determine the durability characteristics.

A humidity control system was designed and integrated with the Mini Traction Machine (MTM) and Spacer Layer Interferometry Method (SLIM) for the first time to evaluate the effect of relative humidity and the tribochemical changes on the tribological performance and tribofilm characteristics of boundary lubricated systems. One of the key aspects in this study is the use of continuous humidity control system, which can provide steady humid environment during the tribological tests. In the

present study, the tribofilm thickness and wear results obtained experimentally were used to develop a semi-deterministic approach to implement the effect of humidity and mixed-water in wear prediction of boundary lubrication.



# Table of Contents

<b>Acknowledgements.....</b>	<b>IV</b>
<b>Abstract.....</b>	<b>V</b>
<b>List of Figures.....</b>	<b>XIII</b>
<b>List of Tables.....</b>	<b>XIX</b>
<b>Chapter 1. Introduction.....</b>	<b>1</b>
1.1 Motivation.....	1
1.2 Aims and objectives.....	4
1.3 Thesis outline.....	6
<b>Chapter 2. Fundamentals of Tribology, Lubrication and Wear.....</b>	<b>7</b>
2.1 Introduction.....	7
2.2 Tribology.....	7
2.2.1 Contact between solids.....	7
2.2.2 Friction.....	9
2.3 Wear.....	10
2.3.1 Running-in.....	12
2.3.2 Wear under rolling-sliding conditions.....	13
2.4 Lubrication.....	14
2.4.1 Introduction.....	14
2.4.2 Lubricants.....	15
2.4.3 Mineral oil.....	16
2.4.4 Synthetic oils.....	16
2.4.5 Additives.....	17
2.4.6 Conclusion.....	18
<b>Chapter 3. Review of the Literature.....</b>	<b>21</b>
3.1 Introduction.....	21
3.2 Water in oil.....	21
3.2.1 Introduction.....	21
3.2.2 Types of water contamination in the lubricated system.....	22
3.2.3 Water absorption properties of lubricants.....	23
3.2.4 The effect of water in dry and lubricated systems.....	25
3.2.5 Effect of water on viscosity.....	28
3.2.6 Effect of water on hydrogen embrittlement.....	29
3.2.7 Effect of water on oil oxidation.....	29



3.2.8	Effect of water on lubricant performance .....	30
3.2.9	Summary of the effect of water on lubricant .....	31
3.3	Zinc Dialkyl Dithiophosphate (ZDDP).....	32
3.3.1	ZDDP as an anti-wear additive .....	32
3.3.2	Mechanical properties and durability of ZDDP tribofilm.....	33
3.3.3	Chemistry of ZDDP .....	36
3.3.4	Growth of ZDDP tribofilm .....	37
3.3.5	Effect of water on tribochemistry of ZDDP.....	39
3.3.6	Summary .....	41
3.4	Modelling approaches .....	42
3.4.1	Introduction .....	42
3.4.2	Modelling of tribocorrosion .....	43
3.4.3	Electrochemical models .....	43
3.4.4	Mechanical models.....	44
3.4.4.1	Wear prediction .....	44
3.4.4.2	Archard wear equation .....	47
3.4.4.3	Modification of Archard wear equation to predict wear in mixed lubricated contact .....	49
3.4.4.3.1	Fractional film defect .....	49
3.4.4.3.2	Fluid and asperities load sharing.....	50
3.4.4.3.3	Determination of the K.....	51
3.4.4.3.4	Calculating $\delta$ .....	52
3.4.4.3.5	Fluid part .....	52
3.4.4.3.6	Asperity part.....	53
3.4.5	Tribochemical wear model.....	54
3.4.5.1	Contact mechanics.....	54
3.4.5.2	Tribofilm development.....	55
3.4.5.3	Wear modelling .....	57
3.5	Conclusion .....	59
<b>Chapter 4.</b>	<b>Experimental Procedures .....</b>	<b>61</b>
4.1	Introduction .....	61
4.2	Bulk oil characterization .....	62
4.2.1	Water concentration measurements .....	62
4.3	Test rig .....	62

4.3.1	Spacer Layer Interferometry Method (SLIM).....	63
4.4	Effect of water experiments .....	64
4.4.1	Materials and test conditions.....	64
4.4.2	Tested lubricants .....	66
4.4.3	Experimental approach.....	66
4.5	Effect of humidity experiments.....	67
4.5.1	Humidity control system .....	67
4.5.2	Calibration.....	68
4.5.3	Materials and test conditions.....	70
4.5.4	Experimental approach.....	71
4.6	Validation of the model experiments .....	72
4.6.1	Materials and test conditions.....	72
4.7	Durability of the tribofilm.....	74
4.7.1	Materials and test conditions.....	74
4.7.2	Tested lubricants .....	75
4.7.3	Methodology .....	76
4.7.4	Cleaning procedure .....	79
4.7.5	Cleaning after suspending the test.....	79
4.8	Chemical and surface analysis techniques .....	80
4.8.1	X-ray Photoelectron Spectroscopy (XPS).....	80
4.9	Wear measurements .....	81
4.9.1	Sample preparation.....	81
4.10	Summary .....	83
<b>Chapter 5.</b>	<b>Water Effect on Tribochemistry and Mechanical Wear .....</b>	<b>84</b>
5.1	Introduction .....	84
5.2	The effect of water on wear .....	85
5.3	Effect of water on tribofilm growth and wear.....	86
5.4	Summary of the effect of water.....	92
<b>Chapter 6.</b>	<b>Humidity Effect on Tribochemistry and Mechanical</b>	
<b>Wear</b>	<b>.....</b>	<b>93</b>
6.1	Introduction .....	93
6.2	Humidity effect on oil .....	94
6.3	Effect of relative humidity on tribofilm evolution and wear performance.....	94
6.4	Effect of relative humidity on tribochemistry.....	99

6.5	The effect of relative humidity on wear performance.....	104
6.6	Summary of the effect of relative humidity .....	106
<b>Chapter 7.</b>	<b>Development of Tribochemical Model .....</b>	<b>109</b>
7.1	Introduction .....	109
7.2	Model calibration procedure .....	111
7.3	Validation of the model.....	112
	7.3.1 Tribofilm thickness .....	112
	7.3.2 Wear results.....	117
	7.3.3 Numerical results .....	120
7.4	Analytical study of the effect of mixed-water.....	126
	7.4.1 First approach: semi-deterministic coefficient of wear.....	127
	7.4.2 Second approach: effect of tribochemistry .....	129
7.5	Analytical study of the effect of relative humidity .....	134
	7.5.1 Semi-deterministic coefficient of wear (approach one).....	134
	7.5.2 Effect of tribochemistry (approach two) .....	137
7.6	Summary .....	145
	7.6.1 Analytical study of the effect of mixed-water.....	145
	7.6.2 Analytical study of the effect of relative humidity .....	146
<b>Chapter 8.</b>	<b>Investigation into the Durability of the Tribofilm Formed by Zinc Dialkyl Dithiophosphate .....</b>	<b>148</b>
8.1	Introduction .....	148
8.2	Tribofilm evolution .....	149
	8.2.1 Early stage tribofilm durability .....	149
	8.2.2 Late stage tribofilm durability.....	151
	8.2.3 Multiple replacement .....	152
8.3	Chemistry of tribofilms .....	152
	8.3.1 Early stage oil replacement .....	153
	8.3.2 Late stage oil replacement.....	155
	8.3.3 Multiple replacement .....	157
8.4	Effect of temperature.....	160
	8.4.1 Chemistry of the tribofilm.....	161
8.5	Effect of load.....	165
	8.5.1 Chemistry of the tribofilm.....	169
8.6	Effect of water.....	170

8.7	Wear .....	173
8.8	Summary .....	178
<b>Chapter 9.</b>	<b>Overall Discussion.....</b>	<b>182</b>
9.1	Water effect on tribochemistry and mechanical wear.....	182
9.2	Humidity effects on tribochemistry and mechanical wear.....	185
9.3	Combined effect of humidity and mixed water.....	193
9.4	Analytical study of the effect of water on tribofilm growth and wear .....	200
9.5	Durability of the tribofilm.....	202
9.5.1	Early stage.....	202
9.5.2	Late stage .....	204
9.5.3	Multiple replacement .....	205
9.5.4	Effect of temperature and load on durability of the tribofilm.....	206
<b>Chapter 10.</b>	<b>Conclusions and Future Work.....</b>	<b>210</b>
10.1	Water effect on ZDDP anti-wear reaction layer and its effect on wear .....	210
10.2	The effect of humidity on the decomposition products of ZDDP anti-wear reaction layer and its effect on wear performance .....	212
10.3	Combined effect of mixed-water in oil and humidity.....	214
10.4	Analytical study of the effect of water and humidity.....	214
10.4.1	Analytical study of effect of mixed-water .....	214
10.4.2	Analytical study of the effect of relative humidity .....	215
10.5	The effect of temperature and load on ZDDP tribofilm structure and its effect on durability of the layer .....	217
10.6	Future work .....	218
10.6.1	Experimental .....	219
10.6.2	Modelling .....	220
<b>Chapter 11.</b>	<b>References .....</b>	<b>221</b>

## List of Figures

Figure 2-1 Real contact area of the rough surface (23) .....	8
Figure 2-2 The transition from static contact to sliding contact for hard asperity on soft contact (23) .....	9
Figure 2-3 Contact stresses between asperities (23).....	9
Figure 2-4 Different modes of two body abrasion (32) .....	12
Figure 2-5 3 <sup>rd</sup> body abrasive particles between surfaces (32) .....	12
Figure 2-6 Running-in and steady state wear versus time (33).....	13
Figure 2-7 Stribeck curve, dependence of the friction coefficient on viscosity, speed and load for a lubricated sliding system (36, 38).....	15
Figure 3-1 The saturation curve for typical oil (52).....	23
Figure 3-2 Forms of water in oil (51).....	24
Figure 3-3 Reverse micelles in oil (2).....	25
Figure 3-4 Effect of relative humidity on wear and friction (54).....	26
Figure 3-5 Effect of water contamination on bearing life (4).....	27
Figure 3-6 Catalytic effect of water and metals on oil oxidation as calculated by total acid number (59).....	30
Figure 3-7 Different structures of ZDDP: (I) neutral monomeric in equilibrium (II) neutral dimeric (III) basic ZDDP (82) .....	33
Figure 3-8 Schematic of multilayer structure of ZDDP (a) before and (b) after washing with solvent (83) .....	35
Figure 3-9 Schematic of the patchy structure of ZDDP tribofilm (62) .....	36
Figure 3-10 Identification of different composition of zinc polyphosphates (98).....	37
Figure 4-1 Mini Traction Machine (MTM) .....	63
Figure 4-2 MTM and the Spacer Layer Interferometry configuration .....	64
Figure 4-3 Humidity control system (a) and (b) humidity chamber c) MTM SLIM integrated to the humidity control system.....	69
Figure 4-4 Schematic representative of humidity control system .....	70
Figure 4-5 Schematic of the experimental approach for replacing oil and surface analysis.....	77
Figure 4-6 SLIM images taken (a) before suspending the test (b) immediately after suspending the test and before starting the rubbing.....	79
Figure 4-7 Shows tribofilm removal from the surface using EDTA(169).....	82
Figure 4-8 Shows wear profile across the wear scar before and after EDTA(2).....	82

<b>Figure 5-1 Effect of water on average wear depth at two different temperatures of 80°C and 100°C .....</b>	<b>86</b>
<b>Figure 5-2 Tribofilm thickness measurement results for 80°C at different water concentrations.....</b>	<b>89</b>
<b>Figure 5-3 Tribofilm thickness measurement results for 100°C at different water concentrations.....</b>	<b>89</b>
<b>Figure 5-4 Final tribofilm thickness results for different water concentrations .....</b>	<b>90</b>
<b>Figure 5-5 Final tribofilm thickness results vs measured wear depth .....</b>	<b>90</b>
<b>Figure 5-6 Comparison between average wear depth and tribofilm thickness at different water concentrations at 100°C .....</b>	<b>91</b>
<b>Figure 5-7 Comparison between average wear depth and tribofilm thickness at different water concentration at 80°C.....</b>	<b>91</b>
<b>Figure 6-1 Measured water concentration at 80°C and 98°C .....</b>	<b>95</b>
<b>Figure 6-2 Tribofilm thickness measurement results for 80°C for different levels of relative humidity.....</b>	<b>96</b>
<b>Figure 6-3 Tribofilm thickness measurement results at 98°C for different levels of relative humidity.....</b>	<b>97</b>
<b>Figure 6-4 Effect of relative humidity on steady state tribofilm thickness for different temperatures.....</b>	<b>98</b>
<b>Figure 6-5 Effect of water concentration measured at different levels of relative humidity on steady state tribofilm thickness for different temperatures.....</b>	<b>98</b>
<b>Figure 6-6 Steady state tribofilm thickness results vs measured wear depth.....</b>	<b>99</b>
<b>Figure 6-7 High resolution X-Ray Photoelectron Spectroscopy (XPS) spectra for ZDDP tribofilm formed at different values of humidity for 80°C .....</b>	<b>102</b>
<b>Figure 6-8 High resolution X-Ray Photoelectron Spectroscopy (XPS) spectra for ZDDP tribofilm formed at different values of humidity for 98°C .....</b>	<b>102</b>
<b>Figure 6-9 Effect of water concentration at different values of relative humidity on polyphosphate chain length at 80°C .....</b>	<b>103</b>
<b>Figure 6-10 Effect of water concentration at different values of relative humidity on polyphosphate chain length at 98°C .....</b>	<b>103</b>
<b>Figure 6-11 Effect of relative humidity on the average wear depth at two different temperatures of 80°C and 98°C.....</b>	<b>104</b>
<b>Figure 6-12 Effect water concentration measured at different levels of humidity on the average wear depth at two different temperatures of 80°C and 98°C.....</b>	<b>105</b>

Figure 7-1 Tribofilm thickness measurements for 100°C at different times ...	113
Figure 7-2 Tribofilm thickness measurements for 60°C at different times .....	113
Figure 7-3 Tribofilm thickness measurements for different temperatures for 1% wt ZDDP in oil.....	114
Figure 7-4 Tribofilm thickness measurements for different temperatures for 0.5% wt ZDDP in oil.....	114
Figure 7-5 Example of numerical and experimental tribofilm growth for 1% wt ZDDP in oil at three different temperatures.....	115
Figure 7-6 2D and 3D images of wear track .....	117
Figure 7-7 2D wear track image and the image profile of the surface after the experiment.....	118
Figure 7-8 Wear measurements for different temperatures and different times for 1% wt ZDDP in oil.....	119
Figure 7-9 Wear measurements for different temperatures for 0.5% wt ZDDP in oil at 2 hours .....	119
Figure 7-10 Simulation of wear for different temperatures at 2 hours for 1%wt ZDDP in oil.....	123
Figure 7-11 Simulation of wear for different temperatures at 2 hours for 1%wt ZDDP in oil .....	124
Figure 7-12 Variation of the average coefficient of wear with time for different temperatures for 1% wt ZDDP in oil .....	125
Figure 7-13 Tribofilm growth simulations for (a) 80°C and (b) 100°C .....	131
Figure 7-14 Numerical wear calculation compared with experimental measurements (a) 80°C and (b) 100°C .....	131
Figure 7-15 xtribo calibrated for different temperatures at different water concentrations at (a) 100°C and (b) 80°C.....	133
Figure 7-16 Tribofilm growth simulations for different values of relative humidity at 80°C .....	139
Figure 7-17 Tribofilm growth simulations for different values of relative humidity at 98°C .....	140
Figure 7-18 Numerical wear calculation in comparison with experimental measurements at 80°C (calculated from second approach) .....	140
Figure 7-19 Numerical wear calculation in comparison with experimental measurements at 98°C (calculated from second approach) .....	141
Figure 7-20 Variation of $h_{max}$ by relative humidity at 80°C.....	144
Figure 7-21 Variation of $h_{max}$ by relative humidity at 98°C .....	144
Figure 8-1 Schematic represensetive of two different stages of replacing the oil. Early stage after 25 minutes and late stage at 180 minutes.....	150
Figure 8-2 Tribofilm thickness results for the early stage durability test .....	150

Figure 8-3 Tribofilm thickness results for the late stage durability test.....	151
Figure 8-4 Tribofilm thickness results for adding fresh ZDDP to the base oil .....	152
Figure 8-5 High resolution X-Ray Photoelectron Spectroscopy spectra for ZDDP tribofilm formed at the end of the test when the oil was replaced by base oil a) O1s b) Zn3s, P2p (Point C <sub>2</sub> in Figure 8-2).....	154
Figure 8-6 High resolution X-Ray Photoelectron Spectroscopy spectra for ZDDP tribofilm formed at the end of the test when the oil was replaced by fresh ZDDP a) O1s b) Zn3s, P2p (Point C <sub>1</sub> in Figure 8-2)...	154
Figure 8-7 High resolution X-Ray Photoelectron Spectroscopy spectra for ZDDP tribofilm formed at the end of the 4hrs test when the oil was replaced with base oil at 3 hrs a) O1s b) Zn3s, P2p (Point C <sub>4</sub> in Figure 8-3).....	156
Figure 8-8 High resolution X-Ray Photoelectron Spectroscopy spectra for ZDDP tribofilm formed at the end of the 4hrs test without replacing the oil a) O1s b) Zn3s, P2p (Point C <sub>3</sub> in Figure 8-3).....	156
Figure 8-9 High resolution X-Ray Photoelectron Spectroscopy spectra for ZDDP tribofilm formed at the end of the test when the oil was replaced by base oil a) O1s b) Zn3s, P2p (Point C <sub>6</sub> Figure 8-4).....	158
Figure 8-10 High resolution X-Ray Photoelectron Spectroscopy spectra for ZDDP tribofilm formed at the end of the test when the oil was replaced by base oil and then with ZDDP a) O1s b) Zn3s, P2p (Point C <sub>5</sub> Figure 8-4) .....	158
Figure 8-11 Tribofilm thickness results and removal behaviour for different temperatures after suspending the test .....	162
Figure 8-12 Tribofilm thickness reduction for different temperatures after one minute of rubbing when the oil is changed with base oil .....	163
Figure 8-13 High resolution X-Ray Photoelectron Spectroscopy (XPS) spectra for ZDDP tribofilm formed before suspending the test at 140°C a) O1s b) Zn3s, P2p (Point A <sub>3</sub> in Figure 8-11) .....	164
Figure 8-14 High resolution X-Ray Photoelectron Spectroscopy (XPS) spectra for ZDDP tribofilm formed after suspending the test at 140°C a) O1s b) Zn3s, P2p (Point B <sub>1</sub> in Figure 8-11) .....	164
Figure 8-15 High resolution X-Ray Photoelectron Spectroscopy (XPS) spectra for ZDDP tribofilm formed at the end of the test at 140°C a) O1s b) Zn3s, P2p (Point C <sub>8</sub> in Figure 8-11).....	165
Figure 8-16 Tribofilm thickness results and removal behaviour for different loads after suspending the test .....	167
Figure 8-17 Tribofilm thickness reduction for different loads after one minute of rubbing when the oil is changed with base oil.....	168
Figure 8-18 Effect of load on the flash temperature rise and the maximum shear stress on the surfaces .....	168



<b>Figure 8-19 Tribofilm thickness results for ZDDP with different water contents at 100°C .....</b>	<b>171</b>
<b>Figure 8-20 Tribofilm thickness results for ZDDP with different water concentrations at 80°C .....</b>	<b>171</b>
<b>Figure 8-21 High resolution X-Ray Photoelectron Spectroscopy (XPS) spectra for ZDDP tribofilm formed at the end of the test for 3wt% water in oil at 80°C a) O1s b) Zn3s, P2p (Point C7 in Figure 8-20) .....</b>	<b>172</b>
<b>Figure 8-22 Schematic of the wear measurement points in the case of ZDDP replaced by fresh ZDDP and ZDDP replaced by base oil .....</b>	<b>174</b>
<b>Figure 8-23 3D-profilometry images taken at the end of experiments.....</b>	<b>174</b>
<b>Figure 8-24 a) 2D-profilometry image of the ball for point 2 b) the average wear depth calculation .....</b>	<b>175</b>
<b>Figure 8-25 Schematic of the wear measurement points in the case of ZDDP replaced by base oil and then fresh ZDDP and ZDDP replaced by only base oil.....</b>	<b>177</b>
<b>Figure 8-26 3D-profilometry images taken at the end of experiments.....</b>	<b>178</b>
<b>Figure 9-1 Water concentration evolution and tribofilm thickness over 2 hrs rubbing time for 3% water concentration at 80°C.....</b>	<b>183</b>
<b>Figure 9-2 Water contents and tribofilm thickness over 2 hrs rubbing time for 95% relative humidity at 80°C.....</b>	<b>186</b>
<b>Figure 9-3 Effect of relative humidity on tribofilm growth rate .....</b>	<b>188</b>
<b>Figure 9-4 Tribofilm evolution at 0% and 95% RH.....</b>	<b>188</b>
<b>Figure 9-5 A 3D visualization of MTM SLIM images and distribution of the tribofilm on the surface for 0% and 95% RH at 80°C.....</b>	<b>189</b>
<b>Figure 9-6 Effect of humidity on the atomic concentration of Zn, S, O and P of ZDDP tribofilm after 2 hrs rubbing.....</b>	<b>191</b>
<b>Figure 9-7 Effect of humidity on the ratio of P/Zn, P/O of ZDDP tribofilm after 2 hrs rubbing .....</b>	<b>192</b>
<b>Figure 9-8 Durability of the tribofilm for ZDDP with different water concentrations at 80°C .....</b>	<b>194</b>
<b>Figure 9-9 Evolution of polyphosphate chain length .....</b>	<b>196</b>
<b>Figure 9-10 Combined-effect of mixed-water and humidity on the evolution of O(a), Zn(b), P(c) and the ratio of P/Zn(d) of the ZDDP reaction layer over the time.....</b>	<b>197</b>
<b>Figure 9-11 Tribofilm evolution at 3% water and 95% RH at 80°C .....</b>	<b>198</b>
<b>Figure 9-12 A 3D visualization of MTM SLIM images and distribution of the tribofilm on the surface for 3% water (point A<sub>2</sub> and C<sub>2</sub>) and 95% RH (A<sub>3</sub> and C<sub>3</sub>).....</b>	<b>199</b>
<b>Figure 9-13 A 3D visualization of MTM SLIM images at point C<sub>1</sub> and C<sub>2</sub>.....</b>	<b>204</b>

**Figure 9-14 A 3D visualization of MTM SLIM images at point C<sub>5</sub> and C<sub>6</sub>..... 206**

## List of Tables

Table 2-1 Chemical structures of mineral oils (12).....	17
Table 2-2 Lubricants and additives (44, 46, 47) .....	19
Table 4-1 Material properties .....	65
Table 4-2 Experimental working conditions .....	65
Table 4-3 Lubricants.....	66
Table 4-4 Experimental working conditions .....	71
Table 4-5 Lubricant properties.....	71
Table 4-6 Material properties .....	73
Table 4-7 Working parameters.....	73
Table 4-8 Material properties .....	74
Table 4-9 Experimental working conditions .....	75
Table 4-10 Lubricant properties.....	75
Table 4-11 Working parameters of the experimental procedure .....	78
Table 5-1 Water concentration measurements before and after tribological test .....	87
Table 5-2 Summary of the effect of mixed-water in oil and temperature on tribological performance .....	88
Table 6-1 BO/NBO ratios at different levels of relative humidity .....	101
Table 6-2 Summary of the effect of relative humidity and temperature on tribological performance .....	106
Table 7-1 Numerical inputs and calibrated parameters.....	116
Table 7-2 Comparison between experimental measurements and numerical wear depth calculations.....	126
Table 7-3 Wear coefficients used in the numerical simulations (Dimensionless).....	128
Table 7-4 $\Psi$ for different water concentrations at different temperatures (Dimensionless).....	128
Table 7-5 Simulation inputs and calibration parameters.....	130
Table 7-6 Dimensionless <i>initial</i> wear coefficients in the numerical simulations in the first approach .....	135
Table 7-7 $\phi$ factors for modifying the Archard equation for different levels of relative humidity.....	136
Table 7-8 Simulation inputs and calibration parameters at 80°C .....	138
Table 7-9 Simulation inputs and calibration parameters at 98°C .....	139

<b>Table 8-1 BO/NBO ratios and the difference between Zn3s and P2p peaks. Tribofilm thickness at points A<sub>1</sub>, C<sub>2</sub> and C<sub>1</sub> is shown Figure 8-2. ....</b>	<b>155</b>
<b>Table 8-2 BO/NBO ratio. Tribofilm thickness at points C<sub>4</sub> and C<sub>3</sub> is shown in Figure 8-3.....</b>	<b>157</b>
<b>Table 8-3 BO/NBO ratios and the difference between Zn3s and P2p peaks. Tribofilm thickness at points A<sub>2</sub>, C<sub>5</sub> and C<sub>6</sub> is shown in Figure 8-4.....</b>	<b>159</b>
<b>Table 8-4 BO/NBO ratios and the difference between Zn3s and P2p peaks. Tribofilm thickness at points A<sub>3</sub>, B<sub>1</sub> and C<sub>8</sub> is shown in Figure 8-11. ....</b>	<b>165</b>
<b>Table 8-5 BO/NBO ratios and the difference between Zn3s and P2p peaks. Tribofilm thickness at points A<sub>4</sub>, B<sub>3</sub>, C<sub>9</sub> and C<sub>10</sub> is shown in Figure 8-16.....</b>	<b>170</b>
<b>Table 8-6 BO/NBO ratios and the difference between Zn3s and P2p peaks. Tribofilm thickness at point C<sub>7</sub> is shown in Figure 8-20.....</b>	<b>173</b>
<b>Table 8-7 Average wear depth measurement results.....</b>	<b>175</b>
<b>Table 8-8 Average wear depth measurement results.....</b>	<b>178</b>
<b>Table 8-9 Summary of the changes in tribofilm characteristics.....</b>	<b>180</b>





# Chapter 1. Introduction

## 1.1 Motivation

There is a new legislation that restricts the use of ZDDP as an anti-wear additive due to the new environmental rules to have Zinc free additives. It makes the lubricant companies to look for an alternative which can provide the same properties as ZDDP. Its unique properties of reducing wear requires a better understanding of the real mechanism in which ZDDP can reduce wear in the tribological system before replacing ZDDP with other additives. There is not only a lack of understanding in the formation, removal and durability of ZDDP reaction layer formed on the surface but also there is a need of investigating the composition of ZDDP tribofilm and its effect on durability and wear performance. To better understand the interfacial mechanisms of tribofilm formed by ZDDP, different factors need to be considered. One of this factors in the tribology industry is the effect of water/humidity on the mechanical, chemical and performance of ZDDP anti-wear film.

Water has been known as a contaminant in the lubricants since many years ago (1-3). It can affect wear performance, especially in bearing systems, in different ways (4-10). In addition, despite being poorly understood, water can greatly affect the performance of lubricants and additives such as ZDDP anti-wear additive. It is widely observed that the effect of water/humidity is not considered in most of the tribological tests (11). Some studies were done to study the effect of humidity in the lubrication system and tribological performance (friction and wear) but these studies are limited to see only the effect of water on the wear performance or tribochemistry of the surface (tribofilm formation). Tribochemistry is defined as the interaction between base stock and additives in the lubricant while tribofilm is forming on the surface (3,

5, 9, 12-16). In this project, the effect of water/humidity on the interfacial mechanisms, durability and chemical composition of ZDDP tribofilm and its effect on wear performance is investigated.

Water changes the chemical and mechanical properties of the interfacial protective film that is formed by the additives presenting in the lubricants. Hence the adsorption of the tribofilm as well as its integrity will be modified. Such a modification of the adsorption behaviour is suspected to cause an increase in the pitting of rolling elements (1, 16, 17). Moreover, water may also affect the elastohydrodynamic film thickness and bulk properties of lubricants, such as viscosity, total acid number (TAN). The mode in which water affects lubricated contacts depends closely on the type of base oil and additives as well as on the working environment (12) .

Duncanson (3) proposed that the effect of water on equipment and lubricants can be classified into:

- Shorter component life
- Water erosion and cavitation wear
- Hydrogen embrittlement
- Oxidation of bearing babbitt
- Water can accelerate oxidation of the oil
- Decomposition of additives

Another parameter that is significant in the tribological systems is temperature. Temperature can affect the tribofilm composition and wear performance. High temperature can change the composition of the tribofilm formed on the surface. This is mainly because the decomposition of additives such as friction modifier and anti-wear additives is temperature dependent. Therefore, temperature can lead to changes in friction and wear (15, 18).



Many researchers tried to study wear of materials considering different parameters such as load, hardness of material, sliding velocity. Archard tried to assess the effect of load, hardness and sliding distance on wear rate. He proposed that in all the experiments and different wear mechanisms, wear is independent of the apparent area and it directly proportional to the applied load for most of the experiment (19). Equation 1 is the form of relation that Archard developed.

$$V = K \frac{WL}{H} \quad (1)$$

In this equation V is the wear volume, W is the normal load, L is the sliding distance, H is the hardness of the material and K is the Archard wear coefficient.

Although extremely powerful, Archard's equation has some limitations. The most important one is that it has been developed for dry contact conditions. So much work has been done to modify the Archard wear equation and adapt it to new conditions. Archard assumed that wear is independent of apparent area which means that he did not consider the effect of surface topography or surface roughness. Effect of transient changes in surface roughness is missing as well (20). Archard equation considers just single material properties which is hardness of the material that it is not sufficient even for unlubricated sliding contacts and it can be seen from some experimental work that sometimes wear does not relate linearly to load and sliding distance (21, 22). These are the main gaps in the Archard equation which attract researchers to develop it to new working conditions. Part of this project is to modify Archard's wear equation to be able to account for the effect of tribochemistry including water/humidity effects.

## 1.2 Aims and objectives

Before discussing the research aims and objectives, it is worth mentioning that this study can be split into three main parts including ex-situ characterisation of ZDDP tribofilm formed on the surface in humid environment, investigation into the durability and characterisation of ZDDP reaction layer to study the different properties of ZDDP anti-wear additive film and finally development and validation of tribochemical model considering the effect of water. This research also concerns with investigating of adsorption, durability and removal (desorption) of ZDDP additive decomposed on the metal surface.

This study not only aims at showing the complication of the relationship between the chemical characterisation and tribological behaviour of the tribofilm but also aims at proposing a new insight into the effect of mixed-water in oil, humidity, temperature, load, rubbing time on interfacial mechanism involved in tribofilm formed by ZDDP. The following objectives can be determined as follows:

1. Forming ZDDP tribofilm using PAO oil containing ZDDP anti-wear additive mixed with different concentration of water to study the effect of water contamination and its tribochemistry on tribocorrosive wear of boundary lubricated system. All the experiments in this part are carried out ex-situ by using Mini Traction Machine integrated with Spacer Layer Interferometry (MTM SLIM) at two different temperatures.
2. Characterisation of the composition of the ZDDP tribofilm by performing X-ray Photoelectron Spectroscopy (XPS) at different times of starting the test in order to evaluate the effect of water on the chemical composition, growth rate and durability of ZDDP reaction layer.

3. Characterisation of tribological properties of ZDDP reaction layer by using 3D-profilometry to measure wear of the MTM ball. In addition to that it is used to study the correlation between wear and chemical composition and durability of the tribofilm formed on the surface at different conditions.
4. Forming ZDDP tribofilm using PAO oil containing ZDDP anti-wear additive at different levels of relative humidity to study the interfacial mechanisms of ZDDP tribofilm in humid environment. To be able to determine the effect of humidity on the chemical composition and durability of the ZDDP reaction layer, a humidity control system was designed and integrated to the Mini Traction Machine (MTM) and Spacer Layer Interferometry Method (SLIM) for the first time. All the experiments are conducted ex-situ by using MTM SLIM at two different temperatures.
5. Characterisation of the tribological properties and chemical composition of ZDDP tribofilm are performed by 3D-profilometry and XPS at different time of starting the test to see how tribofilm evolves in time at different conditions.
6. Investigation into the durability of the tribofilm and the correlation between durability, chain-length of glassy polyphosphate and rubbing time. The role of additive depletion on the pre-formed tribofilm thickness under mechanical stress has also been studied in this part. The tribological test were carried out by using MTM SLIM and chemical composition of tribofilm is evaluated by XPS at different running conditions.
7. In the current study the tribofilm thickness and wear results obtained experimentally are used to develop a semi-deterministic approach to implement the effect of humidity and mixed-water in wear prediction of boundary lubrication for the first time.

### **1.3 Thesis outline**

The report is divided into ten chapters. The first chapter discusses the motivation and objectives of the PhD project. It also introduces the gaps of the study due to the lack of understanding of the effect of water/humidity on the durability, tribological and mechanical properties of ZDDP anti-wear layer. The second chapter provides a theoretical background and an overview of the basics of tribology. The third chapter discusses the state-of-the-art regarding the effect of tribochemistry on the tribological behaviour of sliding and rolling contacts. It also discusses ZDDP additive, different properties of formed layer and the effect of water lubricant. Additionally, the different models used to study wear will be discussed and a new model that is capable of overcoming the limitations of the existing models will be proposed. The fourth chapter discusses the materials and the experimental procedure and techniques used in this study. The fifth chapter describes the effect of water on the tribofilm characteristics and its effect on wear. The sixth chapter shows humidity effects on ZDDP tribofilm characteristics and its effect on wear performance. The seventh chapter delivers the development of tribochemical model to take in to account the effect of water. An investigation into the durability of the tribofilm formed by ZDDP is presented in Chapter 8. The overall discussion of the thesis is described in Chapter 9. Finally, in the last chapter, the conclusions are drawn from this study and the future plans will be discussed.

## **Chapter 2. Fundamentals of Tribology, Lubrication and Wear**

### **2.1 Introduction**

This chapter provides an overview of the basics of tribology. It is divided into three sections. In section one, contact mechanics, friction and wear will be introduced. In addition, a distinction will be made between dry and lubricated contacts as well as between rolling and sliding contacts. The second section of this chapter gives a general overview of the different lubrication regimes and the different lubricants and additives, which are used to achieve certain tribological properties. Finally, a brief summary of this chapter will be given in section three.

### **2.2 Tribology**

Tribology is derived from the Greek word **Tribos** that means rubbing or sliding. The definition of tribology is the science of interacting surfaces in relative motion (23). Tribology investigates wear, friction and the effect of lubricants where two surfaces are interacting; this includes the interaction between gases, solids and liquids (24). Therefore, applying tribology to bearing applications provides a better understanding of the different conditions that any new equipment needs to meet and hence better designs can be achieved (23).

#### **2.2.1 Contact between solids**

The contact between interacting bodies is restricted to a small area, which is the region of the apparent area between high spots of both contacting surfaces. Only high contact stresses at considerable depths below the surface can make the real contact area ( $A_i$ )

between contacting bodies close to the true contact area (23). The contact between two solid surfaces is illustrated in Figure 2-1.

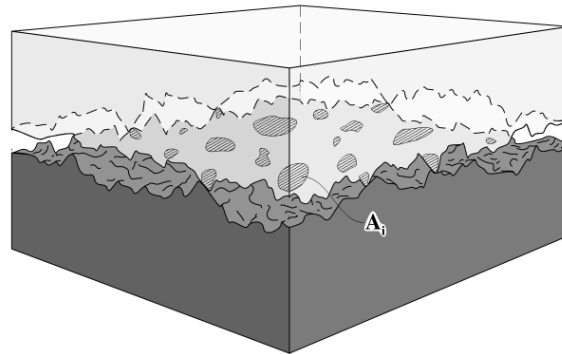


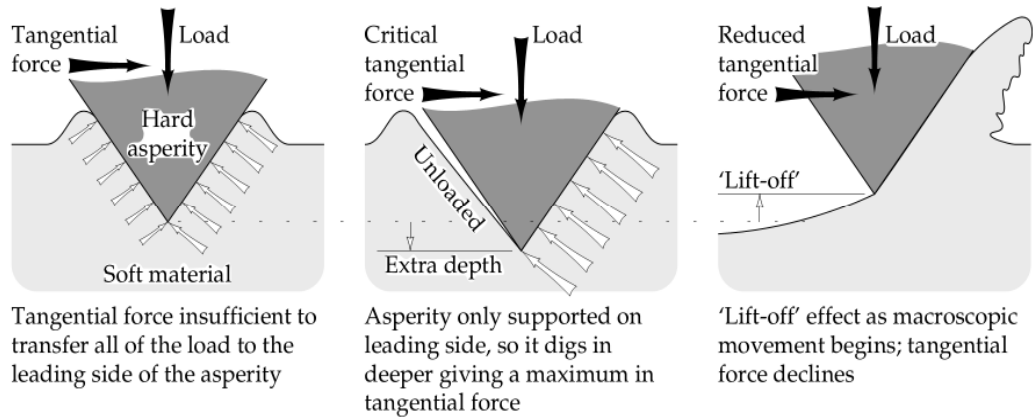
**Figure 2-1 Real contact area of the rough surface (23)**

Deformation of the high spots of contacting bodies, which are known as asperities, is responsible for the real contact area between two surfaces. The contact between asperities is responsible for wear and friction and the average contact stresses under sliding conditions. Three types of contact between solids have been reported (23):

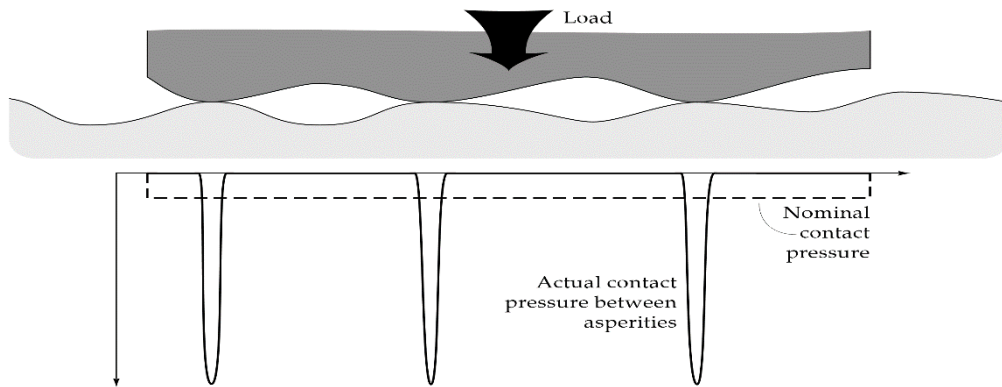
- Static contact where the tangential force is small
- Gross movement of the asperity when the tangential is at the maximum rate
- Unrestricted movement of asperity

Figure 2-2 shows three types of contact between surfaces.

Due to the high contact pressure between asperities, as shown in Figure 2-3, localized plastic deformation among the asperities can occur. Nevertheless, it has been reported that a large proportion of the contact between the asperities is completely elastic (25, 26). As the asperities are the load carriers, the correlation between the real contact area and load is of great importance in terms of friction and wear (26).



**Figure 2-2 The transition from static contact to sliding contact for hard asperity on soft contact (23)**



**Figure 2-3 Contact stresses between asperities (23)**

### 2.2.2 Friction

Friction is defined as the resistance to movement of one body relative to another.

Amontons stated four empirical laws for the friction force (27):

- The maximum tangential force before sliding is proportional to the normal force when a static body is subjected to increasing tangential load.
- The tangential friction force is proportional to the normal force in sliding.
- Friction force is independent of the apparent contact area.

- Friction force is independent of the sliding speed.

These empirical laws can be applied for most tribosystems including metals under dry and boundary lubricated conditions but it cannot be used for polymers (23).

Amontons' second law indicates that the relationship between normal load (P) and tangential force (F) can be described in the equation 2-1.

$$F = \mu P \quad 2-1$$

Where  $\mu$  is defined as the coefficient of friction.

### **2.3 Wear**

Wear is defined as the removal of material from solid surfaces caused by mechanical action (26). Generally, wear is divided into mild and severe wear. Using suitable materials, adequate lubricant and choice of operational variables are vital in order to obtain mild wear conditions; otherwise severe wear will be inevitable (26). Transferring from mild wear conditions to severe wear is mainly related to the topography of the contacting surfaces (25). That is because severe wear always occurs when the rough surfaces rubbing against each other generate rougher surface than the original one (27, 28). Throughout the wear process, wear debris can be generated.

Wear debris generation is significantly high during the running-in process but slows down after the initial smoothing of the contacting surfaces. Two types of wear debris may form, i.e. hard and soft particles as compared to the material of contact. The hard particles can cause wear, e.g. abrasive and erosive, whereas soft particles can cause indentation (29).

Wear mechanisms can be divided into four main categories: adhesive, abrasive, fatigue, and tribocorrosion wear (30). Adhesive wear occurs primarily in dry contacts



where asperities adhere to each other forming junctions. When the contacting surfaces start moving past each other, shear force is generated. This force may break the junctions between asperities and hence wear commences. Abrasive wear may occur due to friction forces generated when a harder surface is moving against a softer one. This form of abrasive wear is called two body abrasion (See Figure 2-4 and Figure 2-5).

On the other hand, wear may also occur due to friction forces generated between hard wear debris and soft contacting surfaces. In this case, wear is called third body abrasion. Fatigue wear takes place after many cycles of loading. Cracks are the main signature of fatigue wear. They may initiate on the surface and propagate to the bulk. This is the case when  $\lambda$  ratio, i.e. ratio between film thickness and surface roughness, is small and therefore an appreciated amount of solid-solid contact occurs. In addition, cracks may initiate inside the solid and propagate towards the surface. This is typically the case when  $\lambda$  ratio is large enough that elastohydrodynamic lubrication dominates Lancaster (30). These types of rolling contact fatigue can also be categorized as (31):

- Subsurface originated which is called spalling
- Subcase fatigue (in surface hardened components) called case crushing
- Surface originated called pitting
- Peeling which is now usually called micropitting
- Section fracture

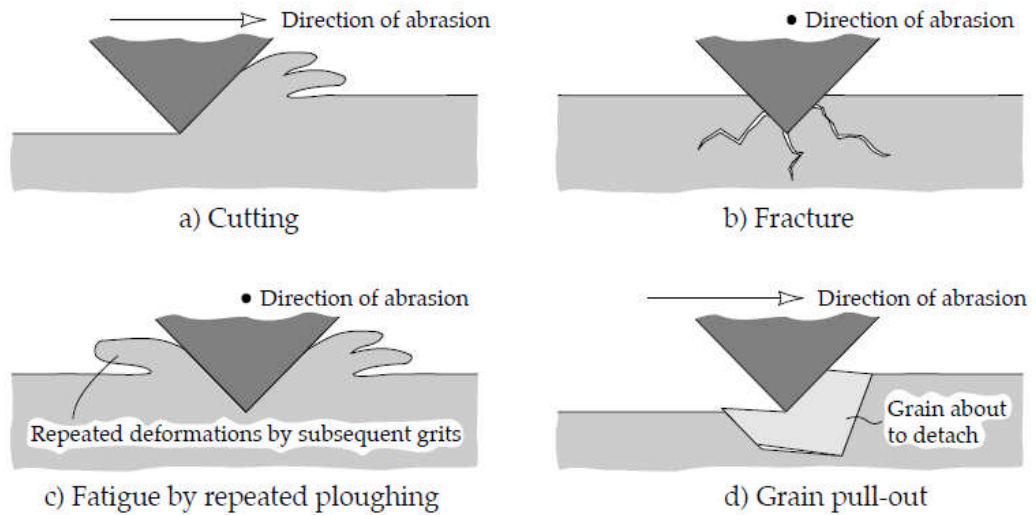


**Figure 2-4 Different modes of two body abrasion (32)**

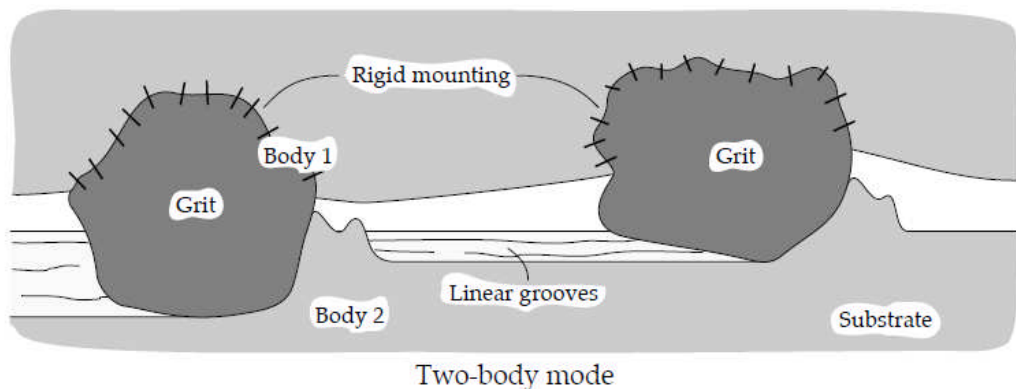


**Figure 2-5 3<sup>rd</sup> body abrasive particles between surfaces (32)**

### 2.3.1 Running-in

The period in which two contacting surfaces start to contact in rolling/sliding conditions is called running-in. This process plays a significant role in altering the physical, chemical and mechanical properties of the interfaces. The phenomena which occurs in this period is complex, therefore the material and lubricant behaviour is not recognised in running-in period.

The real-time wear measurement versus time is shown in Figure 2-6. Higher wear happens during the running-in period compared to the steady state wear because of the physical and chemical changes happening during this complex period. It can be attributed to the asperities which are not smoothed enough during the running-in process their sizes have not been changed.

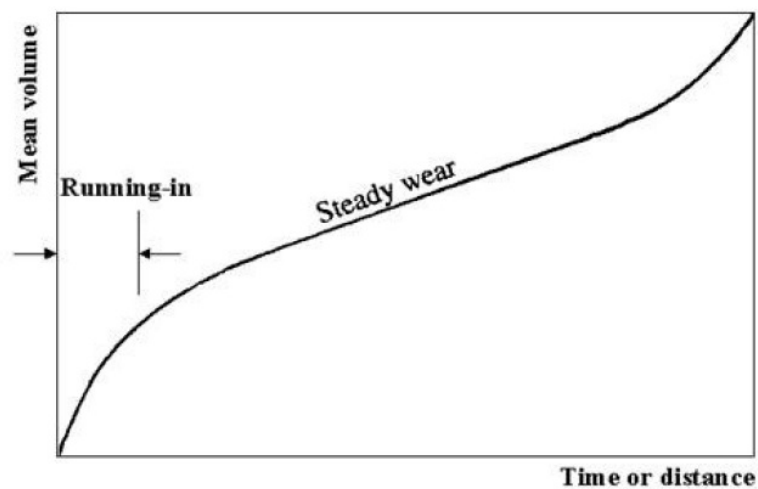


**Figure 2-6 Running-in and steady state wear versus time (33)**

### **2.3.2 Wear under rolling-sliding conditions**

The contacting surfaces in relative motion can be categorised into two zones: stick and slip. Stick can be related to the situation where there is no relative motion between the contacting surfaces. Slip zone is encountered when the contacting bodies are moving past each other. Sliding contact occurs when slip is the only process involved whereas rolling contact occurs when only stick between the contacts occurs. If both stick and slip take place, the system is subjected to a rolling and sliding contact (28).

## 2.4 Lubrication

### 2.4.1 Introduction

To reduce friction and improve wear resistance of the contacting surfaces, these interacting surfaces should be separated. This is achieved using different types of lubricants depending on the material of the interacting surfaces and the operational conditions (34). Different types of lubricants, e.g. air, liquid oils and grease, can be used (35).

Before considering the appropriate choice of lubricants, one should consider in which regime the lubrication system under study is operating. Depending on the speed, normal load and viscosity, the lubrication regime can be hydrodynamic lubrication (HL), elasto-hydrodynamic lubrication (EHL), mixed lubrication (ML) or boundary lubrication. These different regimes are illustrated in Figure 2-7.

Hydrodynamic lubrication is applied when the load is completely carried by the lubricant film. In this case, the interacting surfaces are separated entirely by a thick lubricating film (35). The thickness of this film is about 1-1000  $\mu\text{m}$  (36).

Elasto-hydrodynamic lubricant regime is always applied when the oil film is thin and the local pressure is very high (34). The plastic deformation caused by additional pressure and load beyond the EHL conditions makes the asperities to be in contact more than EHL regime. Consequently, the number of contacting asperities and interacting surfaces will increase and the lubricant film thickness would be decreased regarding the high load and pressure (37). The lubricating film in this regime usually has a thickness of 0.1-1  $\mu\text{m}$  (36).

Mixed lubrication regime occurs between the elasto-hydrodynamic regime and boundary regime (38). Here, the asperities of the counterparts in motion carry part of

load and the other part of the load is carried by the lubricant film (34, 39). The lubricating film in this regime usually has a thickness of 0.01-1  $\mu\text{m}$  (36).

In the boundary lubrication regime, the asperities of both interacting surfaces are in direct contact (34, 39). The interaction between asperities of counterpart's surfaces generates energy that is transformed to friction, wear and heat. Thus, the local temperature at the tip of these asperities increases to a very high level. This high temperature is defined as the flash temperature (36). The average lubricant thickness in the boundary lubrication regime is between 1-100 nm (36).

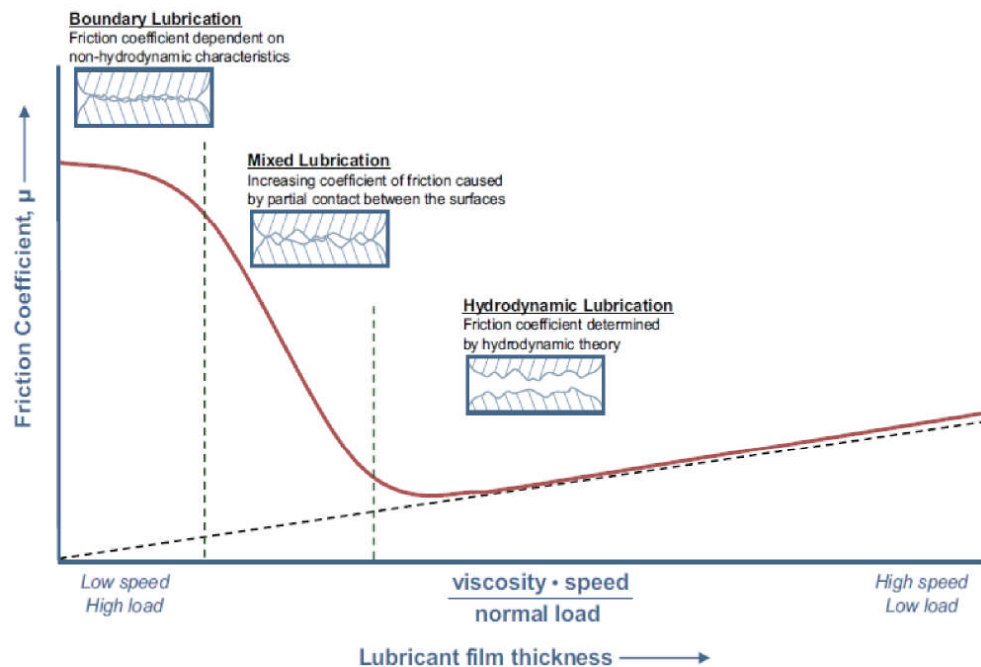


**Figure 2-7 Stribeck curve, dependence of the friction coefficient on viscosity, speed and load for a lubricated sliding system (36, 38).**

### 2.4.2 Lubricants

Lubricant is a composition of base oil and different additives. Different formulations of lubricants can be designed for various applications and processes depending on the

operating conditions, material properties, and temperature. Base oil is generally divided into two types: mineral oil and synthetic oil.

### **2.4.3 Mineral oil**

Mineral oil is widely used as a base stock in the industries. It is produced from the crude oil collected from different parts of the world (40). The general composition of mineral oils consists of carbon chains that contain 20-40 carbon atoms in each molecule. The small percentage of heteroatoms like sulphur, nitrogen and oxygen replaces hydrogen in the hydrocarbon chains. These heteroatoms play a significant role in keeping the oil stable. They are also capable of reacting with lubricant additives and thus affecting the properties of the lubricant (12).

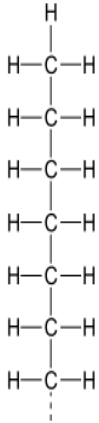
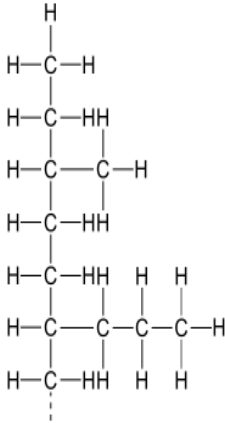
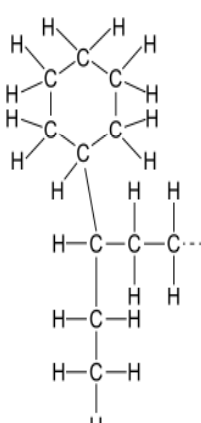
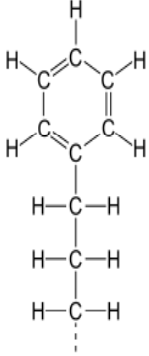
Mineral oils can be classified based on the chemical forms, sulphur content and viscosity. Based on the chemical composition, they can be divided into paraffinic oils, naphthenic oils and aromatic oils. The chemical structures of these oils are summarized in Table 2-1. It should be noted that the relative proportion of paraffinic, naphthenic and aromatic components can also be used as a basis for the classification of mineral oils.

### **2.4.4 Synthetic oils**

Because mineral oils have some drawbacks such as the oxidation and viscosity loss at high temperature, synthetic oils become more popular among different industries (12). Synthetic oils in terms of wear resistance and energy loss are more effective than mineral oils. In addition, they are capable of being used in a wide range of temperature (41). Because of their high oxidative resistance, synthetic oils can provide a longer lubricant life. This lengthens the lubrication intervals and reduces the overall oil consumption as well as waste disposal (12).

Poly- $\alpha$ -olefins, esters and polyglycols are most widely used and most well-known synthetic oils. Poly- $\alpha$ -olefins (PAO) are unsaturated hydrocarbons with the general structure  $(-\text{CH}_2-)_n$ . These oils have high viscosity index, low volatility and good oxidation stability. PAO and polyglycol provide less frictional loss than mineral oils (42-44).

**Table 2-1 Chemical structures of mineral oils (12).**

PARAFFIN		NAPHTHENE	AROMATIC
Straight	Branched		
			

Ester oils, which are formed from the reaction of alcohol and a fatty acid, are used when high temperature resistance and low flammability are needed. Esters are more polar than other synthetic oils. This high polarity makes them more sensitive to water contamination due to their high affinity towards water (45).

### 2.4.5 Additives

Different types of additive can be added to the lubricant to achieve certain properties (12). These additives play a significant role in reducing friction and wear by decomposing over the load carrying asperities and forming a protective tribofilm (37).

A wide variety of additives are available, e.g. friction modifiers, anti-wear, corrosion inhibitors and extreme pressure additives. A summary of well-known additives, including their chemical structure and purpose, is presented in Table 2-2.

Based on the information presented in the previous table regarding the different additives used in industry for different applications, ZDDP can be used as an oxidation inhibitor, corrosion inhibitor and anti-wear additive. There is a new legislation that restricts the use of ZDDP as an anti-wear additive. It makes the lubricant companies to look for an alternative which can provide the same properties as ZDDP.

Its unique properties of reducing wear require a better understanding the real mechanism in which ZDDP can reduce wear in the tribological system before replacing ZDDP with the other additives. Therefore, this additive will be used in this study, which is concerned with studying the tribological properties, i.e. wear and tribofilm characteristics formed on the surfaces by ZDDP reaction layer.

#### **2.4.6 Conclusion**

This project aims to investigate the interfacial mechanism of the tribofilm formed by ZDDP including the effect of water on the mechanical properties, chemical composition of ZDDP anti-wear layer and its effect on wear performance; durability of the ZDDP tribofilm and its correlation with the mechanical and chemical properties of ZDDP in lubricated sliding-rolling contacts under extreme pressure conditions.

The chapter introduces different aspects of the field of tribology including contact mechanics, friction and wear. In addition, a distinction was made between dry and lubricated contacts as well as between rolling and sliding contacts. Moreover, this chapter reviewed the different lubrication regimes and the different lubricants and additives that are used to achieve certain tribological properties.



**Table 2-2 Lubricants and additives (44, 46, 47)**

<b>Types of additive</b>	<b>Chemical compound</b>	<b>purpose</b>	<b>Mechanism of action</b>
Oxidation Inhibitors	Hindered phenol, amines, organic sulphides, Zinc phosphorodithioates	Minimize polymerization to form resin, varnish, sludge, acids or polymerizes	Decrease acid formation by reduced oxygen absorption of the oil inhibits catalytic reactions.
Anti-wear additive	Zinc-phosphoro-dialkyl-dithioates, Tricresylic phosphates	Reduce excessive wear between metal surface	The reaction with metal surfaces leads to the formation of layers which undergo a plastic deformation and improve the contact pattern.
Extreme pressure additives	Sulphurized greases and olefines, chlorinated hydrocarbons, lead salts of organic acids, aminophosphates	Prevent microscopic welding between metal surfaces under high pressure or temperature	The reaction with metal surfaces leads to new compounds with a lower shear stability than the base metal. A continuous process of Shearing-off and rebuilding.
Friction modifier	Fatty acids, fatty amines, Solid lubricants	Reduce friction between metal surface	Molecules with a high polarity are adsorbed on metal surfaces and separate the surfaces.

As discussed before, mineral oils have several drawbacks such as the oxidation and viscosity loss at high temperature whereas synthetic oils have better oxidation resistance and higher viscosity index. Poly- $\alpha$ -olefin (PAO) is the most widely used and most well-known synthetic oil. Therefore, in this project PAO will be used as model oil.

As mentioned earlier, this project aims at studying the tribological and tribochemical properties under extreme pressure conditions. Many additives that are suitable for extreme pressure conditions were reviewed. ZDDP was found to be compatible with PAO and can be used as anti-wear additive in extreme pressure conditions. Therefore, it will be used as model additive in this study.

Water is envisaged to affect the mechanism of ZDDP decomposition and the formation of the tribofilm. In addition, owing to their high polarity, PAO are sensitive to water contamination, which may alter their lubrication properties and the ability to dissolve additives and form protective tribofilms. These aspects have significant effects on the tribological properties especially under extreme pressure conditions where tribochemistry can play a major role. Hence, in the next chapter the state-of-the-art of the effect of water, tribochemistry on the tribological behaviour of sliding and rolling contacts will be discussed in more details.

## **Chapter 3. Review of the Literature**

### **3.1 Introduction**

This chapter reviews the state-of-the-art of the effect of tribochemistry on the tribological behaviour of sliding and rolling contacts. The chapter is divided into four main sections. In the first section, the effect of water on tribochemistry, will be introduced. Different aspects will be discussed including the water absorption properties of lubricants and the effect of water on wear as well as on lubricant, additives, and solid surfaces. In the second section, composition of ZDDP antiwear film as well as mechanical and tribological properties and chemistry of ZZDP will be discussed in detail. A critical review will be provided in Section 3.4 for the very few models that describe the tribochemistry and tribocorrosion phenomena under mechanical work, e.g. friction and wear. The strengths and limitations of every model will be highlighted. Finally, the literature findings will be summarised and some conclusions drawn regarding the design of the experiment and the models to be used or introduced to fit the experimental data.

### **3.2 Water in oil**

#### **3.2.1 Introduction**

The presence of water in the lubricated tribosystems particularly in bearing applications can cause corrosion and hydrogen embrittlement, which can increase wear and friction (8). In addition, the small amount of water even in part per million (ppm) may accelerate the oxidation of oil (12). Water can enter the oil in different ways (48):

- Absorption: oil can get the moisture from the air directly. The amount of water absorbed by oil can be attributed to the saturation point, which is the maximum amount of water which is able to dissolve in the oil, the relative humidity and temperature.
- Condensation: the moisture in air can enter the oil as of the different operating temperatures may result in condensation.
- Combustion or oxidation or neutralization: one of the by-products of fuel combustion is water and it can be combined with water entered from the air.
- Free water entry: The addition of additives or some other fluids can be a source of water in the lubricated system as free water.

### **3.2.2 Types of water contamination in the lubricated system**

To investigate the effect of water contamination on the performance of lubricated systems, it is essential to know the form of water existing in oil (49). Water can present in oil in two different forms (2):

- dissolved water
- free water

Dissolved water case occurs when the amount of water in oil is less than the saturation point (1, 50). The saturation curve for typical oil is illustrated in Figure 3-1. Free water occurs when the amount of water in oil is more than saturation point. In this case, droplet of water will be formed in oil resulting in an emulsion formation (50). Figure 3-2 indicates a description of different forms of water in oil. Typically, water droplets will not be stable from coalescence unless an emulsifier is added. This emulsifier consists of a polar hydrophilic head that surrounds water and a hydrophobic tail that is attracted to the oil. In order to stabilize water droplets, the emulsifier forms micelles

(2) as illustrated in Figure 3-3. The most well-known forms of water in oil is the reverse micelle.

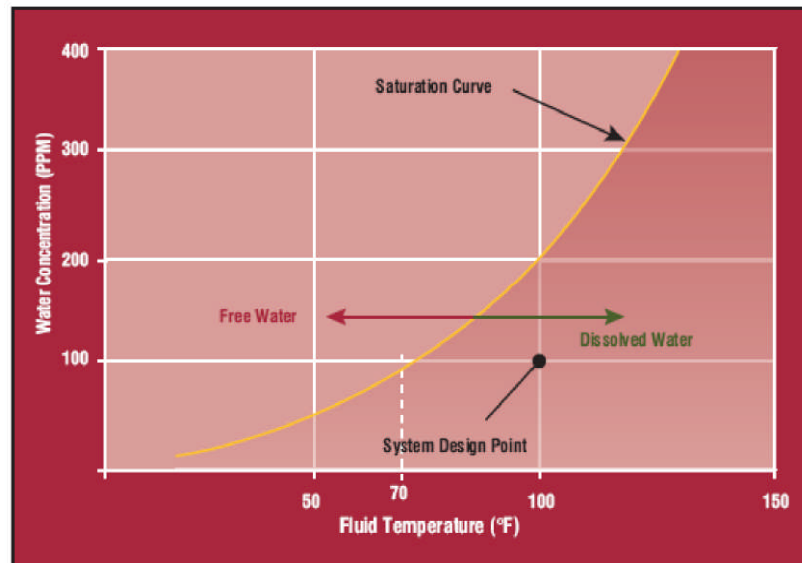


**Figure 3-1 The saturation curve for typical oil (52)**

### 3.2.3 Water absorption properties of lubricants

The factors determining the absorption properties of lubricants are the oil composition, physiochemical properties, concentration of additives, contaminants and local environment, e.g. temperature and pressure (42). Cantley (4) investigated the effect of relative humidity, i.e. 20, 60 and 100%, on 12 different oils, including mineral oils, synthetic oils and oils with EP additives. The results showed that the higher the non-polarity of a lubricant the higher the hydrophobicity and hence the lower the affinity towards absorbing water, which is in accordance with theory. These results also suggested that the addition of additives to oil increases the absorption of water due to their effect in decreasing the extent of hydrophobicity of the oil. For instance, SAE mineral oil absorbed approximately 100 ppm at 100% relative humidity whereas the same oil with EP additive absorbed approximately 700 ppm at the same relative humidity. In addition, Cantley (4) revealed that, generally, synthetic oils

absorb more water than mineral oils. This was evident from observing that Diester synthetic oil absorbed approximately 3000 ppm at 100% relative humidity as compared to 100 ppm in the case of SAE mineral oil.

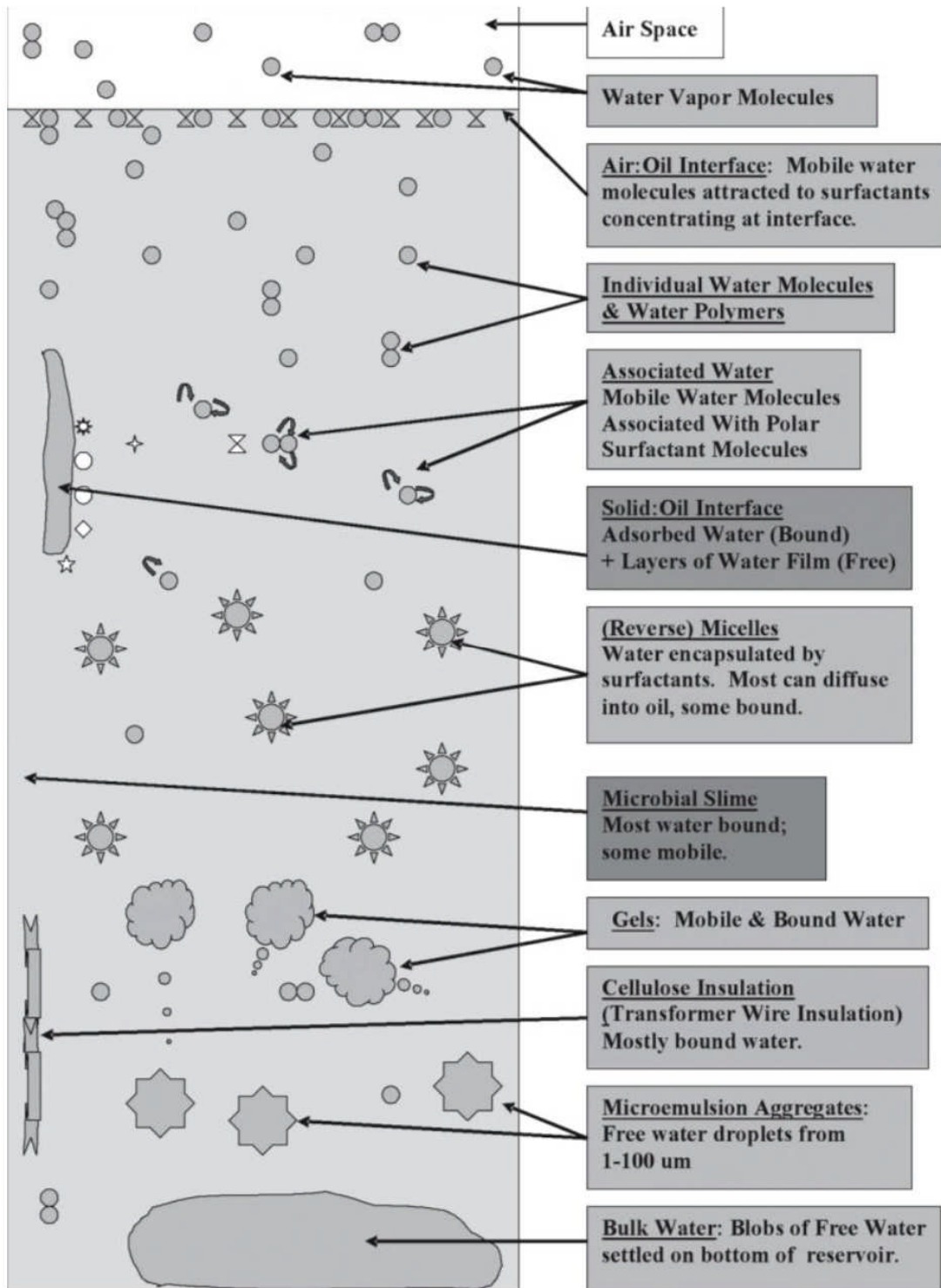
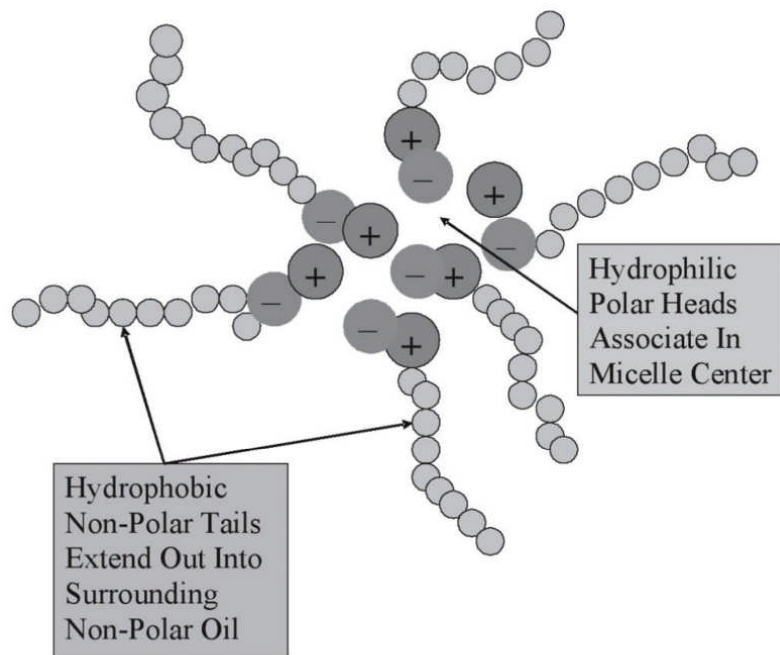


Figure 3-2 Forms of water in oil (51)



**Figure 3-3 Reverse micelles in oil (2).**

### **3.2.4 The effect of water in dry and lubricated systems**

Water can affect friction and wear of lubricated systems in three different ways (53). Firstly, water may affect the formation and removal of the tribofilm by altering the capability of long chain molecules to adhere to the surface. Secondly, it may modify the chemical composition of the tribofilm. Thirdly, water can increase pitting especially in rolling elements. (44, 53). These effects are manifested in altering the bearing performance by modifying friction and wear.

Hamaguchi (43) investigated the effect of water on the film thickness in EHD lubrication regime. They prepared emulsion of water of different concentrations in liquid paraffin. The results showed that the film thickness is not affected by the presence of water. The authors concluded that only the pure oil determines the EHD properties without any adverse effect of water.

Goto and Buckley (54) studied the effect of relative humidity on friction and wear under fretting condition of different metals in dry contact. In case of iron, it was found that for values of relative humidity under 10%, the friction coefficient was constant whereas wear volume increased steadily, which is shown in Figure 3-4. At a relative humidity of 10%, friction and wear dropped drastically. For higher values of relative humidity, wear and friction exhibited distinctive plateau where no further change in friction and wear was noticed.

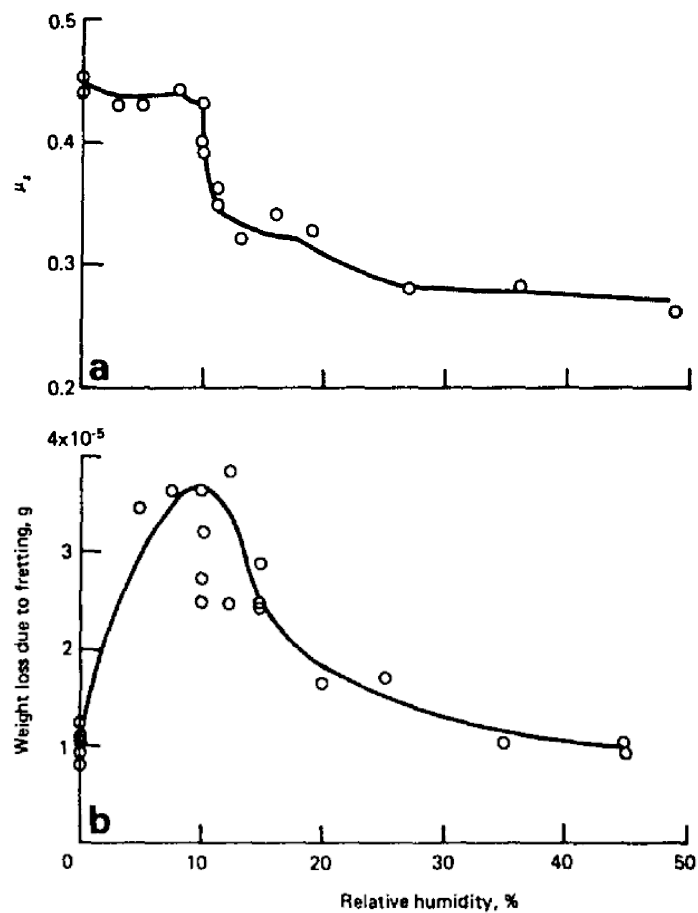


**Figure 3-4 Effect of relative humidity on wear and friction (54)**

After a large number of loading cycles, strain and stress accumulation in the contacting surfaces cause fatigue to occur (12). Fatigue is responsible for the incident of pitting where the detachment of large parts, compared to asperities size, of the



surface occurs. This mainly takes place when  $\lambda$ , the ratio of film thickness to surface roughness, is small (53).

Cantley (4) investigated the effect of water on oil lubricated tapered roller bearing. The author studied different cases of a full-scale bearing lubricated with 12 different oils. These oils were subjected to three levels of relative humidity, i.e. 20, 60 and 100%. The water concentration in the oils was in the range of 25-400 ppm as determined by Karl Fischer titration method. The results revealed an exponential reduction in bearing fatigue life with the increase in water concentration as shown in Figure 3-5.

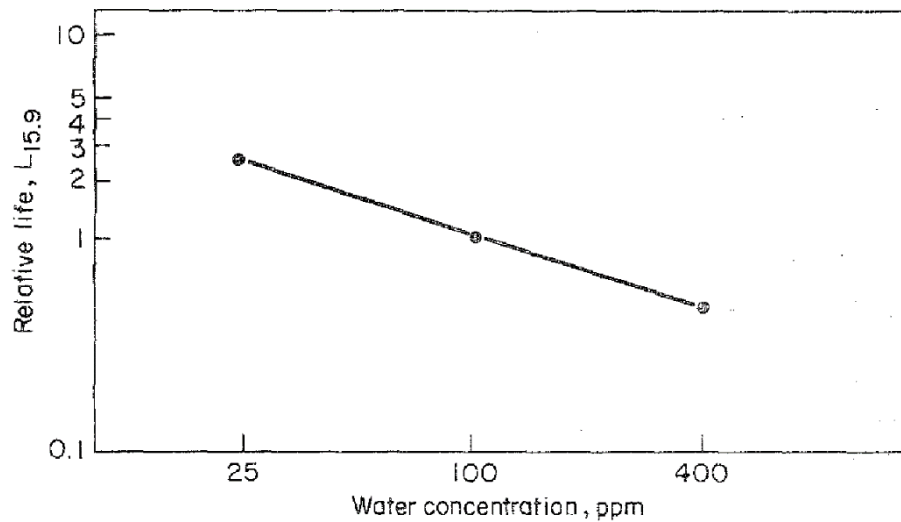


**Figure 3-5 Effect of water contamination on bearing life (4)**

Cantley proposed that the relative bearing life,  $L$ , could be estimated at different water concentrations,  $X$ , in ppm, using equation 3-1:

$$L = \left(\frac{100}{X}\right)^{0.6} \quad 3-1$$

Where the factor 100 corresponds to a bearing life of 1.

Similarly, the effect of water and oxygen on rolling contact lubrication was investigated by Schatzberg and Felsen (55). Their experimental work focused on the performance of the angular contact ball bearing lubricated with different paraffinic oils. The authors considered two levels of dissolved water concentration, i.e. < 10 ppm and 100 ppm. The results showed a significant reduction in bearing fatigue life even at concentrations as small as 100 ppm. Schatzberg and Felsen suggested that this reduction might be attributed to the condensation of small amount of water in the microcracks, which are chemically more reactive, in the metallic surface. This leads to corrosion and hydrogen embrittlement, due to atomic hydrogen, within the microcracks and hence accelerated fatigue.

### **3.2.5 Effect of water on viscosity**

Water contamination may affect oil viscosity and in turn, the change in the oil viscosity can change the lubrication regime from elastohydrodynamic to severe lubrication regimes such as mixed or boundary lubrication regime.

Liu *et al.* (56) studied the effect of free water of concentrations between 8 and 36 vol. % on the viscosity of four different paraffinic mineral oil. At this large concentrations, water and oil form emulsion. In order to stabilize this emulsion, Liu *et al.* added emulsifying agent with concentrations between 1 and 8 vol. %. They noticed that although the viscosity of the emulsion is larger than the one of oil, a thinner EHD film is formed. It was also observed that small amount of water (dissolved water) does not change the bulk properties, i.e. viscosity and TAN, of the oil (12).

The effect of water on viscosity seems to be strongly dependent on the amount of water in oil. Smaller amount appears to have no effect on water, which is evident from Chen *et al.* (12) results. On the other hand, at larger amount of dissolved or free water, viscosity is expected to increase, which is evident from the results of Liu *et al.* (56).

This suggests that it is not sufficient to report only the relative humidity values but the exact amount of water in oil is required as well.

### **3.2.6 Effect of water on hydrogen embrittlement**

Ciruna and Szieleit (8) suggested that the main sources of atomic hydrogen are water and lubricant decomposition. They studied the effect of hydrogen on rolling contact fatigue life using steel balls that were electrolytically charged with different concentrations of atomic hydrogen. The results showed that the higher the concentration of hydrogen in steel the smaller the fatigue life. Their study confirmed that hydrogen embrittlement is one of the main factors that inversely affect the life of bearings.

Vincent *et al* (57) investigated hydrogen embrittlement of a ball bearing of stainless steel. The authors introduced hydrogen to the ball by cathodic charging. Their results revealed that the hydrogen tends to be localized at the carbide-martensite interfaces. In addition, the results showed that the hydrogen traps increases with load by an amount that is different depending on the load whether static or dynamic.

Likewise, the hydrogen embrittlement mechanisms of ferritic steels was assessed by Neeraj *et al.* (58) . They conducted two sets of experiments. In the first one, samples were electrochemically hydrogen pre-charged whereas in the other set samples were tested in high-pressure hydrogen, i.e. 5.5 MPa, 21 MPa and 103 MPa. The results revealed that in the presence of atomic hydrogen, sub-grain structure refinement, enhanced plastic flow as well as nanovoids coalescence might occur.

### **3.2.7 Effect of water on oil oxidation**

The interaction of heat, pressure and air in the lubricated system can result in oil oxidation. The oil oxidation can be enhanced by water contamination by orders of magnitude (59) as shown in Figure 3-6. The by-products of oil oxidation are always

acids, which can make the environment more corrosive. This corrosive environment can accelerate the wear rate (45).

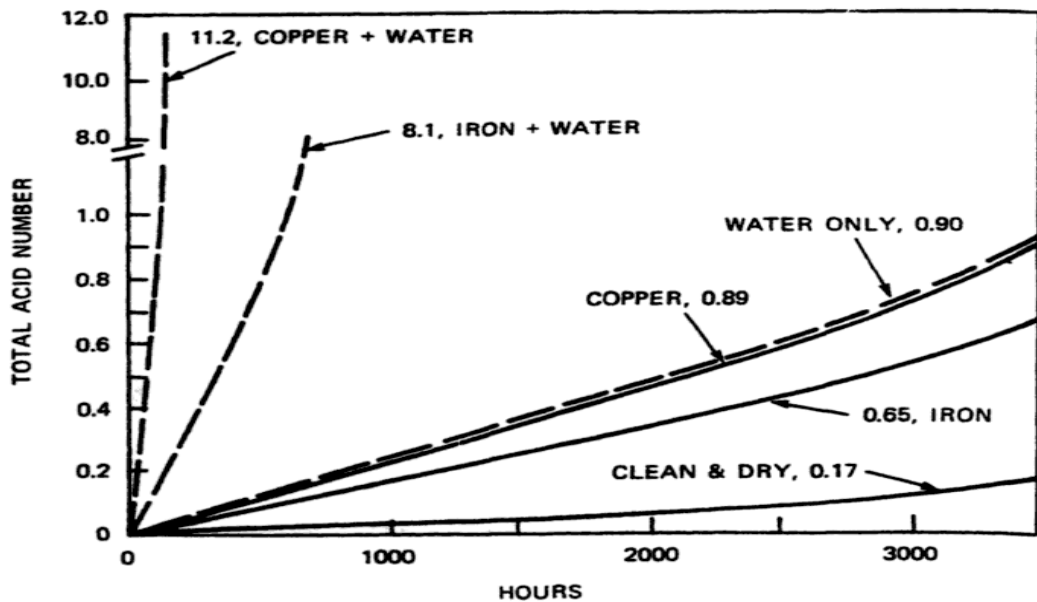


**Figure 3-6 Catalytic effect of water and metals on oil oxidation as calculated by total acid number (59)**

Ciruna and Szieleit (8) suggested that the main sources of atomic hydrogen are water and lubricant decomposition. The interaction of heat, pressure and air in the lubricated system can result in oil oxidation (51).

Interacting surfaces can be affected directly by water or they can be affected indirectly when the water oxidises the lubricants and additives or generates atomic hydrogen that leads to hydrogen embrittlement.

### **3.2.8 Effect of water on lubricant performance**

A review of the effect of water on friction and wear of lubricated systems is made by Lancaster *et al.* (53) and more recently by Cen *et al.* (60). Firstly, water may affect the formation and removal of the tribofilm by altering the capability of long chain molecules to adhere to the surface. Secondly, it may modify the chemical composition

of the tribofilm. Thirdly, water can increase pitting especially in rolling elements. These effects are manifested in altering the bearing performance by modifying friction and wear. Sheiretov *et al.* (61) investigated the effect of dissolved water on the tribological properties of three oils, i.e. Polyalkylene Glycol (PAG) with water content from 200 to 17000 ppm and two Polyolester (PE<sub>1</sub> and PE<sub>2</sub>) oils with water content from 70 to 1600 ppm. In all the measurements conducted in an air atmosphere, the wear of cast iron plates shows a decrease with increasing the water content. Different additives can be added to lubricants to achieve certain properties. These additives can be viscosity-index improvers, anti-wear, friction modifier and extreme pressure additives (60).

It has been widely reported that ZDDP acts as an antiwear additive in the boundary lubrication regime by forming a relatively thick tribofilm on the contacting asperities. This solid-like tribofilm increases the load carrying capacity of the surfaces and protects the surfaces by being partially removed and preventing the direct solid-solid contact of substrates. Chemical, physical and mechanical properties of this tribofilm control the wear behaviour of the system (62).

### **3.2.9 Summary of the effect of water on lubricant**

The main drawbacks of water contamination on lubricants are corrosion, increased wear and premature failure of lubricated metal surfaces. Interacting surfaces can be affected directly by water or it can be affected indirectly when the water damages the lubricants and additives effectiveness or generates atomic hydrogen that leads to hydrogen embrittlement.

### 3.3 Zinc Dialkyl Dithiophosphate (ZDDP)

#### 3.3.1 ZDDP as an anti-wear additive

Zinc Dialkyl Dithiophosphate (ZDDP) is the most commonly used antiwear additive. Based on the new environmental legislations, using ZDDP in lubricant oils is restricted. This results in finding new alternatives for ZDDP that can act as a good antiwear additive. Therefore understanding the true mechanisms in which ZDDP acts as an antiwear additive is essential.

It is reported that ZDDP reacts with the steel surface to generate amorphous reaction layer (63, 64). X-ray absorption spectroscopy and X-ray Photoelectron Spectroscopy (XPS) have been used to evaluate the chemical characterisation of ZDDP reaction layer including durability, structure and reactivity of ZDDP molecules (63, 65, 66). It was found that ZDDP molecules has three different structures: the monomeric form consists of  $Zn_2 [PS_2 (OR)_2]_2$  which has Zinc atom surrounded by four Sulphur atom, neutral form consisting  $Zn_2 [PS_2 (OR)_2]_4$  which has Zinc atom attached to two dithiophosphate groups and the basic form  $Zn_2 [PS_2 (OR)_2]_6 O$  which attributed to the structure proposed by Burn and Smith (67) by using X-ray Absorption Fine Structure (XAFS) spectroscopy (66, 68-70)( see Figure 3-7). It has been suggested that in this structure, Oxygen atoms surrounded by four Zinc shown tetrahedral configuration (71). One of the most well-known structures of ZDDP is the neutral structure which is shown in Figure 3-7. ZDDP can be categorised as primary, secondary and tertiary based on the carbons atoms that could be attached to the alkyl (R) groups.

It is reported that the diffusion or adsorption of the ZDDP molecules on the substrate is necessary prior to the formation of any surface films (62, 72). Surface studies show that ZDDP thermal films are different from tribofilms (73-75). It has been reported that the tribofilm, unlike thermal films, needs asperity-asperity contact and sliding to

be formed on the surface. They form at much lower temperatures than the thermal films and only form on rubbing tracks (62, 76-78). The thickness of the tribofilm is reported to be in the range of 50-150 nm on steel surfaces (77, 79, 80). ZDDP tribofilms grow initially on small single patches and after some time cover the surface in pad-like structures (81).

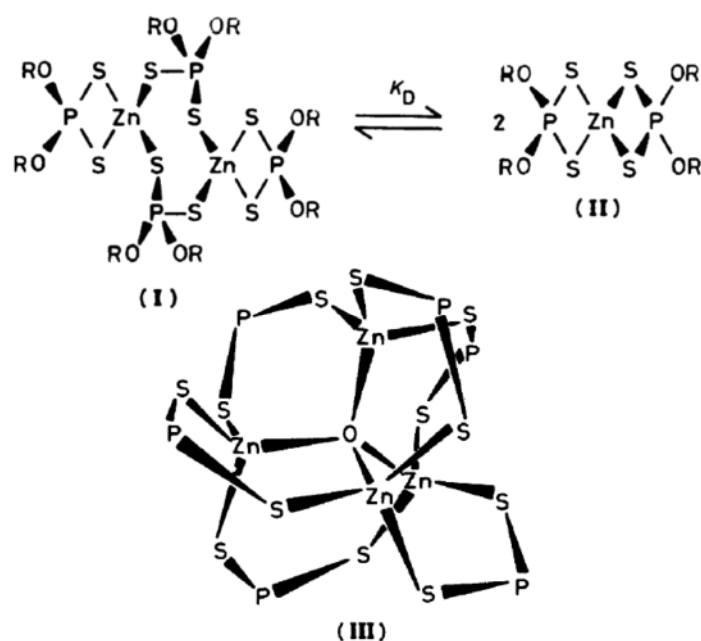


**Figure 3-7 Different structures of ZDDP: (I) neutral monomeric in equilibrium (II) neutral dimeric (III) basic ZDDP (82)**

### 3.3.2 Mechanical properties and durability of ZDDP tribofilm

There are several works which study the mechanical properties of ZDDP tribofilms formed in boundary lubricated contacts (81, 83-88). They found that the properties of the tribofilm layers are dependent on applied load and can be adapted to conditions (89). They also showed that the mechanical properties of tribofilms vary from surface to substrate (90). A schematic figure of the multilayer structure of ZZDP tribofilm is shown in Figure 3-8 and Figure 3-9 illustrate the patchy structure of ZDDP tribofilm formed on the surface. Figure 3-9 shows that the first layer of the tribofilm formed on

the steel surface consists of more FeS/ZnS due to the presence of higher iron concentration in the tribofilm close to the surface. The topmost layer of the tribofilm contains more zinc polyphosphates as the iron concentration is lower compared to the bulk of the tribofilm. It is also shown that the chain length of the polyphosphates varies within the tribofilm. The higher iron concentration results in the shorter chain polyphosphates formed on the surface.

Mosey *et al* (89) developed a new theory for the functionality of ZDDP tribofilms at the molecular level. They suggested that pressure-induced cross-linking is the reason for chemically-connected networks and many aspects of experimentally-observed behaviour of ZDDP can be explained by this theory. It was reported that the high pressure at the surface of the film will lead to higher cross-linking and result in longer chain phosphates. The different mechanical properties of long and short chain polyphosphates were simulated and reported in the work. ZDDP forms different types of tribofilm on various surfaces such as Al/Si alloys, DLCs and steel. The tribofilm on steel surfaces is more durable in comparison with the ones on DLC or other inert surfaces (91, 92). The effect of the steel substrate in changing the nano-indentation results of tribofilm has been reported and different models for extracting the tribofilm properties were developed (83, 90). All these studies give good insights of mechanical characteristics of ZDDP tribofilm under severe conditions that might explain some of the experimentally-observed behaviour (62).

It was suggested by Morina *et al* (93) that the durability of tribofilm can be evaluated by the chemistry of the tribofilm formed on the surface. The experiments were based on investigating the formation, stability and removal of the tribofilm by changing the oils during the tests and monitoring the friction coefficient. It was reported that ZDDP tribofilm is durable once it is formed. The concept of tribofilm removal was also



reported by Lin *et al* (94). Based on the experimental wear results, they suggested that a comparison between the rate of formation and removal of the tribofilm can characterise wear in boundary lubrication.

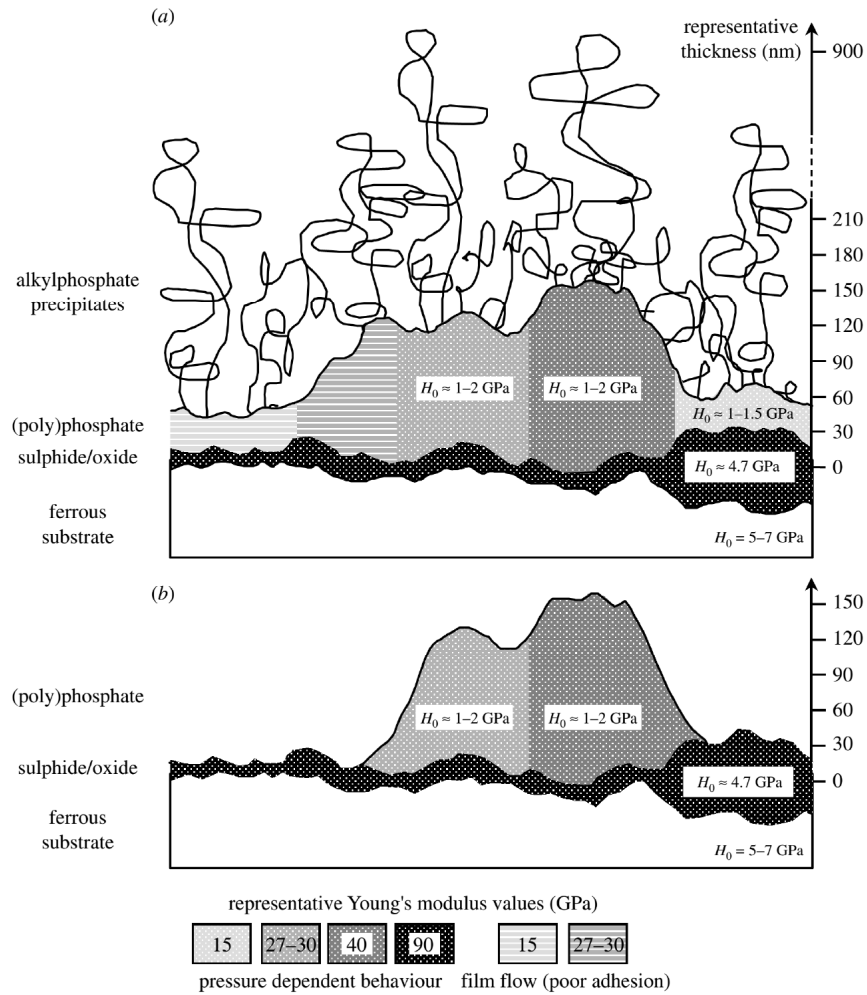


**Figure 3-8 Schematic of multilayer structure of ZDDP (a) before and (b) after washing with solvent (83)**

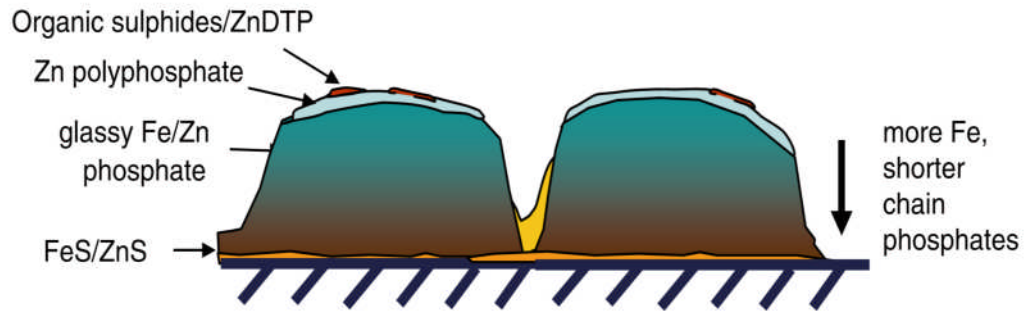


**Figure 3-9 Schematic of the patchy structure of ZDDP tribofilm (62)**

### 3.3.3 Chemistry of ZDDP

The chemical composition of the ZDDP tribofilm in boundary lubrication condition on steel surfaces has been extensively characterized. It is reported that there is a viscous layer of physically adsorbed additive on the top layer of the tribofilm which can be easily removed by means of solvents and washing. Underneath this viscous layer, there is a chemically adsorbed layer of amorphous zinc and iron polyphosphates with different chain lengths (62, 95-97).

It has been reported that the ZDDP tribofilm has a layered structure with different chain lengths at different positions in the layer (95, 97). Shorter chain polyphosphate layers are present at the bottom adjacent to the substrate interlinked with the iron oxide. The top layer is reported to be thinner consisting of mainly longer chain polyphosphates. It is not clearly reported experimentally that an interface is present between the layers and it is most likely to be gradual changes in the structure of the tribofilm.

Crobu *et al.* (95, 98) characterised the surface chemistry of zinc polyphosphates using XPS and Time-of-Flight Secondary-Ion Mass Spectroscopy (ToF-SIMS) by assessing the intensity ratio of bridging oxygen (P-O-P) and non-bridging oxygen (P=O and P-O-M) and. It has been suggested that the chain length of the glassy phosphates in the

tribofilm can be identified by a combined use of bridging oxygen/non-bridging oxygen (BO/NBO) intensity ratio, Zn3s-P2p<sub>3/2</sub> binding energy difference and a modified Auger parameter. This combined method allows characterisation of polyphosphate chain composition ranging from zinc orthophosphate to zinc metaphosphate (See Figure 3-10).

Phosphate Glass	BO/NBO
Metaphosphate	0.48±0.02
Polyphosphate	0.37±0.05
Pyrophosphate	0.20±0.05
Orthophosphate	----

**Figure 3-10 Identification of different composition of zinc polyphosphates (98)**

### 3.3.4 Growth of ZDDP tribofilm

An important aspect in the study of ZDDP tribofilms has been its growth and thickness. The growth of ZDDP tribofilm on contacting surfaces has been subject of several studies (81, 88, 99-103). Almost all of the works report similar observations of ZDDP tribofilm growth on steel surfaces with the reported thickness reaching 50-150 nm. Fujita *et al* (104, 105) studied the growth of ZDDP tribofilm using a Mini Traction Machine and Spacer Layer Interferometry. They investigated the effect of temperature and concentration of both primary and secondary ZDDPs on the growth of the tribofilm on the surface. They concluded that higher temperature leads to faster growth and thicker tribofilms. The same pattern was observed for different concentrations of ZDDP. Higher concentrations result in faster rate of growth. The

experimental results were then used to extract semi-empirical relationships for the growth of the tribofilm.

The tribofilm growth model used in that work was a combined formation and removal model. It was suggested that ZDDP tribofilms are very durable when rubbed in base oil once they are formed. A base oil containing dispersant was found to be essential to remove the tribofilm patches. It was shown that secondary ZDDPs reach to a maximum film thickness very rapidly and then a removal of the tribofilm occurs due to different surface phenomena. They suggested that a combined model of formation and removal can explain such a behaviour. It was hypothesized that the removal process only begins after some time of rubbing. The reason for this is the maximum film thickness reached at the beginning stages of rubbing (104, 105). There was a difference between the growth patterns for primary and secondary ZDDPs. Results revealed that primary ZDDP generally follows a straightforward increase in the thickness while secondary ZDDP grows to a maximum value and then levels out to a steady-state.

Recently, Gosvami *et al* (106) designed an experiment to monitor the growth of the ZDDP tribofilm in a single asperity contact. They used Atomic Force Microscopy (AFM) to generate the tribofilm and monitor the growth *in-situ*. It was reported that temperature and stress play a significant role in the initiation of the tribochemical reactions. They also reported that the tribofilm can form on inert surfaces such as DLCs and did not highlight the effect of substrate on the formation of chemically-reacted tribofilms on surfaces. They have stated that the durability of the tribofilm formed on the surfaces varies with the nature of the surfaces which is in line with the results reported in the literature (91, 92).

Ghanbarzadeh *et al* (107) recently reported a theoretical model with a hypothesis that formation and removal of the tribofilm happen at the same time (107). The hypothesis was based on the experimental observations of removal of the tribofilm and wear of the system even in the presence of fully formed tribofilms (86, 103, 108). The wear hypothesis was then validated against some wear measurement experimental results (109, 110) and has shown good agreement. Testing the model in different conditions suggests that the removal of the tribofilm at different times of the experiment might be different from a fully formed tribofilm and this is in agreement with the experimental reports of (93, 104).

The aim of this study is to investigate the effect of different physical parameters such as temperature and load on the durability of the ZDDP tribofilm. The tribofilm chemical characteristics were also evaluated using XPS. The change in the tribofilm thickness was correlated to the chemistry of the glassy polyphosphates.

### **3.3.5 Effect of water on tribochemistry of ZDDP**

Different additives can be added to lubricants to achieve certain properties. These additives can be viscosity-index improver, anti-wear, friction modifier and extreme pressure additives (12). The properties of additives such as the solubilisation characteristics in oils can be changed by the water contamination. Therefore, desolubilisation of some additives may happen (40). Water contamination can react with oil additives and create destructive and harmful material such as sludge or acid, which make the additives chemically unusable. For instance, some sulfurized additives such as ZDDP can be decomposed by water contamination into the hydrogen sulphide or sulphuric acid which damages bearing surfaces (40).

Rounds (16) studied the effect of free water on the decomposition of ZDDP and the results showed that water seems to accelerate the rate of ZDDP decomposition and

the formation of tribofilm. Therefore, they suggested that the decomposition of ZDDP is due to not only thermal decomposition but also hydrolysis. In contrast, Faut and Wheeler (111) found that for another type of phosphate additives, i.e. Tricresyl Phosphate (TCP), water inhibits the tribofilm formation.

Nedelcu *et al.* (44) studied the effect of water in lubricated sliding and rolling contacts with PAO and ZDDP additive. Three concentrations, i.e. 0.5, 1 and 2 wt. %, of added water were used. The results showed that water affects the decomposition of ZDDP and inhibits the growth of the ZDDP tribofilm. This effect manifests itself in the formation of shorter polyphosphate chains. The authors attributed these effects to the depolymerisation reactions of the long polyphosphate chains and to the increased surface distress in the presence of water.

Likewise, the effect of relative humidity, i.e. 20, 60 and 100% on ZDDP anti-wear performance was assessed by Cen *et al.* (12) in lubricated steel/steel contacts under extreme pressure and pure sliding conditions using ball-on-disc test rig. In addition to the tribological tests at duration of 2 h, they performed tests at shorter times, i.e. 5, 20, 30 and 60 min, to study the variation of water concentration and wear with testing time. Similar to the findings of Nedelcu *et al.* (44) . It was observed that the ZDDP additive inhibits the formation of the protective tribofilm. They also noticed the formation of shorter phosphate chains with increasing the amount of water in oil.

The effect of water on additives seems to be system dependent. Therefore, a detailed systematic study is needed to reveal such discrepancies in the published data. While recent research has increased the understanding on ZDDP tribofilm, the effect of water in oil on tribological performance is still not fully understood. In addition, wear prediction in these systems is still very limited. The current study aims to

experimentally assess the impact of water in oil on tribofilm growth rates with the purpose of developing models capable to predict wear.

### **3.3.6 Summary**

Throughout this chapter the state of the art of different aspects of the composition of ZDDP anti-wear additive was discussed. First and foremost, an overview of ZDDP as antiwear additive was provided. It was shown that the diffusion or adsorption of the ZDDP molecules on the substrate is necessary prior to the formation of any surface films and the tribofilm, unlike thermal films, needs asperity-asperity contact and sliding to be formed on the surface. They form at much lower temperatures than the thermal films and only form on rubbing tracks. All the recent studies confirmed that the concentration of Fe increases towards the substrate whereas Zn concentration decreases. It was also discussed that ZDDP reaction layer formed on the surface has a patchy layered structure of large and small pads.

The mechanical properties of ZDDP anti-wear additives was explored in this chapter. It was found that the mechanical properties of the ZDDP reaction layer vary from the surface to substrate. The tribofilm chain length decreases towards the substrate and the bulk of the tribofilm consists of more short chain polyphosphates. The chemical composition of the ZDDP tribofilm in boundary lubrication condition on steel surfaces has been extensively discussed in literature. It is proposed that there is a viscous layer of physically adsorbed additive on the top layer of the tribofilm which can be easily removed by means of solvents and washing. Under this viscous layer, there is a chemically adsorbed layer of amorphous zinc and iron polyphosphates with different chain lengths. It was shown that the polyphosphate chain composition ranging from zinc orthophosphate to zinc metaphosphate.

## **3.4 Modelling approaches**

### **3.4.1 Introduction**

For more than 50 years, researchers have studied friction and wear as individual sciences but because of the emergence of challenging applications and new technologies, they had to adapt this science to include more parameters with more realistic assumptions. Therefore, the effect of different parameters such as humidity, temperature and the various lubricant properties becomes crucial in reducing the failures and increase the life time of equipment. In the beginning, most of the researchers used simple equations such as Archard equation to calculate wear volume. Nowadays, due to the fact that most tribological systems are exposed to corrosive environment and that makes researchers to study both mechanical wear and chemical wear (112) in conjunction. Considering only the mechanical aspects or only the chemical aspects is insufficient to completely understand many systems like the failure and reliability of offshore wind turbines (113), performance of biological implants (114) and chemical mechanical polishing (115).

It has been reported that mechanical and chemical parameters can affect each other significantly (112) and this interaction is not simply additive. It may be greater than or less than the individual wear processes (mechanical and chemical) depending upon the nature of contact. In the corrosive environment, the total material loss from the surface cannot be calculated from the material loss due to pure wear or pure corrosion (116, 117). Thus, it can be concluded that the synergistic effect between mechanical and electrochemical wear plays a significant role in the tribocorrosion system. Mechanical parameter like friction, wear, deformation and contact geometry can change the electrochemical properties of the tribocorrosion system.



The excess energy at the interface may change the activation energy for reactions, also the mechanical wear may generate fresh metal surfaces, restoring the corrosion potential (118) . On the other hand, electrochemical process decreases the mechanical strength of surface layers which in turn affects tribological performance such as friction, wear and the lubricant performance (112).

### **3.4.2 Modelling of tribocorrosion**

The theoretical approaches used to model the tribocorrosion phenomenon are various. In fact the ways in which these different approaches are categorized is also different. A recent review of the modelling approaches has categorized them to be one of the three: Empirical (119), Fatigue (120) or kinetic (32) models (118). The empirical models are the most straight forward ones but the terms and parameters of the model do not have physical meanings. These are mainly based upon fundamental observations of physical phenomenon. The fatigue models also involve basic kinetics to quantify the crack initiation and growth. The kinetic models on the other hand have quite well rooted basis but require much effort in describing the activation energy for each wear cycle. Thus, among all three, the empirical models are the most relevant in engineering applications.

The above categorization is not quite famous among the tribocorrosion practitioners and researchers. Instead, the following two are considered to be, generally, the two types of models that are in use and in current research nowadays.

### **3.4.3 Electrochemical models**

Electrochemists are interested, mainly, in investigating the repassivation kinetics in tribocorrosion of sliding systems and they try to model the current density during sliding (112). Many electrochemical methods have been used previously to investigate the effect of repassivation kinetics on the sliding conditions (121) .

The film growth kinetics and the ohmic drop have been taken in to consideration in the electrolyte among the wear scar and the reference electrode (122). Synergistic effect among wear and corrosion is responsible for the non-additivity of the chemical and mechanical material loss (116). Regarding the research that have been done so far, local abrasion of passive film may result in an increase in wear rate because corrosion would be increased, hard oxide particle which is originated from the surface due to corrosion can lead to abrasive wear and transferring material from one body to another (123, 124). It can be said that the plastic deformation can be related to the relationship between mechanical wear and tribochemical wear in the tribocorrosion system (125). In 1998, Mischler *et al.* (116) proposed a model which is explained how wear can accelerate corrosion and in this model he considered the effect of load and hardness of the material. The problem with this model is that calculation of repassivation charge was not related to the fundamental kinetics and film growth (122). Two models have been proposed to investigate the repassivation of activated surface in aqueous sliding wear conditions which are surface coverage model and film growth model.

### **3.4.4 Mechanical models**

#### **3.4.4.1 Wear prediction**

Predicting wear is one of the greatest challenges in the tribology. There have been many attempts to predict wear in lubricated systems for different tribological configurations. Evaluating wear in boundary lubrication has been extensively the subject of many studies. There are almost 300 equations for wear/friction in the literature which are for different conditions and material pairs but none of them can fully predict the wear based on first principles including the whole physics of the problem (126, 127). Some examples of these models are Suh delamination theory of

wear (128), Rabinowicz model for abrasive wear (129) and the Archard's wear equation (130, 131).

Wear occurs by different interfacial mechanisms and all these mechanisms can contribute in changes in the topography. It has been widely reported that 3<sup>rd</sup> body abrasive particles play an important role in the wear of the surfaces. The model proposed by Archard (130) was investigated in a wide range of studies, different contact configurations and also different scales. Archard's model was initially developed for sliding in dry conditions and no effect of lubricant or chemistry was involved in the model. By the current understanding of the wear problem and the development of advanced surface analytical techniques, it is clear that the chemical and mechanical properties of the tribofilms play a very important role in the wear behaviour of the tribosystems and should be considered when developing wear models for lubricated contacts. There is therefore a need to see the chemical effects incorporated into any new wear models growing forward.

Some researchers have suggested modifications to the Archard's model. A mathematical model developed by Sullivan (132) describes oxidative wear in boundary lubrication contacts. The model is based on different parameters that together can be assumed as Archard's wear coefficient. Another attempt to investigate the wear in micro contacts is made by Zhang *et al* (133). They used classical wear models to calculate the probability of contact to be covered by physically and chemically adsorbed layers. Flash temperatures, real area of contact and friction force were also calculated by the model. The model suggests that higher lubricant/surface reactivity or substrate hardness enhance the micro-contact behaviour therefore affecting the wear of the system.

In work by Andersson *et al.* (134), a mathematical and chemical model was developed to capture the growth of the tribofilm at a local scale which changes the geometry of contacting surfaces. Archard's wear equation was then used to calculate wear at the asperity scale. They predicted the growth of the tribofilm on the contacting asperities for different surface roughnesses. The same coefficient of wear was considered for tribofilm and substrate which was one of the drawbacks of the model. Another model developed by Bosman *et al.* (135) proposes a numerical formulation for mild wear prediction under boundary lubrication systems. They suggest that chemically-reacted layers are the main mechanisms responsible for protecting boundary lubricating systems and when these layers are worn off, the system will restore the balance and the substrate will react with the oil to produce a tribofilm. The effect of tribofilm was then considered in the model and the amount of substrate atoms in the depth of the tribofilm was reported to be the reason for the wear of the system in the presence of the tribofilm.

Recently, a wear model was proposed by Ghanbarzadeh *et al.* (107) which considers the growth of ZDDP tribofilm on the contact asperities in boundary lubrication systems. The model takes into account the effect of ZDDP tribofilm in changing Archard's wear coefficient. The analytical results were validated with experiments in rolling-sliding conditions reported in another work (109). The model considers the partial removal of the tribofilm and relates it to the wear of the substrate in the case of ZDDP on steel surfaces. The tribochemistry model was an important part of the whole semi-deterministic model because it defines the behaviour of tribofilm growth on the contacting asperities.

#### **3.4.4.2 Archard wear equation**

During the early stages (1950 to 1956) many researchers tried to study wear of materials and developed simplified theories. Many experiments were done with different materials to find the relation between wear and different parameters such as load, hardness of material and sliding velocity. The deformation of the interacting surface showed that real area of the contact which is responsible for wear is much more less than the apparent area of the contacting surfaces. It was postulated that the wear rate is related to the small region of the apparent area which is known as hot spots (136). But the breakthrough came when Archard proposed his wear theory whereby wear rate is independent of the apparent area of the contacting surface (130). Although Holm (136) reached the same conclusion earlier but the incomplete explanation of results by Holm is the main reason why Archard is mainly attributed for this idea. Some work was done between 1953 and 1955 by Hughes and Krushchov to investigate the effect of hardness of material on wear rate. They proposed that wear rate is inversely proportional to hardness of material (19).

Archard wear equation is used to calculate wear volume on the macro scale (20). A large numbers of experiment were done in 1956 by Archard to assess the effect of load, hardness and sliding distance on wear rate and he tried to find an equation to relate wear to these parameters. The experiments were done under dry sliding by using two pin-and-ring machines (19). He calculated wear by measuring wear scar at low wear rate and for high wear rate he used weighting method to measure wear. These experiments were done by using different combination of materials in unlubricated conditions. Loads between 50 g to 10 kg were applied in the tests. Based on these experiments, he proposed that in all the experiments and different wear mechanisms, wear is independent of the apparent area and it directly proportional to the applied

load for most of the experiment and there was a small deviation in terms of load for some experiments. He observed two forms of wear which are mild and severe wear in the experiments due to the different loads (19). Equation 3-2 is the form of relation that Archard developed.

$$V = K \frac{WL}{H} \quad 3-2$$

In this equation V is the wear volume, W is the normal load, L is the sliding distance, H is the hardness of the material and K is the Archard wear coefficient.

Although extremely powerful yet the Archard equation has some limitations. The most important one is that it has been developed for dry contact conditions. So much work has been done to modify the Archard wear equation and adapt it to new conditions. Archard assumed that wear is independent of apparent area which means that he did not consider the effect of surface topography or surface roughness. There effect of transient changes in surface roughness is missing as well (20).

Archard equation was derived from the experiments which were done under unlubricated sliding contact and it cannot be used for the lubricated system. Archard equation considers just single material properties which is hardness of the material that it is not sufficient even for unlubricated sliding contacts and it can be seen from some experimental work that sometimes wear does not relate linearly to load and sliding distance (21, 22). These are the main gaps in the Archard equation which attract researchers to develop Archard equation to adapt it to the new conditions. In the following pages we will try to address some of the case studies that will address the ways in which people have tried to modify the Archard wear equation.

### 3.4.4.3 Modification of Archard wear equation to predict wear in mixed lubricated contact

The Archard equation can just be used for dry sliding conditions. In a recent study (39), a methodology has been proposed to adapt Archard equation to the mixed lubricated contacts. Two major modifications were made: they proposed that by considering fractional film defect to modify Archard wear coefficient and the load-sharing concept to consider the lubricant (137), modified Archard equation can be implemented for mix lubricated contacts (39).

#### 3.4.4.3.1 Fractional film defect

In the lubricated system, oil molecules exist between the interacting surfaces can reduce wear coefficient and wear rate compared with the unlubricated system. In this model by considering fractional film coefficient  $\Psi$  and multiply it by dry wear coefficient ,modified Archard wear coefficient for mixed lubricated system can be calculated (137). Fractional film defect defined as a probability in which an asperity comes into contact with another asperity in the region which is not covered by lubricant molecules (39). Thermal desorption theory is used to calculate  $\Psi$ . Equation 3-3 was suggested by Kingsbury and Rowe (138, 139). It indicates fractional film defect.

$$\Psi = 1 - e^{-\left\{ \left[ \frac{a_x}{u_s t_0} e^{-\frac{E_a}{R_g T_s}} \right] \right\}} \quad 3-3$$

In the equation  $u_s$  is the sliding velocity,  $a_x$  is the diameter of the area with an adsorbed molecule,  $t_0$  is the fundamental time of vibration of the molecule in the adsorbed state,  $E_a$  represents the heat of adsorption of the lubricant on the surface,  $R_g$  is the gas constant and  $T_s$  symbolizes the absolute temperature of the surface. A thermal model

developed by Akbarzadeh and Khonsari (140) is used to calculate the surface temperature.

### 3.4.4.3.2 Fluid and asperities load sharing

In mixed lubrication contacts, it is believed that apart of load is carried by asperities and a part of the load is carried by fluid. This load sharing concept was for the first time introduced by Johnson and Greenwood (141) The load is carried by asperities is considered to be mainly responsible for wear in mixed lubrication regime. They proposed that the total load can be estimated by using equation 3-4:

$$W = W_f + W_a \quad 3-4$$

Where the first one is the load carried by fluid and the second one is the load carried by asperity. The total interface pressure is divided in to two parts, asperity pressure and fluid pressure:

$$P = P_a + P_f \quad 3-5$$

Regarding the load sharing ratios (scaling factors) are presented in equations 3-6 and 3-7:

$$\gamma_1 = \frac{W}{W_f} = \frac{P}{P_f} \quad 3-6$$

$$\gamma_2 = \frac{W}{W_a} = \frac{P}{P_a} \quad 3-7$$

Equation 3-8 shows the relationship between scaling factors:

$$\frac{1}{\gamma_1} + \frac{1}{\gamma_2} = 1 \quad 3-8$$

By substituting load sharing and fractional film defect into Archard equation :



$$V = K\psi \frac{W_a S}{H} = \frac{\left(\frac{K\psi}{\gamma_2}\right) WS}{H} = K_1 \frac{WS}{H} \quad 3-9$$

$K_1$  can be considered as the wear coefficient for the mixed lubrication system. These parameters  $K$ ,  $\Psi$  and  $\gamma_2$  have to be calculated in modified archard equation.

#### 3.4.4.3 Determination of the K

$K$  can be calculated experimentally by conducting pin-on-disc experiments. Furthermore, values for  $K$  in different contacting surfaces can be found in literature (129). But in this study authors measured  $K$  based on the fatigue theory of adhesive wear by using a method that they developed previously (142). By using fatigue theory  $K$  can be calculated from equation 3-10:

$$K = \frac{1}{N} \quad 3-10$$

$N$  is the total number of cycle for the asperity to break which can be calculated from the equation developed by authors. A thermodynamic framework model proposed by Bhattacharya and Ellingwood (143) can be used to calculate the number of cycle needed for the asperity to break and then from the equation 3-10 , wear coefficient can be calculated mathematically. Equation 3-11 can give  $D_i$ , the damage in the  $i$ th cycle and once the damage per cycle reaches the critical value  $D_c$  after  $N$  cycle, this shows the number of cycle required for the asperities to break.

$$D_i = 1 - (1_{i-1})F_i \quad \text{if } S_{max} > S_e \quad 3-11$$

$$F_i = \frac{\left[ \left(1 + \frac{1}{m}\right)^{-1} \Delta \varepsilon_{oi}^{1+\frac{1}{M}} - \Delta \varepsilon_{p1i}^{\frac{1}{M}} \Delta \varepsilon_{oi} + C_i \right]}{\left[ \left(1 + \frac{1}{m}\right)^{-1} \Delta \varepsilon_{pmi}^{1+\frac{1}{M}} - \Delta \varepsilon_{p1i}^{\frac{1}{M}} \Delta \varepsilon_{pmi} + C_i \right]}$$

And

$$C_i = \frac{3S_f}{4K_m} - \frac{\Delta\epsilon_{0i}^{1+\frac{1}{M}}}{1+\frac{1}{M}} + \Delta\epsilon_{p1i}^{\frac{1}{M}} \Delta\epsilon_{0i} \quad \text{otherwise if } S_{max} < S_e$$

$$D_i = D_{i-1}$$

#### 3.4.4.3.4 Calculating $\delta_2$

In this study, as mentioned before, the load sharing concept is considered to adapt Archard equation to the mixed lubrication system (141).

#### 3.4.4.3.5 Fluid part

Authors used Pan and Hamrock's (144) central film thickness equation instead of Dowson-Higginsons (1962) and Ertel-Grubin (1949) because it is more accurate and it can be used for high load. They proposed modified equation 3-12 to calculate the load carried by fluid part.

$$\bar{h}_c = 2.922 \left(\frac{\bar{W}}{2}\right)^{-0.166} \left(\frac{\bar{U}}{2}\right)^{0.692} (2G)^{0.47} \gamma_1^{0.222} \quad 3-12$$

Where  $h_c$  is the central film thickness and the dimensionless parameters defined as:

$$\bar{h}_c = \frac{h_c}{R} \quad \bar{W} = \frac{W}{lE'R} \quad \bar{U} = \frac{\mu_0 u_r}{E'R} \quad G = \alpha E' \quad 3-13$$

Where  $R$  is the effective radius curvature,  $l$  is the length of the contact,  $E$  is the modulus of elasticity,  $\mu_0$  is the lubricant viscosity  $u_r$  is the entrainment speed and  $\alpha$  is the pressure viscosity index.

### 3.4.4.3.6 Asperity part

To calculate the load carried by the asperity, workers proposed the combination of the smooth EHL and dry rough contact model to find the part of load carried by asperity (39, 145-147). The equation 3-14 which has the load carried by asperity as an unknown parameter ( $\delta_2$ ) is proposed to calculate  $\delta_2$ .

$$\frac{1}{\gamma_2 \sqrt{1 + (1.1188 \bar{n}^{-0.1531} \bar{\beta}^{-0.1203} \bar{\sigma}^{0.6304} \bar{W}^{-0.7161} \Omega^{-0.1423} \gamma_2^{-0.2954})^{1.1396}}} \quad 3-14$$

$$= \xi \left( \sqrt{\frac{\pi}{W}} \right) \left[ \phi_{ke} (2.922 \left( \frac{\bar{W}}{2} \right)^{-0.166} \bar{U}^{0.692} (2G)^{0.47} \left( \frac{\gamma_2}{(\gamma_2 - 1)} \right)^{0.222} \right]$$

By calculating  $\delta$ ,  $\Psi$  and  $K$  and substituting these values into the Modified Archard equation, wear for the mixed lubricated contact can be calculated.

Both the above cases discussed have limitations, especially when discussing the tribocorrosion systems. Baheshti and Khonsari (39) verified their model against experimental results from Wu and Cheng (148). The experiments were done by Wu and Cheng at the rolling speed and maximum contact pressure of 1.83 m/s and 2 GPa, respectively and the slide to roll ratio was varied from pure rolling (SRR = 0.001) to pure sliding (SRR = 2). But the model cannot predict wear at high slide to roll ratio accurately because they assumed that the central film thickness is constant for the entire area which is not the case in high slide to roll ratio systems. Furthermore, this model cannot be used for tribocorrosion conditions due to the fact that it has been developed for simple tribological systems with no humidity or corrosion.

Wu and Cheng (148) used small scale two disc machine to be able to get different slide to roll ratio to verify their model. They used mineral oil with the viscosity of 37.5 cSt at 35 °C. Their model shows a good agreement with the experimental data

they obtained. They considered the effect of temperature as well. The main limitations of this model were that it could not account for the effect of viscosity of the oil, Humidity or moisture in the oil and corrosion apart from the fact that their experimental set up was not much reliable.

### **3.4.5 Tribochemical wear model**

The mode of wear in which chemical reactions due to rubbing (known as tribochemical reactions) play an important role, is called tribochemical wear. In this condition, the chemistry of lubricant additives and surfaces determine the severity of the wear. In the recent years there have been attempts in incorporating such wear mechanisms in prediction of tribosystem wear and friction. The important components of such models have been explained briefly in this section.

#### **3.4.5.1 Contact mechanics**

There have been many attempts at simulating the contact of rough surfaces in contact mechanics (107, 149-156). The contact mechanics model developed by Tian and Bhushan (157) which considers the complementary potential energy will be used in this work. By applying the Boussinesq method and relating the contact pressures to surface deformations, the problem would be to solve the contact mechanics only for finding contact pressures at each node and then the related contact deformations can be calculated. For this model, surfaces should be discretised into small nodes and it is assumed that the nodes are small enough and the contact pressure is constant at each node.

The problem is to minimize the complementary potential energy as follows:

$$V^* = \frac{1}{2} \iint p \bar{u}_z dx dy - \iint p \bar{u}_z^* dx dy \quad 3-15$$

Where  $p$  is the contact pressure and  $V^*$ ,  $\overline{u_z}$  and  $\overline{u_z^*}$  are complementary potential energy, surface deformation and prescribed displacement respectively.

The Boussinesq solution for relating contact pressure and surface deformation usually considers only normal forces and the solution is:

$$\mathbf{u}(x_1, x_2) = \frac{1}{\pi E^*} \iint_{-\infty}^{\infty} \frac{p(s_1, s_2)}{\sqrt{(x_1 - s_1)^2 + (x_2 - s_2)^2}} ds_1 ds_2 \quad 3-16$$

In which  $E^*$  is the composite elastic modulus of two surfaces. The contact mechanics model has been discussed in detail in the Ref (107, 156).

It is assumed that the material acts as a half space. It means that applying a load on one node of the surface consequently deforms all other nodes on the surface based on the Boussinesq approximation. This model encompasses several limitations. Firstly, surfaces has linear elastic behaviour. Secondly, material faces pure plasticity while it reaches the hardness threshold. Thirdly, the frictionless contact mechanics is used in this model.

### 3.4.5.2 Tribofilm development

Friction is an irreversible process due to energy dissipation at interfaces which is a non-equilibrium process and should be studied using non-equilibrium thermodynamics (156, 158-160).

Many results show that not only the flash temperature but also the entropy changes at interfaces are very important in tribochemical reactions. Hence the tribochemical reaction and the tribochemical film growth models should consider entropy and the factors affecting the entropy of the system. The concept of thermodynamics in the tribosystems has been the subject of many recent studies. There are some attempts to

model tribofilm growth based on temperature dependency of tribochemical reactions (161) and also diffusion-reaction mechanisms (162). Attempts were made to relate tribochemical reactions to non-equilibrium thermodynamics and changes in the entropy of the system.

It has been reported that the mechanical stress can play a significant role in inducing the tribochemical reactions. It is assumed that tribochemical reactions follow reaction theory but these reactions are activated not only by temperature but also by mechanical rubbing (163, 164). The current model is developed in a way that considers flash temperature as a parameter responsible for the formation but more importantly is the term  $x_{tribo}$  which is responsible for the mechanical activation of chemical compounds. The discussion on the tribofilm kinetics model can be found in (107, 156).

Ghanbarzadeh *et al* (107, 109) suggested that the tribofilm is being removed and formed at the same time. The process of formation and removal of the tribofilm in combination, will lead to growth of the film on the substrate. It was also reported by Lin *et al* (94) that the tribofilm is formed and removed at the same time and the balance between the rate of formation and removal explains the behaviour of the system. Removal plays an important role in the behaviour of tribosystems and the current model offers an insight into the removal processes and how these relate to wear of the system. Assuming that tribofilm removal also follows an exponential form, equation 3-17 is to

$$h = h_{max} \left( 1 - e^{\left( -\frac{k_1 T}{h'} x_{tribo} t \right)} \right) - C_3 (1 - e^{-C_4 t}) \quad 3-17$$

In which  $C_3$  and  $C_4$  are removal constants. These removal terms were calibrated with experimental results (156, 165).

### 3.4.5.3 Wear modelling

The wear model proposed in (107, 156) is based on the conventional Archard wear formulation; the local wear depth of each point of the surface is calculated using:

$$\Delta h(x, y) = \frac{K}{H} \cdot P(x, y) \cdot \Delta t \cdot v \quad 3-18$$

In which  $H$ ,  $K$ ,  $P$  and  $v$  are the material hardness, dimensionless Archard's coefficient, local contact pressure and sliding speed respectively, and  $\Delta t$  is the time step in which contact occurs.

The wear coefficient is assumed to vary across the thickness of the tribofilm. It is assumed that in the areas where a tribofilm is formed, the coefficient of wear is less than in the areas where a tribofilm is not formed. The coefficient of wear is assumed to change linearly with tribofilm height. Assuming that the coefficient of wear is at its maximum for steel-steel contact and at its minimum when the tribofilm has its maximum thickness, the equation for calculating coefficient of wear is as follows:

$$CoW_{tr} = CoW_{steel} - (CoW_{steel} - CoW_{min}) \cdot \frac{h}{h_{max}} \quad 3-19$$

$CoW_{tr}$  is the coefficient of wear for tribofilm with thickness  $h$ .

$CoW_{steel}$ ,  $CoW_{min}$  and  $h_{max}$  are coefficient of wear for steel and coefficient of wear corresponding to maximum ZDDP tribofilm thickness and maximum film thickness respectively (107, 156).

The wear modelled in this work is considered to be mild wear, which is the case for thick tribofilms. It was reported experimentally (62, 107, 108, 156, 166) that, even in the areas where the tribofilm is fully formed, wear is occurring. It can be interpreted as partial removal of the tribofilm and at the same time formation of the film to restore the balance. Therefore formation and removal of the tribofilm will lead to wear of the substrate (167), however this wear is much less than the wear resulting from solid-solid interactions. Studies show that the concentration of substrate atoms decreases towards the top of the tribofilm produced by ZDDP (167, 168) on steel. If material detaches from the tribofilm due to the contact, some amount of the substrate atoms are removed from the surface.

This decrease in the atomic concentration of the substrate as the distance from the substrate/tribofilm interface increases supports the fact that less wear of the substrate occurs if a thicker tribofilm exists. This mechanism was reported by Bosman *et al.* (167), who considered the volumetric percentage of Fe over the depth of the tribofilm and assumed lower concentration in upper layers of the tribofilm. It can be seen in the Ref (107) that the tribofilm can be removed as a result of the severe contact of the asperities and in this case a limited number of the substrate atoms present in the uppermost part of the tribofilm are detached from the surface.

At the same time, more substrate atoms diffuse into the tribofilm and move towards the upper parts of the film to restore the chemical balance. This movement can be due to different mechanisms as explained in the introduction section. Replenishment of the tribofilm then might occur due to different surface phenomena including the tribochemical reactions and mechanical mixing due to combined effects of material removal and shear stress.



### 3.5 Conclusion

This chapter discusses the state-of-the-art of the effect of water, tribochemistry and tribocorrosion on the tribological behaviour of sliding and rolling contacts and an overview of the state-of-the-art of different aspects concerning ZDDP reaction layer formed on the surface.

The presence of water in the lubricated tribosystems particularly in bearing applications can cause corrosion, hydrogen embrittlement, oil oxidation and shorter fatigue life. Nevertheless, there is a discrepancy in the published data regarding the effect of water on friction, wear, viscosity of the lubricant and the decomposition of ZDDP additive to form a protective tribofilm.

Even though the effect of water seems to be system dependent, the different ways of reporting experimental data have an adverse contribution. It was found that the effect of water seems to be strongly dependent on the exact amount of water in oil rather than the relative humidity value. This suggests that it is not sufficient to report only the relative humidity condition but the exact amount of water in oil is required as well.

Hence, it can be concluded that a detailed systematic study is needed to reveal such discrepancies in the published data.

On the basis of all above discussion regarding different models, we can conclude some important ideas and clarify the direction of our project:

1. The electrochemical methods and techniques for the tribocorrosion phenomenon yet are all based on aqueous environment and no lubricant. This is mainly because there has been no model yet that is capable of handling the tribocorrosion systems especially when water is present in oil.

2. The aim is to develop a model and to observe the effect of water and humidity on tribochemistry wear. Our approach will be to perform a series of experiments that would give the general behaviour of the tribofilm growth and its effect on wear performance. This will lead towards a semi-deterministic model using two different approaches.
3. Once this semi-deterministic model is achieved, this equation will be used along with the enormous amount of experimental data to tune the Archard wear coefficient to account for the effect of water. This will give the modified Archard's wear equation for the tribological systems.

## **Chapter 4. Experimental Procedures**

### **4.1 Introduction**

The experimental work in this project is divided into four parts, i.e. effect of water experiments, effect of humidity tests, experiments to validate the semi-deterministic model developed discussed in modelling part and durability of the tribofilm experiments. For sliding-rolling condition, Mini Traction Machine (MTM) will be used to investigate the effect of different parameters, e.g. temperature, humidity, lubricant and on wear, tribofilm characteristics and durability of the tribofilm. A humidity chamber was designed for MTM SLIM for the first time in this work to control the humidity during the experiments.

This chapter discusses the materials and methods that will be used in this study. The chapter consists of nine sections. Section 4.1 gives a general overview of the chapter. Section 4.2 discusses the characterization of bulk oil. In this section, water concentration will be discussed. The third section discusses the test rig was used for this study. Section 4.4 discusses the water effect experimental procedure. Section 4.5 discusses the humidity experimental procedure. The fifth section focuses on the test conditions and material properties of the experiments applied for the validation of the model (Section 4.6). Section 4.7 presented the experimental procedure and methodology for the investigation of durability of the tribofilm. The seventh section presents chemical and surface analysis techniques to discern the composition of tribofilm. Section eight, the wear measurement methodology and sample preparation discussed. The last section provides a summary of the chapter.

## 4.2 Bulk oil characterization

### 4.2.1 Water concentration measurements

Coulometric Karl Fischer Titration was used to measure water concentration before and after each test, which has an accuracy of  $\pm 0.01$ . It is worth mentioning that this method can be used to measure water concentration in the oil but it cannot determine whether the water is free or dissolved.

## 4.3 Test rig

A Mini Traction Machine (MTM, *PCS Instruments UK*) (See Figure 4-1) is used to assess the effect of water on wear under rolling and sliding conditions. One of the key points in using MTM is that slide-to-roll ratio (SRR) can be changed in the experiments and it is possible to run the experiment in the wide range of slide to roll ratio ( $0 < \text{SRR} < 5$ ) (169). SRR is defined as the following:

$$\text{SRR} = \frac{U_A - U_B}{\left(\frac{U_A + U_B}{2}\right)} \quad 4-1$$

In which  $U_A$  and  $U_B$  are the speed of surfaces A and B respectively. The SRR is the ratio of the sliding and the entrainment speeds.

In the standard configuration the test specimens are a 19.05 mm (3/4 inch) steel ball and a 46 mm diameter steel disc. The ball is loaded against the face of the disc and the ball and disc are driven independently to create a mixed rolling and sliding contact. The frictional force between the ball and disc is monitored by a force transducer. The applied load and the lubricant temperature are monitored by sensors.



**Figure 4-1 Mini Traction Machine (MTM)**

#### **4.3.1 Spacer Layer Interferometry Method (SLIM)**

Spacer Layer Interferometry Method (SLIM) was used to measure tribofilm thickness *in-situ* (170). The glass disc is coated with a thin layer of silicon oxide which has a semi-reflective layer of chromium on top. The contact of the ball with the glass is shined by white light through the microscope and the coated glass. Part of the light is returned back from the semi-reflective chromium layer on top of the coated glass and other part goes through the silicon oxide layer and tribofilm formed on the surface and is reflected back from the steel ball. These light paths are captured by RGB colour camera and it can be analysed by the software to evaluate the tribofilm thickness during the experiments. This method is capable of measuring the film thickness of any reaction layer as they are being formed on the surface (See Figure 4-2).

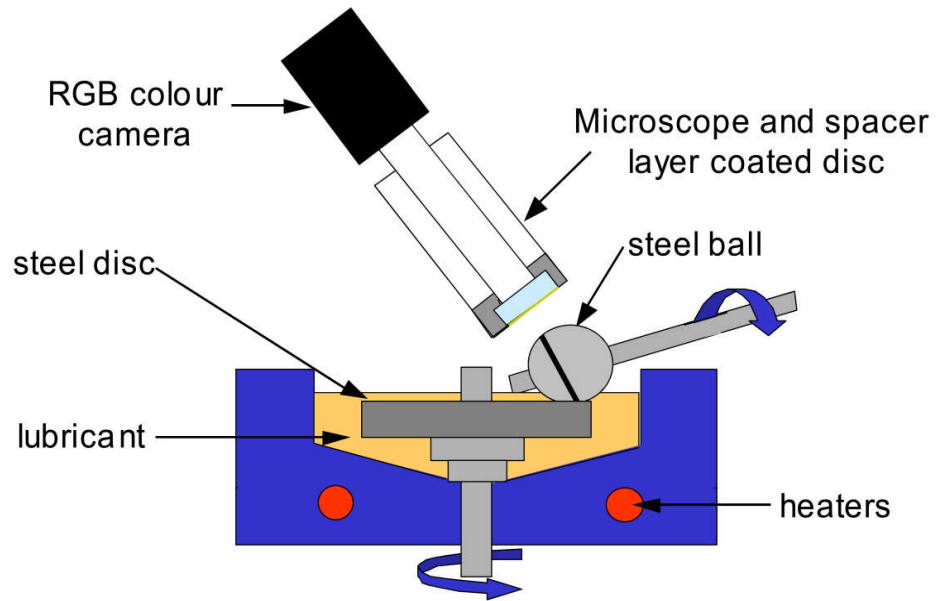


**Figure 4-2 MTM and the Spacer Layer Interferometry configuration**

## **4.4 Effect of water experiments**

### **4.4.1 Materials and test conditions**

In this study the balls and disc used were both of AISI 52100 steel with hardness of 6 GPa. New balls and discs were used for each experiment. They were cleaned up before each test by immersing in isopropanol and petroleum ether in an ultrasonic bath for 20 minutes. All the experiments were conducted at an applied load of 60 N. According to the diameter of the ball which is 19 mm, the maximum Hertzian contact pressure of 1.2 GPa was calculated. The material properties are shown in the Table 4-1. Experiments were carefully designed to study wear in boundary-lubricated contacts at different temperatures, water concentration. A small entrainment speed was chosen for this purpose. The working conditions and the corresponding  $\lambda$  ratios are reported in Table 4-2. Water and oil were mixed at four different levels of water concentration in the ultrasonic bath for 5 minutes.

**Table 4-1 Material properties**

<b>Material properties</b>	<b>Value</b>
Hardness (Ball/Disc) (GPa)	6
Elastic modulus (Ball/Disc) (GPa)	210
Ball surface roughness ( $R_a$ )	20 nm
Disc surface roughness ( $R_a$ )	130 nm

**Table 4-2 Experimental working conditions**

<b>Parameters</b>	<b>Value</b>
Maximum contact pressure (GPa)	1.2
Temperature (°C)	80,100
Water contents (wt%)	0%, 0.5%, 1.5%, 3%
Entrainment speed ( $\frac{m}{s}$ )	0.1
SRR	5%
Test duration (min)	120
$\lambda$ ratio	0.04
Oil used	PAO+ZDDP
Dimensions (mm)	Ball = 19.05 Disc = 46

#### 4.4.2 Tested lubricants

In this study, PAO+ZDDP and PAO+ ZDDP+water were used. Water and oil were mixed in ultrasonic bath for 5 minutes to have four different concentrations of water as mentioned in Table 4-3. PAO+ZDDP+water shows an emulsion state (free water) at room temperature but at 80°C and 100°C the water seems to be dissolved. It is in agreement with this concept that higher temperature leads to the higher saturation point and likewise, there is no free water after each tribological test.

**Table 4-3 Lubricants**

<b>Details</b>	<b>Designation</b>
PAO+ZDDP(0.08 mass% phosphorus)	PAO+ZDDP
PAO+ZDDP (0.08 mass% phosphorus) + (0.5 mass %) Distilled water	PAO+ZDDP+water (0.5)
PAO+ZDDP (0.08 mass% phosphorus) + (1.5 mass %) Distilled water	PAO+ZDDP+water (1.5)
PAO+ZDDP (0.08 mass% phosphorus) + (3 mass %) Distilled water	PAO+ZDDP+water (3)

#### 4.4.3 Experimental approach

The experimental part of this study can be split into two. All tribological experiments were carried out by MTM to simulate rolling/sliding conditions in boundary



lubrication with four different water concentration values. The tribofilm thickness was measured using Spacer Layer Interferometry to evaluate the tribofilm formation in-situ. Finally the tribofilm was removed from the samples and wear was measured using White Light Interferometry. The sub-sets of tribological experiments are:

- I. Experiments at 80°C for different levels of water concentration to investigate the effect of water on tribofilm formation and removal and tribological performance
- II. Experiments at 100°C for different water concentration values to study the effect of water on tribological performance and tribofilm formation and removal

## **4.5 Effect of humidity experiments**

### **4.5.1 Humidity control system**

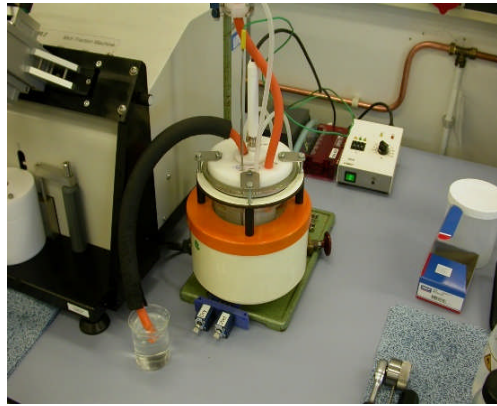
To evaluate the effect of different levels of relative humidity on tribological performance and tribofilm characteristics, a humidity control system was designed and integrated to the MTM SLIM for the first time in this study. This system is capable of producing continuous steady humidity to expose the lubricant in the tribological experiment to a humid environment. To simulate rolling/sliding conditions and monitor tribofilm evolution during the test under controlled humid environment, the humidity system is mounted on an MTM/SLIM configuration. The humidifier is connected to the PC by a controller system and relative humidity is monitored by LUBCHECK program at a time interval of one second. The humidity could be varied between 0%-100% ( $\pm 1\%$ ). The humidity control system consists of different parts described as followings (Figure 4-3 and Figure 4-4):

- 1) Heater: to heat up the water up to the desired temperature. The advantage of using heated water to produce humid air is to avoid the presence of water droplets in the humid air
- 2) Insulation part: to isolate the chamber from the environment to keep the temperature and humidity constant during the experiment
- 3) Humidity sensor : to control and monitor humidity during the test
- 4) Thermocouple : to control the temperature of the water during the experiment
- 5) Dry air and wet air valves: to apply the desired level of humidity in the range of 0% (dry air) to 100%
- 6) Bubbler : to produce bubble in the water which facilitates generating the humid air

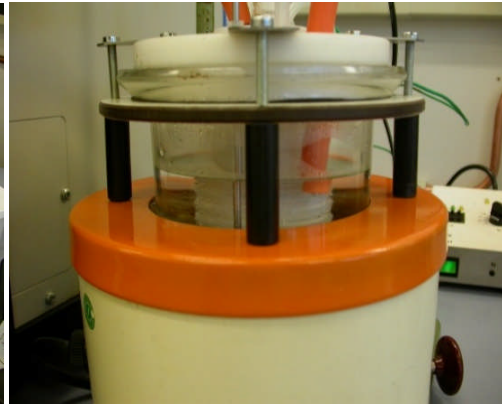
The humid air is transferred from the chamber to the MTM oil bath using a heated tube. The tube is heated to the same temperature as the oil bath and the chamber to avoid any condensation of the water in the system.

#### **4.5.2 Calibration**

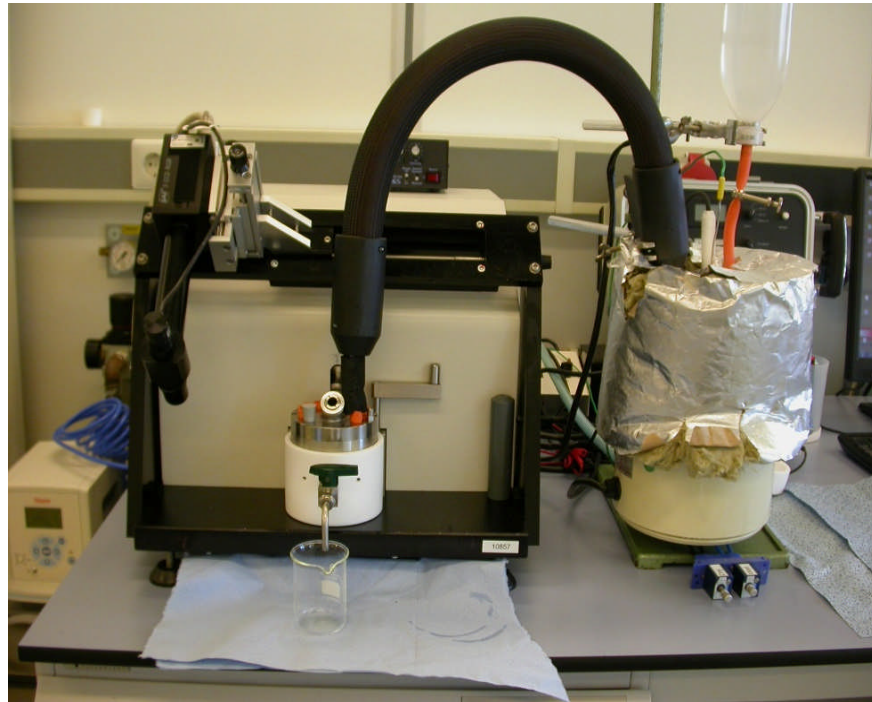
To calibrate the humidity control system, a calibration kit was used. The humidity calibration kit provides an accurate method to calibrate the humidity sensor by using two different salt solutions. It includes lithium chloride (LiCl) to produce 11.3 % relative humidity at 25°C and sodium chloride (NaCl) to produce 75.3 % relative humidity at 25°C. The kit has two bottles which are sodium chloride and lithium chloride and two fitting caps. Distilled water was used to prepare the salt solutions. Then, humidity sensor must be placed into the bottle close to the solution. The sensor should be isolated from the environment to measure the relative humidity of the salt accurately. In addition, the sensor should be left about half an hour to be stabilized above the solution then the humidity value can be read afterwards.



(a)



(b)



(c)

**Figure 4-3 Humidity control system (a) and (b) humidity chamber c) MTM**

**SLIM integrated to the humidity control system**

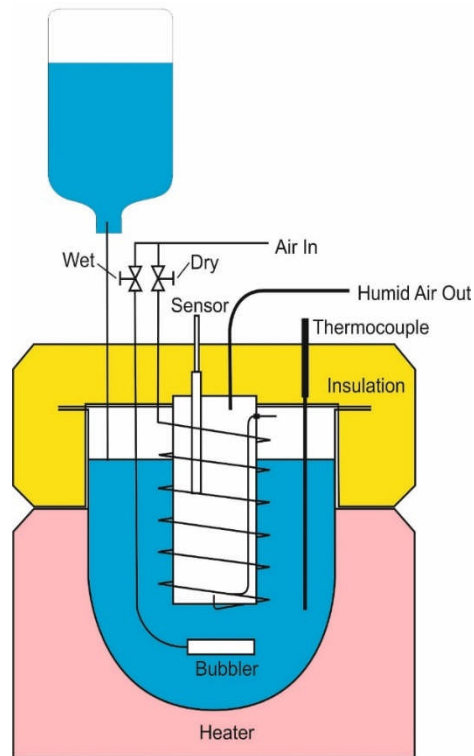


**Figure 4-4 Schematic representative of humidity control system**

### 4.5.3 Materials and test conditions

In this study the balls and discs used were both of AISI 52100 steel with hardness of 6 GPa. A new ball and disc were used for each experiment. They were cleaned up before each test by immersing in Isopropanol and petroleum ether in ultrasonic bath for 20 minutes. All the experiments were conducted at applied load of 60 N. According to the diameter of the ball which is 19 mm, the maximum Hertzian contact pressure of 1.2 GPa was calculated. The materials used in the experiments are shown in the Table 4-1. Experiments were carefully designed to study wear in boundary lubricated contacts at different temperatures, different levels of relative humidity and a small entrainment speed was chosen for this purpose. The working conditions and the corresponding  $\lambda$  ratios are reported in Table 4-4. PAO+ZDDP was used to carry out the experiments (See Table 4-5).

**Table 4-4 Experimental working conditions**

<b>Parameters</b>	<b>Value</b>
Maximum contact pressure (GPa)	1.2
Temperature (°C)	80, 98
Relative humidity (%)	0, 20, 30, 40, 50, 60, 70, 80, 95
Entrainment speed ( $\frac{m}{s}$ )	0.1
SRR	5%
Test duration (min)	120
$\lambda$ ratio	0.04
Oil used	PAO+ZDDP
Dimensions (mm)	Ball = 19.05 / Disc = 46

**Table 4-5 Lubricant properties**

<b>Details</b>	<b>Designation</b>
PAO+ZDDP(0.08 mass% phosphorus)	PAO+ZDDP

#### **4.5.4 Experimental approach**

All the tribological tests were conducted by MTM SLIM integrated to the humidity control system to simulate rolling-sliding conditions in boundary lubricated system. One of the key aspects in this study is the use of continues steady humidity control system which provides lubricant exposed to the humid environment. In this system,

water can be absorbed from the air by lubricant during the experiments. The humidity level was monitored to be constant during the experiment. Each test was carried out two times to check the reproducibility of the results and the range of data are plotted in the graphs.

The reaction layer thickness was measured by Spacer Layer Interferometry Method to evaluate tribofilm thickness in-situ at different levels of humidity.

- I. Experiments at 80 °C for different levels of humidity to investigate the effect of humidity on tribofilm characteristics and tribological performance
- II. Experiments at 98 °C for different levels of humidity to study the effect of humidity on tribological performance and tribofilm characteristics

## **4.6 Validation of the model experiments**

### **4.6.1 Materials and test conditions**

The material used in this work was AISI 52100 steel for both ball and disc with a hardness of 6 GPa. The balls and discs are carefully cleaned by immersing in Isopropanol and petroleum ether before starting the experiments. All the experiments were conducted at an applied load of 60 N which corresponds to the maximum Hertzian pressure of 1.15 GPa. The materials used in the experiments are shown in Table 4-6.

Experiments were carefully designed to study wear in boundary lubricated contact at different ZDDP concentrations and temperatures, and a small entrainment speed was chosen for this purpose. This experimental matrix is chosen to produce several different growth behaviours of ZDDP tribofilm on steel surfaces and at the same time to be able to measure wear at different times corresponding to those growth behaviours. The lubricating oil is selected to be Poly- $\alpha$ -Olefin (PAO) with 0.5% and

1% wt ZDDP as antiwear additive. The working conditions and the corresponding  $\lambda$  ratios are reported in Table 4-7.

**Table 4-6 Material properties**

<b>Material properties</b>	<b>Value</b>
Hardness (GPa)	6
Elastic modulus (GPa)	210
Ball surface roughness (nm)	20
Disc surface roughness (nm)	130

**Table 4-7 Working parameters**

<b>Parameters</b>	<b>Value</b>
Maximum contact pressures (GPa)	1.15
Temperature (°C)	60,80,100
Entrainment speed ( $\frac{m}{s}$ )	0.1
SRR	5%
Test durations (min)	30, 45, 120
$\lambda$ ratios	Around 0.04
Oil used	PAO+0.5% wt ZDDP PAO+1% wt ZDDP

## 4.7 Durability of the tribofilm

### 4.7.1 Materials and test conditions

In this study balls and discs were both made from AISI 52100 steel with hardness of 6 GPa. New balls and discs were used for each experiment. They were cleaned before each test by immersing in isopropanol and petroleum ether in an ultrasonic bath for 20 minutes. The materials used in the experiments are shown in Table 4-8. Experiments were carefully designed to investigate the effect of different parameters such as temperature, load, stopping time and running in on the tribofilm formation/removal and wear performance of the system. Small entrainment speed was chosen for this purpose to remain in the boundary lubrication regime. The working conditions and the corresponding  $\lambda$  ratios are reported in Table 4-9. The methodology used to study the formation and removal behaviour of the tribofilm by using MTM SLIM is reported in detail in the experimental approach.

**Table 4-8 Material properties**

<b>Material properties</b>	<b>Value</b>
Hardness (GPa)	6
Elastic modulus (GPa)	210
Ball surface roughness (nm)	20
Disc surface roughness (nm)	10



**Table 4-9 Experimental working conditions**

<b>Parameters</b>	<b>Value</b>
Load (N)	30, 40, 60, 75
Temperature °C	80, 100, 120, 140
Entrainment speed ( $\frac{m}{s}$ )	0.1
SRR	5%
Test durations (min)	120
$\lambda$ ratios	0.03-0.06
Oil used	PAO+ZDDP
Ball diameter (mm)	19.05
Disc track diameter (mm)	32

#### 4.7.2 Tested lubricants

In this study, Poly- $\alpha$ -olephin (PAO) +ZDDP and PAO were used to investigate the durability of the tribofilm. The lubricant properties are listed in Table 4-10.

**Table 4-10 Lubricant properties**

<b>Designation</b>	<b>Details</b>
PAO+ZDDP(0.08 mass% phosphorus)	PAO+ZDDP
PAO+ZDDP (0.08 mass% phosphorus) + (3 mass %) Distilled water	PAO+ZDDP+water
Base oil	PAO

### 4.7.3 Methodology

It has been hypothesized that the balance between formation and durability of the tribofilm significantly affects the wear performance of the tribological system (94, 107, 109). To investigate this, a set of experiments was designed to study the durability of the tribofilm. Tribofilm durability is assessed by measuring its thickness and how this changes once rubbed in base oil.

Experiments are designed in order that the rate of tribofilm formation is significantly lower than the loss of tribofilm thickness. For this purpose, experiments were carried out for two hours in total; the first 25 minutes run with PAO+ZDDP (oil A) to form the tribofilm and the rest of the test run by base oil (oil B). The test was suspended after different times of starting the oil and different removal behaviour was observed. In addition, a set of tests was conducted to assess the durability of the film formed after 3 hours of rubbing. The oil was replaced after 3 hours and the results were compared with the test when the oil was replaced at 25 minutes.

The experimental part of this study contains different steps. Tribological experiments were carried out by MTM in rolling/sliding conditions in boundary lubrication. Spacer Layer Interferometry was used to monitor tribofilm thickness during the experiments *in-situ*. The disc was then analysed using XPS to assess the chemical characteristics of the tribofilm. This experimental sequence leads to growth of the tribofilm and correlating its chemical and durability characteristics. This experimental approach is demonstrated schematically in Figure 4-5.

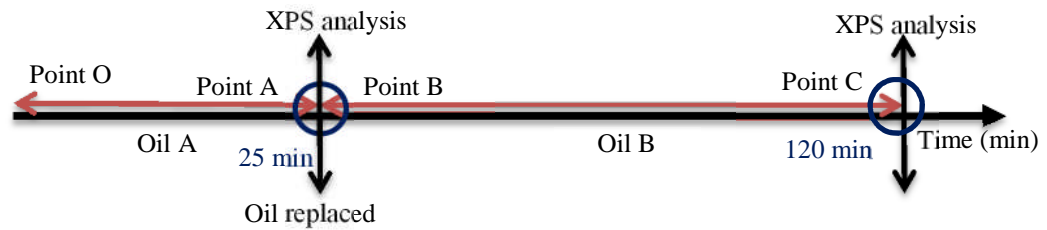


**Figure 4-5 Schematic of the experimental approach for replacing oil and surface analysis.**

The first set of experiments was to study the tribofilm evolution and was conducted in three sub-steps as following:

- I. Early-stage tribofilm durability
- II. Late-stage tribofilm durability
- III. Multiple oil replacement durability test

The second part of the experiments also includes the following sub-steps:

- III. Study the effect of temperature on the durability of the tribofilm by applying different temperatures after suspending the test (ie. When the tribofilm is formed)
- IV. Different loads were applied after suspending the test to see the effect of load on the durability of the tribofilm.
- V. Effect of water on durability of the tribofilm
- VI. Investigating the relationship between tribofilm formation/durability and wear performance of the tribological system for part I and III

The working parameters for the second part of the experiments are summarized in Table 4-11.

**Table 4-11 Working parameters of the experimental procedure**

Tests	Points	<i>O</i> → <i>A</i>	<i>B</i> → <i>C</i>
I	Temperature (°C)	80	80
		60	60
	Load (N)	Oil A (PAO+ZDDP)	Oil B (PAO)
		Oil	
Water concentration	0%, 3%	0%, 3%	
II	Temperature (°C)	100	100
		60	60
	Load (N)	Oil A (PAO+ZDDP)	Oil B (PAO)
		Oil	
Water concentration	0%, 3%	0%, 3%	
III	Temperature (°C)	100	80, 100, 120, 140
	Load (N)	60	60
	Oil	Oil A (PAO+ZDDP)	Oil B (PAO)
IV	Temperature (°C)	100	100
		60	30, 40, 60, 75
	Load (N)	Oil A (PAO+ZDDP)	Oil B (PAO)
	Oil		

#### 4.7.4 Cleaning procedure

#### 4.7.5 Cleaning after suspending the test

Cleaning the oil bath and MTM accessories used for the test is important to study the durability of the tribofilm accurately. The cleaning process was carried out in three different steps. First of all, MTM accessories were immersed in the ultrasonic bath for 30 minutes including 15 minutes in isopropanol and 15 minutes in petroleum-ether. Secondly, the disc was immersed in isopropanol in the ultrasonic bath to remove the attached ZDDP remaining additive from the discs. Thirdly, to avoid altering the tribofilm formed on the balls, they were cleaned by a tissue stained by isopropanol to remove the remaining ZDDP on the ball. To make sure that any tribofilm on the ball was not removed during the cleaning process by isopropanol, two images were taken by SLIM , one before suspending the test and one exactly before starting the rubbing again and the images are shown in Figure 4-6 as an example. Comparison between these two images shows that the thickness of the tribofilm before and after cleaning the ball is almost the same and the only thing which was removed from the ball is the excess unreacted oil (as shown in Figure 4-6). The difference in the images is the spots of oil remaining on the ball at the time of imaging.

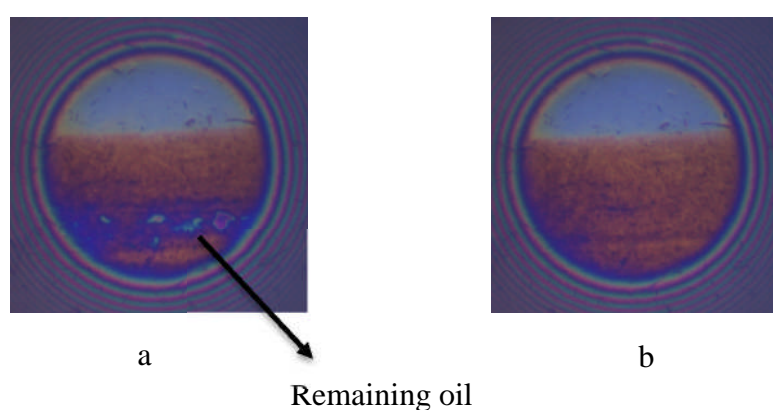


**Figure 4-6 SLIM images taken (a) before suspending the test (b) immediately after suspending the test and before starting the rubbing**

## 4.8 Chemical and surface analysis techniques

### 4.8.1 X-ray Photoelectron Spectroscopy (XPS)

The chemistry of the tribofilm generated by ZDDP containing-oil at different levels of applied relative humidity was evaluated by using X-ray Photoelectron Spectroscopy (XPS) in this work. Analyses have been conducted at the end of each tribological test for different levels of relative humidity at two different temperatures of 80°C and 98°C (60). The samples were cleaned by Isopropanol and put into the ultrasonic bath for 5 minutes after the test and before the XPS analysis. PHI (Model 5000) Versa Probe spectrometer (ULVAC-PHI, Chanhassen, MN, USA). A monochromatic Al K<sub>α</sub> exciting line (23.7 W, 1486.6 eV) with a beam diameter of 100 μm was used to acquire the different spectra. The source analyser angle was fixed at 45° and the signals were collected in fixed analyser transmission (FAT) mode. The surface analysis of every sample started with a survey scan, which was conducted using a pass energy of 187.85 eV and an energy step size of 0.5 eV. This was followed with a high resolution scan of six regions of interest, i.e. C1s, O1s, Fe2p, P2p, Zn2p and S2p, using a pass energy of 46.95 eV and energy step size of 0.05 eV. CasaXPS software (v2.3.17) was used to analyse the different acquired spectra. Due to the spin-orbit splitting of the signals of Fe2p, P2p, S2p and Zn2p, which splits the total signal into a doublet of 2p<sub>3/2</sub> and 2p<sub>1/2</sub>, only the prominent signal of 2p<sub>3/2</sub> was reported in this study. Generally, the analysis comprised two main steps. Firstly, a standard Shirley line type was used as a baseline to subtract the background signal. Secondly, a Gaussian/Lorentzian product formula line shape was used for the different peaks fitted to the different signals in order to recognise the different components contributing to the total signal. The C1s signal was used to calibrate the other signals to compensate for any charging during acquisition. This was performed by shifting the measured

binding energy of the aliphatic component (C–C, C–H) to its expected position at 285.0 eV and thus shifting the other signals by the same value (95).

## **4.9 Wear measurements**

The samples were analysed after each experiments and wear measurements were carried out by an interferometer. Samples are taken out of the experimental set up after the complete tribo-tests. The tribofilm formed on the surfaces are carefully cleaned by using EDT. A White Light Interferometry (NPFLEX from Bruker) was used to measure wear on the balls and analyse the profile of the wear track. The equipment is capable of moving in 3-dimensions to be able to produce the image of the scanned surface. White light interferometry is a non-contact optical method to measure height, volume loss and roughness and other surface parameter. The ‘Vision 64’ software was used to analyse and interpret the data produced by NPFLEX. 2D and 3D images were taken from the wear track and the average wear depth of different areas inside the wear track is calculated. The experiments were repeated 2 times for each working condition and wear was measured in all cases. The wear reported results include the error bars and the variation of the experimental results from the mean value. It should be also noted that the wear depth was measured for 6 different points inside the wear track for each experiment and the average value was reported for the analysis.

### **4.9.1 Sample preparation**

Sample preparation plays a significant role in the experiments. EDTA is used to remove tribofilm from the surface. Figure 4-7 shows surface before and after using EDTA to remove tribofilm (169). Figure 4-8 indicates wear profile among the wear scar before and after using EDTA. It is observed that tribofilm can be interpreted as a

wear and needs to be removed by EDTA from the surface before the wear measurements to be able to accurately measure wear of the system.

It can be clearly seen that EDTA can completely remove tribofilm from the surface and samples would be ready for the wear measurement (see Figure 4-7). EDTA (0.05 M in distilled water) was prepared and it was placed on part of wear scar for 2 minutes and then it is removed by tissue. The process must be repeated 2 times to make sure that tribofilm is completely removed.

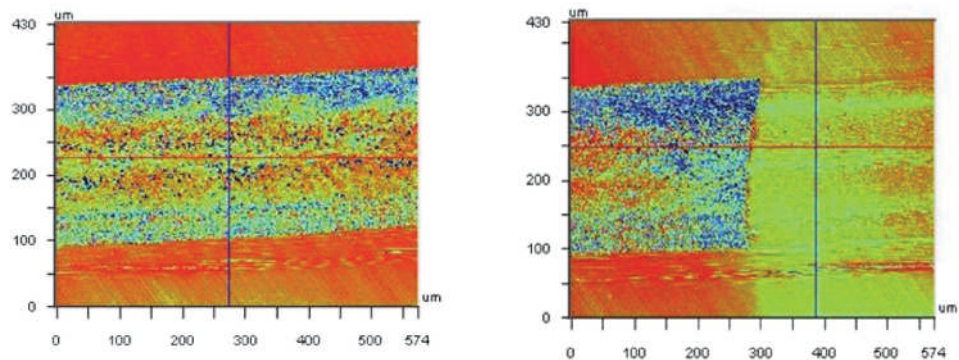


**Figure 4-7 Shows tribofilm removal from the surface using EDTA(169)**

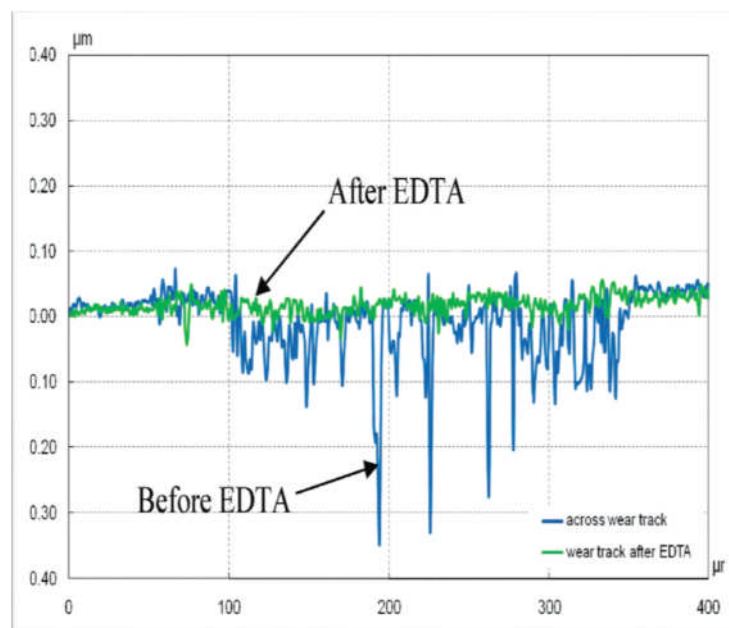


**Figure 4-8 Shows wear profile across the wear scar before and after EDTA(2)**



## **4.10 Summary**

In this chapter, all the details about the methodology and the materials which are used in studying the effect of humidity, temperature, slide to roll ratio and lubricants on wear performance and tribofilm characteristic under rolling-sliding conditions are introduced.

In the next chapter, the results will be presented and discussed and key findings will be disseminated.

## **Chapter 5. Water Effect on Tribochemistry and Mechanical Wear**

### **5.1 Introduction**

Water in lubricants has been known to be a contaminant for many systems (3, 51, 171). It is shown to affect the wear performance, especially in bearing systems, in different ways (4-10). The presence of water in lubricated tribosystems, particularly in bearing applications, can cause corrosion and hydrogen embrittlement, which can increase wear and friction (8). In addition, even small amounts of water in parts per million (ppm) may accelerate the oxidation of oil (60). To investigate the effect of water contamination on the performance of lubricated systems, it is essential to know the form that water exists in the oil (172). Water can be present in oil in two different forms which are dissolved water and free water (42). Dissolved water occurs when the amount of water in oil is less than the saturation point (171). Free water occurs when the amount of water in oil exceeds the saturation level. In this case, droplets of water will be formed in oil resulting in emulsion formation (60).

The effect of water and its tribochemistry on the tribocorrosive wear of boundary lubricated systems with ZDDP-containing oil at different temperatures has been studied experimentally in this work. The experimental part of this study can be split into two. All tribological experiments were carried out by MTM to simulate rolling/sliding conditions in boundary lubrication with four different water concentration values. The tribofilm thickness was measured using Spacer Layer Interferometry to evaluate the tribofilm formation in-situ. Finally the tribofilm was removed from the samples and wear was measured using White Light Interferometry. The sub-sets of tribological experiments are:

- I. Experiments at 80°C for different levels of water concentration (ambient humidity) to investigate the effect of water on tribofilm formation and removal and tribological performance
- II. Experiments at 100°C for different water concentration (ambient humidity) values to study the effect of water on tribological performance and tribofilm formation and removal

## **5.2 The effect of water on wear**

The effect of water on wear performance is shown in Figure 5-1. According to the results, it can be seen that higher water concentration leads to higher wear. These results are in agreement with the works published by Lancaster (53) and Cen (60). They proposed that water plays more significant role in increasing wear compared to the effect on friction. The comparison between two temperatures suggests that the lower temperature results in higher wear. It can be attributed to the lower water content at higher temperature due to the evaporation of water. There is also less wear observed for 100°C compared to 80°C at zero percent water content. This can be related to the thicker tribofilm formed at higher temperatures. The results are in qualitative agreements with the recent studies (109, 173). It is interesting to see that water concentration in oil for the case of 100°C is less than 80°C. It should be noted that the effect of temperature in changing the viscosity of the oil and therefore changing the severity of the contact is negligible in this case as the lambda ratio for both temperatures was calculated to be around 0.04. The water concentrations have been measured by Karl Fischer Titration Method before and after each experiment and the results are reported in Table 5-1.

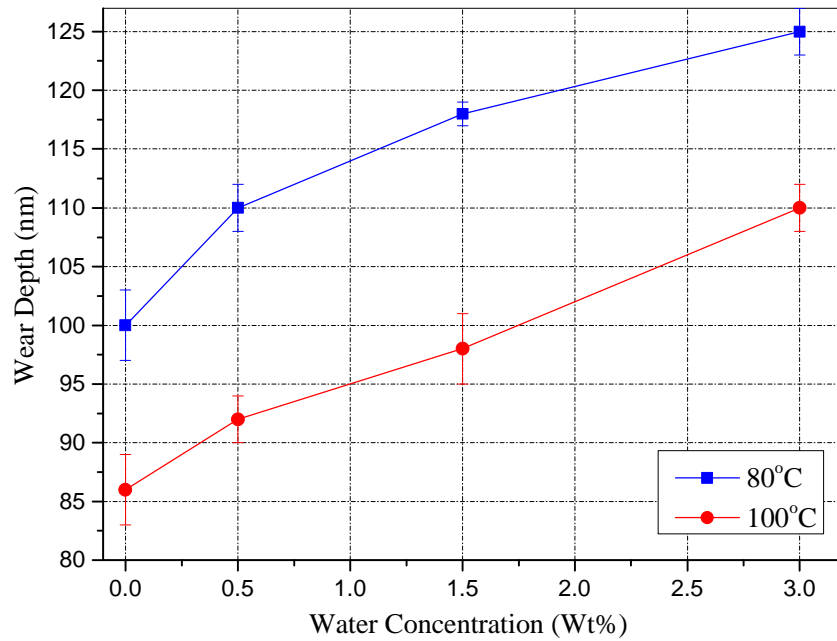


**Figure 5-1 Effect of water on average wear depth at two different temperatures of 80°C and 100°C**

### 5.3 Effect of water on tribofilm growth and wear

The slower and less extensive tribofilm growth was observed for higher water concentration (Figure 5-2 and Figure 5-3) and this effect is more significant at lower temperature. The tribofilm growth in the running-in period is very different than the time water is present. It can affect the wear process due to the fact that the running-in period plays a significant role in the wear of the system. The results show that increasing the water concentration accelerates wear and it can be related to the effect of water on tribofilm growth at the beginning of the experiment. Steady state tribofilm thickness is also affected by water concentration in the oil; the more water concentration the less the tribofilm thickness. The results are in line with the previous research by Nedelcu *et al.* (174) and Cen *et al.* (60). It can be linked to the formation

of shorter chain polyphosphates due to the depolymerisation of the longer chain polyphosphates by water molecules (60).

**Table 5-1 Water concentration measurements before and after tribological test**

Lubricants	Water content before test (ppm)	Water content after 2hr test (ppm)	
		80°C	100°C
PAO+ZDDP	71	11	6
PAO+ZDDP+water (0.5 wt)	4736	62	11
PAO+ZDDP+water (1.5 wt)	16540	121	37
PAO+ZDDP+water (3 wt)	38920	274	42

The same pattern was observed at 80 °C and 100 °C in terms of tribofilm growth rate (Figure 5-2 and Figure 5-3). The only difference is that the effect of water on tribofilm growth is clearly distinguishable at lower temperature indicating that the effect of water on the growth of the tribofilm in the running-in period at 80 °C is more significant compared to 100 °C. The steady state tribofilm thickness follows the same pattern for both temperatures; lower tribofilm thickness is observed for higher water concentration (Figure 5-4). It is also reported in Figure 5-4 that higher temperature leads to the higher tribofilm thickness and it is in line with the results Fujita *et al.* (104) published previously regarding ZDDP antiwear formation and removal. They

proposed that both the tribofilm growth and steady state tribofilm thickness increase with temperature. For comparison purposes, the steady-state tribofilm thickness is plotted against the measured wear depth for both temperatures in Figure 5-5.

It can be seen while the steady-state tribofilm thickness is higher, less wear occurs. However, tribofilm thickness in steady-state does not give a full picture of the wear behaviour in boundary lubricated systems. There are more physical, chemical and mechanical parameters responsible for the wear. In fact, the whole growth behaviour of the tribofilm on the surfaces is important for capturing the wear behaviour. It is important how the tribofilm was formed during the running-in process.

**Table 5-2 Summary of the effect of mixed-water in oil and temperature on tribological performance**

<b>Changes with the increase of mixed-water in oil and temperature using PAO+ZDDP in rolling/sliding conditions</b>		<b>Mixed-water in oil</b>	<b>Temperature</b>
Tribofilm information on ball wear scar	Final tribofilm thickness	decrease	increase
	Growth rate	decrease	increase
Wear		increase	decrease

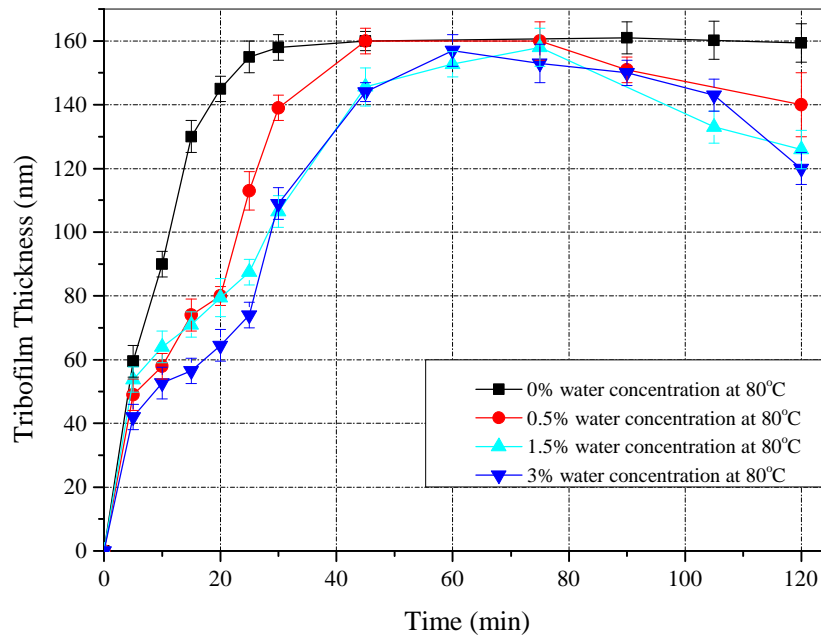


**Figure 5-2 Tribofilm thickness measurement results for 80°C at different water concentrations**

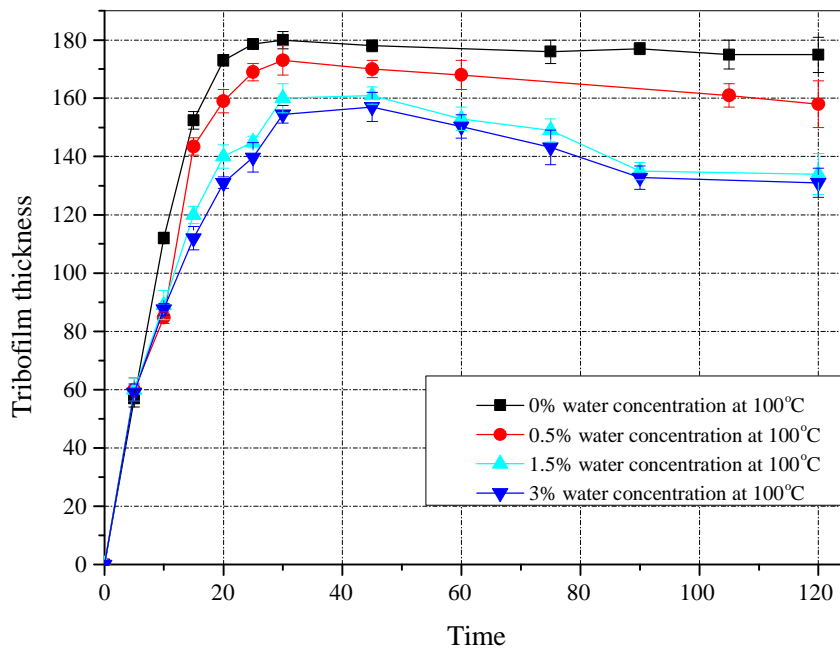


**Figure 5-3 Tribofilm thickness measurement results for 100°C at different water concentrations**

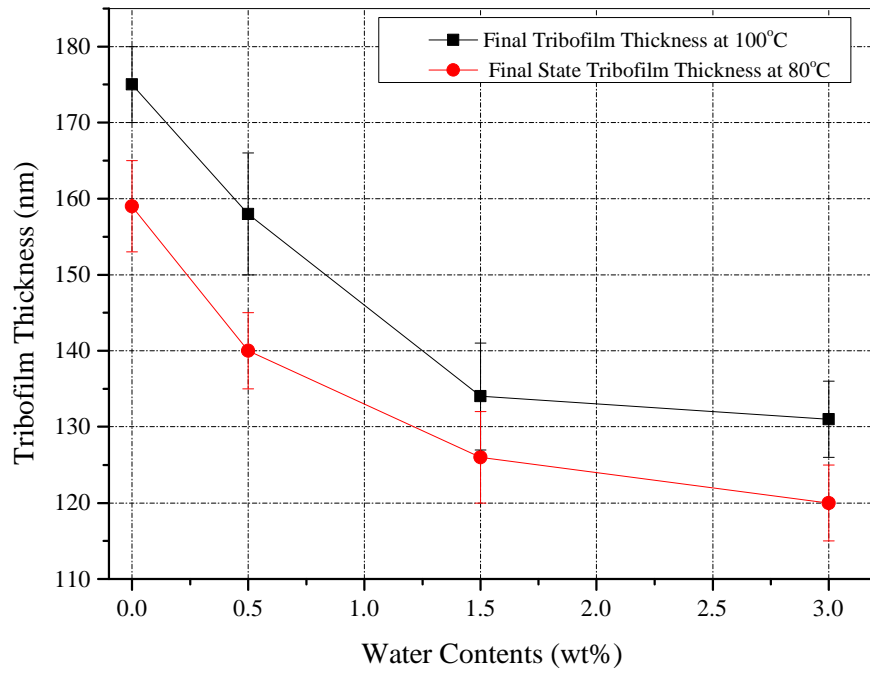


**Figure 5-4 Final tribofilm thickness results for different water concentrations**

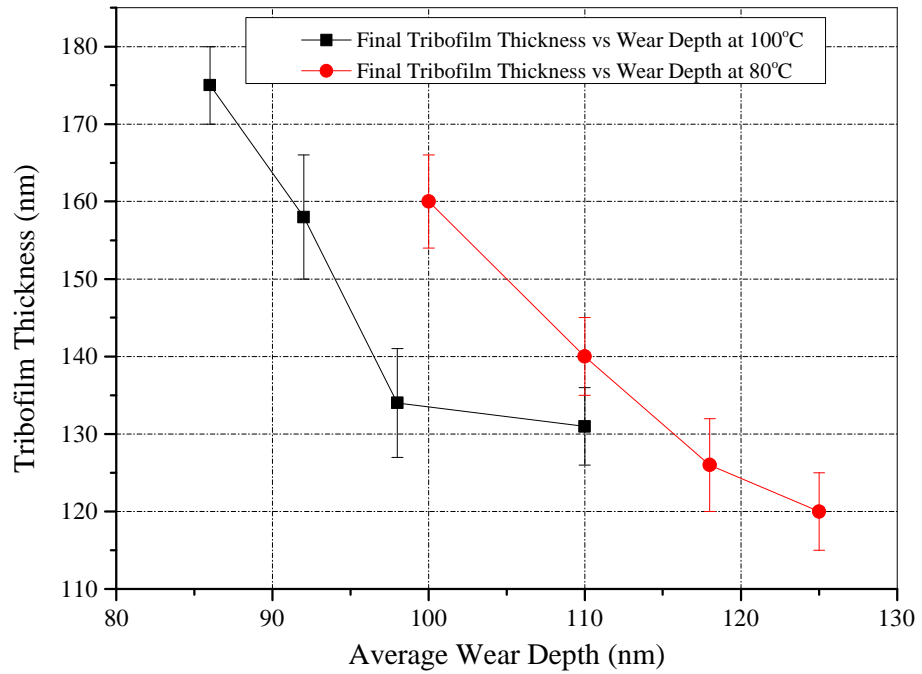


**Figure 5-5 Final tribofilm thickness results vs measured wear depth**



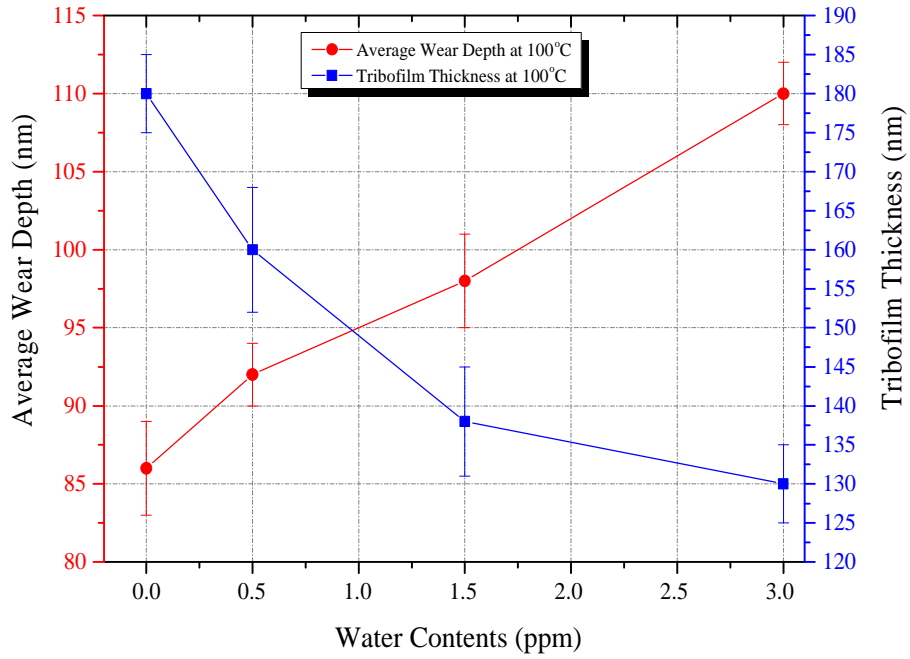


**Figure 5-6 Comparison between average wear depth and tribofilm thickness at different water concentrations at 100°C**

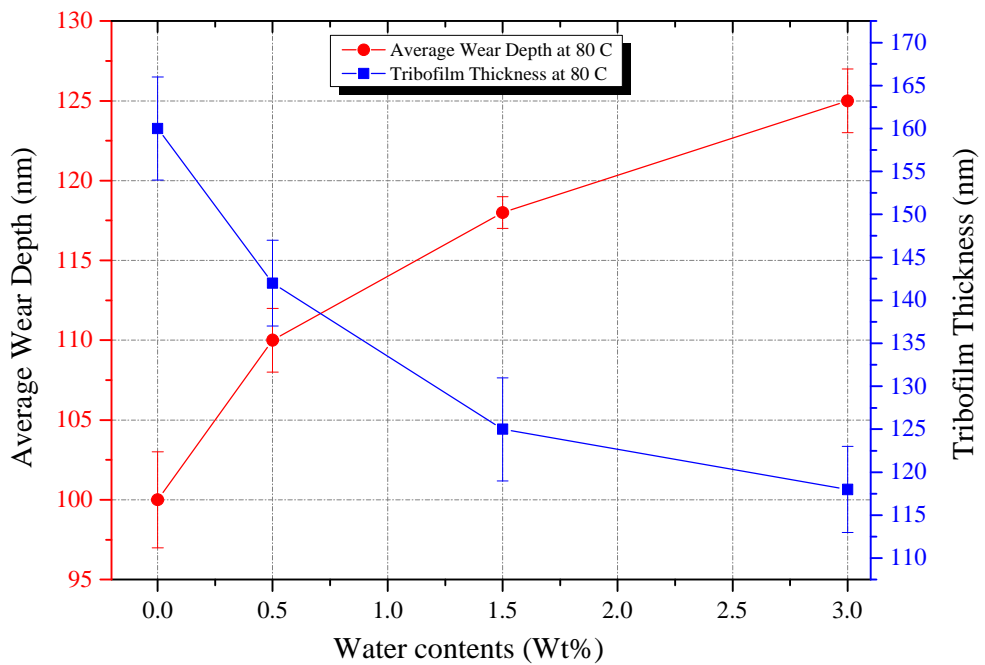


**Figure 5-7 Comparison between average wear depth and tribofilm thickness at different water concentration at 80°C**

A detailed discussion on this can be found in Ref (109). Comparisons made between the effect of water on steady state tribofilm thickness and the average wear depth for 80°C and 100°C are plotted in Figure 5-6 and Figure 5-7 for 100°C and 80°C respectively. The trends indicate that increasing the water content in the oil affects wear by decreasing the steady state tribofilm thickness.

#### **5.4 Summary of the effect of water**

Section 5.2 and Section 5.3 have studied the effect of water on wear behaviour of boundary lubricated tribosystem in a rolling-sliding contact. The main results are summarized in this section.

1. Water influences the growth behaviour of the tribofilm on the surfaces and more water in the oil results in lower rate of the growth on contacting surfaces
2. Water in oil can delay the growth of the tribofilm in the running-in period and it can significantly affect wear performance in boundary lubricated system. This effect is more significant for the tests at 80°C in comparison with tests at 100°C due to more water in the oil
3. Higher water concentration leads to a reduction in growth rate of the tribofilm which in nature results in an increase in the wear of the system. This reduction in growth rate might be because of the difficulty that ZDDP molecules have in reacting with the substrate in the presence of the water. (See Figure 5-5)
4. It was shown that tribofilm thickness in steady-state condition is not a good representative of the wear behaviour of the system. However other important physical, chemical and mechanical parameters are involved. The whole growth behaviour of the tribofilm is important to characterize wear. This means that running-in period is also important in determining the wear of boundary lubricated systems.

## **Chapter 6. Humidity Effect on Tribochemistry and Mechanical Wear**

### **6.1 Introduction**

Wear performance of any tribological system can be influenced in a complex way by water contamination. Water can be the cause of steel corrosion which, in turn, can accelerate wear. It can decompose the additives in the oil and create a more corrosive environment which leads to the higher wear in the system. The aim of this chapter is to investigate the effect of relative humidity on tribological performance and tribofilm characteristics in boundary lubricated system in rolling-sliding conditions. A key novelty of this study is that the effect of relative humidity and the tribochemical changes on the tribological performance and tribofilm characteristics of boundary lubricated systems by means of designing a humidity control system integrated to the Mini Traction Machine (MTM) and Spacer Layer Interferometry Method (SLIM) for the first time. The system is capable of simulating rolling-sliding conditions continuously where lubricant can be contaminated with water.

The reaction layer thickness was measured by Spacer Layer Interferometry Method to evaluate tribofilm thickness in-situ at different levels of humidity.

- I. Experiments at 80 °C for different levels of humidity to investigate the effect of humidity on tribofilm characteristics and tribological performance
- II. Experiments at 98 °C for different levels of humidity to study the effect of humidity on tribological performance and tribofilm characteristics

## **6.2 Humidity effect on oil**

In Figure 6-1 the water content at two temperatures of 80°C and 98°C for different levels of relative humidity are shown. It should be noted that before starting each experiment, oil was exposed to the relative humidity for 30 minutes to be saturated and all experiments were conducted at steady state relative humidity. Figure 6-1 shows that there is no significant changes in water concentration while the humidity level is adjusted between 20% RH and 50% RH. Water concentration dramatically increases at higher values of humidity. It can be clearly seen that the level of water adsorption due to the relative humidity reaches a maximum of 0.079% at 95% RH. The same trend was observed for 98°C (Figure 6-1). The comparison between two temperatures of 80°C and 98°C confirms that the level of water content is reduced at higher temperature. It is likely attributed to the evaporation of the water molecules from the oil. It can also be interpreted from the results that only 18°C differences in temperature leads to a significant change in water concentration in the oil and it is more noticeable at higher values of relative humidity.

## **6.3 Effect of relative humidity on tribofilm evolution and wear performance**

The effect of relative humidity on tribofilm growth at 80°C is shown in Figure 6-2. It can be clearly seen that the curves cluster together into three groups. The curves in the first group called low humidity range correspond to the relative humidity between 0% RH to 40% RH. Second and third groups represent curves for humidity in the range of 50%RH to 70% RH (medium humidity) and 80%RH to 95%RH (high humidity) respectively.

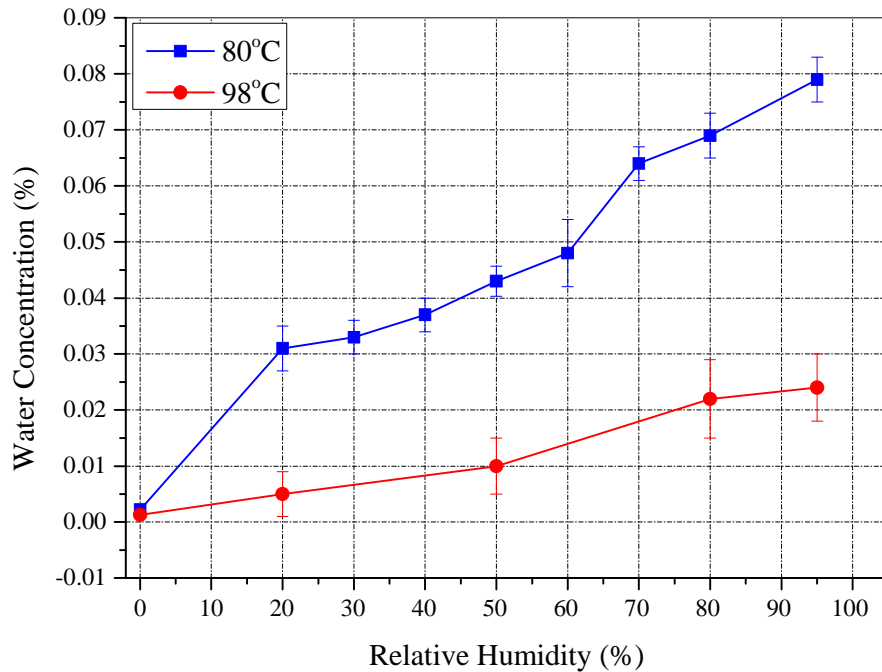


**Figure 6-1 Measured water concentration at 80°C and 98°C**

The higher tribofilm thickness was observed in the first group due to the lower water concentration in the oil (Figure 6-3). The lower tribofilm thicknesses were found in the high humidity group including the humidity in the range of 80% to 95%. Results indicate higher water concentration in higher humidity tests (Figure 6-3). It can be concluded that the higher the relative humidity thinner tribofilm is formed. The same trend was observed at 98°C in terms of tribofilm thickness (Figure 6-3). Tribofilm thickness was decreased by increasing the relative humidity.

The comparison between these two temperatures show that the differences between the steady state tribofilm thicknesses for the low humidity values and high humidity values are more distinguishable at low temperature (80°C). The results are in a good agreement with the recent study by the authors (110). They proposed that when the mixed-water in oil increases, the steady state tribofilm thickness decreases. Cen *et al* (44) found the same trend in their work. It is interesting to note that based on the results presented in Figure 6-2 and Figure 6-3, relative humidity can reduce the rate

of formation and eventual thickness of the tribofilm and it can significantly affect the wear process (202).

The effects of water concentration at different values of relative humidity on steady state tribofilm thickness at two different temperatures of 80°C and 98°C are plotted in Figure 6-4 and Figure 6-5. It can be understood from the graph that the steady state thickness of the tribofilm reduces while the water concentration (relative humidity) increases for both temperatures. However, it is more significant and noticeable at lower temperature due to the fact that more water is present in the oil. It is observed that an increase of temperature seems to increase the ZDDP decomposition rate thus increasing the tribofilm thickness.

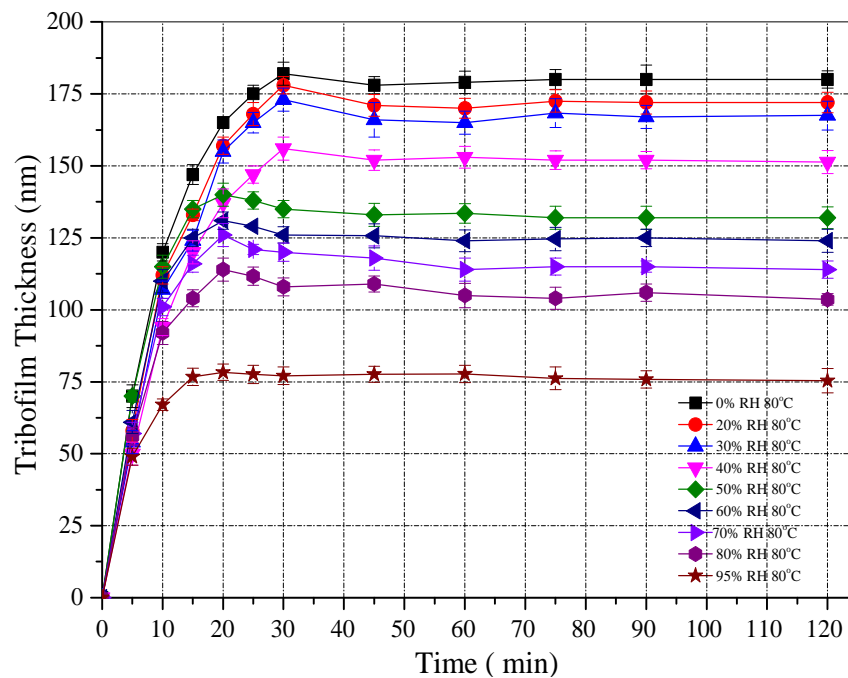


**Figure 6-2 Tribofilm thickness measurement results for 80°C for different levels of relative humidity**

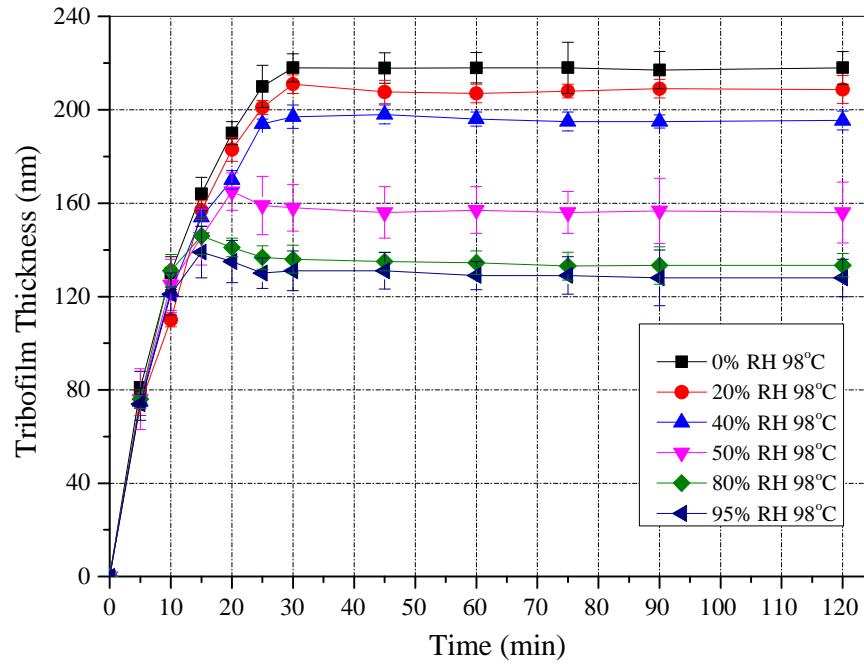


**Figure 6-3 Tribofilm thickness measurement results at 98°C for different levels of relative humidity**

It can be clearly understood that at the same values of humidity, tribofilm thickness is higher at higher temperature. The same trend was observed by Morina *et al* (15, 175). Figure 6-6 indicates how steady state tribofilm thickness influences wear performance.

The following conclusion can be drawn from the graph; first and foremost, thicker the ZDDP tribofilm leads to lower wear in the system. Secondly, it can be noted that at the same thicknesses of the tribofilm, the higher wear occurs at lower temperature (80°C) which can be attributed to the higher dissolved water concentration in the oil at lower temperature. This difference indicates that thickness of the tribofilm is only one of the dominant factors in affecting wear performance and composition of the tribofilm is also significant and needs to be explored.

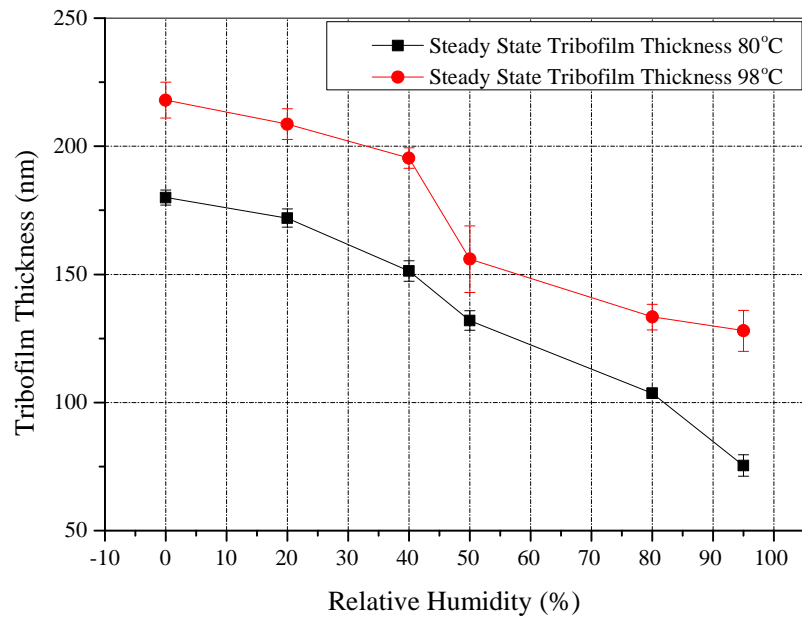


**Figure 6-4 Effect of relative humidity on steady state tribofilm thickness for different temperatures**

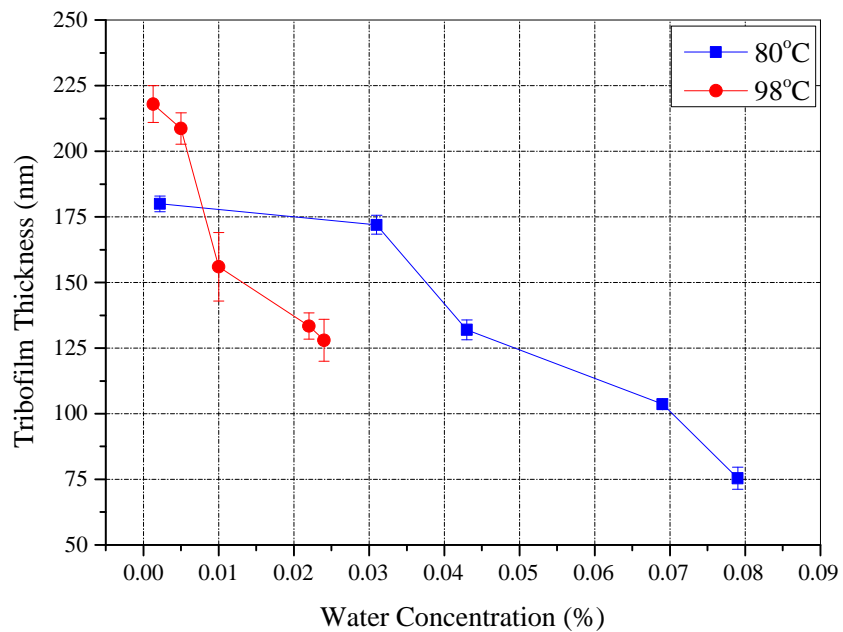


**Figure 6-5 Effect of water concentration measured at different levels of relative humidity on steady state tribofilm thickness for different temperatures**



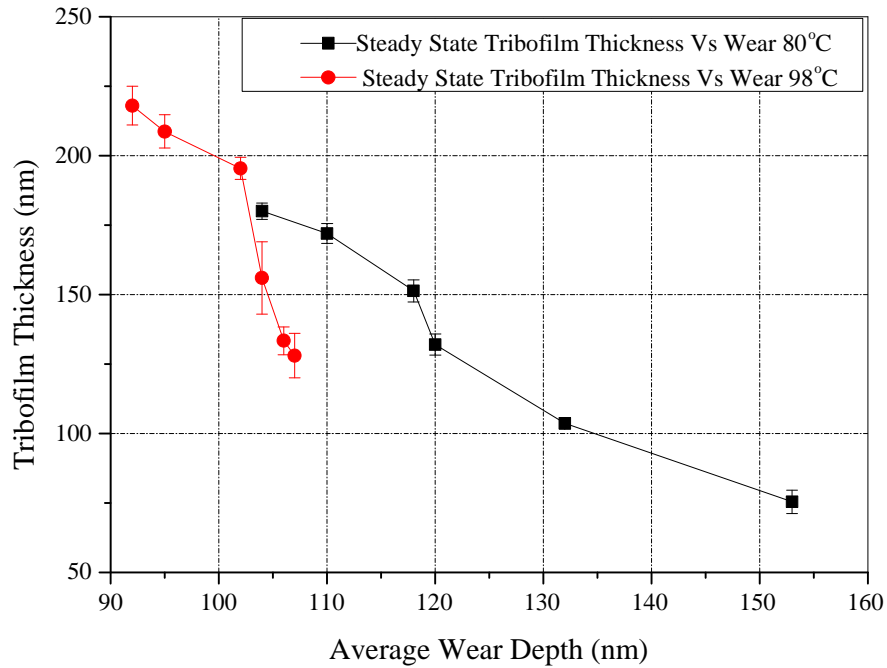


**Figure 6-6 Steady state tribofilm thickness results vs measured wear depth**

#### **6.4 Effect of relative humidity on tribochemistry**

Crobu *et al.* (95, 98) showed the surface chemistry of zinc polyphosphates can be characterised using XPS based on the integrated intensity ratio of bridging oxygen (P-O-P) and non-bridging oxygen (P=O and P-O-M). It has been suggested that the chain length of glassy phosphates tribofilm can be identified by a combined usage of bridging oxygen/non-bridging oxygen (BO/NBO) intensity ratio, Zn3s-P2p<sub>3/2</sub> binding energy difference and a modified Auger parameter.

This combined method allows characterisation of polyphosphate chain composition ranging from zinc orthophosphate to zinc metaphosphate. In this study, the ratio of bridging oxygen to non-bridging oxygen is used to identify the chain length of glassy polyphosphate by dividing the ratio of BO to NBO intensity obtained from XPS analysis (Figure 6-7 and Figure 6-8). For the above mentioned experiments in Section

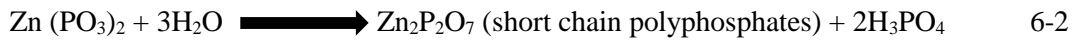
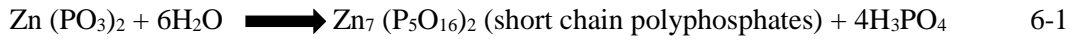
6.3 XPS analysis was conducted and the oxygen peaks are plotted. This approach has been demonstrated in the literature (176-184).

Table 6-1 represents the results for BO/NBO at different levels of relative humidity. It can be seen that the value of BO/NBO decreases while the humidity increases for both temperatures of 80°C and 98°C. It can be interpreted that higher values of humidity correspond to shorter polyphosphates chain length ranging from zinc orthophosphate to zinc metaphosphate (95, 98).

Based on the BO/NBO ratios, the shortest polyphosphate chain length was observed for 95% relative humidity at 80°C while 0% relative humidity at 98°C was found responsible for the longest polyphosphate chain length. The test at 80°C and 0% RH showed very short-chain structure predominate in orthophosphate composition and the long-chain structure (metaphosphate) belongs to 0% RH and 98°C.

It suggests that humidity can affect the mechanical properties of the tribofilm especially at lower temperatures and higher levels of humidity due to the higher water concentration in the oil. Figure 6-1 illustrates the water concentrations at different values of humidity. The lowest water content belongs to 98°C and 0% RH which is responsible for the longest polyphosphate chain (metaphosphate) and the highest water concentration is for 95% RH at 80°C found 0.079 which has the shortest glassy polyphosphate chain length (202).

The results are in a good agreement with literature. Fuller *et al* (74) and Nichollas (86) *et al* pointed out that longer chain polyphosphates could also be depolymerised by water to shorter chain polyphosphates. The proposed mechanisms of depolymerisation of polyphosphates chain are described in Equation 6-1 and Equation 6-2 . In the presence of water, hydrolysis of polyphosphates occurs, creating short-chain polyphosphates and phosphoric acid.



It supports the fact that when higher water concentration is present in the oil at higher values of humidity and lower temperature, the tribofilm formed on the surface consists of shorter polyphosphates due to the depolymerisation of the longer polyphosphates chains (44, 174).

The effect of humidity on tribofilm chain length for different temperatures of 80°C and 98°C are shown in Figure 6-9 and Figure 6-10 respectively. Interpreting the graphs confirms that the difference between BO/NBO ratios of 0% RH and 95% RH at 80°C is more significant than 98°C due to the evaporation of water at higher temperature and lower water concentration presented in the oil.

**Table 6-1 BO/NBO ratios at different levels of relative humidity**

Tests	BO/NBO	
	80°C	98°C
0% Relative Humidity	0.43	0.56
20% Relative Humidity	0.39	-----
30% Relative Humidity	0.30	-----
50% Relative Humidity	0.14	0.2
70% Relative Humidity	0.1	-----
95% Relative Humidity	0.04	0.15

Figure 6-5 showed that higher temperature leads to the thicker steady state tribofilm thickness. The comparison between the ratios of BO/NBO of two temperatures reveals that the higher the tribofilm thickness the longer the polyphosphates chain (Table 6-1). Figure 6-5 and Table 6-1 results indicate that the higher test temperature results a thicker tribofilm containing longer polyphosphates.

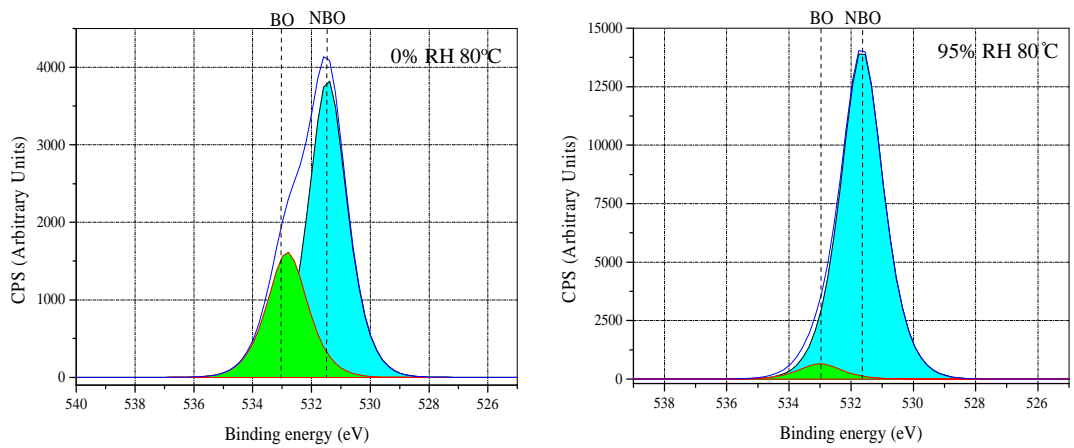


**Figure 6-7 High resolution X-Ray Photoelectron Spectroscopy (XPS) spectra for ZDDP tribofilm formed at different values of humidity for 80°C**

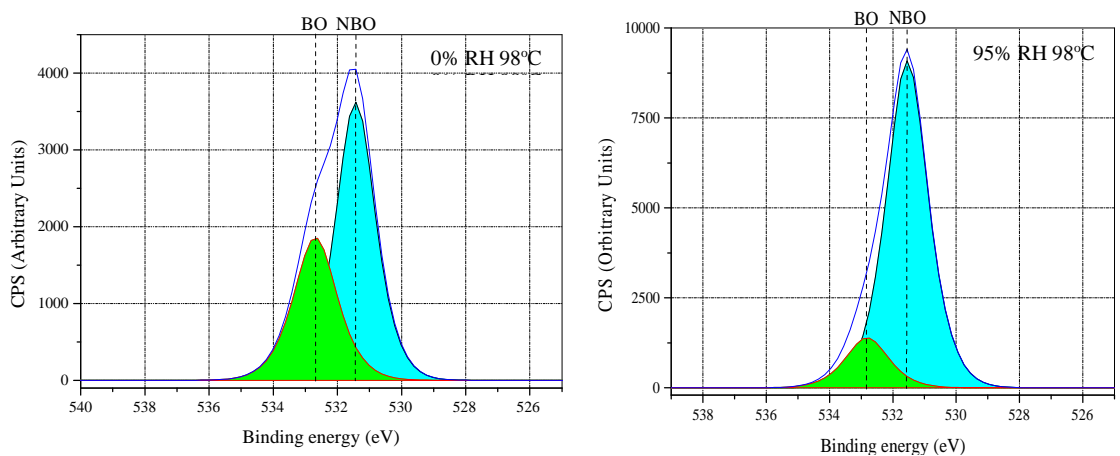


**Figure 6-8 High resolution X-Ray Photoelectron Spectroscopy (XPS) spectra for ZDDP tribofilm formed at different values of humidity for 98°C**

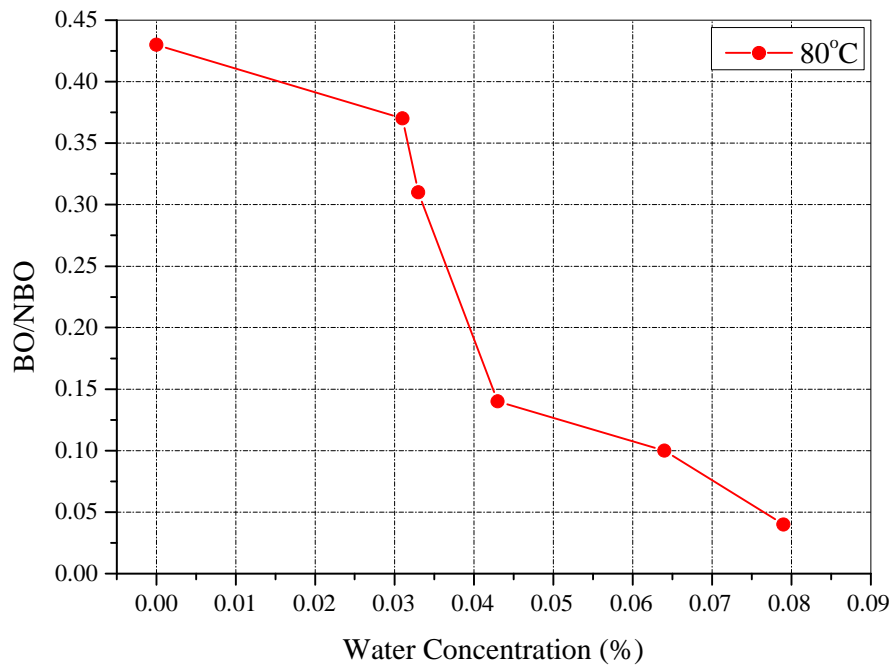


**Figure 6-9 Effect of water concentration at different values of relative humidity on polyphosphate chain length at 80°C**

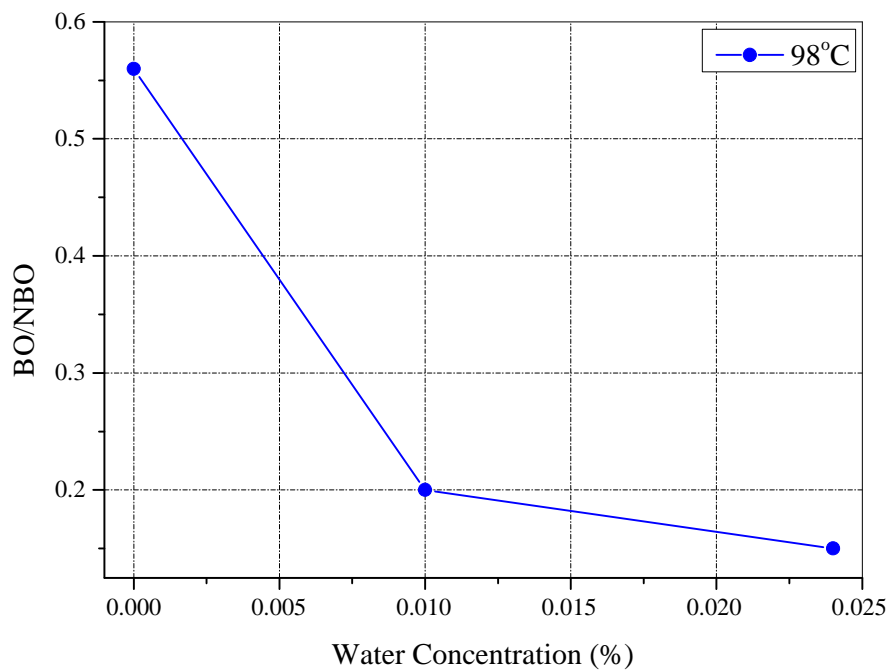


**Figure 6-10 Effect of water concentration at different values of relative humidity on polyphosphate chain length at 98°C**

## 6.5 The effect of relative humidity on wear performance

The tribological tests were performed using MTM SLIM with different levels of relative humidity to investigate the relationship between relative humidity and wear performance. Figure 6-11 and Figure 6-12 illustrates the effect of different levels of humidity on wear performance of the lubricant. Based on the wear results, it can be noted that the higher the relative humidity the higher the wear of the system. The reason for the increase of wear at higher relative humidity is attributed to the higher level of water adsorption.

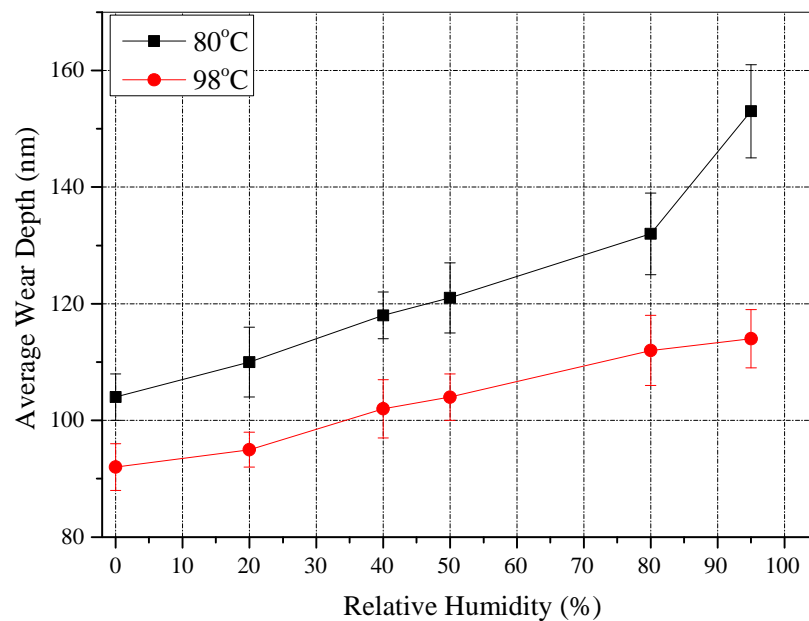


**Figure 6-11 Effect of relative humidity on the average wear depth at two different temperatures of 80°C and 98°C**

The following conclusion can be drawn that relative humidity results in the acceleration of wear of the system. Figure 6-11 confirms that the average wear depth is dramatically increasing when the relative humidity is reaching the higher values (more than 50%) at 80°C. It supports the fact that the level of water absorption of the oil in the presence of humid environment increases to a maximum of 0.079 volume percent at 95% RH which produces 153 nm average wear depth. The water contents

and wear depth follow the same trend at 98°C as 80°C but it should be mentioned that the effect of higher relative humidity on wear performance is more noticeable at 80°C compared to 98°C.

These results are in a good agreement with the studies done by Lancaster *et al* (53) and Cen *et al* (44, 60). It was proposed that water contamination plays a significant role in accelerating wear of the system in comparison with the effect of water on friction. Cen *et al* (44) found recently that increasing the relative humidity leads to the higher water adsorption and higher wear under pure sliding condition.

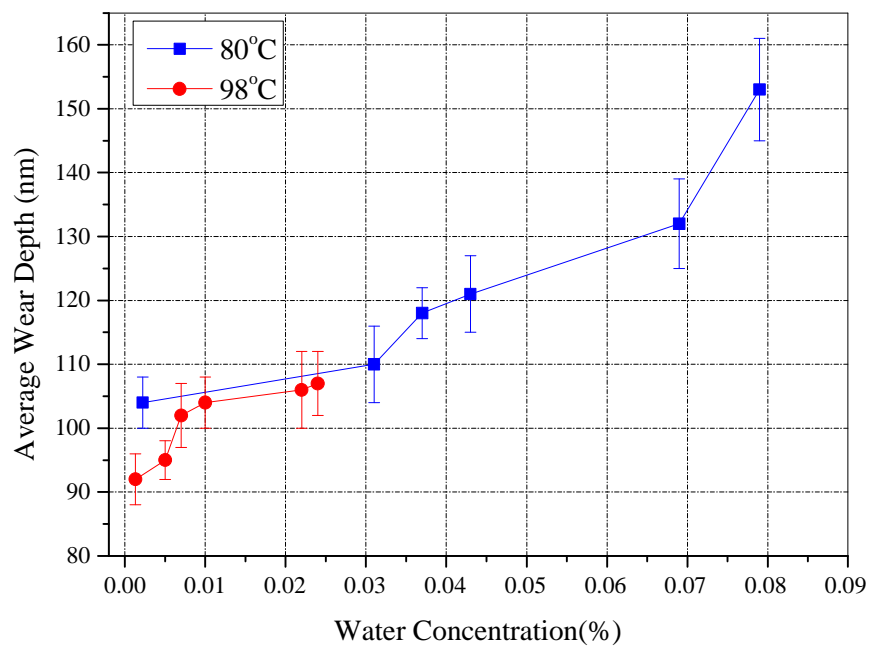


**Figure 6-12 Effect water concentration measured at different levels of humidity on the average wear depth at two different temperatures of 80°C and 98°C**

Recent work published by Parsaeian *et al* (110) indicates that average wear depth is increasing by mixing more water in the oil. It was also found by Cai *et al* (185) that water contamination above the saturation level in the oil (emulsion) is detrimental

for the system in terms of wear behaviour. In this study, it is also observed that the lower temperature results in higher wear. It can be related to the more evaporation of water at higher temperature. It can also be said that the higher temperature leads to the thicker tribofilm formed by ZDDP. The same trends were proposed by Cen *et al* (44) and Ghanbarzadeh *et al* (109).

**Table 6-2 Summary of the effect of relative humidity and temperature on tribological performance**

Changes with the increase of relative humidity and temperature using PAO+ZDDP in rolling/sliding conditions		Relative humidity	Temperature
Tribofilm information on ball wear scar	Steady state tribofilm thickness	decrease	increase
	Growth rate	No trend	increase
	Phosphate chain length decided by BO/NBO ratio	decrease	increase
Wear		increase	decrease

## 6.6 Summary of the effect of relative humidity

The effect of relative humidity on tribofilm characteristics and wear performance of the boundary lubricated system in rolling-sliding conditions has been investigated for the first time in this chapter by using MTM SLIM integrated to the humidity control system. Notable observations in this chapter are summarized as follow:



1. The increase of relative humidity increases the tribocorrosive wear of the system for both temperatures of 80°C and 98°C. It can be attributed to the higher water concentrations when higher humidity values are applied. It is worth mentioning that the higher the temperature the less the tribocorrosive wear due to the thicker tribofilm thickness formed on the surface. The effect of humidity on wear performance is more significant at lower temperature in comparison with higher temperature.
2. Higher water contents in oil results in reducing the growth of the tribofilm which causes higher wear in the system. Reducing tribofilm growth might be because of the difficulty that ZDDP molecules have to access to the surface and react with the substrate in the presence of higher amount of water.
3. Relative humidity can significantly affect the mechanical properties of the tribofilm. It was found that the effect of humidity on tribofilm formation is more significant at higher humidity and lower temperature (80°C) due to the more water content in the oil.
4. It can be interpreted from the results that humidity hinders the growth of the tribofilm and it can considerably affect the tribocorrosive wear of the system. The higher the relative humidity the lower the steady state tribofilm thickness and the higher the tribocorrosive wear.
5. XPS results show that shorter chain poly phosphates present in the tribofilm at higher relative humidity. It can be linked to the depolymerisation of longer polyphosphate chain to shorter chain. The higher the relative humidity the lower the ratio of BO/NBO.

The results indicate that the higher water concentration observed in the higher humidity test and thinner tribofilm containing shorter chain poly phosphates is formed

on the surface (Table 6-2). This experimental results are used to develop a semi-analytical model considering the effect of relative humidity on the tribofilm thickness and the corresponding wear for the first time which is the subject of the next chapter of this study.

## Chapter 7. Development of Tribochemical Model

### 7.1 Introduction

Relative humidity, addition of water and their effects on tribochemistry and wear of boundary lubricated systems were examined experimentally in Chapter 5 and Chapter 6. In the current study the tribofilm thickness and wear results obtained experimentally are used to develop a semi-deterministic approach to implement the effect of humidity and mixed-water in wear prediction of boundary lubrication for the first time. Two approaches were used for this purpose; firstly, a modification factor was found to be suitable for Archard's wear equation to be able to account for the effect of relative humidity. Secondly, the effect of humidity on the tribofilm growth on the surfaces was captured in the model and its effect on the wear was tested based on a recent model developed in Leeds (107, 156). Although the model components are explained briefly in this section, the details of the contact model and the wear mechanism can be found in Ref (107) and (109) respectively.

The model consists of the following main parts:

- A deterministic contact model for rough surfaces using elastic-perfectly plastic theory
- A semi-analytical tribofilm growth model based on thermodynamics of interfaces
- Tribofilm mechanical properties which include the values reported previously in the literature
- A new proposed modification of Archard's wear model considering the effect of ZDDP tribofilm

In this model, digitized surfaces have been used as the inputs. This method is explained in detail by Tonder *et al.* (186) and Ghanbarzadeh *et al* (107). The contact mechanics model is a plastic-perfectly plastic approach using the complementary potential energy formulation (107).

In order to consider tribochemistry, this model contains the tribofilm formation part which is based on kinetics of tribochemical reactions and is combined with a phenomenological term that accounts for the dynamic removal of the tribofilm (107) and is shown by equation 7-1 .

$$h = \underbrace{h_{max} \left( 1 - e^{\left( \frac{-k_1 T}{h'} x_{tribo} \cdot t \right)} \right)}_{\text{Formation}} - \underbrace{C_3 (1 - e^{-C_4 t})}_{\text{Removal}} \quad 7-1$$

In which  $k_1$  and  $h'$  are the Boltzmann and the Plank's constants,  $T$  is the flash temperature and  $C_3$  and  $C_4$  are removal constants. The term  $x_{tribo}$  was interpreted as the mechanoactivation in inducing the tribochemical reactions. A detailed discussion can be found in (107). A tribochemical wear model was developed in that work that accounts for the dynamic, formation and removal of the tribofilm. Since the wear model is developed further to take into account the effect of water in this thesis, a detailed description is given in this chapter.

The wear model used in the numerical approach is a modified version of Archard's wear equation that accounts for the growth of the ZDDP tribofilm on the surface. The wear model is local and is space and time-dependant. Assuming that the coefficient of wear is at its maximum for steel-steel contact and at its minimum when the tribofilm has its maximum thickness, the equation for calculating the coefficient of wear is as follows:

$$K_{tr} = K_{steel} - (K_{steel} - K_{min}) \cdot \frac{h}{h_{max}} \quad 7-2$$

Where  $K_{tr}$  is the coefficient of wear for a tribofilm with thickness  $h$ ,  $K_{steel}$ ,  $K_{min}$  and  $h_{max}$  are coefficients of wear for steel and the maximum ZDDP tribofilm thickness and maximum film thickness, respectively. It was reported that wear can occur due to the removal of the tribofilm from the surface. There is limited number of the substrate atoms in the bulk of the tribofilm due to different surface phenomena (168, 187, 188). Therefore the dynamic process of the formation and removal of the tribofilm on the contacting asperities will lead to the removal of the substrate atoms (109). This is a simple mathematical formulation for studying the effect of ZDDP tribofilm on reducing wear on steel surfaces. This wear model is explained in detail in (107, 156) and is validated against experimental results in Section 7.3.

## 7.2 Model calibration procedure

There are several parameters in the complete model that require calibration before predictions of wear can be made. The details of the model calibration has been reported in (107) in detail. However a brief explanation is given here. For the wear calculation part of the model, the parameters needed are the *initial* wear coefficient,  $K$ , and the *minimum* coefficient of wear  $CoW_{min}$ . These are determined using experimental results for one operating condition and then used for all other simulations under different conditions. For the tribofilm growth part of the model, the four parameters  $x_{tribo}$ ,  $h_{max}$ ,  $C_3$  and  $C_4$  need to be determined for each set of experimental conditions in order to capture the tribofilm behaviour, which is different in each case. This is achieved by fitting equation 7-1 to experimental measurements of tribofilm thickness.

The procedure for determining the initial wear coefficient involves conducting simulations with different initial coefficients of wear to identify the coefficient value that exactly matches the wear behaviour observed in the calibration experiment. The same initial coefficient of wear can then be used in all other simulations under different conditions.

For simplicity, the value of  $CoW_{min}$  is chosen to be one tenth of the initial coefficient of wear for the case of steel on steel contact. This is based on the experimental observations that wear in the presence of the ZDDP tribofilm has been reported to be approximately one tenth of the wear in the absence of the ZDDP (74, 86, 189-191). The numerical prediction results confirm that this is a reasonable approximation.

## **7.3 Validation of the model**

### **7.3.1 Tribofilm thickness**

MTM-SLIM configuration results are shown in this section for two ZDDP concentrations at three temperatures and three times. Thickness measurements for 1% wt ZDDP concentrations in oil at two temperatures of 60 and 100°C for three different test durations are shown in Figure 7-1 and Figure 7-2. All the experiments were conducted at applied load of 60 N. In addition, the measurement results with the same concentration for different temperatures for 2 hours test duration are plotted in Figure 7-3 . Spacer Layer imaging results are also plotted for 0.5% wt ZDDP concentration in oil at three different temperatures of 60, 80 and 100° C in Figure 7-4.

The tribofilm measurement results are used to calibrate the tribochemical model of Equation 7-1 and the calibrated parameters are reported in Table 7-1. The goodness of the fitting is also shown in the Figure 7-5 for one case of 1% wt ZDDP in oil. Figure

7-5 shows the tribofilm thickness predicted by the simulation and measured experimentally for the three temperatures (60°C, 80°C and 100°C) for 1% wt ZDDP.

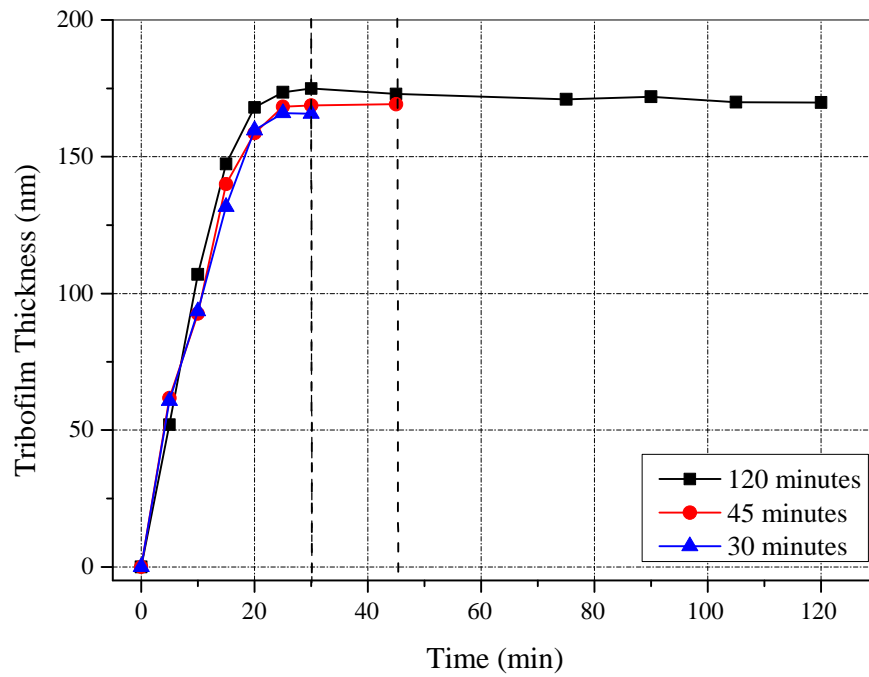


Figure 7-1 Tribofilm thickness measurements for 100°C at different times

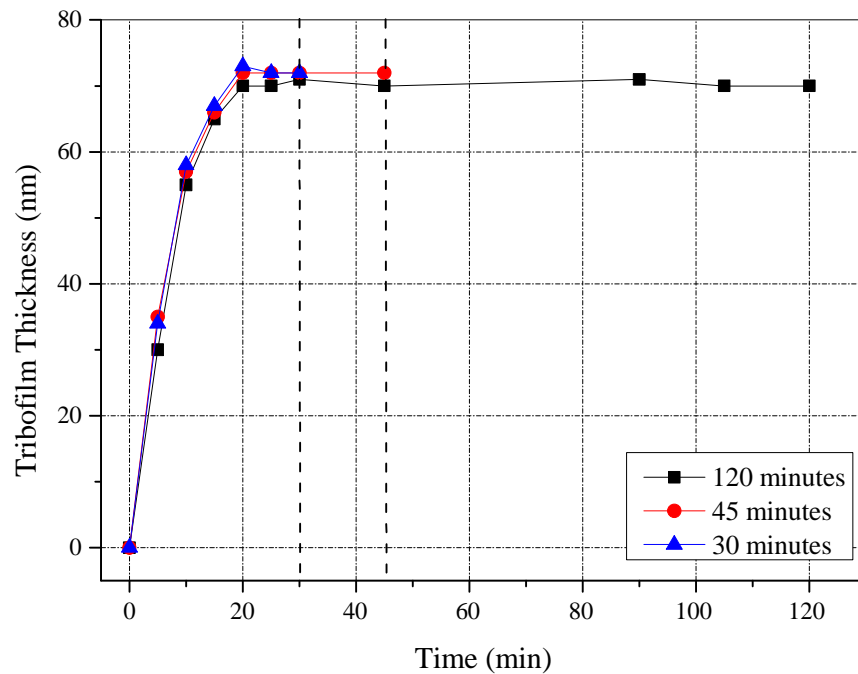
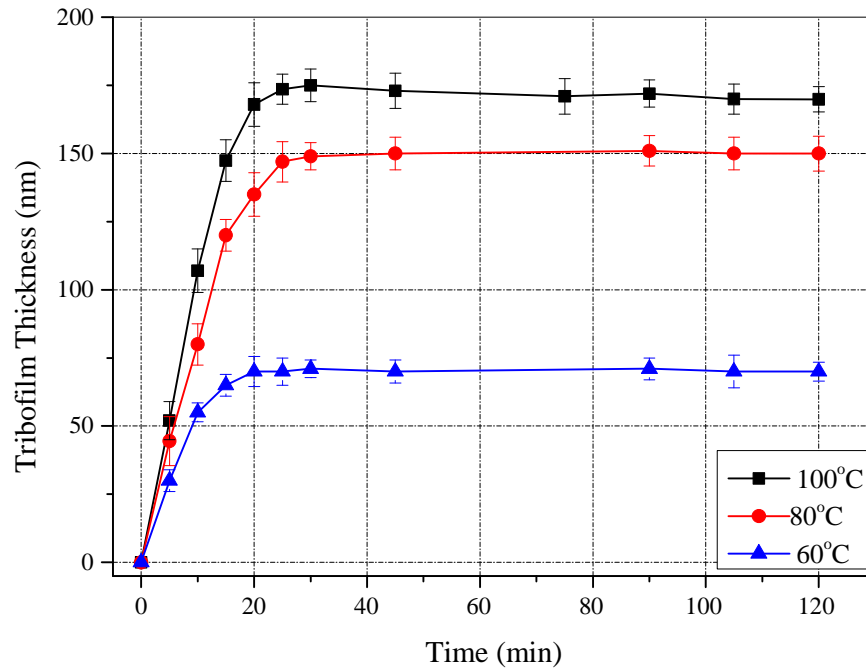
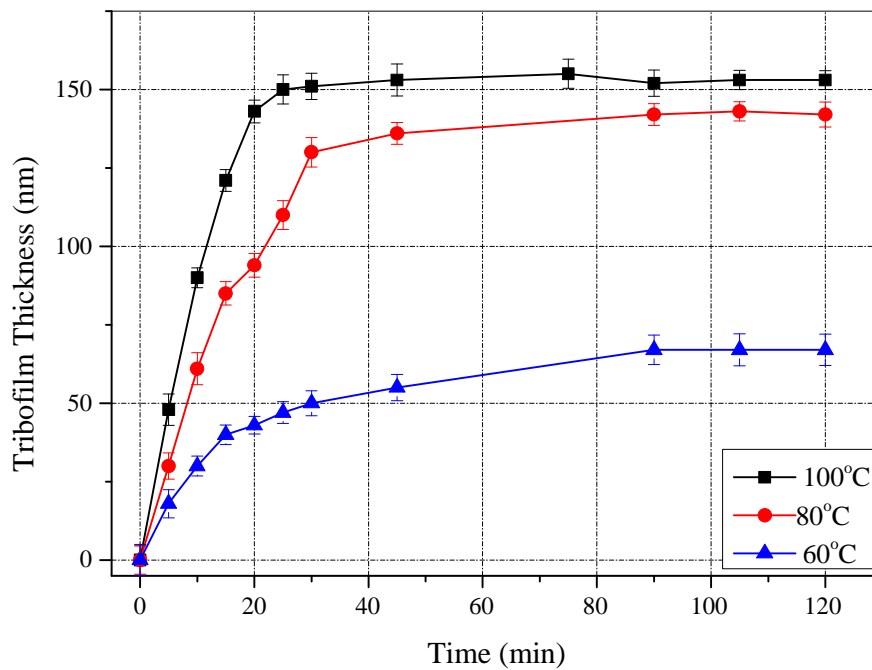


Figure 7-2 Tribofilm thickness measurements for 60°C at different times



**Figure 7-3 Tribofilm thickness measurements for different temperatures for 1% wt ZDDP in oil**



**Figure 7-4 Tribofilm thickness measurements for different temperatures for 0.5% wt ZDDP in oil**



There is very good agreement between simulation and experiment, and both show that the tribofilm formed under these different conditions has a different thickness. The tribochemical model predicts the growth of the tribofilm at asperity scale. Therefore the next step would be to examine the effect of this formed tribofilm on wear of the system using the proposed wear model. Wear measurement results are shown in the next section and the predicted numerical results are reported in Section 7.3.2 and 7.3.3.

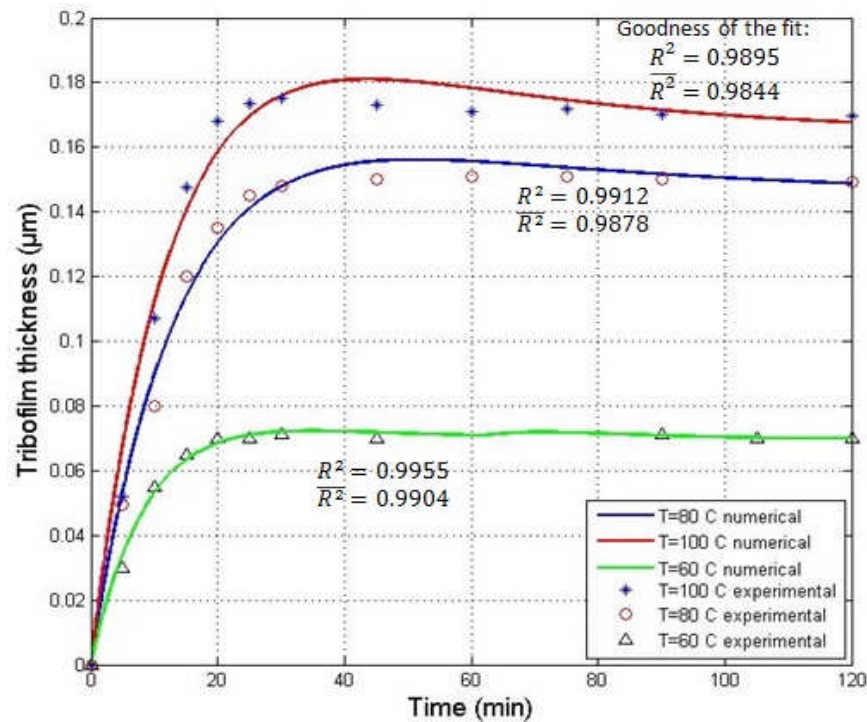


**Figure 7-5 Example of numerical and experimental tribofilm growth for 1% wt ZDDP in oil at three different temperatures**

**Table 7-1 Numerical inputs and calibrated parameters**

Parameter	1% Wt ZDDP			0.5% Wt ZDDP	Description
	100°C	80°C	60°C	100°C	
<b>K</b>	$5.45 \times 10^{-8}$	$5.45 \times 10^{-8}$	$5.45 \times 10^{-8}$	$5.45 \times 10^{-8}$	Initial Dimensionless wear coefficient for steel
<b><math>COW_{min}</math></b>	$5.45 \times 10^{-9}$	$5.45 \times 10^{-9}$	$5.45 \times 10^{-9}$	$5.45 \times 10^{-9}$	Dimensional wear coefficient for maximum film thickness
<b><math>h_{max}</math></b>	250 nm	200 nm	150 nm	250 nm	Maximum local tribofilm thickness in the formation process
<b><math>x_{tribo}</math></b>	$1.66 \times 10^{-16}$	$1.66 \times 10^{-16}$	$1.66 \times 10^{-16}$	$1.30 \times 10^{-16}$	Tribofilm formation rate constant
<b><math>C_1</math></b>	0.08566	0.05432	0.08052	0.08052	Tribofilm removal constant
<b><math>C_2</math></b>	0.000457	0.0004022	0.0004033	0.000406	Tribofilm removal exponential factor
<b><math>E_1, E_2</math></b>	209 GPa	209 GPa	209 GPa	209 GPa	Young's modulus of two surfaces
<b><math>\nu_1, \nu_2</math></b>	0.3	0.3	0.3	0.3	Poisson ratio
<b><math>H_{steel}</math></b>	6 GPa	6 GPa	6 GPa	6 GPa	Hardness of the steel substrate
<b><math>H_{tr}</math></b>	2 GPa	2 GPa	2 GPa	2 GPa	Hardness of the tribofilm at steady state tribofilm thickness

### 7.3.2 Wear results

White Light Interferometry using NPFLEX from Bruker was used to measure wear on the discs. An example of wear measurement images is shown in Figure 7-6.

The wear analysis in this work is based on the average wear depth profile and is compared to the numerical results. Wear depth is measured by comparing the average heights of points inside and outside the wear track. An example of this comparison is shown in Figure 7-7.

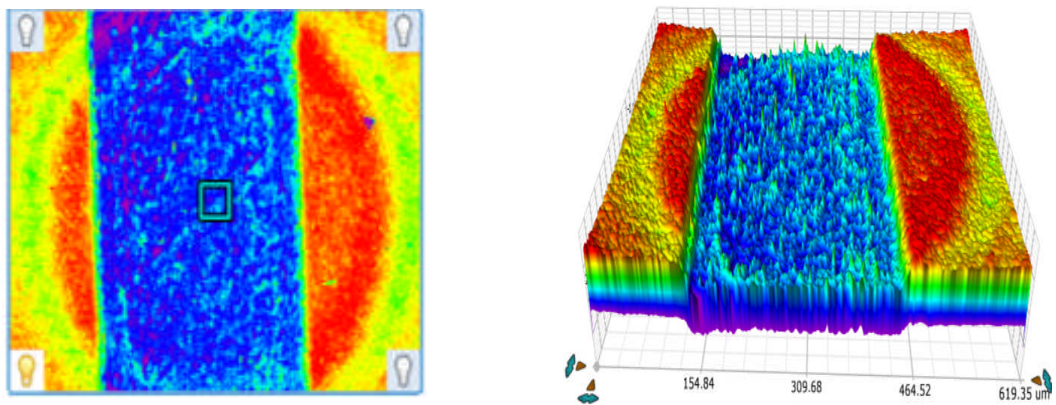


**Figure 7-6 2D and 3D images of wear track**

The measurement results for different working conditions as reported in Table 7-1 are shown in Figure 7-8 for 1% wt ZDDP in oil and Figure 7-9 for 0.5% wt ZDDP which give the wear depth measured for different samples. The experiments were conducted for different times for 1% wt ZDDP to see the evolution of wear and validating the model but only 2-hour experiments were carried out for 0.5% wt ZDDP in the oil.

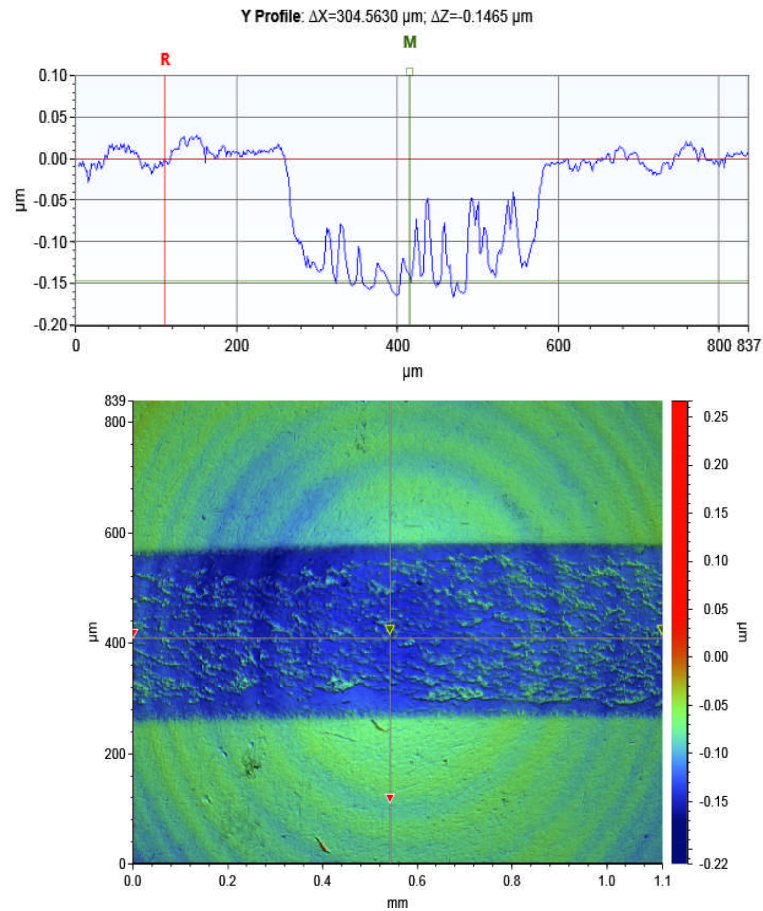


**Figure 7-7 2D wear track image and the image profile of the surface after the experiment**

From the comparison of the experimental results, it can be interpreted that a higher concentration of ZDDP in the oil increases the growth rate of the ZDDP tribofilm. It is also shown that a higher concentration of ZDDP results in less wear in the system. These conditions are simulated by the model and the results are reported in the next sections.

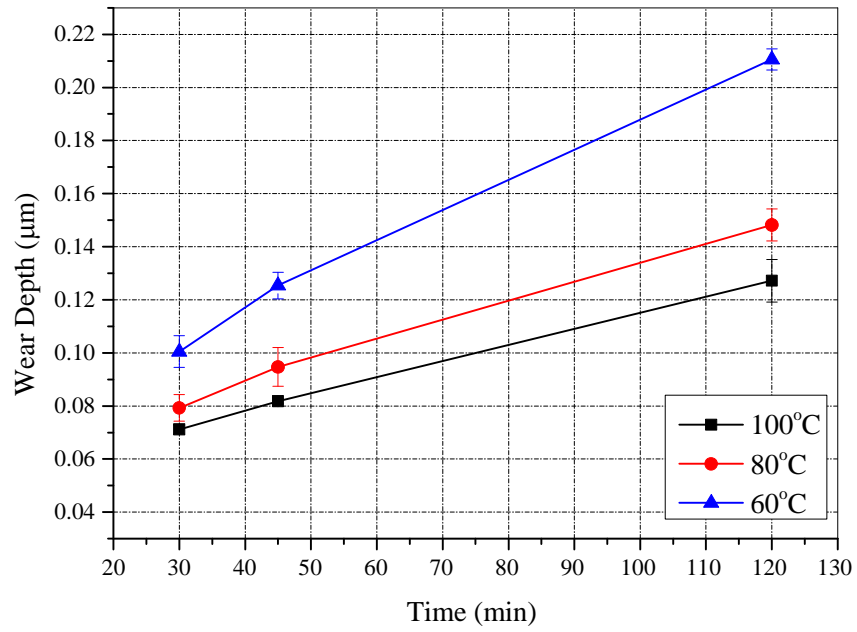


**Figure 7-8 Wear measurements for different temperatures and different times for 1% wt ZDDP in oil**

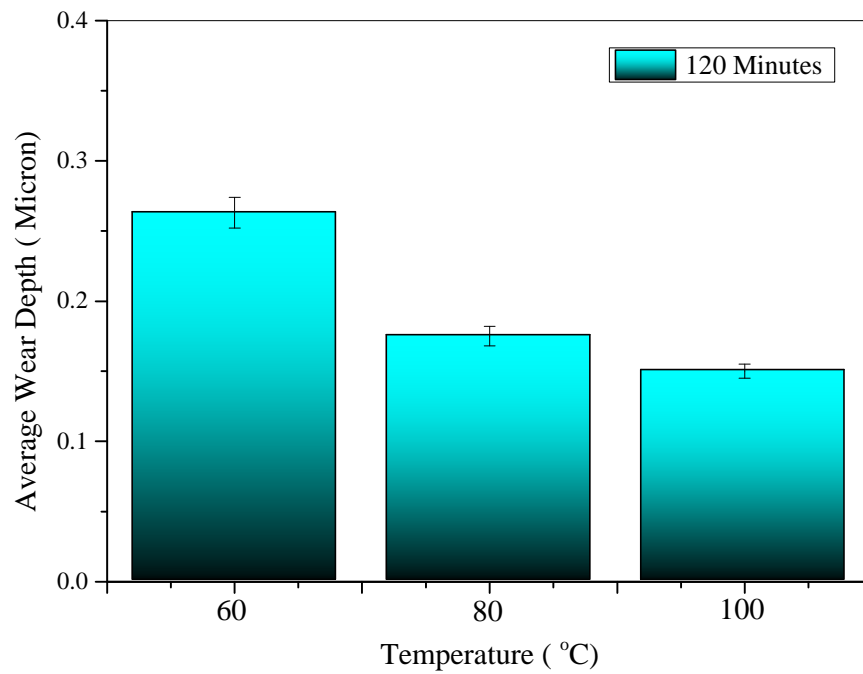


**Figure 7-9 Wear measurements for different temperatures for 0.5% wt ZDDP in oil at 2 hours**

### 7.3.3 Numerical results

The experimental wear depth measurements for 80°C at two hours were used to calibrate the wear model as described in Section 7.2. The initial coefficient of wear found agreed well with values reported in the literature (161, 167, 192). Wear is calculated at every time step of the simulation using the wear model described in Section 0, and plastic deformation is calculated in the elastic-perfectly plastic contact model.

The amount of wear is accumulated in time at every asperity in contact and the wear depth can be calculated at the end of simulation. The experiments reported in Section 7.3.2 were simulated via the model, and the predicted wear depth as a function of time is shown in Figure 7-10 for 1% wt ZDDP in oil and Figure 7-11 for 0.5% wt ZDDP. This strategy shows that if the model is able to capture the tribofilm growth on the surface it is also able to capture wear in the systems with this specific mechanism. The authors believe that this model in combination with the experiments can open new insights in the mechanisms of wear reduction of ZDDP on steel surfaces and relate it to the tribofilm formation and removal properties and can be extended to systems where tribochemical reactions form reactive layers and these layers offer a physical barrier to the surface. This would be the case for most P-containing antiwear additives.

For comparison with experiments, calculations of wear depth and tribofilm thickness are made by averaging values over the entire computational surface. The calibration parameters were then used to simulate the model to see the pattern of surface topography and wear of the system. No validation of such physical parameters was then reported and only the numerical model development and its capabilities were

studied. In this work experiments were conducted on MTM and the tribofilm growth results are based on the new measurements.

Tribofilm thickness experimental results are used to capture the growth behaviour by setting the simulation values with respect to the experimental results. It is important to notice that once the tribofilm behaviour is captured, the model is able to predict the wear behaviour for the case of ZDDP on steel surfaces. So far in this research, capturing the tribofilm behaviour was dependent on the experimental results due to the lack of comprehensive analytical understanding of the real mechanisms of tribofilm formation and removal. Despite all the complexities, such simplified semi-analytical models for tribofilm growth can be good starting points for the problem. As explained in detail in the previous work (107), there is more need for experimentation to develop the proposed tribofilm growth even further.

The parameters used in the tribofilm growth model such as  $x_{tribo}$ ,  $h_{max}$ ,  $C_3$  and  $C_4$  for different sets of experiments are reported in Table 7-1. It can be seen from Table 7-1 that the fitting parameters are different for different experiments and this is not surprising due to the different growth behaviour in each experiment. The calibration results in this work reported in Table 7-1 are in line with the theories explained in (107). It can be seen that  $x_{tribo}$  is the same for different temperatures of the same condition. It is also reasonable to have smaller  $x_{tribo}$  for lower concentration of ZDDP in the oil.

These results are in agreement with the concept of  $x_{tribo}$  which was explained in details in (107, 156). In principle, this term relates to the proportion of transition states in the tribochemical reaction that result from mechanical activation; in practice it is a fitting parameter to be calibrated via experiments providing *in-situ* measurements of tribofilm thickness. The advantage of this model is the ability to link

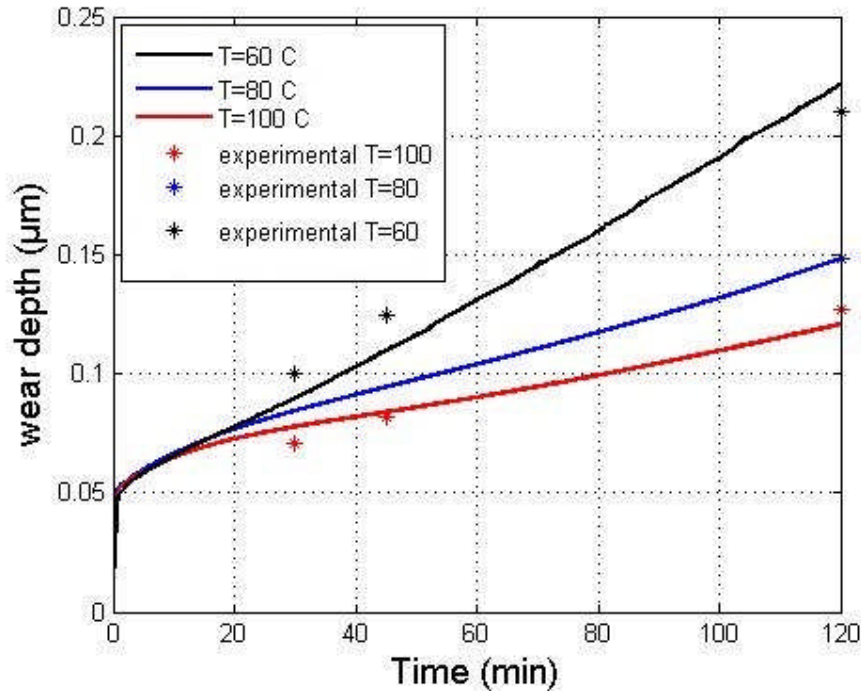
to component scale measurements. It must be noted that the work strongly supports the fact the tribofilm reactions need shear stress to initiate. The temperature dependency of the kinetics is not exponential like conventional Arrhenius type equations. The term  $\alpha_{tribo}$  is independent of the temperature and it is confirmed in the numerical results reported in Table 7-1. It shows that concentration of lubricant additives can be considered in the growth modelling of their tribofilm. Since this is not the focus of this work, further discussion on the growth model is not presented here.

As explained in Section 7.3.3, the coefficient of wear in the simulation is time and position-dependent. Therefore the average coefficient of wear at each time in the simulation can be obtained by averaging the values for coefficient of wear for all contacting points. The variation of the average coefficient of wear with time for different temperatures in the case of 1% ZDDP in the oil is plotted in Figure 7-12. It can be interpreted from the results that growth of the tribofilm on the contacting spots can reduce the average wear coefficient and that results in the overall wear reduction. The average wear coefficient tends to stabilize when the tribofilm thickness stabilizes and this is where the steady-state wear can start.

The predicted pattern of wear depth seen in Figure 7-10 and Figure 7-11 shows that a relatively fast plastic deformation happens in the beginning of the contact and the rate of the wear reduces as the rate of plastic deformation reduces. The wear of material still remains and is responsible for the reduction in depth of the contact. Formation of the tribofilm on the contact spots results in the reduction of wear rate and is responsible for less wear being observed in numerical results. The amount of wear observed experimentally after 30 minutes and 45 minutes at 100°C and 60°C for 1% wt ZDDP in oil are also shown as discrete data points in Figure 7-10. The simulation



predictions show reasonably good agreement with the experimental measurements; see also Table 7-2 for comparison of the data values.



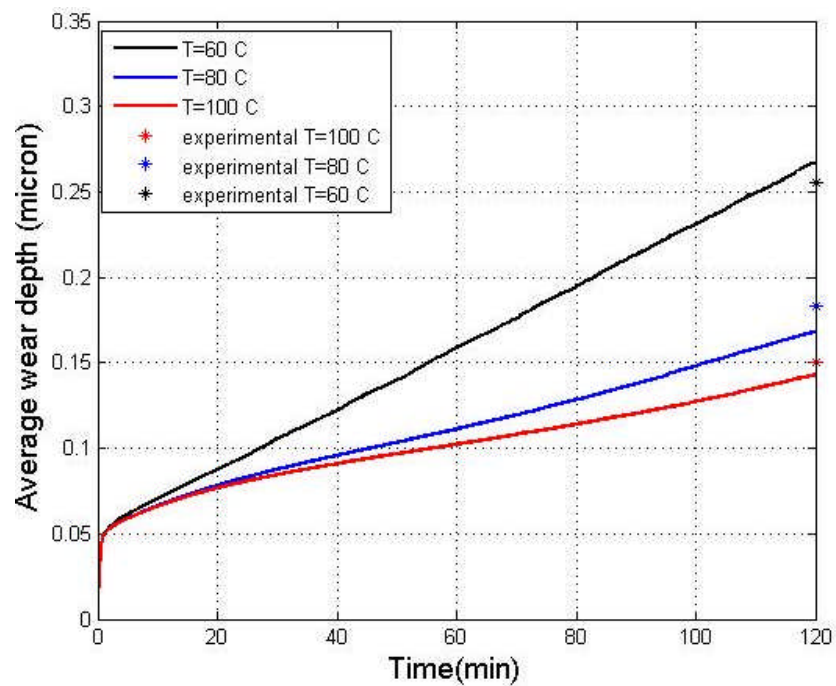
**Figure 7-10 Simulation of wear for different temperatures at 2 hours for 1% wt ZDDP in oil**

Figure 7-10, Figure 7-11 and Figure 7-9 together therefore highlight that the effect of the ZDDP tribofilm on the coefficient of wear is well captured by the model. The tribochemical wear model tested in this study can be applied to systems similar to the one reported here; where a reacted film with varying chemistry through the thickness is formed. As the tribofilm starts to grow on the surface, the rate of this growth plays a significant role in the rate of reduction of the coefficient of wear.

The thickness reported in most experimental studies is the steady-state tribofilm thickness, but the coefficient of wear in this work is a function of time and changes with the gradual changes in the thickness of the tribofilm. Therefore it is possible to

have a thicker tribofilm in the simulation at steady-state while also having a higher wear.

The tribofilm thickness measurements resulting from Spacer Layer Interferometry were used to calibrate the tribochemical model of Equation 7-1. Simulations were carried out using the calibrated parameters and working conditions. The simulation results show that the assumption of a lower time and spatially-dependent coefficient of wear for thicker tribofilms is reasonable for the case of different temperatures and different concentrations of ZDDP in the oil.



**Figure 7-11 Simulation of wear for different temperatures at 2 hours for 1% wt ZDDP in oil**

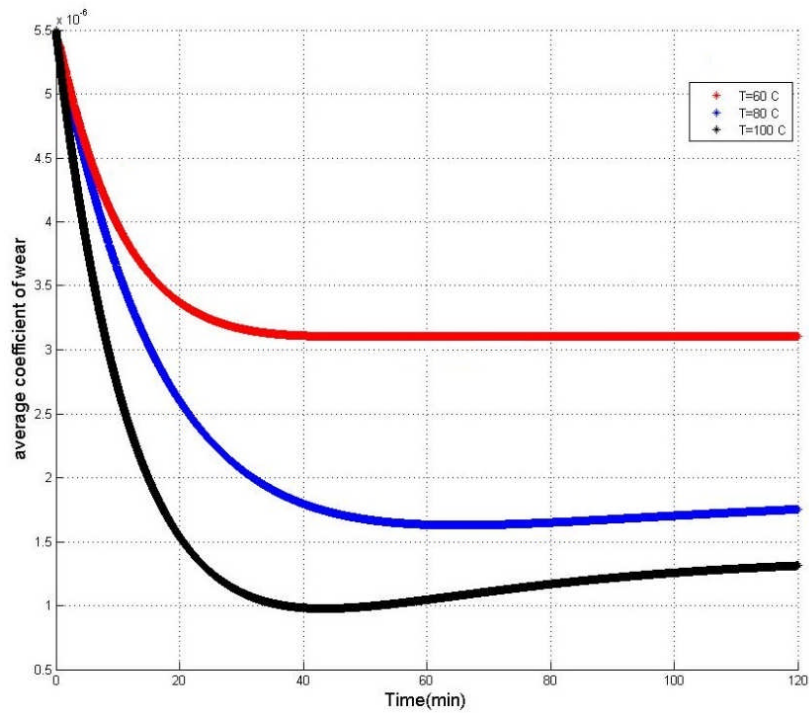


**Figure 7-12 Variation of the average coefficient of wear with time for different temperatures for 1% wt ZDDP in oil**

It can be seen in Figure 7-10 and Figure 7-11 that at the start of the tribo-contact, simulations show almost the same wear because of high plastic deformation. At some point, when the tribofilm starts to grow, and because of variable reaction rates (indicated by  $x_{tribo}$  values), the coefficient of wear starts to decrease and the rate of this decrease depends on temperature and concentration of additive. This fact is also confirmed in Figure 7-12. The experimental results support the model.

**Table 7-2 Comparison between experimental measurements and numerical wear depth calculations**

	<b>Test</b>	<b>Experimental wear depth measurements (<math>\mu\text{m}</math>)</b>	<b>Numerical wear depth results (<math>\mu\text{m}</math>)</b>
1% wt ZDDP	100°C_30 min	0.0712	0.0778
	100°C_45 min	0.0818	0.0839
	100°C_120 min	0.1272	0.1208
	80°C_30 min	0.0793	0.0798
	80°C_45 min	0.0947	0.0952
	80°C_120 min	0.1482	0.1484
	60°C_30 min	0.1006	0.0917
	60°C_45 min	0.1252	0.1121
	60°C_120 min	0.2102	0.2215
0.5% wt ZDDP	100°C_120 min	0.1505	0.1430
	80°C_120 min	0.1830	0.1682
	60°C_120 min	0.2550	0.2676

#### **7.4 Analytical study of the effect of mixed-water**

The experimental results reported in Chapter 5 are used in this section in two different approaches to predict wear of the boundary-lubricated contact with the oil containing ZDDP additive.

#### 7.4.1 First approach: semi-deterministic coefficient of wear

In this approach it is assumed that the tribofilm thickness is following the same behaviour for all levels of water concentration. It means that the growth of tribofilm is the same for all water concentration experiments and the same amount of tribofilm is formed on the surfaces for all different experiments. This is not accurate in reality and experimental results reported in chapter 5 show otherwise. But this approach is used to see if the same tribofilm growth behaviour is modelled for all experiments, a modification to Archard's wear equation can predict the wear of the system. The only parameter that can be affected by water is assumed to be the *initial* coefficient of wear. The calibration procedure for the *initial* coefficient of wear is reported in Ref (109). This approach is applied to semi-deterministically find the true coefficient of wear corresponding to the different levels of water concentration. The value of the average wear depth measured experimentally and reported in Section 5.2 was used to match the average wear depth results from the simulations for every level of water concentration. The procedure for determining the initial wear coefficient involves conducting simulations with different initial coefficients of wear to identify the coefficient value that exactly matches the wear behaviour observed in the experiment. The difference between the value of the calculated wear and the wear measured experimentally in Section 5.2 was set to be less than 0.1 nm in order to get the best match. The *initial* wear coefficients calculated from the simulations are reported in Table 7-3 for different water concentrations for 80°C and 100°C.

A factor  $\psi$  is added to the proposed wear model of Equation 7-2 that is responsible for the effect of water on tribocorrosive wear of the system. Equation 7-2 is then converted to Equation 7-3.

$$K_{tr} = \Psi K_{steel} - (\Psi K_{steel} - K_{min}) \cdot \frac{h}{h_{max}} \quad 7-3$$

$\psi$  is calculated between 1 and 2.5 in all ranges of water concentrations and is more for higher concentrations. These simulation results show that the coefficient of wear can be modelled for different levels of water concentration to predict wear. If the appropriate  $\Psi$  value is assigned in the simulation of wear in the presence of water, wear values can be successfully predicted by Equation 7-3.  $\Psi$  is then reported in Table 7-4 for different levels of water concentration.

**Table 7-3 Wear coefficients used in the numerical simulations (Dimensionless)**

Temperature	0%	0.5 %	1.5%	3%
100 °C	$10^{-8}$	$1.64 \cdot 10^{-8}$	$1.65 \cdot 10^{-8}$	$2.3 \cdot 10^{-8}$
80 °C	$2 \cdot 10^{-8}$	$2.7 \cdot 10^{-8}$	$3.1 \cdot 10^{-8}$	$3.5 \cdot 10^{-8}$

**Table 7-4  $\Psi$  for different water concentrations at different temperatures (Dimensionless)**

Temperature	0%	0.5 %	1.5%	3%
100 °C	1	1.35	1.55	1.75
80 °C	1	1.64	1.65	2.30

### 7.4.2 Second approach: effect of tribochemistry

To study the effect of tribochemistry, unlike the first approach, the starting coefficient of wear is assumed to be the same in the numerical model for different levels of water concentration. Following that, the effect of water in changing the growth behaviour of the tribofilm observed experimentally in Chapter 5 has been used to capture the behaviour in the model. The changes in growth behaviour of the tribofilm will change the wear coefficient locally at the asperity scale. For the tribofilm growth part of the model, the four parameters  $x_{tribo}$ ,  $h_{max}$ ,  $C_1$  and  $C_2$  need to be determined for each set of experimental conditions in order to capture the tribofilm behaviour, which is different in each case. This is achieved by fitting Equation 7-1 to experimental measurements of tribofilm thickness of Section 5.3. These parameters are reported in Table 7-5 for different water contents. The wear is then calculated with respect to this growth behaviour and the results have been compared to the experimental wear depth results obtained experimentally.

The tribofilm growth simulation results are plotted Figure 7-13. The simulation wear results corresponding to the different levels of water concentrations for 100 °C and 80 °C are also shown in Figure 7-14 and are compared with the experimental results of section 5.3 . It can be seen that tribofilm affects the wear of the system. In the higher concentrations of water a lower rate of formation of the tribofilm is being observed. This lower rate of formation results in higher coefficient of wear according to Equation 7-2. It is important to notice that once the tribofilm behaviour is captured (Figure 7-13), the model is able to predict the wear behaviour for the case of ZDDP on steel surfaces (Figure 7-14).

**Table 7-5 Simulation inputs and calibration parameters**

<b>T=100°C</b>				
Water Concentration (wt %)	0	0.5	1.5	3
$x_{tribo}$	$1.66 \times 10^{-16}$	$1.56 \times 10^{-16}$	$1.41 \times 10^{-16}$	$1.35 \times 10^{-16}$
$h_{max}$ (nm)	250	250	250	250
$C_1$ (nm)	85.86	95.92	132.7	134
$C_2$	0.000457	0.000408	0.0003149	0.000331
<b>T=80°C</b>				
Water Concentration (%)	0	0.5	1.5	3
$x_{tribo}$	$1.66 \times 10^{-16}$	$9.65 \times 10^{-17}$	$8.85 \times 10^{-17}$	$7.45 \times 10^{-17}$
$h_{max}$ (nm)	200	200	200	200
$C_1$ (nm)	54.32	100	120	120
$C_2$	0.0004022	0.000098	0.0001067	0.0001042

So far in this research, capturing the tribofilm behaviour was dependent on the experimental results due to the lack of comprehensive mechanistic understanding of tribofilm formation and removal. Despite all the complexities, such simplified semi-analytical models for tribofilm growth can be good starting points for the problem.



This is therefore a good approach for modelling wear in boundary lubricated contacts which can include the effect of water in the tribological behaviour of the system.

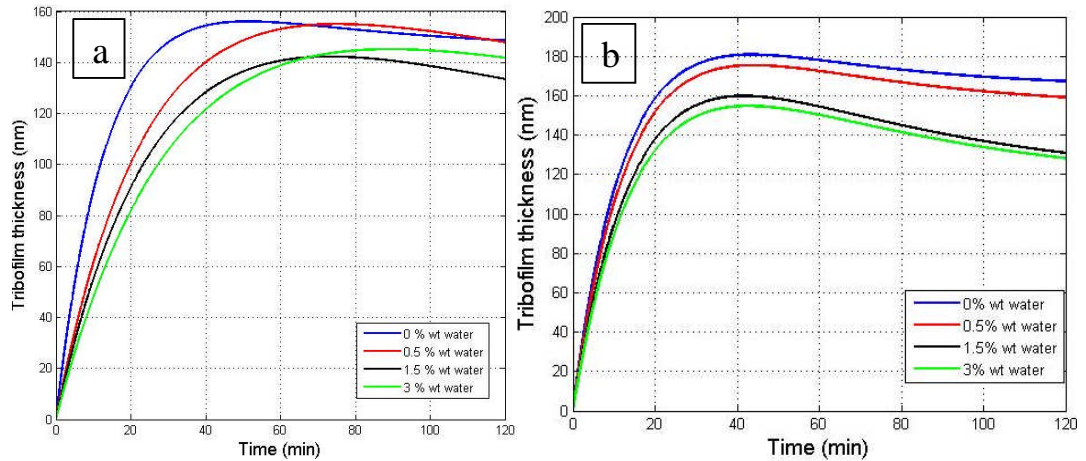


**Figure 7-13 Tribofilm growth simulations for (a) 80°C and (b) 100°C**

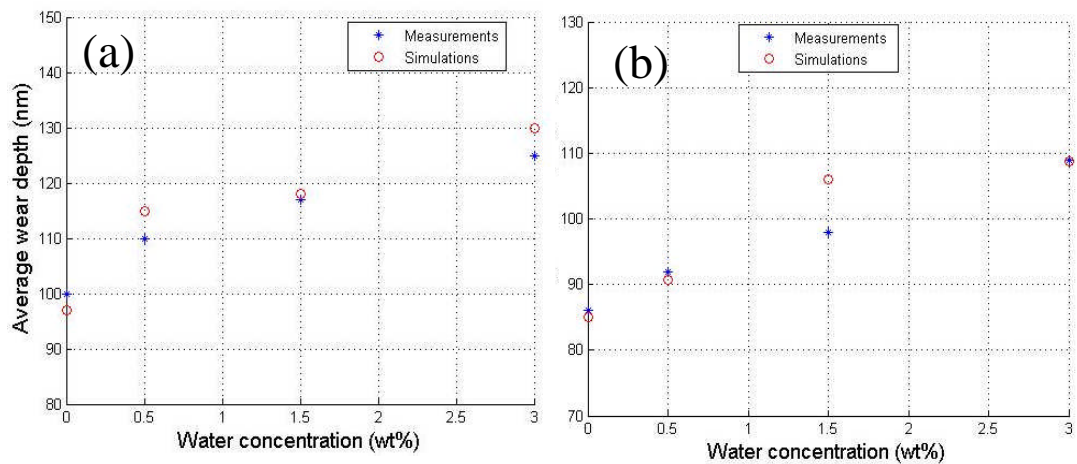


**Figure 7-14 Numerical wear calculation compared with experimental measurements (a) 80°C and (b) 100°C**

Tribocorrosive wear of the boundary lubricated system by oil containing a ZDDP antiwear additive has been modelled in this work considering the tribochemistry of the antiwear additive. It is shown that considering growth behaviour of the tribofilm

for ZDDP on steel surfaces is a reasonable approach for modelling wear in tribocorrosive tribological systems. Experiments were designed to monitor the tribofilm growth in addition to the measurement of wear to be able to make a link between them. Two numerical approaches were tested in this work in order to study the effect of water in tribocorrosive wear of the boundary lubrication contacts and the results were shown in the previous section. For the first approach, coefficients of wear were semi-deterministically obtained from the simulations to satisfy the wear measurements.

This approach suggests that for different water concentrations wear of the system is different and Archard's wear equation needs to be modified accordingly. It was reported in Section 7.4.1 of the numerical results that a modification parameter can be used to modify the Archard's wear coefficient in the previously reported tribochemistry wear model. This parameter ( $\psi$ ) is calculated from the simulations and the range was between 1 and 2.5 for all water concentrations used in this study. It is shown that, without changing the growth behaviour of the tribofilm (tribochemistry), simulations can predict the wear of tribocorrosion systems by changing the Archard's wear coefficient. In the second approach, unlike the first one, the effect of water on the growth of the ZDDP tribofilm was considered.

The growth model was calibrated for all different tribofilm growth cases and the simulations were carried out using those growth behaviours. The coefficient of wear was assumed to be constant for all the simulations in this approach unlike the first approach and the only parameter changing the coefficient of wear was the difference in tribofilm thickness of the different cases. Wear results in this case were shown in the previous section and good agreement can be seen with experimental results.

As shown in Table 7-5 Simulation inputs and calibration parameters the rate of formation of tribofilm is different for different levels of water concentration at the same temperature. The term  $x_{tribo}$  which is responsible for the effect of mechanical rubbing on the initiation of tribochemical reactions (107) is reported in Table 1-6. It is clear both from experimental and numerical results that the formation rate decreases when water concentration increases. The term  $x_{tribo}$  for different levels of water concentration is plotted in Figure 7-15.

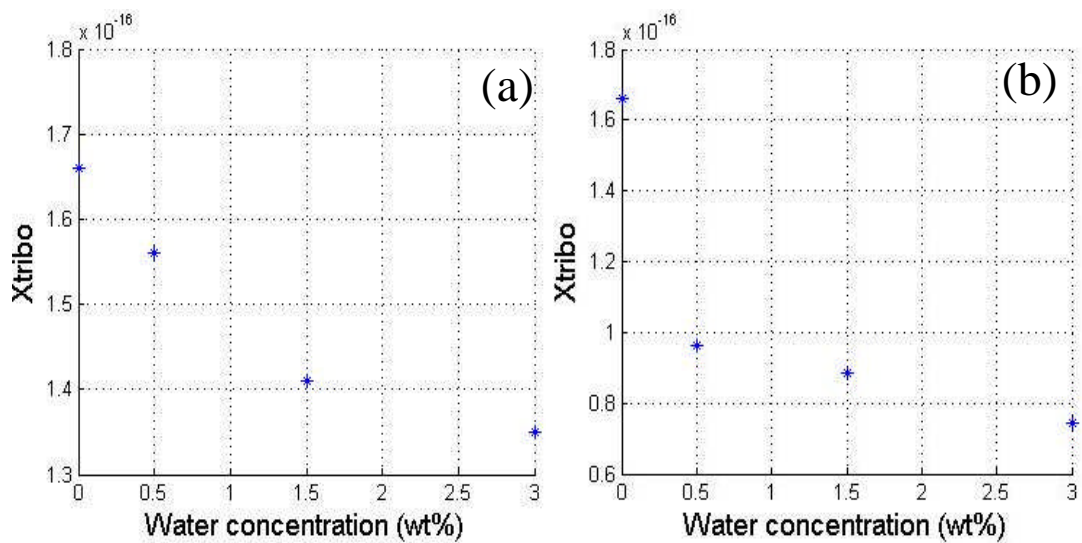


**Figure 7-15**  $x_{tribo}$  calibrated for different temperatures at different water concentrations at (a) 100°C and (b) 80°C

The simulation results based on the second approach show that if a good prediction in the growth behaviour of the tribofilm is calculated, it can lead to a good prediction in the wear of the system. In previous work by Ghanbarzadeh *et al* (109), the wear model and the effect of tribofilm in reducing wear have been studied and the numerical model showed good predictive capabilities for wear. The term  $x_{tribo}$  that is a major part in the growth behaviour of the tribofilm will be the subject of future work of the authors with a focus being on how different oils and tribological parameters affect the value. Understanding and being able to quantify this term for tribocorrosion

conditions will help to obtain a more robust predictive tribofilm growth model. Tribofilm growth prediction then impacts the prediction of wear according to Equations 7-1 and 7-2. In this stage of the work, only the predictive capability of the model in tribocorrosive conditions was tested and the results are promising. More results and development of this model will be reported in the future.

## **7.5 Analytical study of the effect of relative humidity**

The wear in this work is predicted in two different numerical approaches. The experimental results of Chapter 6 are used to both calibrate and validate the model. Both numerical approaches are described in detail below.

### **7.5.1 Semi-deterministic coefficient of wear (approach one)**

In this approach, it is assumed that the tribofilm thickness is following the same trend in all levels of humidity and the tribofilm growth model of Equation 7-1 is not modified for different levels of humidity. This is not correct in reality and the experimental results of Chapter 6 show otherwise. But the rationale for this is to see the effect of humidity on modifying the Archard wear equation without taking care of the tribofilm properties. So one can model the humidity and predict wear without considering changes in the tribofilm and only using Archard's wear equation.

The only parameter that can be affected by humidity in Equation 7-2 is assumed to be the *initial* coefficient of wear ( $K_{steel}$ ). The calibration procedure for the initial coefficient of wear is reported in detail in Ref (109). This approach is applied to semi-deterministically find the true coefficient of wear corresponding to the different levels of humidity. The value of the average wear depth measured experimentally and reported in Section 6.5 was used to match the average wear depth results from the simulations for every level of humidity. The procedure for determining the initial wear

coefficient involves conducting simulations with different initial coefficients of wear to identify the coefficient value that exactly matches the wear behaviour observed in the experiment. The difference between the value of the calculated wear and the wear measured experimentally in Section 6.5 was set to be less than 0.1 nm in order to get the best match. The initial wear coefficients calculated from the simulations are reported in Table 7-6 for different levels of humidity at 80 °C and 98 °C.

**Table 7-6 Dimensionless *initial* wear coefficients in the numerical simulations in the first approach**

Relative Humidity	Temperature 80°C	Temperature 98°C
0	$2.2 \times 10^{-8}$	$1.2 \times 10^{-8}$
20	$2.5 \times 10^{-8}$	$1.3 \times 10^{-8}$
30	$2.6 \times 10^{-8}$	-----
40	$2.95 \times 10^{-8}$	$2 \times 10^{-8}$
50	$3.1 \times 10^{-8}$	$2.2 \times 10^{-8}$
60	$3.5 \times 10^{-8}$	-----
70	$4 \times 10^{-8}$	-----
80	$4.2 \times 10^{-8}$	$2.3 \times 10^{-8}$
95	$6 \times 10^{-8}$	$2.35 \times 10^{-8}$

A factor  $\phi$  is added to the proposed wear model of Equation 7-2 that is responsible for the effect of humidity on tribocorrosive wear of the system. These values are reported in Table 7-7. Equation 7-2 is then converted to Equation 7-4 as follows:

$$K(h) = \varphi \cdot K_{steel} - (\varphi \cdot K_{steel} - K_{min}) \cdot \frac{h}{h_{max}} \quad 7-4$$

In which  $\varphi$  is the modification parameter used to take into account the effect of humidity in Archard's wear equation. This approach is a good approach for designers of machine elements to include the tribochemical effects of humidity on the wear of boundary lubricated systems without any detailed chemical analysis only by modifying Archard's wear equation. If the appropriate  $\varphi$  value is assigned in the simulation of wear in humid environment, wear values can be successfully predicted by Equation 7-4.

**Table 7-7  $\varphi$  factors for modifying the Archard equation for different levels of relative humidity**

Relative Humidity	Temperature 80°C	Temperature 98°C
0	1	1
20	1.13	1.08
30	1.18	-----
40	1.34	1.66
50	1.41	1.83
60	1.6	-----
70	1.81	-----
80	1.90	1.91
95	2.72	1.95

### 7.5.2 Effect of tribochemistry (approach two)

In this approach, unlike the first approach, the *initial* coefficient of wear ( $K_{steel}$ ) is assumed to be constant and the effect of humidity on the growth of tribofilm on contacting asperities is investigated numerically. The tribofilm growth results reported 6.3 was used to capture the behaviour in the model. As discussed in 6.3, the changes in growth behaviour of the tribofilm will change the wear coefficient locally at the asperity scale based on Equation 7-2.

The parameters ( $x_{tribo}$ ,  $h_{max}$ ,  $C_3$  and  $C_4$ ) are obtained by fitting the mathematical expression of Equation 7-1 to experimental tribofilm thickness results in 6.3. Inevitably a semi-deterministic model such as the one used here involves a number of parameters that must be determined by reference to experimental data. It is therefore natural to ask: what is the sensitivity of the model to the values of these parameters, and how can such parameters be determined in the absence of experimental data? Indeed, the model of equation 7-1 has been adapted to the pool of experimental results available in the literature, to provide a good indication of the range of the parameters and to allow selection of a reasonable set of calibration parameters in the absence of specific experimental data (see Ref (193)). The calibration parameters are reported in Table 7-8 and Table 7-9 for different levels of humidity. The wear is then calculated with respect to this growth behaviour using Equation 7-2 and the results have been compared to the experimental wear depth results obtained experimentally.

The tribofilm simulation results are shown in Figure 7-16 and Figure 7-17 for 80°C and 98°C respectively. The wear results corresponding to the tribofilm simulations results are plotted in Figure 7-18 and Figure 7-19 and the simulation results are compared with experiments. It is clear that the different growth behaviour of the tribofilm on contacting asperities at various levels of relative humidity, affect the mild

wear of boundary lubricated contacts. This shows that higher level of humidity lower to thickness of the tribofilm which leads to higher wear based on Equation 7-2. It is important to note that while the growth of the tribofilm is captured, the model is successfully predicting wear of boundary lubricated contacts even in humid environments.

**Table 7-8 Simulation inputs and calibration parameters at 80°C**

<b>Relative Humidity %</b>	<b><math>h_{\max}</math> (nm)</b>	<b><math>X_{\text{tribo}}</math></b>
0	300	$1.88 \times 10^{-16}$
20	257	$1.74 \times 10^{-16}$
30	218	$1.75 \times 10^{-16}$
40	184	$1.75 \times 10^{-16}$
50	179	$1.83 \times 10^{-16}$
60	140	$1.89 \times 10^{-16}$
70	121	$1.84 \times 10^{-16}$
80	126	$1.9 \times 10^{-16}$
95	83	$1.93 \times 10^{-16}$



**Table 7-9 Simulation inputs and calibration parameters at 98°C**

Relative Humidity %	$h_{\max}$ (nm)	$X_{\text{tribo}}$
0	365	$1.54 \times 10^{-16}$
20	323	$1.47 \times 10^{-16}$
40	246	$1.75 \times 10^{-16}$
50	225	$1.86 \times 10^{-16}$
80	183	$1.93 \times 10^{-16}$
95	171	$1.85 \times 10^{-16}$

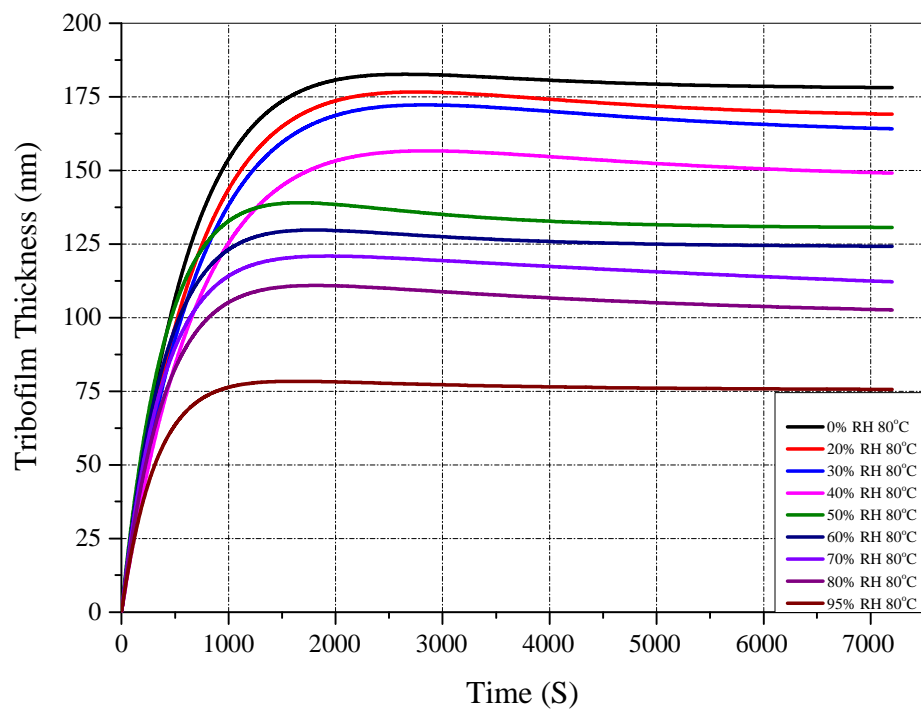


**Figure 7-16 Tribofilm growth simulations for different values of relative humidity at 80°C**

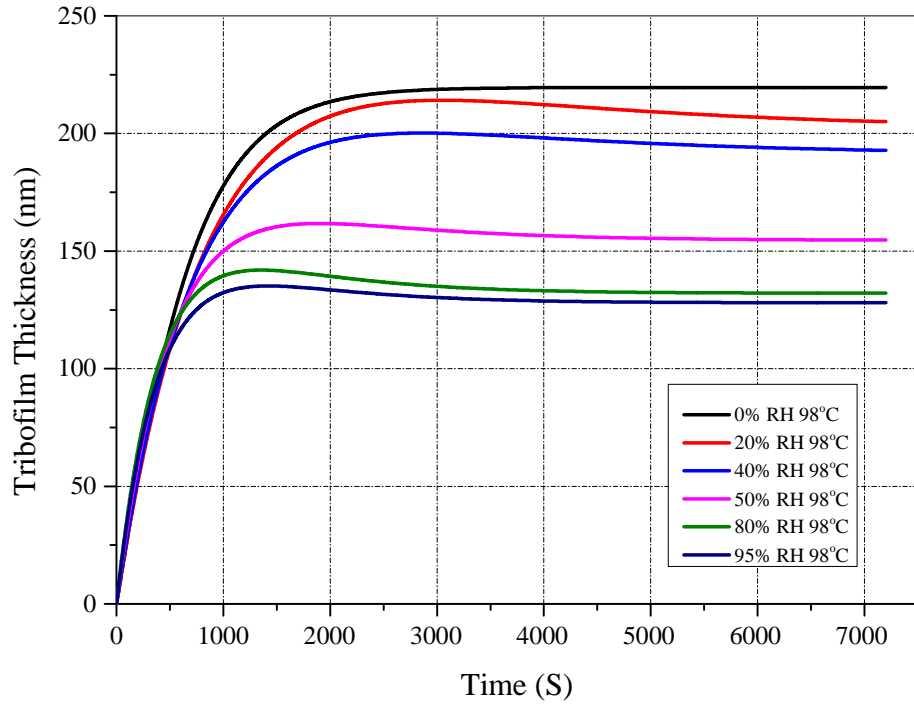


**Figure 7-17 Tribofilm growth simulations for different values of relative humidity at 98°C**

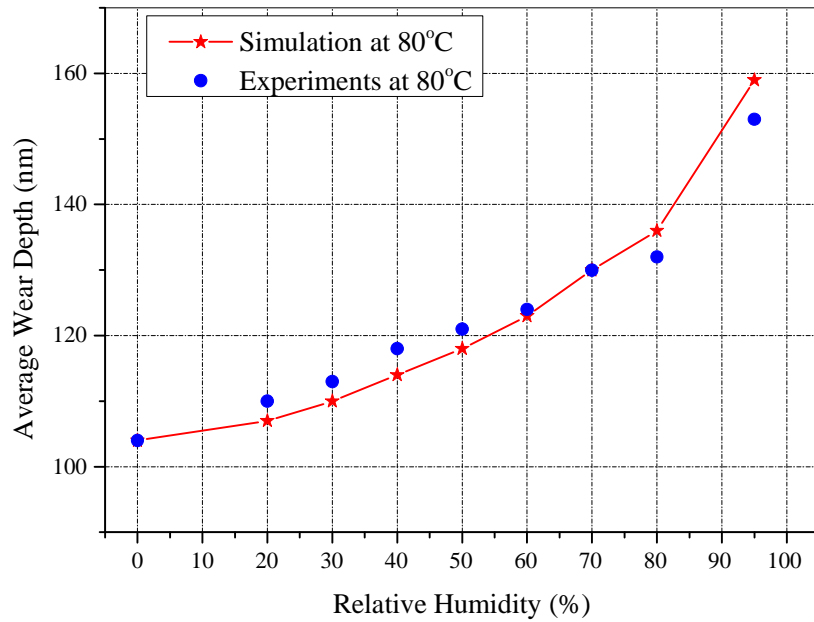


**Figure 7-18 Numerical wear calculation in comparison with experimental measurements at 80°C (calculated from second approach)**

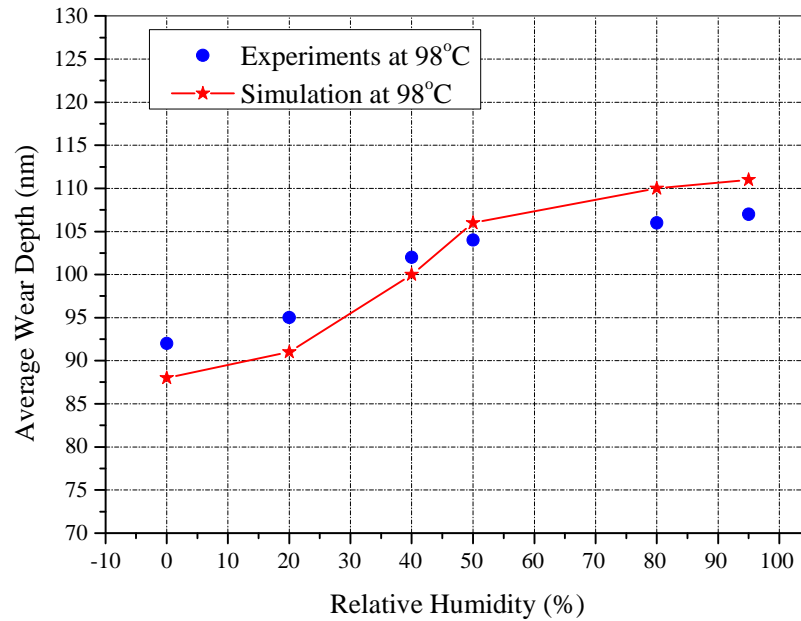


**Figure 7-19 Numerical wear calculation in comparison with experimental measurements at 98°C (calculated from second approach)**

The wear of boundary lubricated system in a tribocorrosive environment in the presence of ZDDP as an antiwear additive has been modelled in this work by considering the tribochemistry for different levels of relative humidity. The wear in this condition was modelled using two numerical approaches. As explained in Section 7.5.1, a modification to Archard's wear equation that accounts for the effect of relative humidity can successfully predict wear in boundary lubrication.

This approach can be simply used in design of machine elements working in humid environments. The modification parameter was reported to be between 1 and 2.8 for both temperatures and is in line with the recent reports of authors in Ref (110). The second approach accounts for the effect of tribofilm and its thickness at different relative humidity levels. The effect of relative humidity on the growth of ZDDP tribofilm was investigated in this approach. The same *initial* coefficient of wear was used in all simulations and the effect of tribofilm thickness in reducing the coefficient of wear was modelled. Wear was then predicted based on Equation 7-2 and fairly

good agreement was found between experimental and numerical results (Figure 7-18 and Figure 7-19 ).

Tribofilm thickness in this case follows Equation 7-1 in all levels of humidity and the model of Equation 7-1 was fit into the experimental tribofilm thickness results reported in Figure 7-16 and Figure 7-17 for 80°C and 98°C respectively. The fitting parameters are reported in Table 7-8 and Table 7-9 . These parameters were then used to run the simulations and predict wear based on Equation 7-2. It is presented that capturing the growth of tribofilm can be the first step for predicting the wear of boundary lubricated systems. Once the tribofilm behaviour is captured, the wear is successfully predicted using Equation 7-2.

It is clear from the experimental results of tribofilm growth, that the humidity hinder the further growth of tribofilm on the contacting asperities. The rate of growth of the tribofilm on the surfaces is almost similar for all humidity levels and this can be seen from the initial stages of the tribofilm growth in Figure 7-16 and Figure 7-17. On the other hand, the steady-state film thickness that tribofilm reaches, is significantly affected by relative humidity (203).

In the tribochemistry model of Equation 7-1, steady-state tribofilm thickness is a combined effect of steady-state tribofilm formation ( $h_{max}$ ) and the steady-state tribofilm removal ( $C_3$ ) terms. Extracting these information from fitting Equation 7-1 into experimental tribofilm growth results, show that the tribofilm formation rate term ( $x_{tribo}$ ) is not significantly dependant on the relative humidity as was expected from the experimental results (the rate of growth seems to be similar for different levels of relative humidity). On the other hand, the term  $h_{max}$  in the model which is a representation of maximum tribofilm formation (not growth) in the absence of tribofilm removal, is significantly affected by relative humidity. In this regard, the

calibrated  $h_{max}$  reported in Table 7-8 and Table 7-9 are plotted for different levels of relative humidity in Figure 7-20 and Figure 7-21 for 80°C and 98°C respectively. It can be seen that the term  $h_{max}$  is clearly reducing linearly with relative humidity values.

The mathematical model representing this behaviour for both temperatures are presented below

$$\begin{aligned} h_{max} &= -2.27 \times RH + 291.31 & T &= 80^{\circ}C \\ h_{max} &= -2.10 \times RH + 352.05 & T &= 98^{\circ}C \end{aligned} \quad 7-5$$

In which RH is the relative humidity percentage ranging from 0 to 100.

In order to modify the tribochemistry model of Equation 7-1 it has been decided to see the effect of relative humidity on the maximum film formation form and averaging the above mentioned equations. The variation of  $h_{max}$  with relative humidity can be expressed as:

$$h_{max} = -2.18 \times RH + 321.68 \quad 7-6$$

Equation 7-6 can be used to predict the term  $h_{max}$  in Equation 7-1 in humid environments which then can lead to a good prediction of tribofilm growth on the surfaces and result in good prediction of wear in boundary lubricated systems in the presence of anti-wear additives. The tribochemical model of Equation 7-1 is then converted to:

$$h(t) = (-2.18 \times RH + 321.68) \left( 1 - e^{\left( \frac{-k_1 T}{h'} \cdot x_{tribo} \cdot t \right)} \right) - C_3 (1 - e^{-C_4 t}) \quad 7-7$$

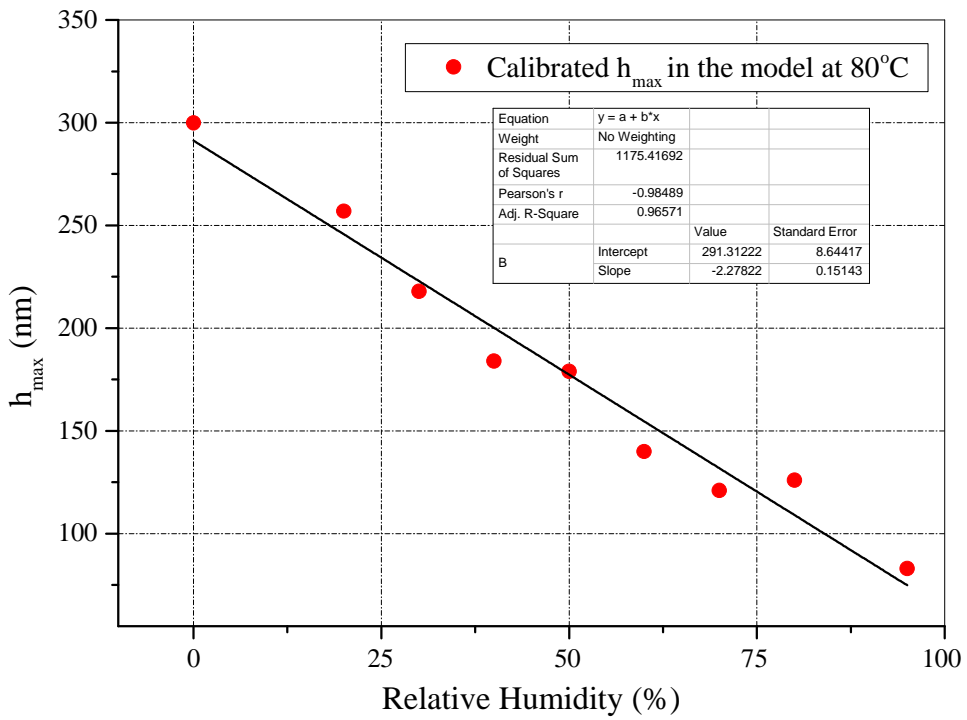


Figure 7-20 Variation of  $h_{\max}$  by relative humidity at 80°C

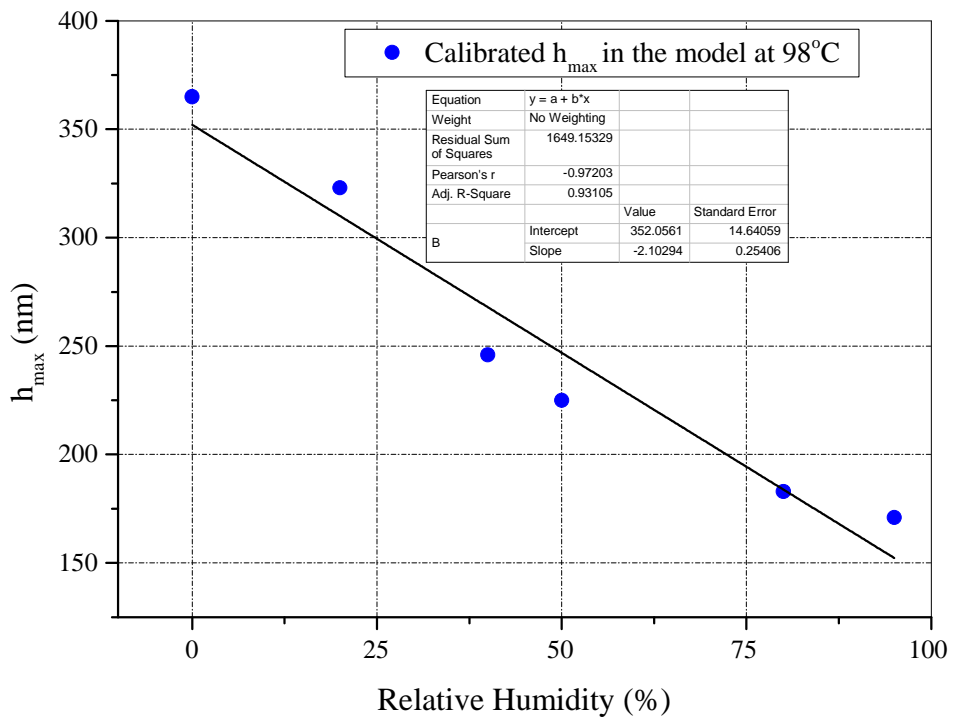


Figure 7-21 Variation of  $h_{\max}$  by relative humidity at 98°C

It should be mentioned that equation 7-7 is valid for the specific range of temperature between 80°-100°C for this experimental conditions. According to the calibration of Equation 7-1 at different humidity levels, the term  $x_{tribo}$  which in principle is responsible for the formation rate of tribofilm, is not significantly affected by altering the humidity. This is because the humidity does not affect the growth rate of the ZDDP tribofilm considerably as shown in Experimental results of 6.3 in comparison with the effect of mixed-water in the oil which can significantly affect the growth rate of the tribofilm (110).

## **7.6 Summary**

A semi-analytical approach was applied to model the effect of relative humidity and mixed-water in oil on tribofilm growth and wear in boundary lubricated system in presence of ZDDP as an anti-wear additive. Two approaches were employed to implement the effect of relative humidity and mixed-water in oil in predictive wear model and experimental results were used to validate the prediction results.

### **7.6.1 Analytical study of the effect of mixed-water**

The experimental results obtained from the effect of mixed-water in oil were used to adapt Archard's wear coefficient to the tribocorrosive conditions. The new wear model considering the effect of water was implemented into the previously-reported numerical model to develop a new semi-deterministic numerical wear model adapted to the tribo-corrosion system in this section (See Section 7.4). The key observations can be summarised as shown below:

1. Two different numerical approaches were used to test the model and also represent the effect of water in wear of the system. With respect to the first approach, tribocorrosive wear can be predicted by modifying the Archard's

wear coefficient. The modification parameter ( $\Psi$ ) increases by increasing the water concentration. The simulation wear results show good agreement with the experimental wear measurements.

2. It is concluded in this work that once the characteristics of the tribofilm growth are captured, the model is capable of predicting tribocorrosive wear in boundary lubrication regime.

### **7.6.2 Analytical study of the effect of relative humidity**

Relative humidity and its effects on tribochemistry and wear of boundary lubricated systems was examined experimentally in Chapter 6. In the current study the tribofilm thickness and wear results obtained experimentally are used to develop a semi-deterministic approach to implement the effect of humidity in wear prediction of boundary lubrication for the first time.

A semi-analytical approach was applied to model the effect of relative humidity on tribofilm growth and wear in boundary lubricated system in presence of ZDDP as an anti-wear additive (See Section 7.5). Two approaches were employed to implement the effect of relative humidity in predictive wear model and the following observations can be drawn:

1. In regards to the first approach, Archard's wear coefficient is semi-deterministically obtained for different levels of relative humidity from the simulations. This can lead to the modification of Archard's wear equation with a modification factor of  $\phi$ . This approach can be used by designers of tribological parts to take in to account the effect of humid environment on the durability.
2. In addition, the modification factor  $\phi$  is increasing while the humidity increases.



3. The second numerical approach was applied to consider the effect of humidity on the tribofilm growth and the corresponding wear behaviour in boundary lubrication. It is shown that successfully capturing the tribofilm growth behaviour leads to predicting the tribochemical wear in boundary lubricated conditions.
4. It was the effect of relative humidity on tribofilm growth behaviour and wear is different from the effect of mixed-water in the oil which was the subject of a recent study by the authors. In the latter case, the maximum film thickness was found the same for different levels of water concentration while the tribofilm growth rate found to be significantly affected which led to different wear rates in running-in stage. In the case of relative humidity, the maximum film thickness is influenced considerably.
5. Calibration of the numerical-tribochemical model suggests a linear variation of  $h_{max}$  (maximum tribofilm formation) with relative humidity and the result is a modification to the tribochemical model to adapt it to the tribocorrosion conditions in humid environment.

## **Chapter 8. Investigation into the Durability of the Tribofilm Formed by Zinc Dialkyl Dithiophosphate**

### **8.1 Introduction**

Understanding the true interfacial mechanisms of the growth of the tribofilms generated by Zinc Dialkyl Dithiophosphate (ZDDP) is important because it is the most widely used anti-wear additive and there is legislative pressure to find efficient environmentally-friendly replacements. The main focus of this chapter is to investigate the durability of the ZDDP tribofilm and correlate it to the chemical properties of the glassy polyphosphates. The effect of parameters such as temperature and load on tribofilm formation and its durability has been studied experimentally by using a Mini Traction Machine (MTM) with the Spacer Layer Interferometry Method (SLIM) attachment.

The role of additive depletion on the pre-formed tribofilm thickness under mechanical stress has also been studied. Results show that physical parameters such as temperature and pressure significantly influence the tribofilm. XPS analyses were carried out before suspending the test and after changing the oil to assess the difference in chemical structure of the tribofilm before and after stopping the test. The chemical analyses suggest that there are different chemical properties across the thickness of the tribofilm and these determine the durability characteristics. Tribofilm durability so far has not been studied extensively. The experimental results in this study, show for the first time that running conditions do not affect only the formation of the tribofilm but also its durability and as such it should be considered in the tribochemical studies of such additives.

## **8.2 Tribofilm evolution**

To investigate the tribofilm durability throughout the time, oil was replaced at two different stages; early stage and late stage. Figure 8-1 illustrates the two stages in which the oil was replaced. In the early stage, the oil was changed after 25 minutes of starting the experiment whereas in the late stage, oil was replaced after 3 hrs of running the test. In both cases, two different experiments were conducted. Firstly oil was replaced by a fresh ZDDP containing oil and secondly by base oil. The growth of the tribofilm for these two different points is reported in the next section as well as the chemistry of the tribofilm formed on the surfaces.

### **8.2.1 Early stage tribofilm durability**

The results of the tribofilm thickness measurements for the early stage oil replacement experiments are shown in Figure 8-2. It can be seen that if the lubricating oil is replaced by a fresh oil containing ZDDP, the tribofilm growth behaviour is not affected significantly by stopping the experiment and starting it again. There is a small drop in the thickness of the tribofilm due to the mechanical action. When the oil is replaced by base oil, there is a larger drop in the thickness of the tribofilm. These two experiments confirm that tribofilm thickness reduces because of the mechanical action.

Once the uppermost layer is removed, the tribofilm is durable and the thickness does not change. It should be noted that the drop in the thickness of the tribofilm is an instantaneous drop. It means that the top soft layer of the tribofilm is removed in the first few load cycles after replacing the oil. It can also be related to the chemical properties of the top and bottom part of the glassy polyphosphates tribofilm formed on the surface.

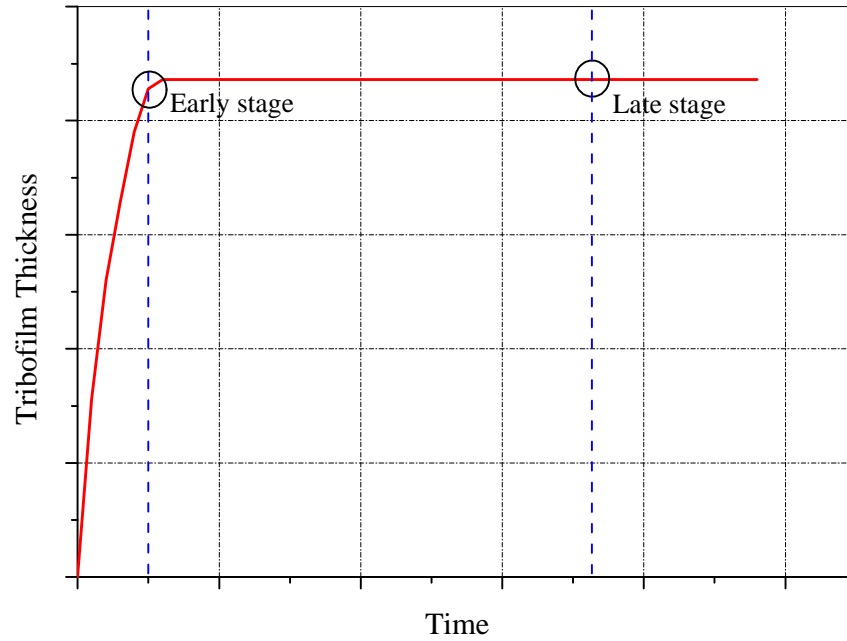


Figure 8-1 Schematic representative of two different stages of replacing the oil.

Early stage after 25 minutes and late stage at 180 minutes.

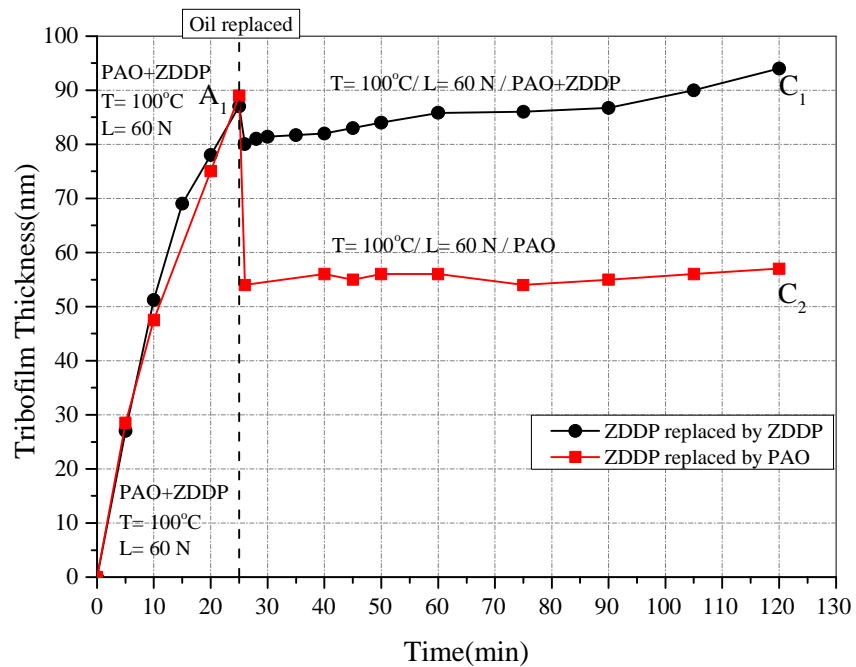


Figure 8-2 Tribofilm thickness results for the early stage durability test

## 8.2.2 Late stage tribofilm durability

It was reported previously that long chain polyphosphates convert to shorter chain polyphosphates due to rubbing (95). The tribofilm evolution experiments were conducted with the same experimental configuration and the oil was replaced by base oil after 180 minutes of starting the test. The tribofilm growth results are plotted in Figure 8-3. Results suggest that lower reduction in the thickness of tribofilm occurs when the oil is exchanged after 3 hours than after 25 minutes. It is clear that the tribofilm is more resistant to rubbing and only a few nanometres of the film are removed. These results are in agreement with the reports of Refs (93, 104) that report a durable ZDDP tribofilm once fully formed. XPS analysis was carried out to differentiate the chemical properties of the tribofilm formed on the surfaces at two different stages and the results are reported in Section 8.3.2.

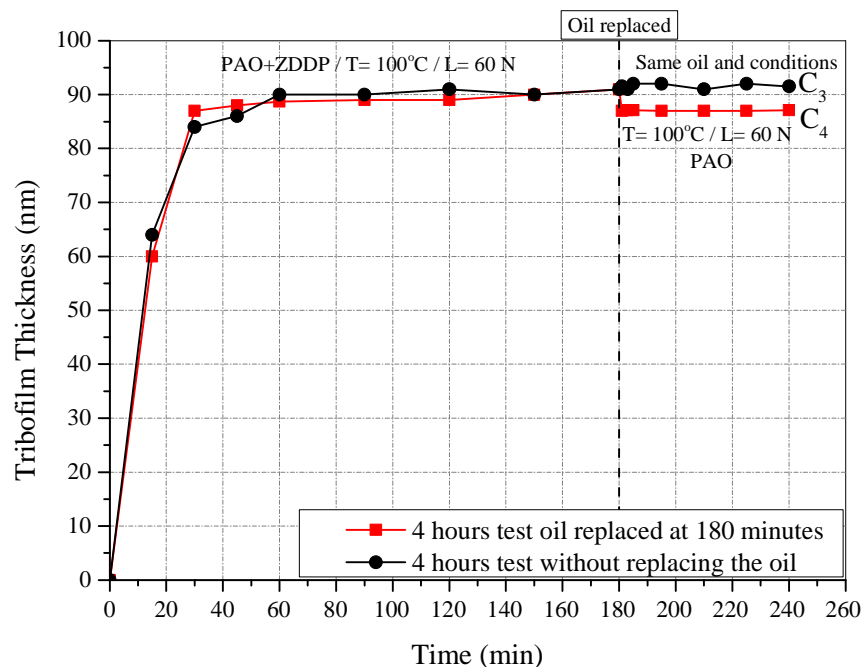
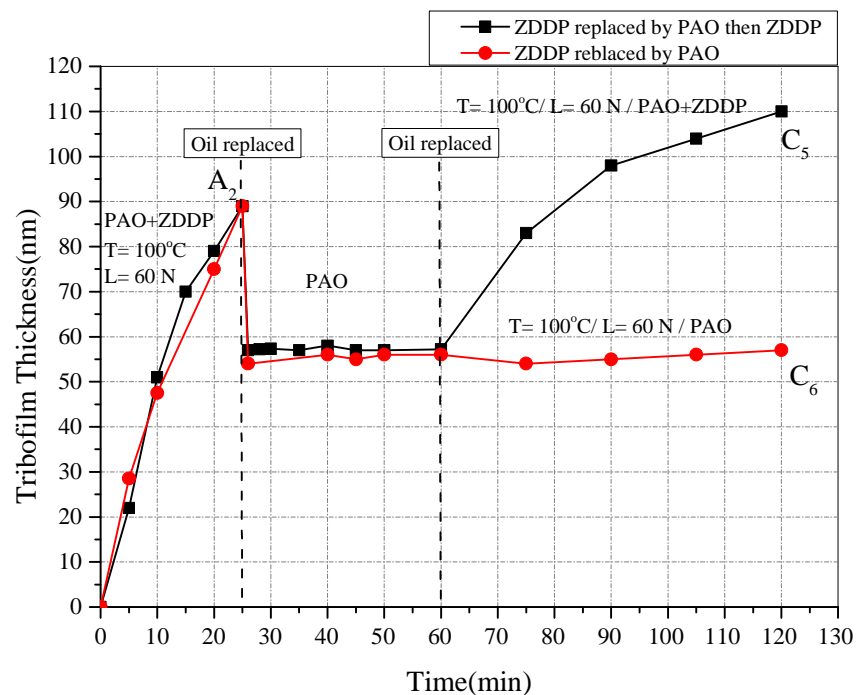


Figure 8-3 Tribofilm thickness results for the late stage durability test

### 8.2.3 Multiple replacement

This experiment was designed to assess whether when a tribofilm partially removed by rubbing in an oil without ZDDP can be replenished when the ZDDP is subsequently replenished. The oil was changed to base oil after 25 minutes of starting the test and the base oil was replaced again by a fresh ZDDP after 1 hour of starting the test and the results are shown in Figure 8-4.



**Figure 8-4 Tribofilm thickness results for adding fresh ZDDP to the base oil**

Results show that replacement of ZDDP in oil leads to continued growth of the tribofilm, the rate being slower than for a fresh clean surface. XPS analysis was carried out at different times of these experiments to correlate the chemistry of the tribofilm and the different layers.

### 8.3 Chemistry of tribofilms

For the above-mentioned experiments in Section 8.2 XPS analysis was conducted at the time of replacing the oil and at the end of each experiment. The oxygen and

phosphorus peaks are plotted, to primarily identify the chain length for the glassy polyphosphates in the tribofilm. The ratio of bridging oxygen to non-bridging oxygen in the polyphosphate glass was calculated by dividing the intensity of BO and NBO peaks obtained from XPS analysis. This approach has been extensively used in literature (176-184). Also the binding energy difference between the Zn3s and P2p peaks in the XPS spectra was used to give complementary information. The XPS analysis results for different experimental cases of Section 8.2 are reported in the following sections (204).

### **8.3.1 Early stage oil replacement**

The BO/NBO ratio for the case of replacing the oil by base oil at 25 minutes of starting the test is identified as 0.31 at the end of the experiment (see Figure 8-5). According to the refs (95, 98), in this case the composition of the tribofilm is zinc pyrophosphate. This value is calculated to be 0.51 when the oil was replaced by a fresh ZDDP-containing oil (point C<sub>1</sub> in Figure 8-2) and the tribofilm is mainly composed of metaphosphates (see Figure 8-6). The results suggest that the tribofilm consists of shorter chain polyphosphates in the case that oil was replaced by base oil. The tribofilm in this case is more durable and not easy to be removed. The BO/NBO ratio before replacing the oil was obtained as 0.47 ( Point A1 Figure 8-2) which shows a long chain polyphosphate in the tribofilm (metaphosphate) (98). Calculation of the binding energy difference between Zn3s-P2p<sub>3/2</sub> peaks shows the same trend in identifying the chain length. The above mentioned results can be found in Table 8-1. Zn3s-P2p<sub>3/2</sub> binding energy difference increases when the tribofilm composition varies from metaphosphate (longer) to orthophosphate (shorter). (As shown in Chapter 3 and Figure 3-10).

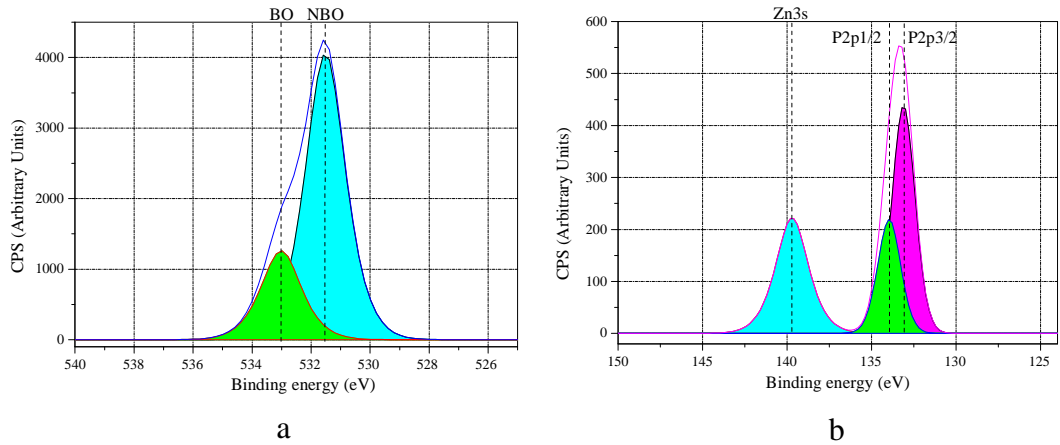


**Figure 8-5 High resolution X-Ray Photoelectron Spectroscopy spectra for ZDDP tribofilm formed at the end of the test when the oil was replaced by base oil a) O1s b) Zn3s, P2p (Point C<sub>2</sub> in Figure 8-2)**

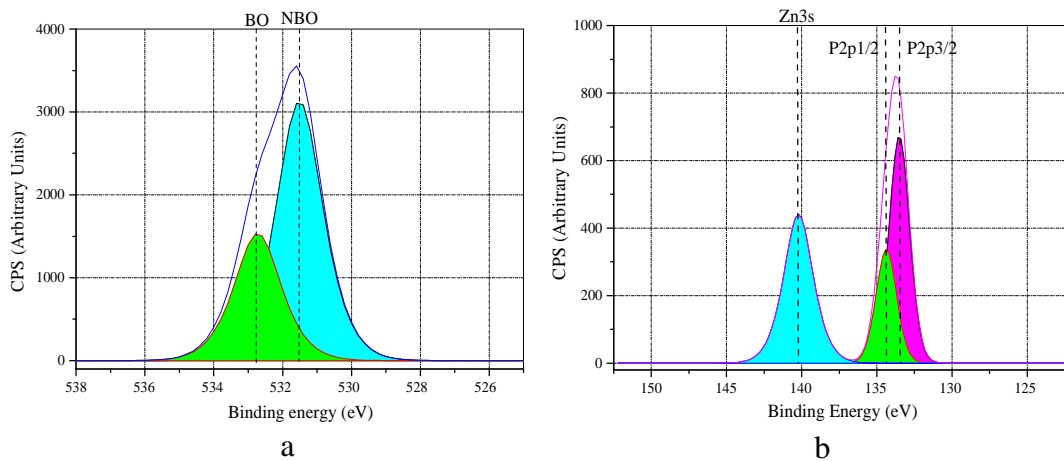


**Figure 8-6 High resolution X-Ray Photoelectron Spectroscopy spectra for ZDDP tribofilm formed at the end of the test when the oil was replaced by fresh ZDDP a) O1s b) Zn3s, P2p (Point C<sub>1</sub> in Figure 8-2)**



**Table 8-1 BO/NBO ratios and the difference between Zn3s and P2p peaks. Tribofilm thickness at points A<sub>1</sub>, C<sub>2</sub> and C<sub>1</sub> is shown Figure 8-2.**

Test	Both tests	ZDDP changed with base oil	ZDDP changed with fresh ZDDP
	Before changing the oil (Point A <sub>1</sub> )	End of the test (Point C <sub>2</sub> )	End of the test (Point C <sub>1</sub> )
BO/NBO ratio	0.47	0.31	0.51
Zn3s – P2p binding energy difference (eV)	6.57	6.70	6.4

### 8.3.2 Late stage oil replacement

The BO/NBO ratio and binding energy difference between Zn3s and P2p are calculated as 0.21 and 6.97 (eV) respectively (see Figure 8-7) for the case of replacing the oil at 3 hours of starting the test (point C<sub>4</sub> in Figure 8-3). The zinc polyphosphates composition can be recognised as pyrophosphate (short chain). These values are 0.23 (pyrophosphate) and 6.92 (eV) when the oil was not replaced (point C<sub>3</sub> in Figure 8-3) by base oil (see Table 8-2 and Figure 8-8). It suggests that short chain polyphosphates are present in the tribofilm. Comparing the chemical structure of the tribofilm when oil replaced after 25 minutes of the experiments and 3 hours with the same conditions shows that rubbing affects the structure and tribofilm contains more short chain polyphosphates at longer time of rubbing. Results are in agreement with the reports of literature (194). The comparison between the experiments while the oil was

exchanged after 25 minutes of rubbing with the one after 3 hours of rubbing suggests that more tribofilm loss happens in the former and it can be related to the chemical structure of the tribofilm.

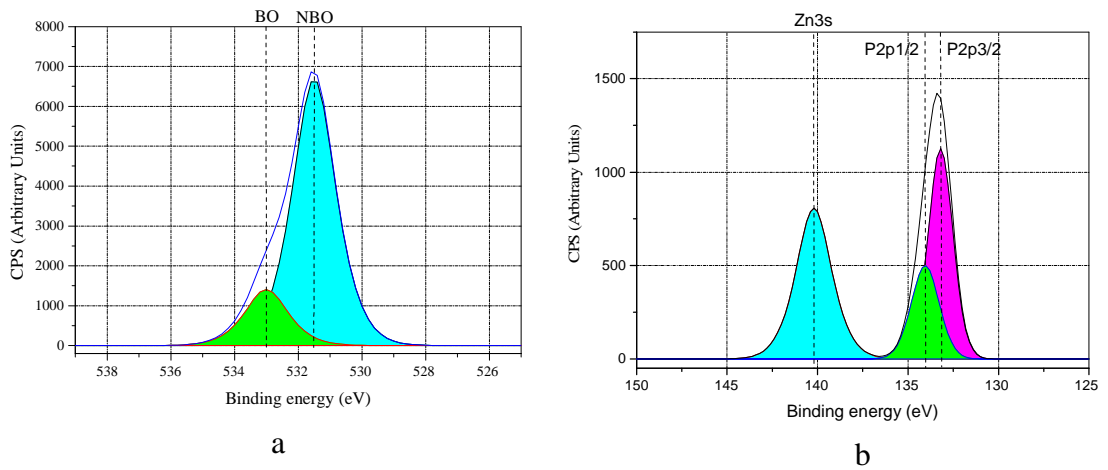


**Figure 8-7 High resolution X-Ray Photoelectron Spectroscopy spectra for ZDDP tribofilm formed at the end of the 4hrs test when the oil was replaced with base oil at 3 hrs a) O1s b) Zn3s, P2p (Point C4 in Figure 8-3)**

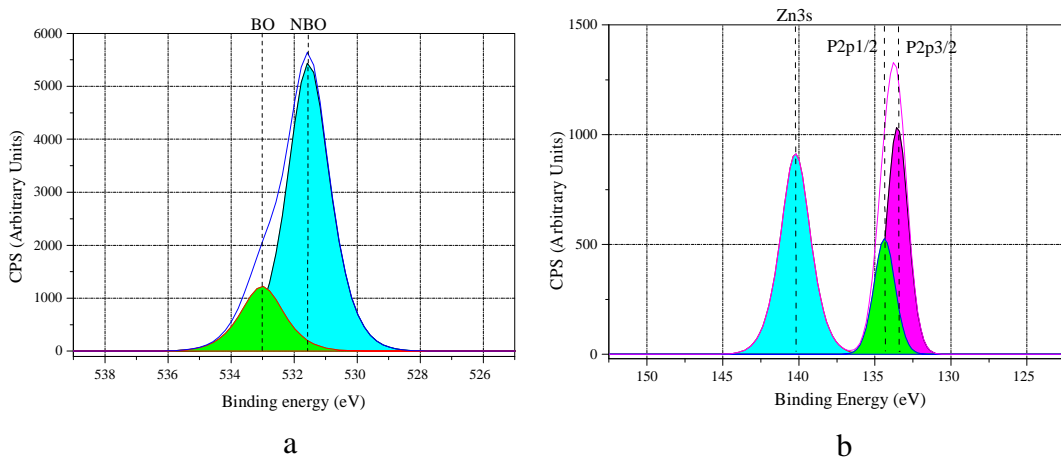


**Figure 8-8 High resolution X-Ray Photoelectron Spectroscopy spectra for ZDDP tribofilm formed at the end of the 4hrs test without replacing the oil a) O1s b) Zn3s, P2p (Point C3 in Figure 8-3)**

**Table 8-2 BO/NBO ratio. Tribofilm thickness at points C<sub>4</sub> and C<sub>3</sub> is shown in**

**Figure 8-3.**

<b>Test</b>	<b>ZDDP changed with base oil at 3 hrs</b>	<b>Without changing the oil</b>
	End of the test (Point C <sub>4</sub> )	End of the test (Point C <sub>3</sub> )
BO/NBO ratio	0.21	0.23
Zn3s – P2p binding energy difference (eV)	6.97	6.92

### **8.3.3 Multiple replacement**

For the multi replacement experiments (Figure 8-4) in which the oil was replaced twice, XPS was carried out at the end of the experiment to compare it with the first test and the results are shown in Figure 8-9 and Figure 8-10.

Results for BO/NBO ratio and binding energy difference between Zn3s and P2p are reported in Table 8-3. The value of BO/NBO ratio was 0.51 (metaphosphate) in case of ZDDP replaced by fresh ZDDP (point C<sub>1</sub> in Figure 8-2) and 0.62 (metaphosphate) when ZDDP changed with base oil and then replaced by fresh ZDDP again (C<sub>5</sub> in Figure 8-4). It has also been shown in the literature that unreacted ZDDP can be replenished in the contact areas and reform glassy polyphosphates (85). The difference in the values of binding energy (eV) between Zn3s and P2p was 6.4 (point C<sub>1</sub> in Figure 8-2) and 6.32 (point C<sub>5</sub> in Figure 8-4), respectively.

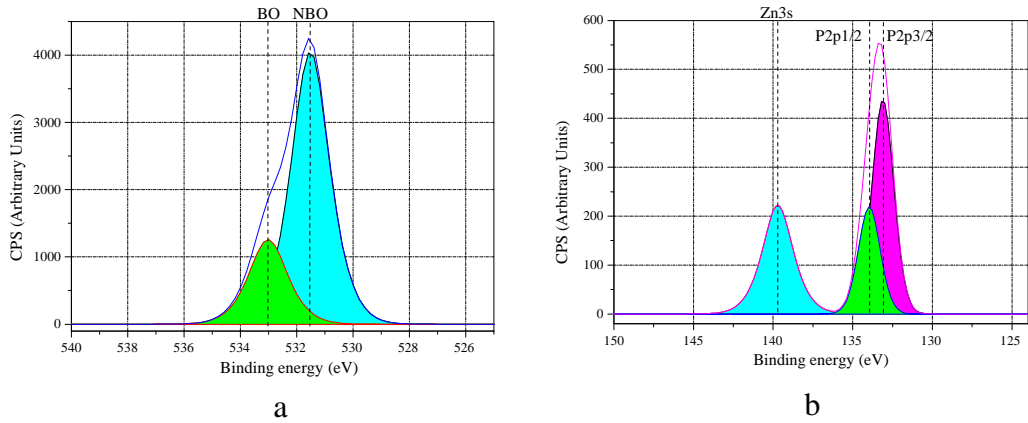


**Figure 8-9 High resolution X-Ray Photoelectron Spectroscopy spectra for ZDDP tribofilm formed at the end of the test when the oil was replaced by base oil a) O1s b) Zn3s, P2p (Point C<sub>6</sub> Figure 8-4)**

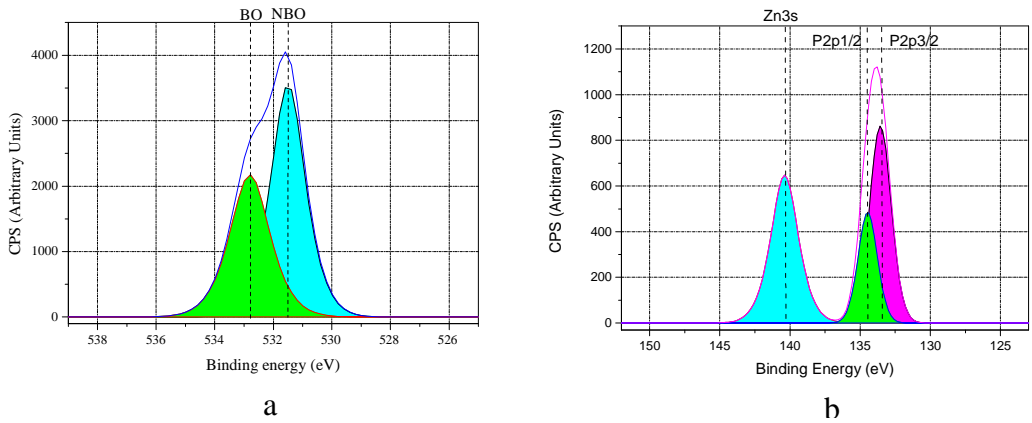


**Figure 8-10 High resolution X-Ray Photoelectron Spectroscopy spectra for ZDDP tribofilm formed at the end of the test when the oil was replaced by base oil and then with ZDDP a) O1s b) Zn3s, P2p (Point C<sub>5</sub> Figure 8-4)**

**Table 8-3 BO/NBO ratios and the difference between Zn3s and P2p peaks. Tribofilm thickness at points A<sub>2</sub>, C<sub>5</sub> and C<sub>6</sub> is shown in Figure 8-4.**

Test	Both tests	ZDDP changed with base oil	ZDDP changed with base oil and then changed with fresh ZDDP
	Before changing the oil (Point A <sub>2</sub> )	End of the test (Point C <sub>6</sub> )	End of the test (Point C <sub>5</sub> )
BO/NBO ratio	0.47	0.31	0.62
Zn3s – P2p binding energy difference (eV)	6.57	6.70	6.32

It can be interpreted from the values that longer chain polyphosphates are present in the tribofilm before exchanging the oil when the tribofilm is relatively thick. Once the oil is exchanged and the tribofilm is partially removed, it is mainly consisting of shorter chain polyphosphates. It has been shown that the mechanical properties and chemistry of the ZDDP tribofilm varies from bulk to the surface (81, 85, 86, 95, 195). This suggests that different chemistries can be correlated for mechanical properties of the film. Comparison between the two experiments shows that while the tribofilm forms again in the presence of the fresh ZDDP, more of longer chain polyphosphates are detected at the end of the experiment.

## 8.4 Effect of temperature

Temperature is reported to affect the tribological performance of ZDDP (162, 196). To study the effect of temperature on the durability of the tribofilm, tribological tests were carried out with the same conditions to form the tribofilm on the surfaces. The tests were stopped after 25 minutes and the temperature was changed when the oil was replaced by base oil to see the effect of temperature on the tribofilm durability. The tribofilm thickness was measured for four different temperatures after the suspension. Figure 8-11 demonstrates the tribofilm thickness measurements for different temperatures. It should be noted that the temperature is the same for all the tests before the suspension to form similar tribofilm and then it is changed at the time of the suspension.

The amount of tribofilm removed at different temperatures in terms of the reduction in the thickness is reported in Figure 8-12. It can be seen that the removal of the tribofilm is almost changing linearly with the oil bulk temperature. One would say these changes in the temperature can change the severity of the contact due to the effect of temperature on the viscosity of the oil. Smaller  $\lambda$  ratio for higher temperature might result in more tribofilm removal. For this reason,  $\lambda$  ratio was calculated for all four temperatures. It was observed that  $\lambda$  ratio varies between 0.03 and 0.06 for all these temperatures. All these conditions are severe and the ratio is small enough to be in boundary lubrication. Therefore the chemical properties of the tribofilms were analysed using XPS to see a correlation between the chemical characteristic of the film and the observed tribofilm durability.

Based on the results from Figure 8-11, there is a more prominent mechanism to support the fact that the higher temperature results in the higher reduction in the tribofilm thickness after changing the oil to base oil (oil B). Increasing the temperature

can affect the mechanical properties of the tribofilm. Interpreting the results for different temperatures revealed that the higher temperatures lead to a significant decrease in hardness of the tribofilm and therefore plastic flow of the tribofilm increases. Due to the lower hardness and higher plastic flow, more indentation occurs into the depth of the tribofilm and more tribofilm thickness reduction is observed. Results are in agreement with the previous study of the temperature effects on the mechanical properties of ZDDP (90, 197).

#### **8.4.1 Chemistry of the tribofilm**

XPS is reported for the highest temperature for comparison reasons. The XPS was conducted before suspending the test, after 1 minute rubbing when the oil is changed and finally at the end of each experiment. The Oxygen and phosphorus peaks are reported in Figure 8-13, Figure 8-14 and Figure 8-15 for three different points shown in Figure 8-11. The intensity ratio of BO to NBO is reported in Table 8-4 as well as the binding energy difference for Zn3s and P2p. The results in Table 8-4 show that before suspending the test, the BO/NBO ratio is 0.47 (Point A<sub>3</sub> in Figure 8-11) and the difference in binding energy for Zn3s and P2p is 6.57.

This suggests that the tribofilm contains longer chain polyphosphates and mainly contains zinc metaphosphates (95, 98). After the suspension of the test and once the oil is replaced, the softer top part of the tribofilm (consisting of long chain polyphosphates) is removed. This is also shown by XPS that the shorter chain polyphosphate (pyrophosphates) present in the tribofilm after the removal (Point B<sub>1</sub> in Figure 8-11) (BO/NBO ratio of 0.19 and  $\Delta$  (Zn3s, P2p) of 6.76 eV). Once the tribofilm is again formed for the case of 140 C, longer chain polyphosphates are present in the tribofilm at the end of the experiments (Point C<sub>8</sub> in Figure 8-11) where

XPS analysis shows a BO/NBO ratio of 0.30 and binding energy difference of 6.70 eV for Zn3s and P2p (polyphosphate).

The XPS results show that the top part of the tribofilm contains mainly the longer chain polyphosphates which can be removed easier than the shorter chain polyphosphates in the bulk of the tribofilm. The comparison between experiments for 80°C and 140°C shows that longer chain polyphosphates are present when tribofilm is removed in the case of 80°C compared to the 140°C. The removal of the tribofilm is more for the case of 140°C and XPS results confirm that shorter chain polyphosphates are present in depth of the tribofilm once it is removed. The difference between the binding energy for Zn3s and P2p also confirms the above mentioned observations (See Table 8-4).

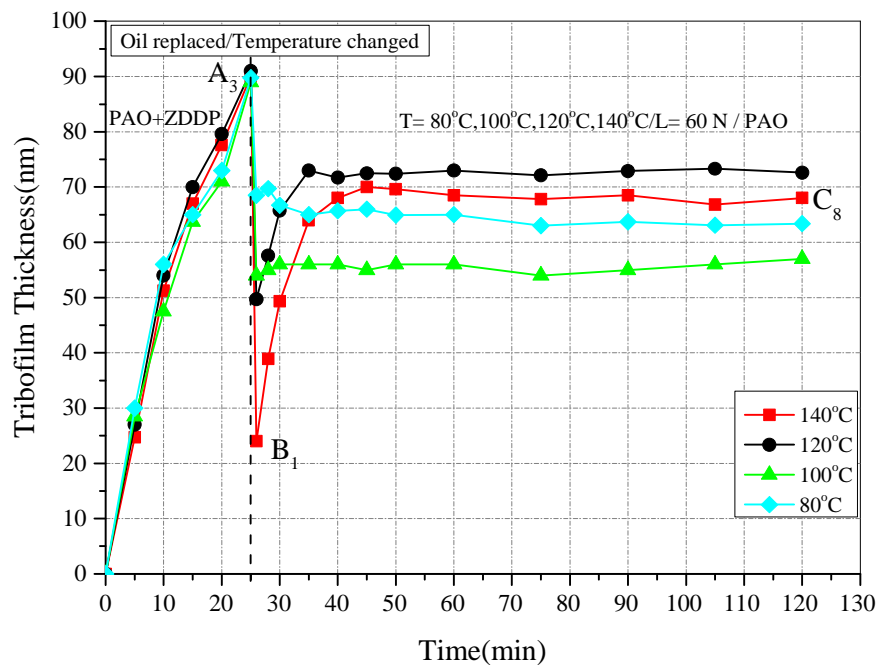


**Figure 8-11 Tribofilm thickness results and removal behaviour for different temperatures after suspending the test**



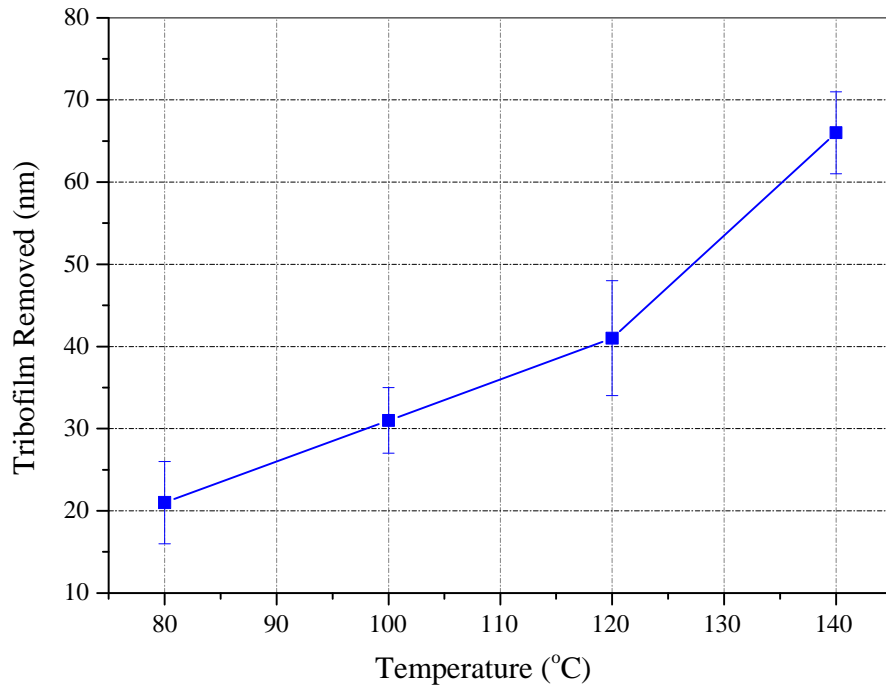


**Figure 8-12 Tribofilm thickness reduction for different temperatures after one minute of rubbing when the oil is changed with base oil**

The comparison between tribofilm growth results of Figure 8-11 suggests that increasing the temperature after replacing the oil results in more removal of the tribofilm. In addition XPS analysis results confirm that the top part of the tribofilm contains mainly longer chain polyphosphates than the bulk (81, 85, 86, 95, 195). It can be interpreted that higher temperature can result in changes in the structure of the tribofilm thus changing the mechanical properties of the glassy phosphates. The changes in the chemical and mechanical properties of the tribofilm due to changes in the temperature can be the reason for the different removal behaviour of the tribofilm.

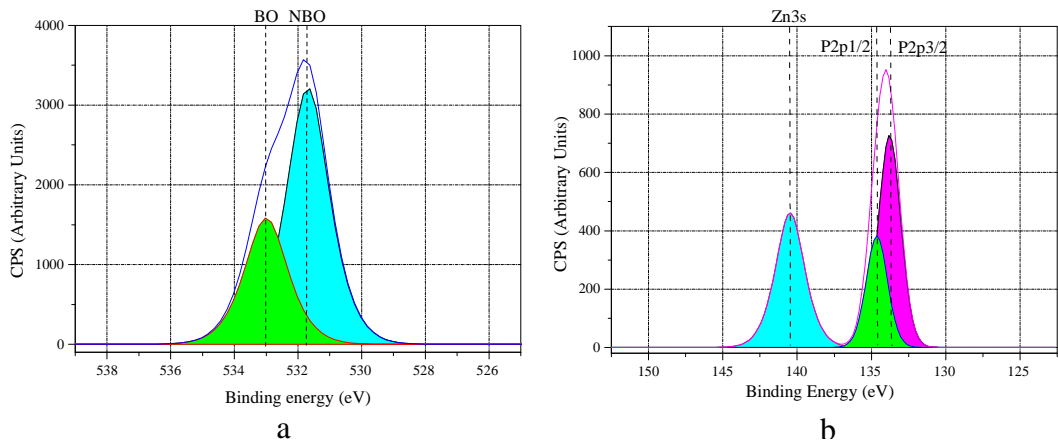


**Figure 8-13 High resolution X-Ray Photoelectron Spectroscopy (XPS)**

**spectra for ZDDP tribofilm formed before suspending the test at 140°C**

**a) O1s b) Zn3s, P2p (Point A<sub>3</sub> in Figure 8-11)**

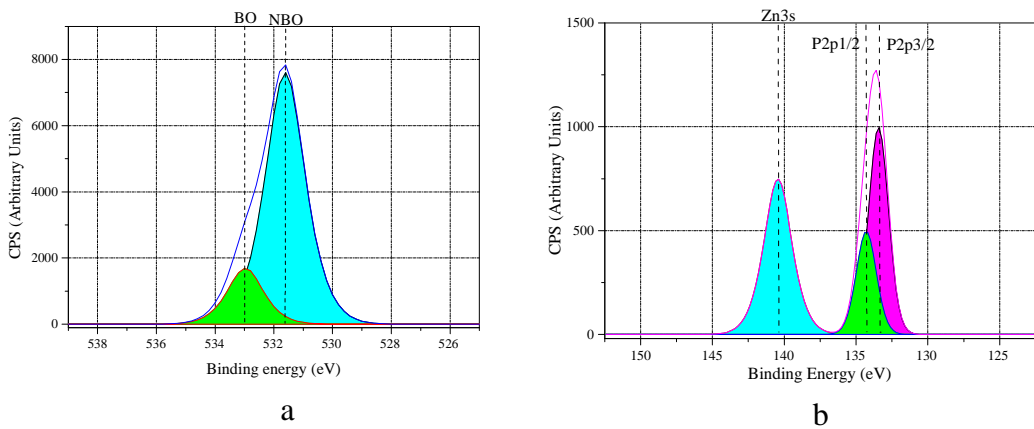


**Figure 8-14 High resolution X-Ray Photoelectron Spectroscopy (XPS)**

**spectra for ZDDP tribofilm formed after suspending the test at 140°C a)**

**O1s b) Zn3s, P2p (Point B<sub>1</sub> in Figure 8-11)**

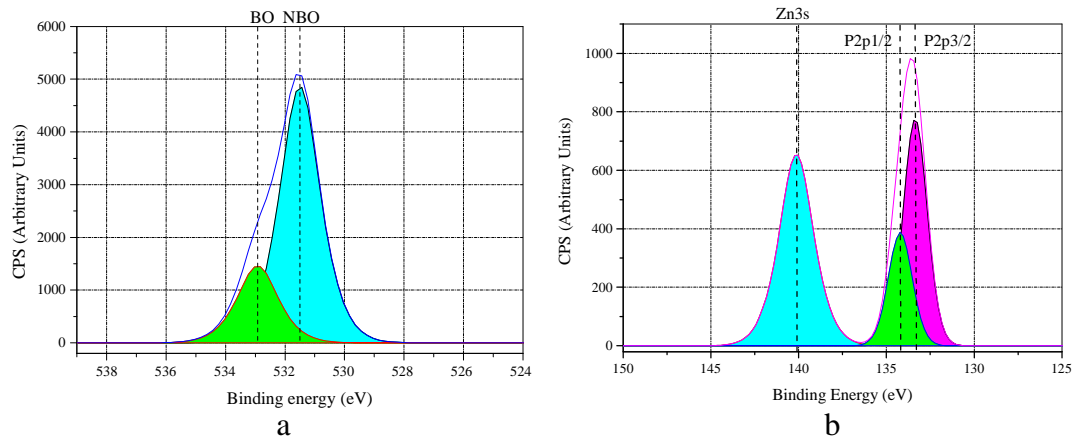


**Figure 8-15 High resolution X-Ray Photoelectron Spectroscopy (XPS) spectra for ZDDP tribofilm formed at the end of the test at 140°C a) O1s b) Zn3s, P2p (Point C<sub>8</sub> in Figure 8-11)**

**Table 8-4 BO/NBO ratios and the difference between Zn3s and P2p peaks. Tribofilm thickness at points A<sub>3</sub>, B<sub>1</sub> and C<sub>8</sub> is shown in Figure 8-11.**

Test	140°C		
	Before suspension (Point A <sub>3</sub> )	After suspension (Point B <sub>1</sub> )	End of the test (Point C <sub>8</sub> )
BO/NBO ratio	0.47	0.19	0.30
Zn3s – P2p binding energy difference (eV)	6.57	6.76	6.70

### 8.5 Effect of load

One important parameter in the mechanical action of removing any material is the load applied on the surfaces. The load affects the penetration depth into the material

and is responsible for the stress fields on the surface. Therefore it is reasonable to see the effect of load on the durability of the tribofilm. Similar to the experiments for the temperature, the tribological tests were conducted with the same conditions to form the tribofilm on the surfaces and the tests were stopped after 25 minutes. Four different loads were then applied after the suspension and images were taken after 1 minute of rubbing with the sequence of every 5 minutes. Figure 8-16 shows the results of the tribofilm thickness evolution for different loads. Higher load results in more thickness reduction of the tribofilm and this variation is plotted in Figure 8-17. Not surprisingly, reduction in thickness of the tribofilm is also linear with the applied load. Similar to the temperature, variation of load may result in changes in the severity of the contact. For this purpose  $\lambda$  ratios have been calculated for all four loads and all the results are very close to 0.04. It shows that variation of loads from 30N to 75N does not change the severity of the contact significantly.

One important parameter in study of the boundary lubrication systems is the flash temperature due to the surface contacts. For this reason, flash temperature was calculated for different applied loads in this work (see Figure 8-18). According to Kennedy *et al* (198), flash temperature can be calculated from Equation 8-1.

$$\Delta T_{max} \approx \frac{2Qb}{K\sqrt{\pi(1+Pe)}} \approx \frac{1.122Qb}{K} \quad 8-1$$

Where  $b$  is the width of the contact and  $K = \frac{k}{\rho C}$  is the thermal diffusivity ( $k$  is the thermal conductivity,  $\rho$  is the density and  $C$  is the specific heat).  $Pe$  is the Peclet number.  $Q$  is the frictional heating (199) at the contact interface and is calculated from Equation 8-2.

$$Q = \mu PV$$

8-2

In which  $\mu$ ,  $P$  and  $V$  are the coefficient of friction, contact pressure and the relative sliding speed between surfaces respectively. Results showed that flash temperature is not significantly increased by load. This is because of the slight difference in the Hertzian contact pressure on the surfaces. The maximum contact pressure is calculated to be 1 GPa and 1.3 GPa for the loads of 30N and 75 N respectively. These pressures result in the flash temperature rise of around 12°C-14°C. This suggests that the changes in thickness due to the different applied load is not because of variation of the flash temperature at these loads. For further investigations, the shear stress was calculated for different loads and is plotted in Figure 8-18. Higher loads lead to the higher shear stress in both substrate and tribofilm and it can affect the material removal of the tribofilm. It is also shown by Archard (130) that that the material removal is proportional to the real area of contact and load.

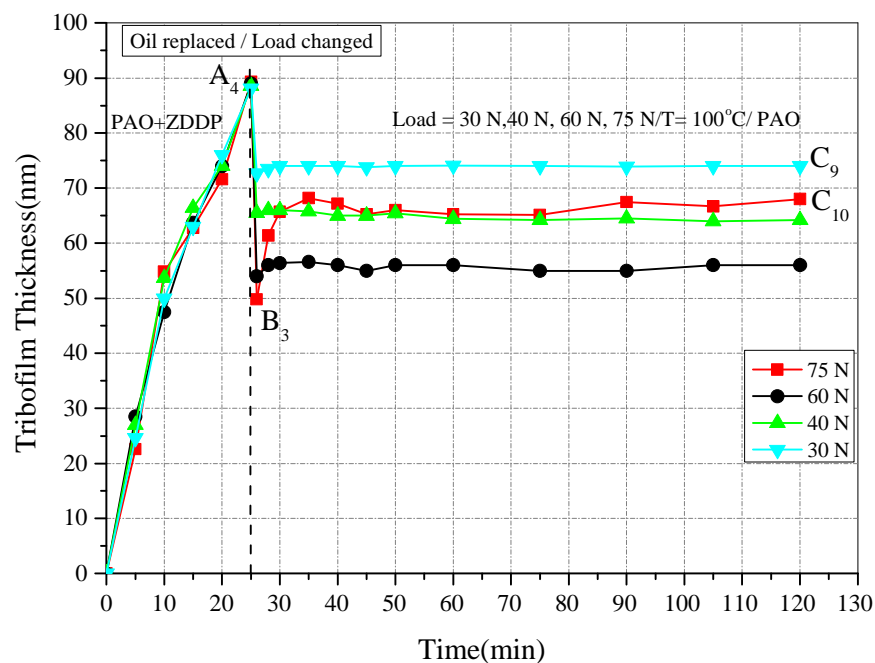


**Figure 8-16 Tribofilm thickness results and removal behaviour for different loads after suspending the test**

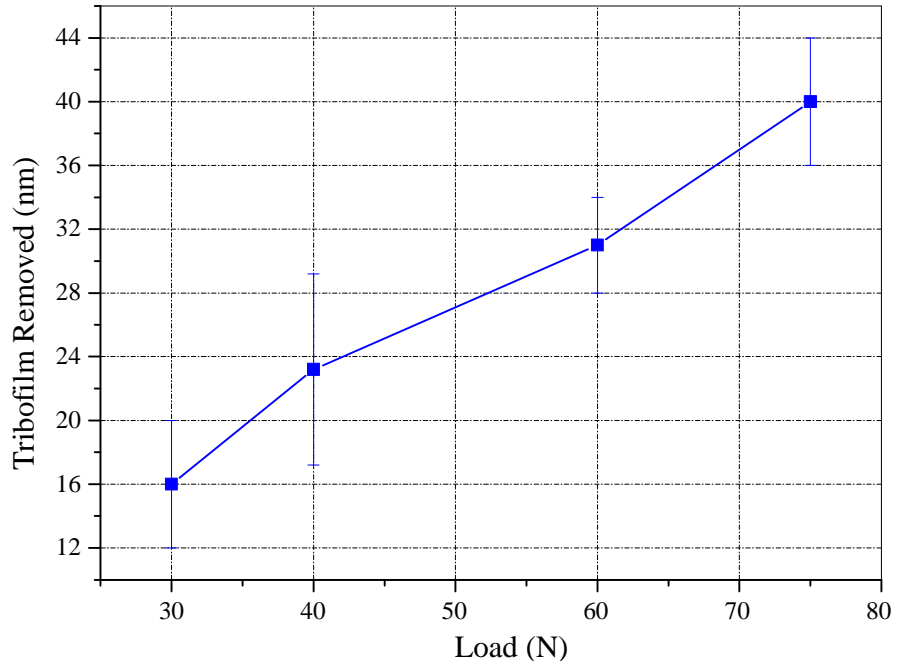


**Figure 8-17 Tribofilm thickness reduction for different loads after one minute of rubbing when the oil is changed with base oil**

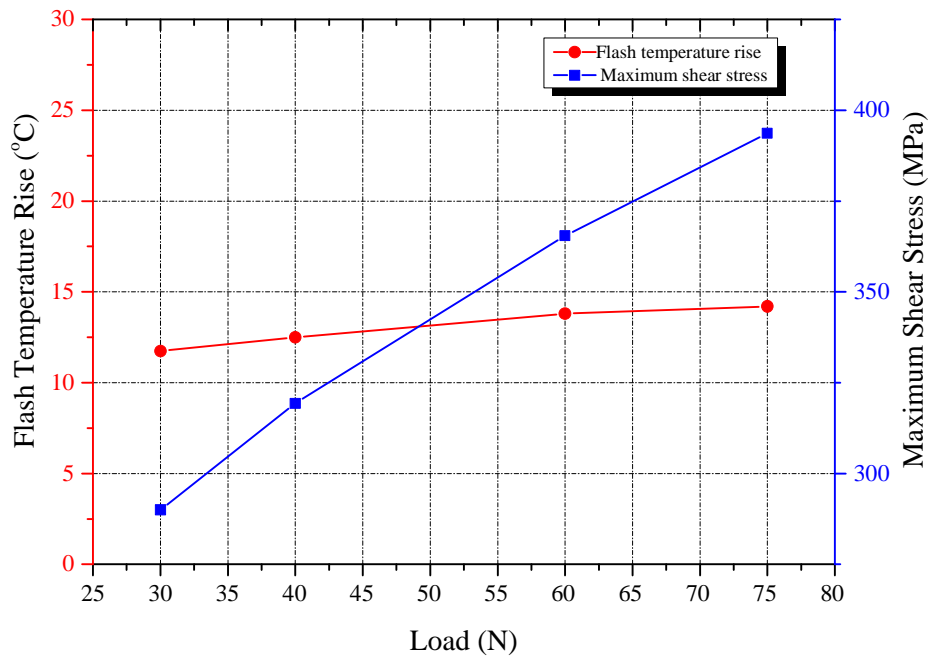


**Figure 8-18 Effect of load on the flash temperature rise and the maximum shear stress on the surfaces**

### 8.5.1 Chemistry of the tribofilm

Analyses were carried out at three different times on the samples to see the change of the chemical structure of the tribofilm and the effect of load on its variations. The intensity ratio of BO to NBO as well as the difference between Zn3s and P2p are reported in Table 8-5 for different positions of Figure 8-16.

The results show that BO/NBO is 0.47 and the binding energy difference for Zn3s and P2p is 6.57 eV before suspending the oil (Point A<sub>4</sub> in Figure 8-16), therefore longer chain polyphosphates (metaphosphates) are present in the tribofilm. BO/NBO ratio is 0.29 (Point B<sub>3</sub> in Figure 8-16) and the binding energy difference for Zn3s and P2p is 6.6 which suggest that the shorter chains (pyrophosphates) are present after the removal of the top layer of the tribofilm when the oil is replaced with base oil. The chain length at the end of the experiments is almost the same as the chain length after the removal process.

The comparison between high load and low load suggests that when the tribofilm is more removed for the case of higher load, there are shorter chain polyphosphates present in its bulk after the removal. Therefore higher load is able to remove more durable glassy phosphates in the bulk of the tribofilm and this behaviour is very similar to the temperature effect on the removal of the tribofilm. For the temperature, it is more reasonable that temperature changes the structure of the tribofilm therefore changing its durability and removal behaviour. On the other hand higher load results in more shear stress applied on the tribofilm which can lead to more removal of the film.

**Table 8-5 BO/NBO ratios and the difference between Zn3s and P2p peaks.**

**Tribofilm thickness at points A<sub>4</sub>, B<sub>3</sub>, C<sub>9</sub> and C<sub>10</sub> is shown in Figure 8-16.**

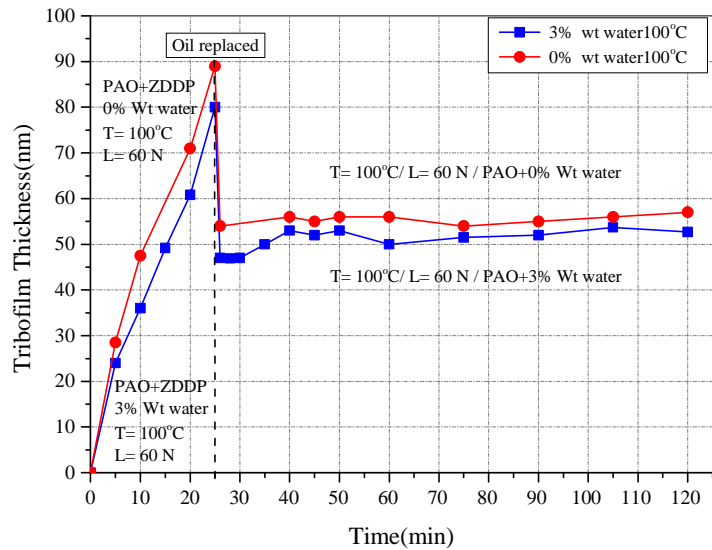
Test	75 N			30 N
	Before suspension (Point A <sub>4</sub> )	After suspension (Point B <sub>3</sub> )	End of the test (Point C <sub>10</sub> )	End of the test (Point C <sub>9</sub> )
BO/NBO ratio	0.47	0.29	0.27	0.45
Zn3s – P2p binding energy difference (eV)	6.57	6.6	6.58	6.54

## 8.6 Effect of water

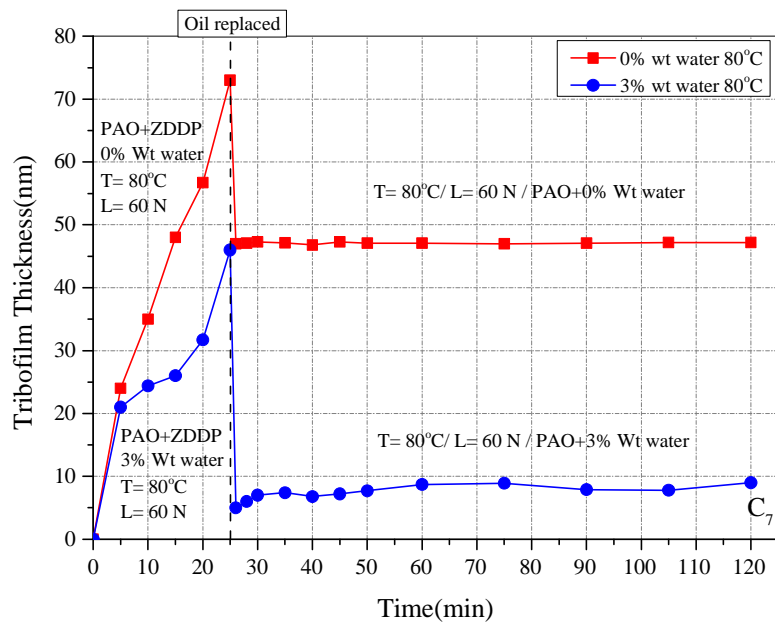
It is reported that water can affect tribochemistry and therefore wear of the tribosystem (110, 200). ZDDP tribofilm thickness in two different levels of water concentration in oil has been plotted in Figure 8-19 and Figure 8-20.

Figure 8-19 indicates that the higher water concentration leads to a lower tribofilm growth rate. It might be because of the effect of water in delaying the tribofilm formation due to the fact that water molecules prevent ZDDP to access the substrate. Another scenario can be delaying the decomposition of the ZDDP on the surface to form the tribofilm (200). It can be seen from the results that water does not significantly affect steady state tribofilm thickness at higher temperature (100°C). One reason for this could be the evaporation of water at higher temperature compared to the lower temperature (80°C). Two experiments were carried out to investigate the synergism effect between temperature and water at 80° C for two different water concentrations.





**Figure 8-19 Tribofilm thickness results for ZDDP with different water contents at 100°C**



**Figure 8-20 Tribofilm thickness results for ZDDP with different water concentrations at 80°C**

Figure 8-20 illustrates that water plays a significant role in both formation and removal of the tribofilm at lower temperature (80°C). This figure suggests that water can affect the mechanical properties of the tribofilm especially at lower temperature

(less than the evaporation temperature) because of the depolymerisation of the polyphosphate chain to shorter chain (200). Water delays the growth rate of the tribofilm at 80°C compared to 100°C. The observed results at 80°C show that the higher water concentration results in the higher removal of the tribofilm and tribofilm thickness reaches to the first few nanometre in the bulk of the tribofilm which consists of shorter chain polyphosphates (86).

The results of Figure 8-20 suggest that water can affect the chemical structure of the tribofilm and makes it weaker and easy to be removed. The tribofilm was characterized by XPS in the case of 80°C when the thickness was reduced to very low values. Results for oxygen and phosphorus peaks are reported in Figure 8-21 and BO/NBO ratio and the difference in binding energy for Zn3s and P2p peaks are reported in Table 8-6.

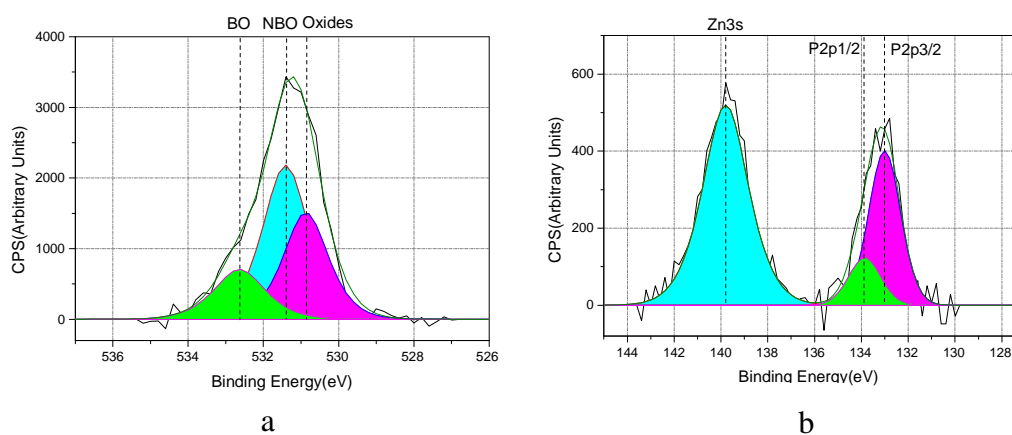


**Figure 8-21 High resolution X-Ray Photoelectron Spectroscopy (XPS) spectra for ZDDP tribofilm formed at the end of the test for 3wt% water in oil at 80°C a) O1s b) Zn3s, P2p (Point C7 in Figure 8-20)**

The BO/NBO ratio and binding energy difference between Zn3s and P2p are calculated as 0.35 and 6.7 (eV) respectively. It suggests that the tribofilm mainly consists of pyrophosphates. Interpreting the results suggest that tribofilm contains

short polyphosphates with high amount of iron oxides and sulphides and high amount of zinc.

**Table 8-6 BO/NBO ratios and the difference between Zn3s and P2p peaks. Tribofilm thickness at point C<sub>7</sub> is shown in Figure 8-20.**

Test	80°C 3wt% water
	End of the test  (Point C <sub>7</sub> )
BO/NBO ratio	0.28
Zn3s – P2p binding energy difference (eV)	6.7

## 8.7 Wear

To investigate the correlation between tribofilm formation/durability behaviour and wear of the system, wear measurements were carried out along with thickness measurements and chemical analysis of XPS. Wear was measured for two sets of experiments reported in Section 8.2.1 and Section 8.2.3 and different points were chosen systematically to be able to find out the role of tribofilm and its effect on wear. Wear was measured at two different points for each experiment, one immediately after replacing the oil and one at the end of each experiment. The measurement points are schematically shown in Figure 8-22. An examples of 3D-profilometry images for two different points at the end of the experiments are demonstrated in Figure 8-23. Average wear depth (Figure 8-24) is a good representative for evaluation of wear on ball samples of MTM. For this reason, average wear depth was calculated at four

different points on the wear track of the balls to obtain a more accurate wear assessment and each experiments was repeated two times.

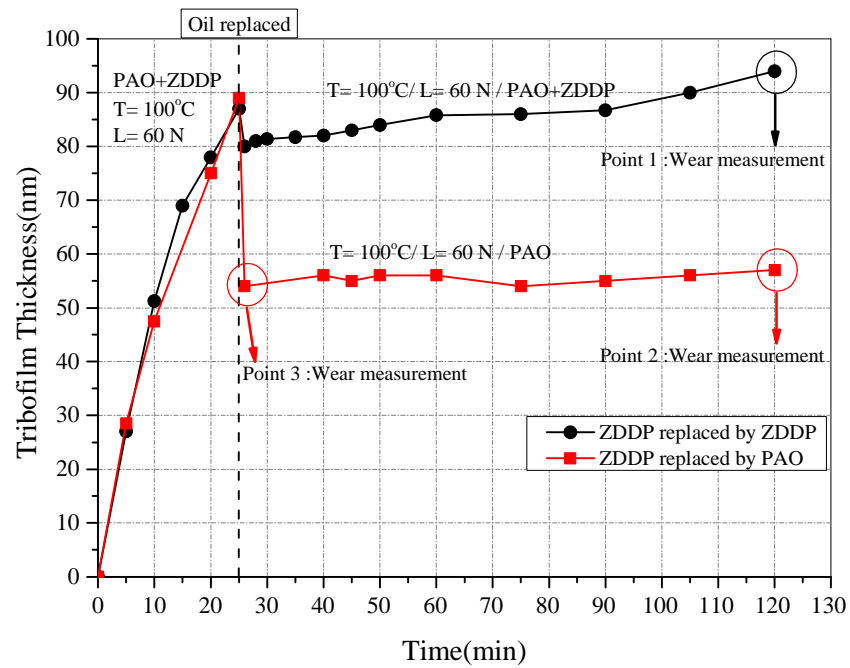


**Figure 8-22 Schematic of the wear measurement points in the case of ZDDP replaced by fresh ZDDP and ZDDP replaced by base oil**

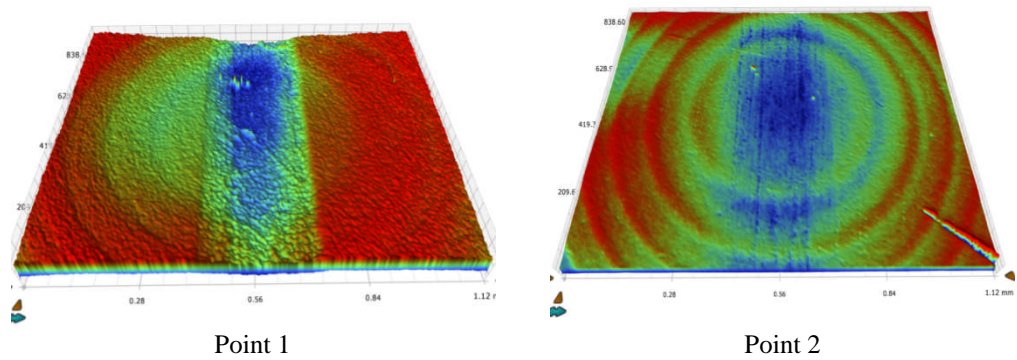
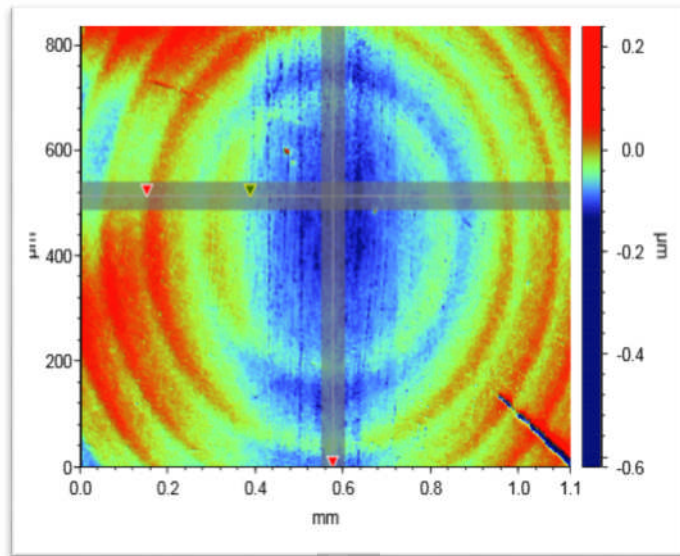
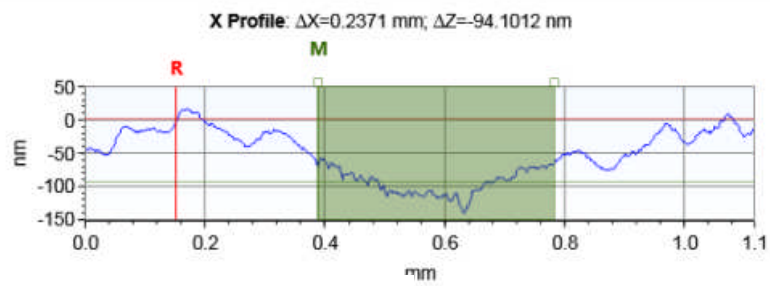


**Figure 8-23 3D-profilometry images taken at the end of experiments**



a



b

**Figure 8-24 a) 2D-profilometry image of the ball for point 2 b) the average wear depth calculation**

**Table 8-7 Average wear depth measurement results**

Measurement point	Average wear depth measurement (nm)
Point 1	216
Point 2	104
Point 3	96

The average wear depth results are reported in Table 8-7 for the first set of experiments. It was hypothesized recently (107, 109, 156, 201) that wear can happen because of the removal of substrate atoms present in the tribofilm due to different tribochemical phenomena and the dynamic loss of material within the tribofilm throughout the growth on the contacting asperities. The results suggest that the dynamic tribofilm thickness reduction does not occur when the formation is not happening. The remaining tribofilm on the surface is a durable layer and it was confirmed by means of XPS presented in 8.3 which shows that the remaining tribofilm consists of shorter chain poly phosphates.

Results in Table 8-7 illustrate that lower wear occurs at point 2 which is the end of the experiments when the ZDDP containing oil was changed with base oil in compare to point 1 which is the end point of the test when the oil was replaced by fresh ZDDP. For the case of the fresh ZDDP the tribofilm started to grow after replacing the oil which means that tribofilm removal is likely to happen at the same time as the formation. On the other hand when the oil was replaced by the base oil , top layers of the tribofilm is immediately removed and the more durable part of the tribofilm still remains on the surface. No more removal was observed because no more formation of the tribofilm occurs. The comparison between these two points indicates that the higher wear takes place when the tribofilm formation and removal happens at the same time. For the case that ZDDP containing oil was changed with the base oil, significant reduction in the wear of the system has been observed.

To investigate the effect of formation/durability on the wear of the system specifically, wear measurements were conducted with the same approach for the second set of experiments reported in Section 8.2.3. In this case, first the ZDDP containing oil was replaced by base oil after 25 minutes of starting the test for both experiments and then

for one of the experiments base oil was changed with fresh ZDDP after 1 hour of starting the test. The wear results for different points reported in Table 8-8 shows the same behaviour as the previous set of experiments mentioned above. The comparison between point 1 from first set of experiment and point 1 from the second set of experiments shows that higher wear happens for the first set of experiment. For the first set of experiments (Figure 8-22 ), the dynamic formation and removal of the tribofilm starts from the beginning of replacing the oil up to the end of the experiment. On the other hand, for the second one (Figure 8-25), the formation and removal starts when the base oil is replaced by fresh ZDDP at 60 minutes. Hence, more formation and removal is happening for the case 1 and that is where more wear is observed. It supports the fact that dynamic formation and removal of the tribofilm plays a significant role in wear of the system.

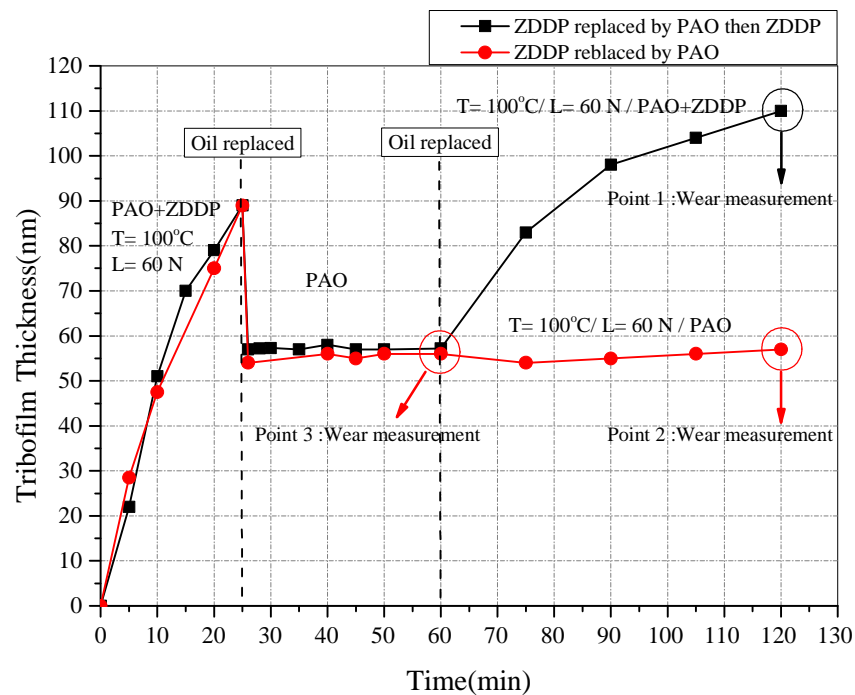


**Figure 8-25 Schematic of the wear measurement points in the case of ZDDP replaced by base oil and then fresh ZDDP and ZDDP replaced by only base oil**

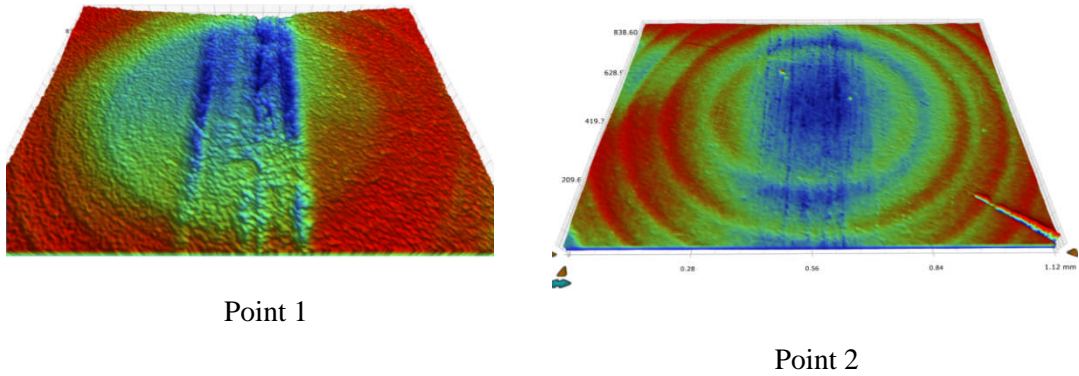


**Figure 8-26 3D-profilometry images taken at the end of experiments**

**Table 8-8 Average wear depth measurement results**

Measurement point	Average wear depth measurement (nm)
Point 1	192
Point 2	104.6
Point 3	98.4

### 8.8 Summary

The main focus of this study is to investigate the durability of the ZDDP tribofilm and correlate it to the chemical properties of the glassy polyphosphates. The effect of parameters such as temperature and load on tribofilm formation and its durability has been studied experimentally by using a Mini Traction Machine (MTM) with the Spacer Layer Interferometry Method (SLIM) attachment. Tribofilm durability so far has not been studied extensively. The experimental results in this paper, show for the first time that running conditions do not affect only the formation of the tribofilm but



also its durability and as such it should be considered in the tribochemical studies of such additives. A methodology for studying the mechanical and chemical aspects of the durability of the tribofilm derived from ZDDP antiwear additive is reported for the first time in this work. The following conclusions can be drawn:

1. The dynamic growth of the tribofilm on the contacting asperities is important for the antiwear mechanism of ZDDP on steel surfaces.
2. The experiments suggest that chemical characteristics and durability of ZDDP tribofilm evolves in time. The results from XPS confirm that longer chain polyphosphates convert to shorter chains when rubbing occurs and tribofilm changes its structure. These changes in the structure are responsible for the increase in the durability of the tribofilm. When the oil was replaced at 25 minutes, the tribofilm mainly consisted of metaphosphates while the structure moved towards containing more pyrophosphates after 3 hrs.
3. ZDDP tribofilm is less durable in the early stages of tribofilm formation. The durability of the ZDDP tribofilm is different at different stages of tribofilm evolution.
4. Physical parameters such as temperature and load significantly affect the resistance of the film to the mechanical rubbing.
5. It was observed that temperature can significantly affect the structure of the glassy polyphosphates in a way that the same applied load can remove more glassy polyphosphates at higher temperature. The structure of the ZDDP tribofilm evaluated by XPS shows that shorter chain polyphosphates (pyrophosphates) are found on the tribofilm when a high amount of tribofilm thickness reduction occurred. In contrast, relatively longer chain polyphosphates were found when the applied temperature was low and a relatively lower amount of tribofilm was removed.

**Table 8-9 Summary of the changes in tribofilm characteristics**

Changes in tribofilm characteristics using PAO+ZDDP in rolling/sliding conditions	PAO+ZDDP replaced by PAO/ Temperature, load and water contents changed				
	Early stage	Late stage	Temperature increases	Load increases	Water content increases
Phosphate chain length decided by BO/NBO ratio and Zn <sub>3</sub> S-P <sub>2P3/2</sub> distance	↓	Not changed	↓	↓	↓
Reaction layer thickness	↓	Not changed	↓	↓	↓
Durability of the tribofilm	↓	↑	↓	↓	↓
Wear	↓	-----	-----	-----	-----

6. Variations in the temperature in this study affect the viscosity of the oil but the calculations of the severity of the contact and  $\lambda$  ratio is not significant.
7. Higher lubricant temperature changes the structure of the glassy polyphosphates which results in higher tribofilm removal once tested in base oil. This observation was supported by XPS and different chain lengths of polyphosphates were found at different depths of the tribofilm.

8. Not surprisingly, higher load results in higher tribofilm thickness reduction and this variation is almost linear. The flash temperature was calculated for different applied loads. It was found that the flash temperature is not varying significantly by the applied load due to the small differences in the maximum Hertzian contact pressures.

A summary of the effect of different parameters such as rubbing time, temperature, load and water on tribofilm characteristics and durability of the tribofilm shown in Table 8-9.

## **Chapter 9. Overall Discussion**

The aim of this chapter is to present the overall discussion derived from this study. This chapter discusses the effect of water and humidity on the tribological and mechanical properties of ZDDP tribofilms as well as it investigates the durability of these anti-wear films. In addition, a detailed discussion is provided on the surface chemistry, properties and composition of ZDDP reaction layer followed by analytical study of the effect of water on the tribofilm formation and wear of the system. This chapter is divided into five sections. Section one discusses the effect of water on ZDDP anti-wear reaction layer and its effect on the tribological performance. Section two examines the humidity effects on the characteristics of ZDDP tribofilm and its effect on wear performance. Section three provides analytical study of the effect of water on the tribofilm growth. The proposed model was used to correlate the growth to wear performance. Finally, section four investigates the interfacial mechanisms of ZDDP tribofilms considering their durability, chemical composition and other mechanical properties and chemical composition.

### **9.1 Water effect on tribochemistry and mechanical wear**

As discussed in Chapter 5, the higher water concentration leads to higher wear in the system for both 80°C and 100°C temperatures. This can be attributed to the effect of water contents on the mechanical and chemical properties of ZDDP tribofilms and its effect on the wear performance. It is also reported in Figure 5-4 that higher temperature leads to the higher tribofilm thickness and it is in line with the results Fujita *et al.* (104) published previously regarding ZDDP antiwear formation and removal. They proposed that both the tribofilm growth and steady state tribofilm thickness increase with temperature. For comparison purposes, the steady-state

tribofilm thickness is plotted against the measured wear depth for both temperatures in Figure 5-5. The lower tribofilm growth rate was observed at high water concentration (Figure 5-2 and Figure 5-3) for both temperatures and this effect is prominent at lower temperature.

The only difference is that the effect of water on the tribofilm growth is clearly distinguishable at lower temperature indicating the effect of water on the growth of the tribofilm at 80°C is more significant than 100°C. Water led to a significant decrease in the growth rate especially in the running-in period. Figure 9-1 shows that water contents dramatically drops after 20 minutes of starting the test due to water evaporation for 3% water concentration at 80°C. It confirms that more water is present in the oil during running-in period for both temperatures. It seems that the higher water concentration present in the oil in running-in period delays the tribofilm formation. This reduction in the growth rate of the tribofilm is more notable at lower temperature due to higher water content in the oil. Figure 9-1 also illustrates that the tribofilm growth rate accelerates once water evaporates from the oil after 25 minutes of rubbing.

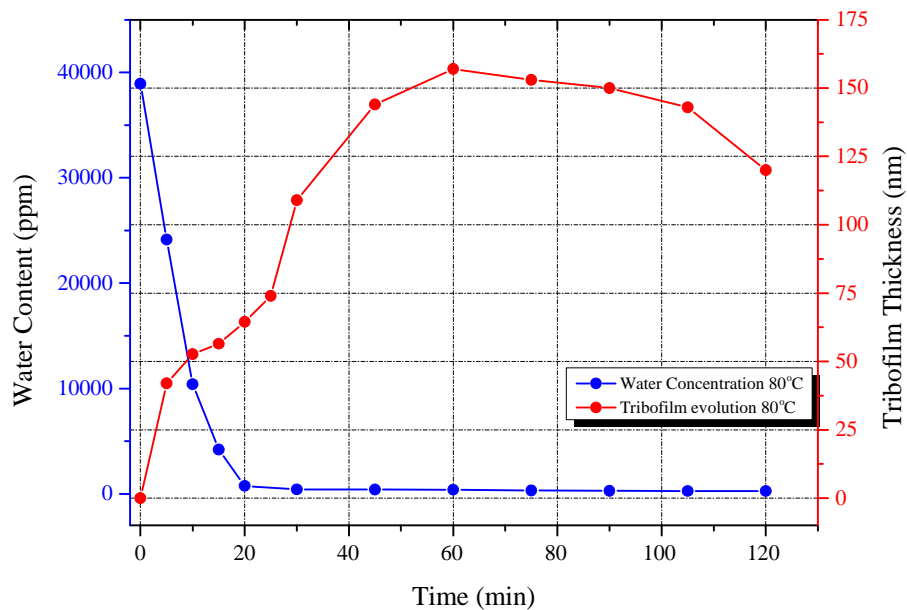


**Figure 9-1 Water concentration evolution and tribofilm thickness over 2 hrs rubbing time for 3% water concentration at 80°C**

One of the possible mechanisms of the delay in the tribofilm growth can be that ZDDP molecules are surrounded by water molecules and thus are prevented from reacting with the surface. This leads to the lower tribofilm growth rate at the beginning. The reduction in the growth rate can noticeably affect the wear process due to the fact that the running-in period plays a significant role in this process. These results are in agreement with the works published by Lancaster (53) and Cen (60). Steady state tribofilm thickness is also affected by water concentration in the oil; the more water concentration the less the tribofilm thickness. It supports the fact that water not only delays the tribofilm formation but also significantly alter the mechanical properties and structure of the ZDDP anti-wear layer. The tribofilm formed in the presence of water seems to be less durable in comparison with the tribofilm formed in the absence of water. This results show that water significantly affects the tribochemistry and chemical composition of zinc polyphosphates.

According to the XPS results shown in Figure 9-9 and Figure 9-10, water molecules can depolymerise longer chain polyphosphates into shorter ones and alter the structure of ZDDP tribofilm. This indicates that presence of water in oil could in fact accelerate the depolymerisation of longer polyphosphate chains into shorter ones. The results are in line with the previous research by Nedelcu *et al.* (174) and Cen *et al* (60). In addition, water seems to change the atomic concentration of O, P and S as well. This could also show that water not only affect the chain length of phosphate species but also alter the chemical bonds. The ratio of BO/NBO also suggests that shorter chain polyphosphates found in the presence of water (see Figure 9-9).It can be summarised that the tribofilm thickness in steady-state condition is not a good representative of

the wear behaviour of the system. However other important physical, chemical and mechanical parameters are involved.

## **9.2 Humidity effects on tribochemistry and mechanical wear**

The effect of relative humidity on oil, tribofilm characteristics and composition and its effect on wear performance were discussed in Chapter 6. It was observed that water concentration dramatically increases at higher values of humidity at 80°C and the same trend was observed for 98°C (Figure 6-1). The comparison between the two temperatures of 80°C and 98°C confirms that the level of water content is reduced at higher temperature. It is likely attributed to the evaporation of the water molecules from the oil. The same conclusion can also be drawn from the observation that only 18°C differences in temperature leads to a significant change in water concentration in the oil and it is more noticeable at higher values of relative humidity (see Figure 6-1).

Figure 9-2 compares the trend of water concentration at 80°C and tribofilm thickness evolution during the 2 hours tribotest for 95% relative humidity. Water concentration seems to keep its value during the test indicating that there is an equilibrium between evaporation and absorption of water in the system. It can be interpreted from Figure 9-2 that in the first 15 minutes (running-in) the decomposition rate of ZZDP is higher than one in the later stages during which the rate levels out.

It can be seen from Figure 6-2 that the higher relative humidity in the range of 80% to 95% leads to the lower tribofilm thickness as well as higher wear at 80°C and the same trend was also found at 98°C (Figure 6-3). Cen *et al* (44) found the same trend in their work. The comparison between these two temperatures shows that the differences between the steady state tribofilm thicknesses for the low humidity values

and high humidity values are more distinguishable at low temperature (80°C) due to the higher water concentration in the oil (see Figure 6-1).

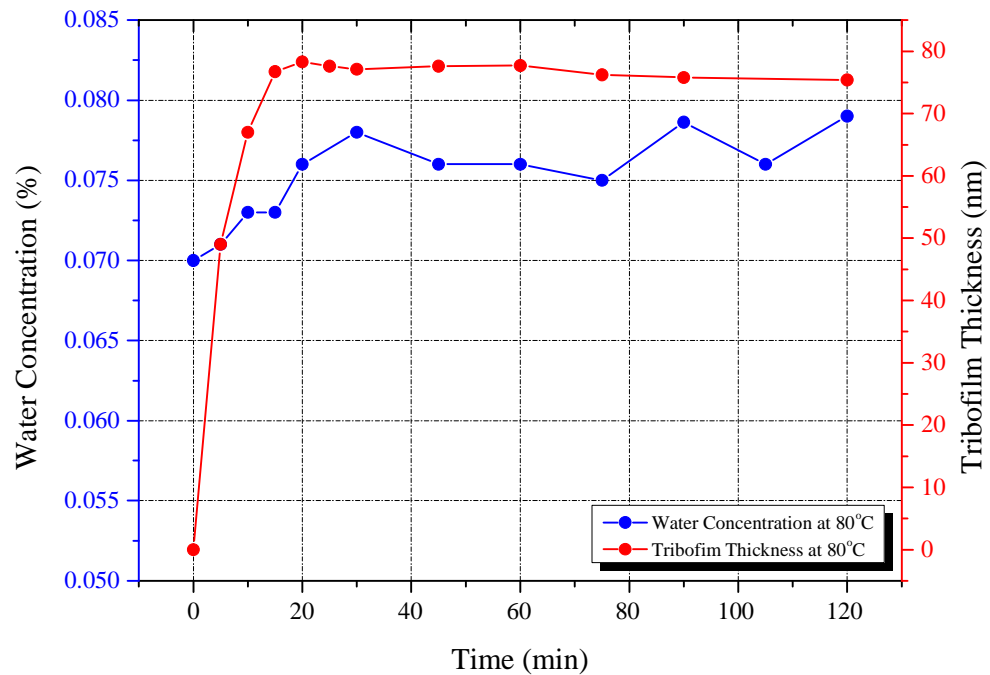


**Figure 9-2 Water contents and tribofilm thickness over 2 hrs rubbing time for 95% relative humidity at 80°C**

As it was shown in Figure 9-2, certain amount of water is present in the oil over the entire rubbing time preventing ZDDP molecules from reacting with the surface to generate tribofilm after first 15 minutes. It was also found that relative humidity hinders the formation of the tribofilm. This could be a reason for the thickness of the ZDDP reaction layer to reach steady-state value and then levels out. This effect is prominent at higher relative humidity for the both tested temperatures (see Figure 6-9 and Figure 9-2).

The growth rate of the tribofilm is also reduced by increasing the relative humidity which supports the fact that relative humidity prevents the formation of ZDDP tribofilms. This effect is significant at higher levels of humidity and lower temperatures as shown in Figure 9-3. For the purpose of better representation, Figure



9-5 shows a 3D visualisation of MTM SLIM images and distribution of the tribofilm within the surface. In the same figure, two different points during the tribotest were considered, i.e. for the lowest and highest relative humidity at 80°C (the points are indicated in Figure 9-4).

It can be clearly observed that the ZDDP tribofilm does not form uniformly on the surface. In addition, higher humidity seems to lead to a patchier form of ZDDP anti-wear layer. The patchiness of the layer is considerably higher at 95% RH in comparison with 0% RH. The 3D map of SLIM image at 95% reveals that the structure of the ZDDP tribofilm can be significantly affected by the presence of humidity (point A3 and C3 in Figure 9-4). The distribution of the tribofilm thickness ranges from 30 nm to 75 nm at 95% RH (see Figure 9-5), which suggests that the tribofilm surface is rougher at higher humidity. The higher roughness was also confirmed from the numerical values obtained from the 3D maps. The roughening effect of relative humidity on the topography of the tribofilm surface might be one of the reasons for the higher wear observed at higher relative humidity (point A3 and C3 in Figure 9-5).

The composition and structure of the tribofilm were investigated by XPS in order to better characterise the ZDDP tribofilm formed in the presence versus absence of humidity. The ratio of BO to NBO area obtained from XPS analysis is used to identify the chain length of glassy polyphosphate (Figure 6-7 and Figure 6-8). This ratio allows characterisation of polyphosphate chain composition ranging from zinc orthophosphate to zinc metaphosphate. It can be clearly seen from Figure 6-9 and Figure 6-10 that the value of BO/NBO decreases while the humidity increases for both temperatures of 80°C and 98°C (see Table 6-1). The higher values of humidity seems to lead to the formation of shorter polyphosphates chain length of zinc orthophosphate

as compared to the case of zinc metaphosphate formed at lower humidity. The results are aligned with the findings of Crobu *et al* (95, 98).

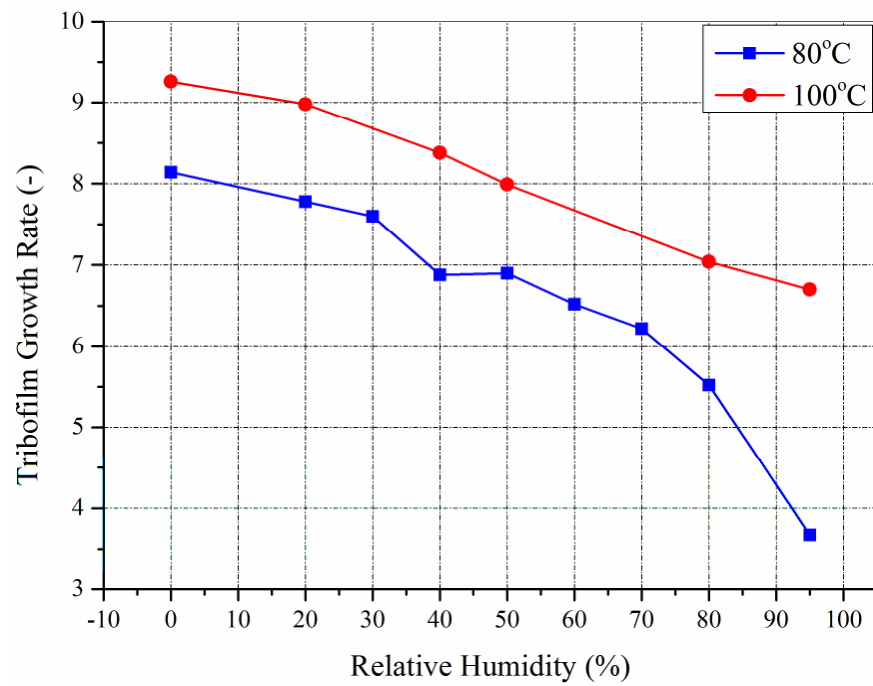


**Figure 9-3 Effect of relative humidity on tribofilm growth rate**

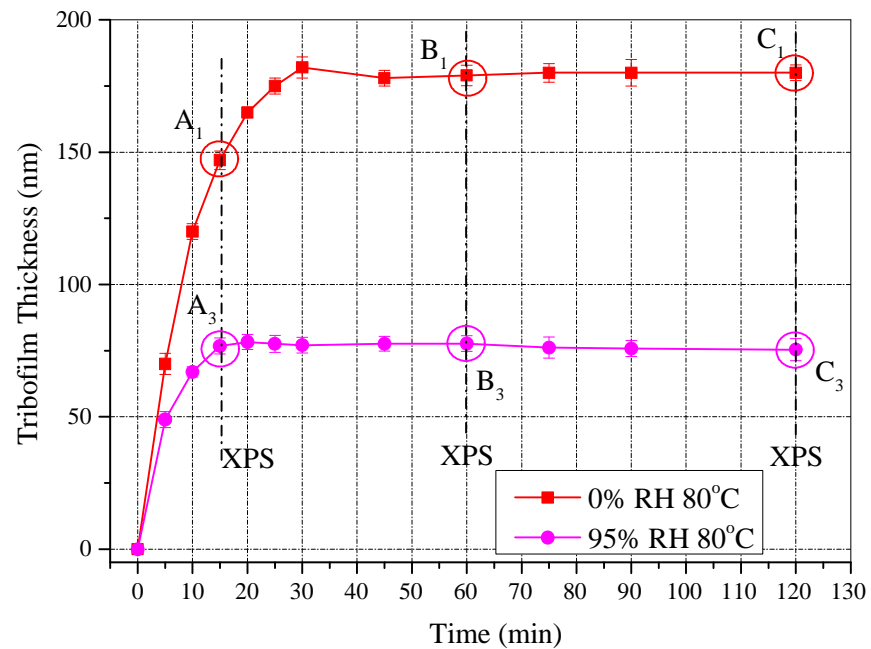


**Figure 9-4 Tribofilm evolution at 0% and 95% RH**

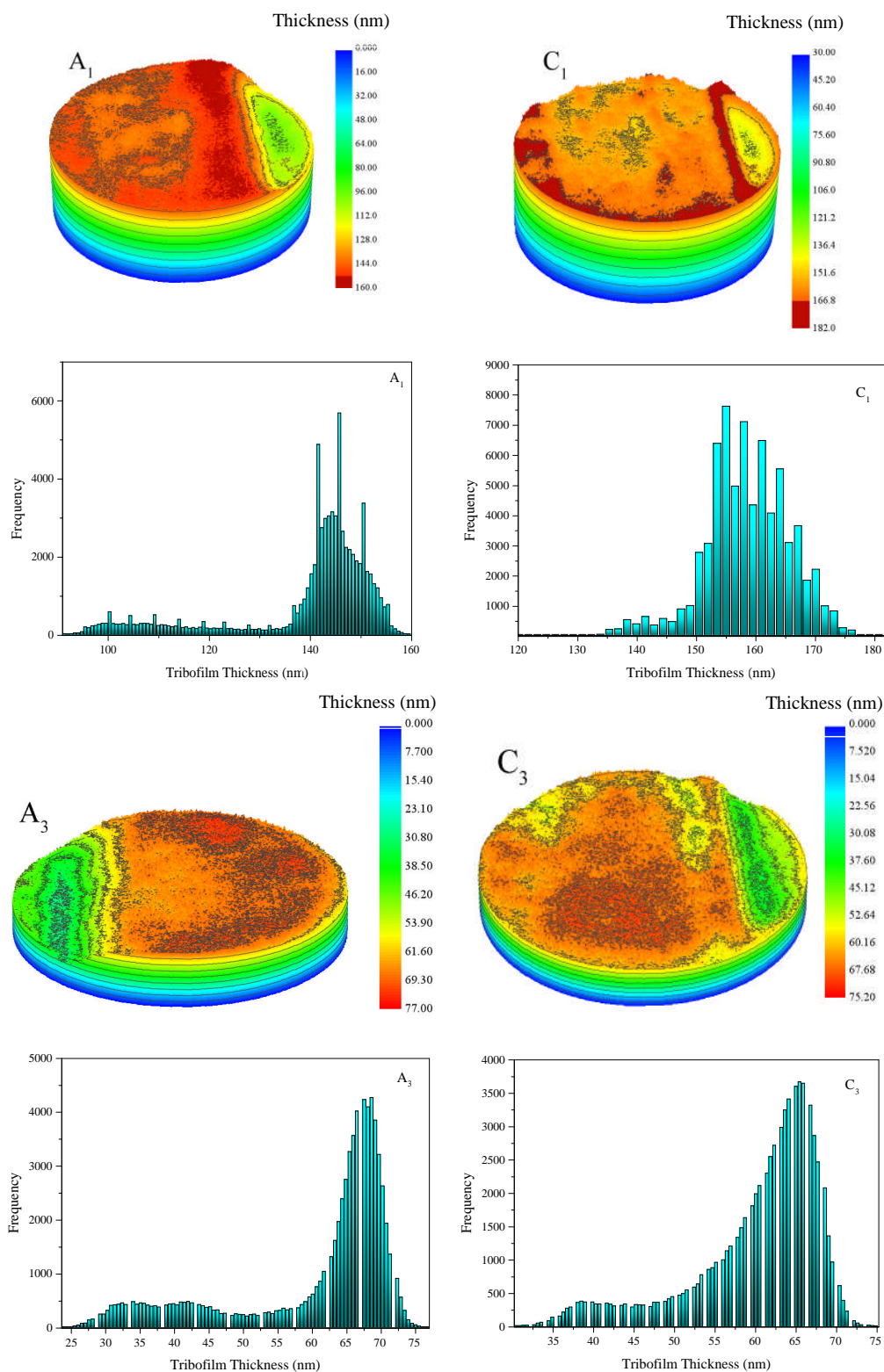


**Figure 9-5 A 3D visualization of MTM SLIM images and distribution of the tribofilm on the surface for 0% and 95% RH at 80°C**

According to the BO/NBO ratios, the shortest polyphosphate chain length was found at 95% relative humidity at 80°C. On the other hand, the longest polyphosphate chain

length was found in the case of 0% relative humidity at 98°C. It suggests that humidity can affect the mechanical properties of the tribofilm especially at lower temperatures and higher levels of humidity due to the higher water concentration in the oil.

Figure 6-1 discusses the water concentrations present in the oil at different values of humidity. The lowest water content was found at 98°C and 0% RH, which is responsible for the longest polyphosphate chain (metaphosphate). However, the highest water concentration, which was found at 95% RH and 80°C, led to the formation of the shortest glassy polyphosphate chain length. It could be interpreted that humidity in fact not only alters the growth rate, topography of the tribofilm surface and roughness of the ZDDP tribofilm but also changes the chain length of polyphosphates and speeds up the depolymerisation reaction of longer chain polyphosphates to shorter ones. The similar findings observed by Fuller *et al* (74) and Nichollas (86) *et al*. They pointed out that longer chain polyphosphates could also be depolymerised by water to shorter chain polyphosphates.

It can be summarised that in the presence of humidity the ZDDP anti-wear additive generates patchier and rougher tribofilms consisting of shorter chain polyphosphates, which leads to thinner tribofilm and higher wear. This detrimental effect might weaken the reaction layer structure formed on the surface. Thus, it results in less durable tribofilm that can be also easily removed from the surface, which eventually causes higher wear. This is further supported by the results shown in Figure 6-11 and Figure 6-12, which indicate that the average wear depth escalates when the relative humidity increases. This trend is prominent at lower temperature and higher humidity, which confirms that the ability of the ZDDP anti-wear additive to reduce wear is sensitive to variations in operating conditions. These results are in a good agreement with the studies done by Lancaster *et al* (53) and Cen *et al* (44, 60). It was proposed

that water contamination plays a significant role in accelerating wear of the system in comparison with the effect of water on friction. Cen *et al* (44) found recently that increasing the relative humidity leads to the higher water adsorption and higher wear under pure sliding condition.

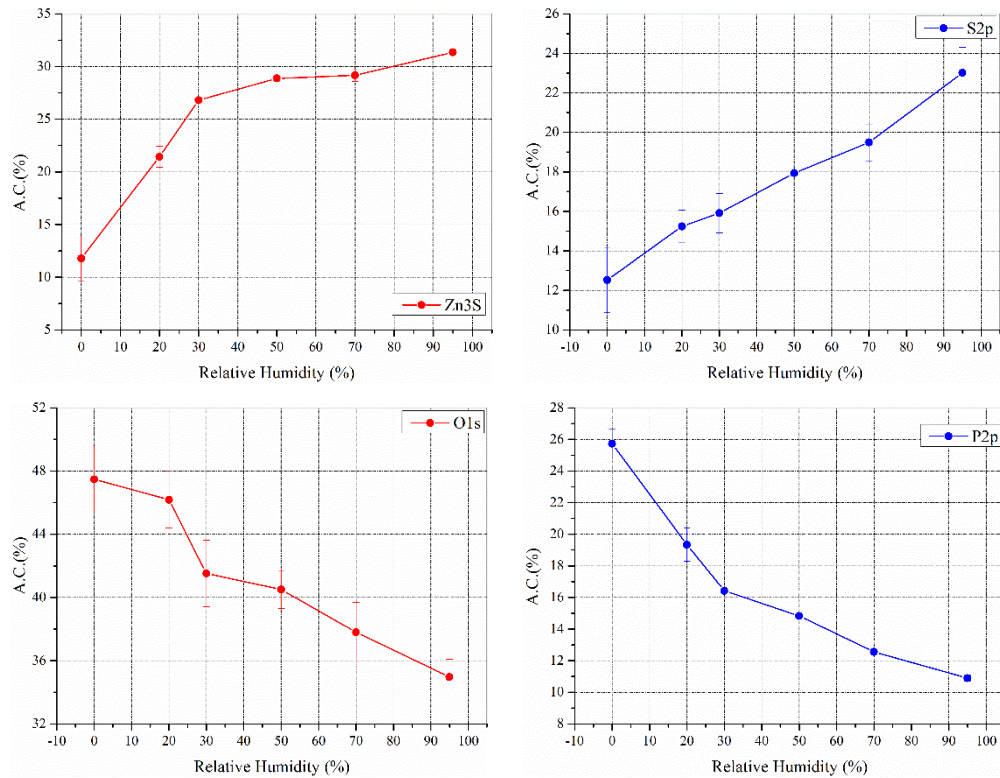


**Figure 9-6 Effect of humidity on the atomic concentration of Zn, S, O and P of ZDDP tribofilm after 2 hrs rubbing**

Figure 9-6 demonstrates the influence of humidity on the atomic concentration of ZDDP decomposition products such as Zn, S, O and P after 2 hrs rubbing. Humidity clearly alters the atomic concentrations of O, S, P and Zn, which are the main decomposition products forming layers of zinc phosphate. Humidity significantly reduces the concentration of O and P. The general trend indicates that the higher the relative humidity the lower the atomic concentration of O and P. On the other hand, humidity accelerates the formation of Zn and S (Figure 9-6). The decrease in the atomic concentration of O and P followed by an increase in the concentration of Zn

can support the fact that shorter polyphosphate chain forming on the surface. This fact is also supported by the significant reduction in the ratio of P/Zn over the 2 hrs test in the humid environment. These findings are also aligned with the trend observed from the ratio of BO/NBO indicating the ZDDP tribofilm consists of shorter chain polyphosphates in the presence of humidity.

It can be summarised that humidity appears to prevent or delay the polymerisation of shorter chain polyphosphates to longer ones. These findings are also aligned with the literature (44, 174). Furthermore, it seems that more vulnerable phosphate chains formed within the tribofilm in the presence of humidity, which can be easily broken down.

The results suggest two possible mechanisms:

- 1- Firstly, humidity appears to be able to deteriorate the long chains polyphosphates (weaker phosphate chains formed), which can be easily depolymerised into shorter ones.
- 2- Secondly, humidity hinders the polymerisation of shorter chain polyphosphates and therefore the longer chain polyphosphates cannot be generated from the beginning of the test.

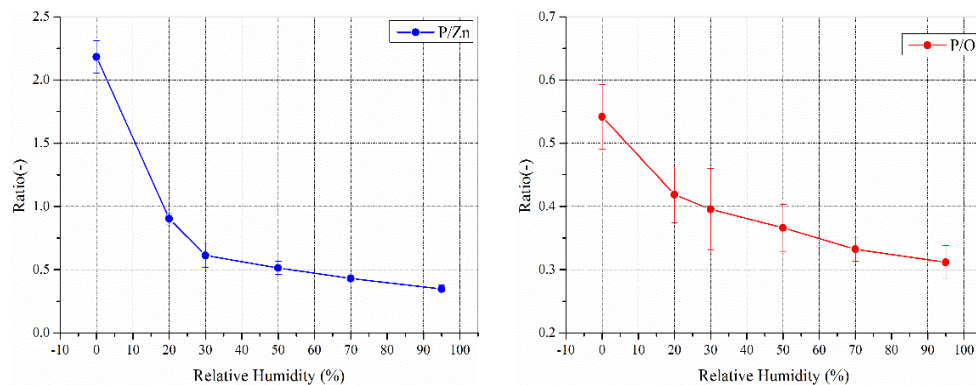


**Figure 9-7 Effect of humidity on the ratio of P/Zn, P/O of ZDDP tribofilm after 2 hrs rubbing**

### **9.3 Combined effect of humidity and mixed water**

As it is discussed in Section 9.1, water concentration in the case of mixed-water in oil does not appear to be constant during the experiment (Figure 9-1). This trend in water content can be split into two stages. Firstly, water concentration largely drops down in the first 15 minutes followed by a second stage of steady state concentration. As shown in Figure 5-2 and Figure 5-3, it seems that water delays the formation of the tribofilm during the running-in period, which is more prominent for higher water concentration and lower temperature. It confirms the observation that the higher the water concentration the lesser the growth rate of the tribofilm. Figure 9-1 reveals that most of the water in the oil evaporates in the first 15 minutes and polymerisation of polyphosphates seems to start in the absence of water. Figure 5-2 illustrates that the lesser tribofilm growth rate results in the lower steady state tribofilm thickness, which is likely related to the weaker tribofilm formed in running-in period in the first stage. It could be concluded that water not only affects the decomposition reaction when it is present in the first 15 minutes but also alters the tribofilm formation even after it evaporates from the oil. The ZDDP anti-wear layer formed in the presence of water is less durable during the time water is present and it can be easily removed as shown in Figure 5-2 and Figure 5-3. As indicated earlier, the general trend shows that the higher the water concentration the lower the steady state tribofilm thickness.

To be able to better understand the effect of water on the durability of the tribofilm, oil containing anti-wear additive was replaced with PAO without any ZDDP in the oil after 25 minutes of starting the test. Figure 9-8 shows that the effect of water on the tribofilm structure in the running-in period cannot be overturned even when water evaporates and thus supports the hypothesis that ZDDP anti-wear layers formed in the

presence of water are less durable. The weaker tribofilm formed in the presence of water leads to higher removal after changing the oil.

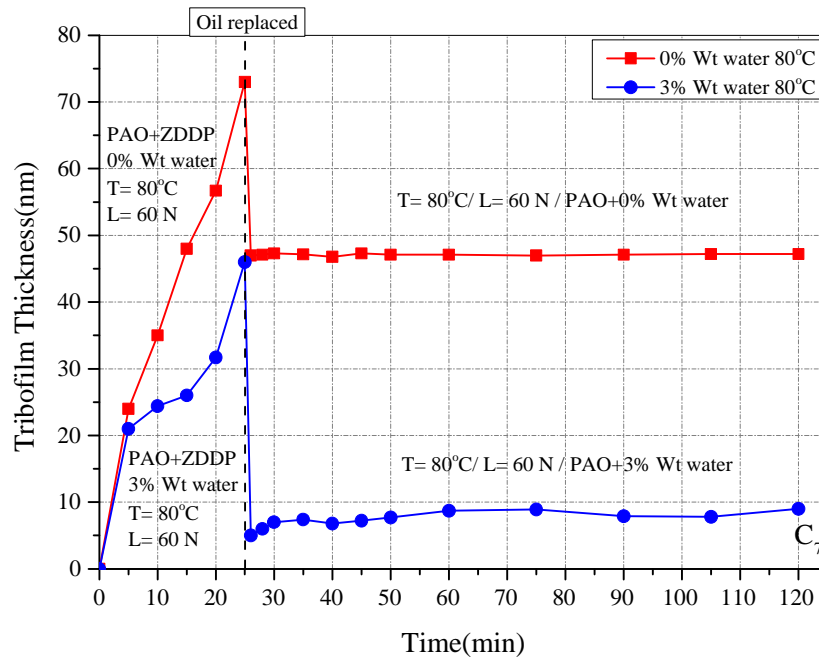


**Figure 9-8 Durability of the tribofilm for ZDDP with different water concentrations at 80°C**

The XPS results also suggest that the tribofilm contains short polyphosphates with high amount of iron oxides and sulphides and high amount of zinc after replacing the oil in the presence of water (see point C<sub>7</sub> in Figure 9-8).

In the case of relative humidity (see Figure 9-2), certain amount of water is present in the oil throughout the test as water evaporation and adsorption reach an equilibrium stage. In this case, the higher relative humidity results in lower steady state thickness of the tribofilm as well as less tribofilm growth rate. It appears that water concentration combined with relative humidity hinder the formation of ZDDP reaction layer during the test and that is the main reason for tribofilm thickness to get levelled out into steady state. Humidity seems also to retard the polymerisation of shorter polyphosphate chains into longer ones and weakens the longer polyphosphate



chain bond formed in the tribofilm, which can be easily converted to shorter ones. This behaviour can be attributed to the high amount of water concentration within the oil throughout the experiment as shown in Figure 9-2.

Figure 9-9 indicates how polyphosphates chain length evolves during the test in the presence and absence of water in the oil based on the ratio of BO/NBO. In the case of 95% relative humidity, the ZDDP reaction layer contains shorter polyphosphate chain even from the beginning and it is lightly decreasing during the test. It is more likely related to the certain amount of water present in the oil throughout the test, which surprisingly results in forming shorter chain polyphosphates than in the case of 3% mixed-water and 0% Humidity.

As it described before in this section, in the case of 3% mixed-water in oil, the ZDDP additive generates shorter chain tribofilm in the first 15 minutes (first stage) and delays the polymerisation of short chains into longer ones as water is present in the oil. It is interesting to notice that the polymerisation reaction seems to immediately start after the evaporating of the mixed-water from the oil. There is a slight reduction in the chain length of polyphosphates even when the water evaporates from the surface and polymerisation process starts to occur, which indicates that the formed polyphosphate chains are less durable during the time water is absent (0% relative humidity). The chemical bonds of the formed polyphosphates appear to be easily broken, which makes the tribofilm more vulnerable to wear and removal (see Figure 5-2 and Figure 5-3).

The combined effect of water and humidity can be observed in Figure 9-10. The results indicate that both mixed water in oil and humidity can largely affect the atomic concentration of P and Zn, which are the main decomposition products generating zinc phosphates within the tribofilm's layers. It appears that Zn formation in the

presence of mixed-water or humidity is considerably speeded up compared to 0% relative humidity although the phosphorous concentration decreases for both cases (see Figure 9-10). It can be determined that the presence of water either as water contamination or water adsorbed from the humid environment can highly alter the composition of ZDDP tribofilm. Further investigation into the Figure 9-10 reveals that the effect of humidity on the acceleration and deceleration of Zn and P respectively, is fairly higher than the case of 3% mixed-water in oil. It can be related to the water evaporation from the oil in the case of 3% water (Figure 9-1 and Figure 9-2).

The atomic concentration of O appears to decrease when water or humidity is present in the system and the effect of water is more prominent in the humid environment. This can be related to the certain amount of water present in the oil throughout the test. The reduction in the concentration of O results in a decrease in the ratio of BO to NBO which shows that the ZDDP reaction layer is made of short polyphosphate chains.

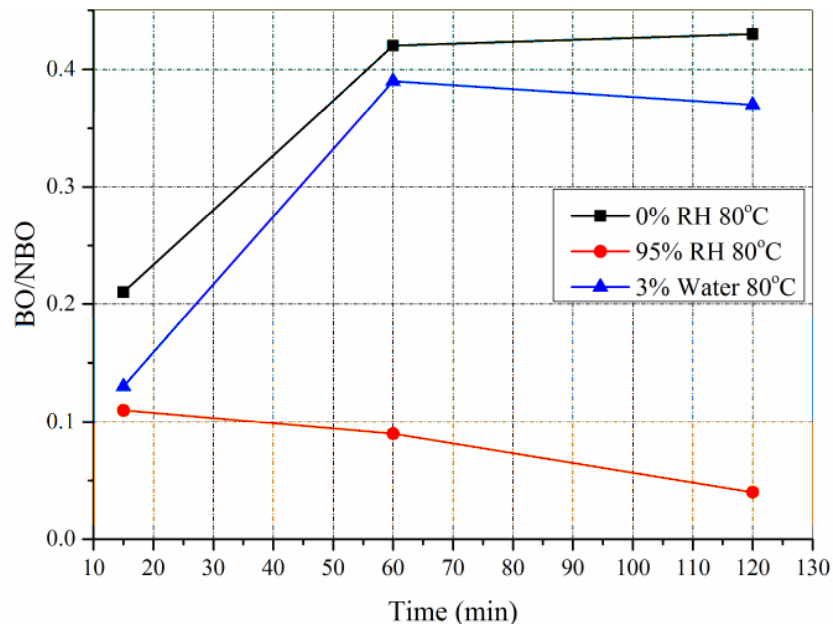
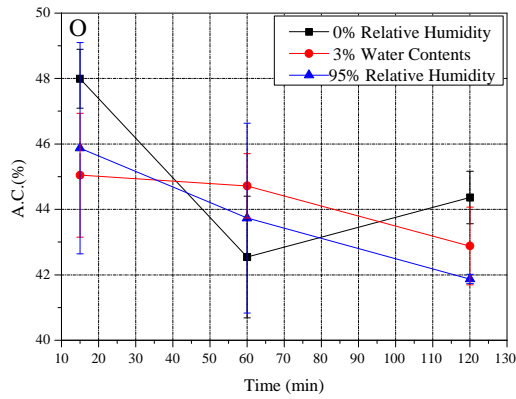
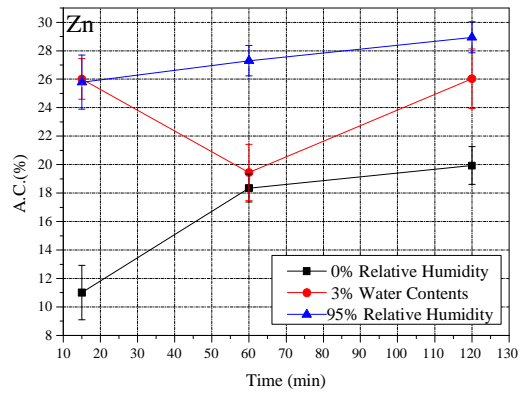


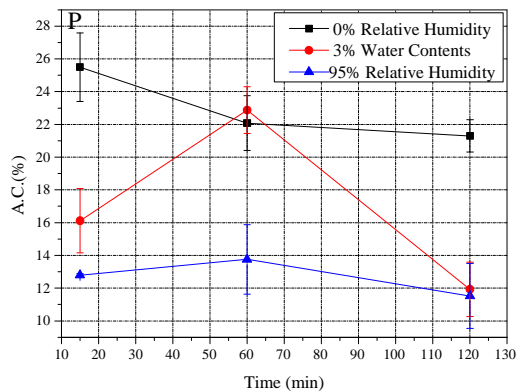
**Figure 9-9 Evolution of polyphosphate chain length**



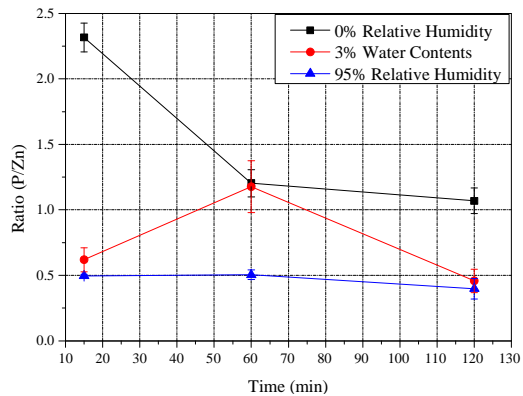
(a)



(b)



(c)



(d)

**Figure 9-10 Combined-effect of mixed-water and humidity on the evolution of O(a), Zn(b), P(c) and the ratio of P/Zn(d) of the ZDDP reaction layer over the time**

As described earlier in this section, water can delay the formation of the tribofilm and hinders the polymerisation reaction of short chain polyphosphates for both cases (mixed-water and humidity). All these observations suggest that the tribofilm consists of shorter polyphosphate chains in humid environment than in the case of mixed-water in oil, which is evident from the evolution of the atomic concentrations of P, Zn and O.

Figure 9-11 shows the tribofilm evolution over rubbing time for 95% relative humidity and 3% water at 80°C. It can be clearly observed that the growth rate of the tribofilm for 3% mixed-water is slightly lower than in the case of 95% RH. The main reason for this can be related to the higher water content present in the oil for 3%

water than 95% relative humidity as shown in Figure 9-1 and Figure 9-2. Generally, the results indicate that the higher the water concentration the lower the tribofilm growth rate. As soon as water molecules start evaporating from the surface, depolymerisation of shorter chain polyphosphates start to occur whereas in the case of relative humidity certain amount of water still exists in the oil throughout the test thus preventing the formation of the tribofilm.

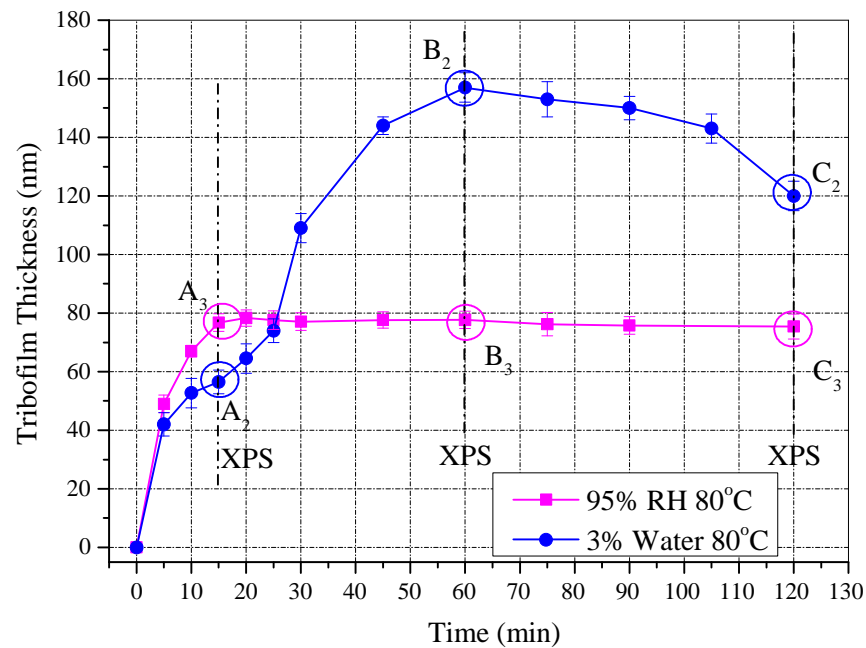


**Figure 9-11 Tribofilm evolution at 3% water and 95% RH at 80°C**

To examine the effect of water on the structure of the formed tribofilm, 3D maps of MTM SLIM images and distribution of the tribofilm within the surface are presented in Figure 9-12 at two different points over the rubbing time. The ZDDP anti-wear layer in the presence of water appears to be patchier and rougher for both humidity and mixed-water than in the case where water is absent. The distribution of the tribofilm within the surface reveals that the tribofilm thickness ranges from 0 to 75 nm at point A<sub>2</sub> and 75 to 145 nm at point C<sub>2</sub> indicating that the topography of the tribofilm for 3% water content is considerably patchier than in the case of 95% RH.

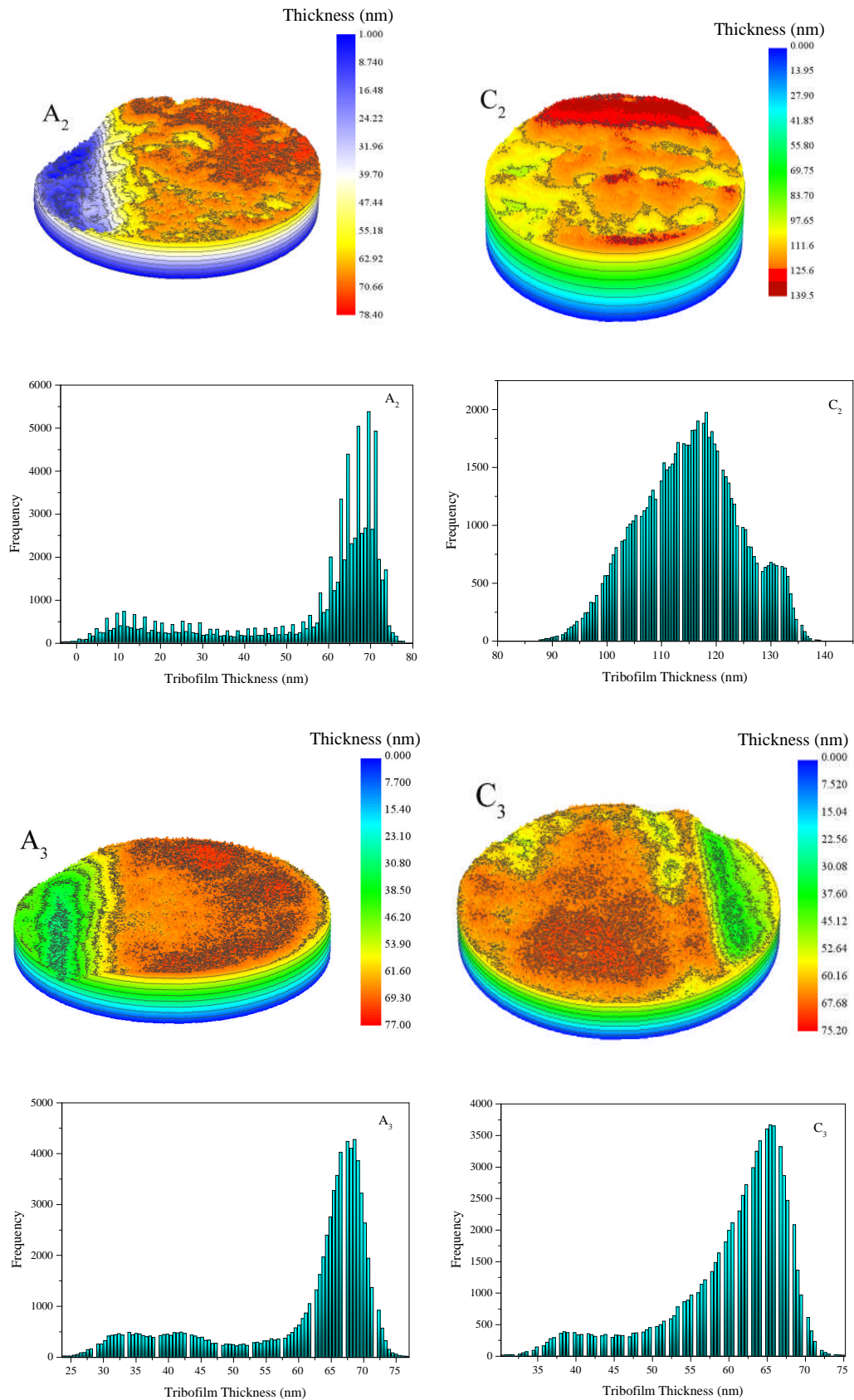


**Figure 9-12 A 3D visualization of MTM SLIM images and distribution of the tribefilm on the surface for 3% water (point A<sub>2</sub> and C<sub>2</sub>) and 95% RH (A<sub>3</sub> and C<sub>3</sub>)**

It can be summarized that water, whether adsorbed from the humid environment or added to the oil before the test, generally is detrimental to the tribofilm and contacting surfaces. Water can significantly affect the tribofilm formation, durability, structure and even composition, which largely influence wear performance of the system. The presence of water can cause delay in the tribofilm formation when the oil is contaminated with water before the test whereas in the humid environment it hinders the formation of the ZDDP reaction layer and the polymerisation of its polyphosphate chains into longer chains. In the presence of water, thinner tribofilms are formed on the surface. This effect becomes more prominent in humid environment as water is present over the entire rubbing time as compared to the running-in period only in the case of oil contaminated with water under low relative humidity. The presence of water seems to make the tribofilm more vulnerable to wear and removal, which results in higher wear of contacting surfaces in both cases. It was also found by Cai *et al* (185) that water contamination above the saturation level in the oil (emulsion) is detrimental for the system in terms of wear behaviour. In this study, it is also observed that the lower temperature results in higher wear. It can be related to the more evaporation of water at higher temperature. The higher temperature leads to the thicker tribofilm formed by ZDDP. The same trends were proposed by Cen *et al* (44) and Ghanbarzadeh *et al* (109).

#### **9.4 Analytical study of the effect of water on tribofilm growth and wear**

As described in Chapter 7 two different approaches were used to analytically study the effect of mixed-water and humidity on the tribofilm growth and how its impacts on wear of the system. The aim of the first approach is set to be an evaluation of the effect of water on the coefficient of wear. For this purpose, a modification factor,  $\psi$

was defined to be added to Equation 7-2 which is assigned to the effect of water on wear. As it is expected from the obtained experimental results in Chapter 5,  $\psi$  which is responsible for the water effects is increasing by increasing the mixed-water in oil (see Table 7-3 and Table 7-4). The results from the model suggests that the higher the water concentration the higher the coefficient of wear. The same trend observed from the model for the effect of humidity.

Table 7-6 clarifies that the higher coefficient of wear and  $\psi$  for both temperatures assigned to the higher relative humidity. The influence of water corresponding to the different humidity on  $\psi$  found to be higher than the case of mixed-water in oil. It supports the fact that wear in humid environment is more detrimental than mixed-water in oil. The model is also capable of capturing the effect of temperature on the wear performance. The results for both cases suggest that the higher temperature appears to reduce the wear due to the thicker tribofilm on the surface and lower concentration of water.

Second approach is meant to capture the effect of water on the tribofilm growth and its effect on wear of the system. Figure 7-13 and Figure 7-14 exhibit the higher water concentration in the oil seems to decelerate the growth rate of the tribofilm as well as steady state tribofilm thickness for both temperatures. It confirms the fact that the model is able to predict the tribofilm growth. The same trend was observed in the humid environment as presented in Figure 7-16 and Figure 7-17 indicating the thickness of the reaction layer is decreasing by increasing the humidity as well as the growth rate of the tribofilm. It can be also seen that the model can predict the formation for both temperatures meaning the higher the temperature the thicker the tribofilm for the both cases (mixed-water and humidity).

As expected from experimental results, numerical wear calculations obtained from the model are in a good agreement with the experimental measurements (see Figure 7-18 and Figure 7-19). The model appears to be able to accurately capture the wear behaviour for two different temperatures. As it can be seen in the graphs, the higher the relative humidity the higher the wear in the system. The mathematical model follows the same behaviour in the case of mixed-water in oil. It can be summarised that the effect of humidity on the growth rate of the reaction layer is different from the effect of mixed-water in oil. The maximum film thickness seems to be the same for all the water concentration whereas the maximum film thickness significantly affected by different levels of relative humidity and it can be estimated by mathematical model.

## **9.5 Durability of the tribofilm**

For the purpose of investigating the tribofilm evolution and the durability of the reaction layer within the time, oil was replaced at two different stages; early stage and late stage as mentioned in Chapter 8.

### **9.5.1 Early stage**

Figure 8-2 displays the replacement of PAO+ZDDP with PAO in the absence of ZDDP at early stage (after 25 minutes of rubbing time) which significantly alters the tribofilm growth behaviour. This replacement results in a large reduction in the thickness of the tribofilm whereas there is no notable drop in the tribofilm thickness when PAO+ZDDP exchanged with a fresh PAO+ZDDP. In this case, ZDDP reaction layer keeps forming on the surface up to 100 nm tribofilm thickness. Mechanical action seems to be responsible for the considerable reduction of the tribofilm thickness when PAO+ZDDP replaced by PAO. The observations suggest that the top layer of the ZDDP reaction layer formed on the surface is less durable than the bulk of the



tribofilm which results in a decrease in the thickness when the oil replaced by PAO. The results show that there is no sufficient ZDDP additive remained in the oil after replacing PAO+ZDDP with PAO and the rate of the mechanical removal of the tribofilm is higher than formation which results in a significant drop in the thickness. It can be also said that the top layer of the ZDDP anti-wear layer is less durable than bulk of the tribofilm and once the uppermost layer is removed, the tribofilm is durable and the thickness does not change.

It is also shown that the drop in the thickness of the tribofilm is a rapid drop indicating the top soft layer of the tribofilm is removed in the first few load cycles after replacing the oil. The results obtained from XPS analysis on the samples (see point A<sub>1</sub>, C<sub>1</sub> and C<sub>2</sub> in Figure 8-2) exhibit the toper layer of the tribofilm consists of longer chain polyphosphate (point A<sub>1</sub> and C<sub>1</sub>) which appears to be softer than the bulk of the reaction layer (point C<sub>2</sub>) which is made of the shorter chain polyphosphates (see Figure 8-5 and Figure 8-6). According to the refs (95, 98), this conclusion can be drawn that the ZDDP reaction layer structure alters from metaphosphate (longer chain) to orthophosphate (shorter chain) in the bulk of the tribofilm.

The results reveal that the mechanical properties of the tribofilm varies within the thickness of the reaction layer that can be assigned to the chemical bonds between the decomposition products of ZDDP such as P, Zn, O and S. The shorter polyphosphate chain in the bulk of the tribofilm shows more durable structure than the top layer which contains longer chain polyphosphates. The longer chain polyphosphates (metaphosphates) seem to be more vulnerable and removable than the shorter chain polyphosphates.

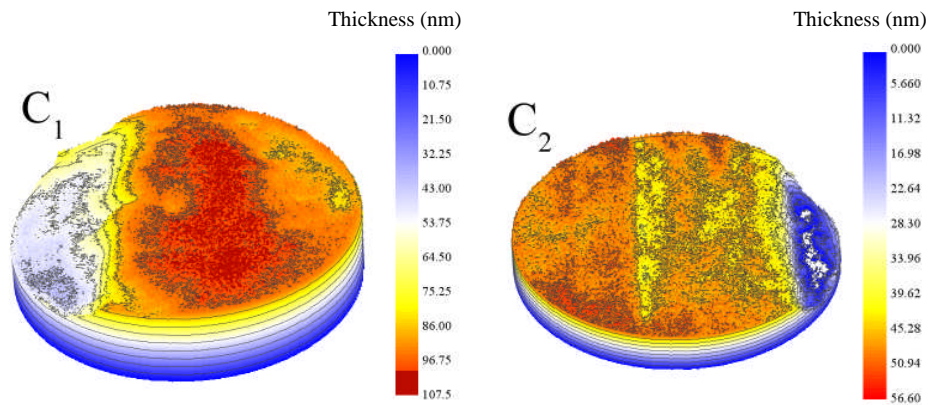


**Figure 9-13 A 3D visualization of MTM SLIM images at point C<sub>1</sub> and C<sub>2</sub>**

A 3D visualization of SLIM images from wear scar at Point C<sub>1</sub> and C<sub>2</sub> (Figure 8-2) shown in Figure 9-13 to better understand the topography of the surface. It can be interpreted from the figures that the tribofilm thickness ranges from 35nm to 105 nm when PAO+ZDDP replaced by Fresh PAO+ZDDP. The 3D images also show that roughness and patchiness of the reaction layer in the case of replacing PAO+ZDDP with PAO is higher than the case in which PAO+ZDDP replaced by PAO. In the latter case, Tribofilm thickness ranges from 5nm to 55nm. According to the change in the mechanical properties of the reaction layer within the tribofilm, the longer chain polyphosphates on the top layer appears to create rougher and patchier surface (point C<sub>1</sub>) than the bulk of the tribofilm which contains short ones (point C<sub>2</sub>).

### 9.5.2 Late stage

Figure 8-3 displays the late stage replacement of the PAO+ZDDP with PAO to assess the effect of rubbing time on the durability of the tribofilm. There is no significant drop in the tribofilm thickness when the oil is replaced with PAO after 3 hrs of rubbing time (Figure 8-3), however Figure 8-2 indicates that there is a large reduction of the tribofilm thickness at early stage replacement of the oil. It could support the fact that the durability of the tribofilm is also changing by rubbing time and it is more resistant

to rubbing. Therefore, only a few nanometres of the film are removed. XPS analysis confirms the presence of short chain polyphosphates at the end of both experiments (point C<sub>3</sub> and C<sub>4</sub> in Figure 8-3). A comparison between early stage and late stage oil replacements indicates that shorter chain polyphosphates exist on the surface compared to the early stage (see Table 8-2). It appears that the durability of the tribofilm is improved by rubbing time which might be a reason why the ZDDP reaction layer is not removed after exchanging the oil with PAO. Results are in a good agreement with the reports of literature (194). As it is observed in XPS analysis (see Figure 8-7 and Figure 8-8), tribofilm contains shorter chain polyphosphates after 3hrs rubbing. Rubbing appears to accelerate depolymerisation of longer chain to shorter ones. The similar trend was observed by Crobu *et al* (95). They reported previously that long chain polyphosphates convert to shorter chain polyphosphates due to rubbing. There is another possibility that rubbing makes the longer chain weaker and after enough rubbing time, longer chain polyphosphates easily broken to shorter ones.

### **9.5.3 Multiple replacement**

Figure 8-4 exhibit when the oil replaced by base oil after 25 minutes of starting the test followed by the exchanging PAO by a fresh ZDDP after 1hour of rubbing time, the reaction layer appears to start forming again up to the higher level of tribofilm thickness even higher than initial stage (see Point A<sub>2</sub> and C<sub>5</sub> in Figure 8-4). It has also been shown in the literature that unreacted ZDDP can be replenished in the contact areas and reform glassy polyphosphates (85) XPS analysis on the wear track at Point A<sub>2</sub>, C<sub>5</sub> and C<sub>6</sub> display the reaction layer at A<sub>2</sub> before replacing the oil by PAO contains longer chain polyphosphates (metaphosphate) when the tribofilm is relatively thick. Once the oil is exchanged and the tribofilm is partially removed, shorter chain polyphosphates found in the tribofilm.

It can be proved that the mechanical properties of ZDDP anti-wear layer varies from the bulk to the top layer of the tribofilm. This behaviour can be assigned to the chain length of polyphosphate varies from the shorter chain in the bulk to the longer ones on the top. Furthermore, the significant drop in the tribofilm thickness, especially from the top layer when the oil replaced by PAO (see point A<sub>2</sub>) can approve that the uppermost layer which consists of longer polyphosphate chain is less durable than the bulk of the tribofilm in which shorter chain ones exist. It has been shown that the mechanical properties and chemistry of the ZDDP tribofilm varies from bulk to the surface (81, 85, 86, 95, 195). This suggests that different chemistries can be correlated for mechanical properties of the film.

A 3D map of SLIM images shown in Figure 9-14 confirms that as a result of replacing the PAO with fresh PAO+ZDDP (see point C<sub>5</sub> in Figure 8-4), patchier structure of the tribofilm found on the surface than Point C<sub>6</sub>.

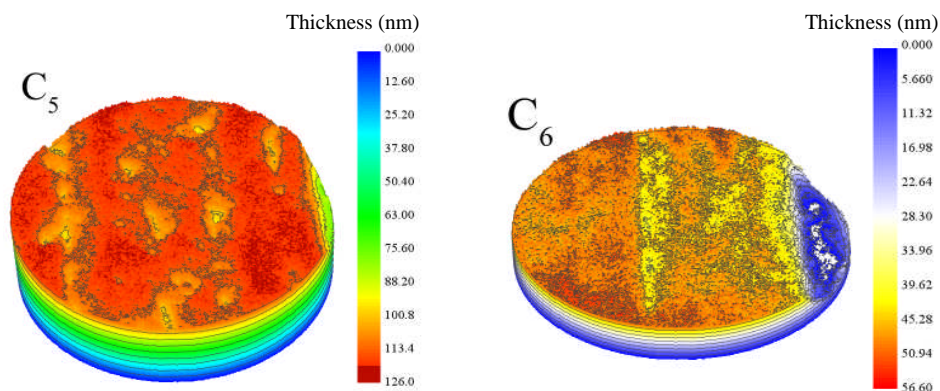


**Figure 9-14 A 3D visualization of MTM SLIM images at point C<sub>5</sub> and C<sub>6</sub>**

#### **9.5.4 Effect of temperature and load on durability of the tribofilm**

As explained in the sections 8.4 and 8.5, tribological test conducted with the same conditions to build up the tribofilm up to 25 minutes of rubbing time and then the oil and temperature/load changed to PAO and different temperatures/loads to be able to

assess the effect of temperature and load on the durability and chemical composition of the ZDDP reaction layer. It can be obviously seen from Figure 8-11 and Figure 8-12 that changing the temperature to the higher temperatures (120°C and 140°C) after replacing the PAO+ZDDP with PAO results in a significant reduction in the thickness of the tribofilm which is an instantaneous drop after a few cycles (see point B1 in Figure 8-11). The higher the temperature the higher the tribofilm removal. Heating up the tribofilm formed within the first 25 minutes of rubbing to the higher temperature appears to alter the durability of the tribofilm.

This leads to the immediate removal of the ZDDP-antiwear layer after starting the test again. Results are supported by the previous study of the temperature effects on the mechanical properties of ZDDP (90, 197). With respect to the BO/NBO ratios and Zn3S-P2p binding energy difference at point A<sub>3</sub> (see Figure 8-13), longer chain polyphosphates found on the surface. As it is seen in the previous sections, longer chain polyphosphates are softer than the short ones and easier to be removed from the surface. This phenomena accelerates when the temperature is increased and makes the structure more vulnerable and detachable. That can be a reason for the highest reduction of tribofilm thickness occurred at 140°C. The same trend is observed for 120°C whereas the lower temperature (80°C) found responsible for the lowest tribofilm removal (see Figure 8-13).

It seems that the cross-linked structure of ZDDP reaction layer becomes weaker and less durable at higher temperature that can be broken and removed from the surface by a few cycles of rubbing. The XPS results at Point B<sub>1</sub> after a few cycles of rubbing reveals that tribofilm contains shorter chain polyphosphates which cannot be removed from the surface due to its durability.

It is interesting to note that the growth rate of the tribofilm in the second stage (after replacing the oil), is increasing by temperature as well. The highest growth rate found in the case of 140°C which is responsible for the highest removal of the tribofilm as well. Tribofilm after a large removal at 140°C immediately starts building up to the 75 nm thickness. The longer chain tribofilm observed at point C<sub>8</sub> at the end of the test (see Figure 8-13). Temperature appears to speed up the polymerisation reaction of shorter polyphosphate chains to longer ones as longer chain polyphosphates found at point C<sub>8</sub>.

It can be understood from the XPS results that temperature not only change the mechanical properties and durability of the tribofilm but also plays a role of catalyser and accelerates the decomposition rate of ZDDP and polymerisation reaction which results in the higher growth rate of the tribofilm in the second stage.

The same behaviour observed for the effect of load on the durability and chemical composition of the tribofilm. Figure 8-16 displays the tribofilm evolution for different loads. Higher load results in the higher removal of the tribofilm. This variation is plotted in Figure 8-17. Not surprisingly, reduction in the thickness of the tribofilm is also linear with the applied load.

The comparison between the high load and low load suggests that when the tribofilm is more removed for the case of higher load, there are shorter chain polyphosphates present in its bulk after the removal. Therefore higher load is able to remove more durable glassy phosphates in the bulk of the tribofilm and this behaviour is very similar to the temperature effect on the removal of the tribofilm. For the temperature, it is more reasonable that temperature changes the structure of the tribofilm therefore changing its durability and removal behaviour. On the other hand higher load results in more shear stress applied on the tribofilm which can lead to the more removal of

the film. The same conclusion can be drawn from the effect of load and temperature that the mechanical properties of the tribofilm changes within the tribofilm as well as tribofilm structure (81, 85, 86, 95, 195).

## **Chapter 10. Conclusions and Future Work**

This chapter discusses the conclusions derived from this work. A combination conclusion of the effect of water on the tribofilm formation, characteristics, durability and its effect on wear performance of the tribological system; the effect of humidity on the decomposition products of ZDDP anti-wear reaction layer and its effect on wear performance; analytical study of the effect of water on ZDDP tribofilm growth and its correlation with wear and finally, the effect of temperature and load on ZDDP tribofilm structure and its effect on durability of the layer. At the end of this chapter, some future work will be presented.

### **10.1 Water effect on ZDDP anti-wear reaction layer and its effect on wear**

Section 5.2 and Section 5.3 have extensively studied the effect of water on wear behaviour of boundary lubricated tribosystem in a rolling-sliding contact. The main results are summarized in this section.

1. Water affects the tribochemistry of the zinc polyphosphates tribofilm on the surfaces.
2. Water influences the growth behaviour of the tribofilm on the surfaces and more water in the oil results in lower rate of the growth on contacting surfaces
3. Water in oil can delay the growth of the tribofilm in the running-in period and it can significantly affect wear performance in boundary lubricated system. This effect is more significant for the tests at 80°C in comparison with tests at 100°C due to more water in the oil
4. Higher water concentration leads to a reduction in the growth rate of the tribofilm which in nature results in an increase in the wear of the system. One



of the possible mechanisms might be that ZDDP molecules can be surrounded by water molecules and prevented from reacting with the surface which leads to the lower tribofilm growth rate at the beginning. (See Figure 5-5)

5. Steady state tribofilm thickness is also affected by water concentration in the oil; the higher the water concentration the lower the tribofilm thickness. It supports the fact that water not only delays the tribofilm formation but also significantly alters the mechanical properties and structure of the ZDDP anti-wear layer. The tribofilm formed in the presence of water seems to be less durable in comparison with the tribofilm formed in the absence of water.
6. It was shown that tribofilm thickness in steady-state condition is not a good representative of the wear behaviour of the system. However other important physical, chemical and mechanical parameters are involved. The whole growth behaviour of the tribofilm can be significantly important to characterize wear. This means that running-in period is also important in determining the wear of boundary lubricated systems.
7. According to the XPS results, water molecules can depolymerise longer chain polyphosphates to the shorter ones and alter the structure of ZDDP tribofilm. This indicates that presence of water in oil could in fact accelerate the depolymerisation of longer polyphosphate chains to shorter ones.
8. Water seems to change the atomic concentration of O, P and S as well. This could also show that water not only affect the chain length of phosphate species but also alter the chemical bonds allowed with the phosphates. The ratio of BO/NBO is also suggested that shorter chain polyphosphates found in the presence of water (see Figure 9-9).

## **10.2 The effect of humidity on the decomposition products of ZDDP anti-wear reaction layer and its effect on wear performance**

The effect of relative humidity on tribofilm characteristics and wear performance of the boundary lubricated system in rolling/sliding conditions has been investigated for the first time in this chapter by using MTM SLIM integrated to the humidity control system. Notable observations in this chapter are summarized as follow:

1. The increase of relative humidity increases the wear of the system for both temperatures of 80°C and 98°C. It can be attributed to the higher water concentrations when higher humidity values are applied. It is worth mentioning that the higher the temperature the less the wear due to the thicker tribofilm thickness formed on the surface. The effect of humidity on wear performance is more significant at lower temperature in comparison with higher temperature.
2. Higher water contents in oil results in reducing the growth of the tribofilm which causes higher wear in the system. Reducing tribofilm growth might be because of the difficulty that ZDDP molecules have to access to the surface and react with the substrate in the presence of higher amount of water.
3. Relative humidity can significantly affect the mechanical properties of the tribofilm. It was found that the effect of humidity on tribofilm formation is more significant at higher humidity and lower temperature (80°C) due to the more water content in the oil.
4. Water concentration seems to keep its value during the test indicating that there is an equilibrium between evaporation and absorption of water in the system. It can be interpreted from Figure 9-2 that the presence of water in the

first 15 minutes (running-in) accelerates the decomposition rate of ZDDP and then it starts terminating the tribofilm formation and it levels out.

5. It can be also determined that relative humidity hinders the formation of tribofilm and that could be a reason for ZDDP reaction layer to growth up to the steady-state thickness and then levels out, and this effect is prominent at higher relative humidity for both temperatures ( Figure 6-9 and Figure 9-2).
6. ZDDP tribofilm does not form uniform on the surface and higher humidity leads to the patchier form of ZDDP anti-wear layer. The 3D map of SLIM image at 95% reveals that the structure of the ZDDP tribofilm can be significantly affected in the presence of humidity
7. It also shows that humidity not only alter the growth rate of the tribofilm but also changes the chemical composition and structure of the reaction layer.
8. XPS results show that shorter chain poly phosphates present in the tribofilm at higher relative humidity. It can be linked to the depolymerisation of longer polyphosphate chain to shorter chain. The higher the relative humidity the lower the ratio of BO/NBO.
9. It is more likely that humidity largely changes the composition of the ZDDP tribofilm by altering the atomic concentrations of P and Zn which are the main decomposition products forming layers of zinc phosphate.
10. The decrease in the atomic concentration of O and P followed by an increase in the concentration of Zn can support the fact that shorter polyphosphate chain forming on the surface. This fact is also supported by the significant reduction in the ratio of P/Zn over 2hrs test in the humid environment.
11. For the purpose of comparison between the effect of mixed-water and humidity, it can be mentioned that water delays the decomposition reaction in running-in period when water mixed with oil (3% water). As soon as water

molecules start evaporating from the surface, depolymerisation of shorter chain polyphosphates start to occur whereas in terms of the humidity case, certain amount of water exists in the oil throughout the test and humidity prevents the formation of the tribofilm.

### **10.3 Combined effect of mixed-water in oil and humidity**

It can be summarized that water generally is detrimental for all the tribological system either water adsorbed from the humid environment or oil contaminated with water before the test. Water can significantly affect the tribofilm formation, durability, structure and even composition which largely influence wear performance of the system. The presence of water can cause delay in the tribofilm formation when the oil is contaminated with water before the test but it hinders the polymerisation of the polyphosphate chain to form longer chains and formation of the ZDDP reaction layer in the humid environment. Thinner tribofilm formed on the surface in the presence of water and it is prominent in humid environment as water present over the rubbing time compared to the time oil contaminated with water before the test.

The observations seem to make the tribofilm more removable and vulnerable which results in higher wear in both cases. The higher the water concentration the higher the wear happening in the system. Running the test in humid environment causes more wear in the system compared to the mixed-water in oil as the consequences of humidity are more detrimental due to the concentration of water throughout the test.

### **10.4 Analytical study of the effect of water and humidity**

#### **10.4.1 Analytical study of effect of mixed-water**

The experimental results obtained from the effect of mixed-water in oil were used to adapt Archard's wear coefficient to the tribocorrosive conditions. The new wear

model considering the effect of water was implemented into the previously-reported numerical model to develop a new semi-deterministic numerical wear model adapted to the tribo-corrosion system in this section (See Section 7.4). The key observations can be summarised as shown below:

1. Two different numerical approaches were used to test the model and also represent the effect of water in wear of the system. With respect to the first approach, tribocorrosive wear can be predicted by modifying the Archard's wear coefficient. The modification parameter ( $\Psi$ ) increases by increasing the water concentration. The simulation wear results show good agreement with the experimental wear measurements.
2. It is concluded in this work that once the characteristics of the tribofilm growth are captured, the model is capable of predicting tribocorrosive wear in boundary lubrication regime.

#### **10.4.2 Analytical study of the effect of relative humidity**

Relative humidity and its effects on tribochemistry and wear of boundary lubricated systems was examined experimentally in Chapter 6. In the current study the tribofilm thickness and wear results obtained experimentally are used to develop a semi-deterministic approach to implement the effect of humidity in wear prediction of boundary lubrication for the first time.

A semi-analytical approach was applied to model the effect of relative humidity on tribofilm growth and wear in boundary lubricated system in presence of ZDDP as an anti-wear additive (See Section 7.5). Two approaches were employed to implement the effect of relative humidity in predictive wear model and the following observations can be drawn:

1. In regards to the first approach, Archard's wear coefficient is semi-deterministically obtained for different levels of relative humidity from the simulations. This can lead to the modification of Archard's wear equation with a modification factor of  $\varphi$ . This approach can be used by designers of tribological parts to take in to account the effect of humid environment on the durability.
2. In addition, the modification factor  $\varphi$  is increasing while the humidity increases.
3. The second numerical approach was applied to consider the effect of humidity on the tribofilm growth and the corresponding wear behaviour in boundary lubrication. It is shown that successfully capturing the tribofilm growth behaviour leads to predicting the tribochemical wear in boundary lubricated conditions.
4. It was the effect of relative humidity on tribofilm growth behaviour and wear is different from the effect of mixed-water in the oil which was the subject of a recent study by the authors. In the latter case, the maximum film thickness was found the same for different levels of water concentration while the tribofilm growth rate found to be significantly affected which led to different wear rates in running-in stage. In the case of relative humidity, the maximum film thickness is influenced considerably.
5. Calibration of the numerical-tribochemical model suggests a linear variation of  $h_{max}$  (maximum tribofilm formation) with relative humidity and the result is a modification to the tribochemical model to adapt it to the tribocorrosion conditions in humid environment.

## **10.5 The effect of temperature and load on ZDDP tribofilm structure and its effect on durability of the layer**

The main focus of this study is to investigate the durability of the ZDDP tribofilm and correlate it to the chemical properties of the glassy polyphosphates. The effect of parameters such as temperature and load on tribofilm formation and its durability has been studied experimentally by using a Mini Traction Machine (MTM) with the Spacer Layer Interferometry Method (SLIM) attachment. Tribofilm durability so far has not been studied extensively. The experimental results in this paper, show for the first time that running conditions do not affect only the formation of the tribofilm but also its durability and as such it should be considered in the tribochemical studies of such additives. A methodology for studying the mechanical and chemical aspects of the durability of the tribofilm derived from ZDDP antiwear additive is reported for the first time in this work. The following conclusions can be drawn:

1. The dynamic growth of the tribofilm on the contacting asperities is important for the antiwear mechanism of ZDDP on steel surfaces.
2. The experiments suggest that chemical characteristics and durability of ZDDP tribofilm evolves in time. The results from XPS confirm that longer chain polyphosphates convert to shorter chains when rubbing occurs and tribofilm changes its structure. These changes in the structure are responsible for the increase in the durability of the tribofilm. When the oil was replaced at 25 minutes, the tribofilm mainly consisted of metaphosphates while the structure moved towards containing more pyrophosphates after 3 hrs.
3. ZDDP tribofilm is less durable in the early stages of tribofilm formation. The durability of the ZDDP tribofilm is different at different stages of tribofilm evolution.

4. Physical parameters such as temperature and load significantly affect the resistance of the film to the mechanical rubbing.
5. It was observed that temperature can significantly affect the structure of the glassy polyphosphates in a way that the same applied load can remove more glassy polyphosphates at higher temperature. The structure of the ZDDP tribofilm evaluated by XPS shows that shorter chain polyphosphates (pyrophosphates) are found on the tribofilm when a high amount of tribofilm thickness reduction occurred. In contrast, relatively longer chain polyphosphates were found when the applied temperature was low and a relatively lower amount of tribofilm was removed.
6. Variations in the temperature in this study affect the viscosity of the oil but the calculations of the severity of the contact and  $\lambda$  ratio is not significant.
7. Higher lubricant temperature changes the structure of the glassy polyphosphates which results in higher tribofilm removal once tested in base oil. This observation was supported by XPS and different chain lengths of polyphosphates were found at different depths of the tribofilm.
8. Not surprisingly, higher load results in higher tribofilm thickness reduction and this variation is almost linear. The flash temperature was calculated for different applied loads. It was found that the flash temperature is not varying significantly by the applied load due to the small differences in the maximum Hertzian contact pressures.

## **10.6 Future work**

This research discussed the effect of water/humidity on the mechanical, chemical properties of ZDDP tribofilms as well as their formation, removal and durability. The correlation between the mechanical properties and the chemical composition of the



ZDDP anti-wear layer was also presented in this study. Additionally, the effect water and humidity on the tribofilm growth and wear performance were analytically studied. There are several factors involved in the interfacial mechanisms of ZDDP tribolayer need to be investigated further.

### **10.6.1 Experimental**

- Investigate the effect of water and humidity on the rheological properties, tribofilm formation and durability of ZDDP additive in nano-scale by using AFM.
- Assess the impact of dissolved water and free water on the ZDDP anti-wear additive and its tribochemistry. In this research, the type of water in the oil cannot be specified as free or dissolved water.
- Investigation into the mechanical properties of ZDDP reaction layer using nano-indentation test. This method can indicate that how water can affect the hardness and modulus of ZDDP tribofilms and how this affect is related to the tribological performance.
- The effect of water and humidity on friction behaviour of the ZDDP-antiwear additive and its relation to the other tribological, mechanical and rheological properties of the system.
- The interactions of the ZDDP antiwear additive with other additives such as MoDTC, DDP, TCP. This will enable us to formulate a better mechanistic understanding of the decomposition process of ZDDP.
- Study the effect of water on the tribofilms formed on different substrates than bearing steel. In one case, the effect of water on non-doped H-DLC and doped DLCs with different dopants can be studied.

### 10.6.2 Modelling

- The effect of water and humidity on the tribofilm growth and its effect on the friction behaviour of ZDDP additive.
- Effect of water and humidity on tribofilm formation and its effect on subsurface stresses; therefore the water effect on micropitting and fatigue
- Adapt the developed model to the other lubricants and additives. This model is only developed for PAO+ZDDP.
- Extend the model for tribocorrosion conditions including the effect of passivation and repassivation of oxide layer on wear performance.

## Chapter 11. References

1. Fitch J, Jaggernauth S. The second most destructive lubricant contaminate, and its effects on bearing life. 1994.
2. Needelman WM. Forms of water in oil and their control. 2006.
3. Duncanson M. Detecting and controlling water in oil. *Practicing Oil Analysis Magazine*. 2005:22-4.
4. Cantley R. The effect of water in lubricating oil on bearing fatigue life. *ASLE TRANSACTIONS*. 1977;20(3):244-8.
5. Felsen I, McQuaid R, Marzani J. Effect of seawater on the fatigue life and failure distribution of flood-lubricated angular contact ball bearings. *ASLE TRANSACTIONS*. 1972;15(1):8-17.
6. Sam Z. The effect of relative humidity on wear of a diamond-like carbon coating. *Surface and Coatings Technology*. 2003;167(2-3):221-5.
7. Schatzberg P, Felsen I. Effects of water and oxygen during rolling contact lubrication. *Wear*. 1968;12(5):331-42.
8. Ciruna J, Szieleit H. The effect of hydrogen on the rolling contact fatigue life of AISI 52100 and 440C steel balls. *Wear*. 1973;24(1):107-18.
9. Grunberg L, Jamieson D, Scott D. Hydrogen penetration in water-accelerated fatigue of rolling surfaces. *Philosophical Magazine*. 1963;8(93):1553-68.
10. Evans MH, Richardson AD, Wang L, Wood RJK. Serial sectioning investigation of butterfly and white etching crack (WEC) formation in wind turbine gearbox bearings. *Wear*. 2013;302(1-2):1573-82.
11. Lancaster J. A review of the influence of environmental humidity and water on friction, lubrication and wear. *Tribology International*. 1990;23(6):371-89.
12. Cen H. Effect of water on the performance of lubricants and related tribochemistry in boundary lubricated steel/steel contacts. 2012.
13. Eachus AC. The trouble with water. *Tribology and Lubrication Technology*. 2005.
14. Gresham RM. When oil and water do mix. *Tribology and Lubrication Technology*. 2008;64(3):22.
15. Morina A, Neville A. Tribofilms: aspects of formation, stability and removal. *Journal of Physics D: Applied Physics*. 2007;40(18):5476.
16. Rounds FG. Some factors affecting the decomposition of three commercial zinc organodithiophosphates. *ASLE TRANSACTIONS*. 1975;18(2):79-89.
17. Haque T, Morina A, Neville A, Kapadia R, Arrowsmith S. Non-ferrous coating/lubricant interactions in tribological contacts: Assessment of tribofilms. *Tribology International*. 2007;40(10-12):1603-12.
18. Graham J, Spikes H, Korcek S. The friction reducing properties of molybdenum dialkyldithiocarbamate additives: part I—factors influencing friction reduction. *Tribology Transactions*. 2001;44(4):626-36.

19. Archard J, Hirst W. The wear of metals under unlubricated conditions. *Proceedings of the Royal Society of London Series A Mathematical and Physical Sciences*. 1956;236(1206):397-410.
20. Thompson JM, Thompson MK, editors. A proposal for the calculation of wear. *Proceedings of the 2006 International ANSYS Users Conference & Exhibition, Pittsburgh, PA–2006*; 2006.
21. Rigney D, Chen L, Naylor MG, Rosenfield A. Wear processes in sliding systems. *Wear*. 1984;100(1):195-219.
22. Sexton M. A study of wear in Cu and Fe systems. *Wear*. 1984;94(3):275-94.
23. Stachowiak GW, Batchelor AW. 8 - Boundary and Extreme Pressure Lubrication. In: Stachowiak GW, Batchelor AW, editors. *Engineering Tribology (Third Edition)*. Burlington: Butterworth-Heinemann; 2006. p. 363-417.
24. Khonsari MM, Booser R. *Applied tribology: bearing design and lubrication*: John Wiley & Sons; 2008.
25. Bowden, Philip F. *The friction and lubrication of solids, part I*. Clarendon Press, Oxford, . 1954.
26. Whitehouse DJ, Archard JF. The properties of random surfaces of significance in their contact. *Proc Roy Soc London*,. 1970; 316(Series A):97-121.
27. Handbook A. Friction, lubrication and wear technology. *International Journal of Fatigue*. 1992;18.
28. Nilsson R. On wear in rolling-sliding contacts. 2005.
29. Dwyer-Joyce R. Predicting the abrasive wear of ball bearings by lubricant debris. *Wear*. 1999;233:692-701.
30. Lancaster JK. Material-specific wear mechanisms: relevance to wear modelling. *Wear*. 1990;141(1):159-83.
31. Littmann W. The mechanism of contact fatigue. *NASA Special Publication*. 1970;237:309.
32. Stachowiak, Gwidon, Batchelor. *Engineering tribology 2013*.
33. Karpinska A. *Running-in and the evolution of metallic surfaces subjected to sliding and rolling contact*: Imperial College London; 2010.
34. Hutchings IM. *Tribology - Friction and wear of engineering materials*: Butterworth-Heinemann Ltd; 1992.
35. Hsu S, Gates RS. Boundary lubrication and boundary lubricating films. *National Institute of Standards and Technology*. 2001;12.
36. Sakamoto, Uetz. Reaction layer formation on bronze with an S-P ,extreme pressure additive in boundary lubrication under increasing load. *Wear*. 1985;105(4):307-21.
37. Chapter 8 - Boundary and extreme pressure lubrication. In: Stachowiak GW, Batchelor AW, editors. *Engineering Tribology (Fourth Edition)*. Boston: Butterworth-Heinemann; 2014. p. 371-428.
38. Spikes HA. Mixed lubrication — an overview. *Lubrication Science*. 1997;9(3):221-53.
39. Beheshti A, Khonsari M. An engineering approach for the prediction of wear in mixed lubricated contacts. *Wear*. 2013;308(1):121-31.

40. Soda N, Kimura Y, Tanaka A. Wear of Some F.C.C. Metals During Unlubricated Sliding Part I: Effects of load, velocity and atmospheric pressure. *Wear*. 1975;33: 1-16.
41. Errichello R. The lubrication of gears. *Gear Technology*. 1991.
42. Echin A, Novosartov G, Popova E. Hygroscopicity of synthetic oils. *Chemistry and Technology of Fuels and Oils*. 1981;17(4):198-200.
43. Hamaguchi H, Spikes H, Cameron A. Elastohydrodynamic properties of water in oil emulsions. *Wear*. 1977;43(1):17-24.
44. H Cen, A Morina, A Neville, R Pasaribu, I Nedelcu. Effect of water on ZDDP anti-wear performance and related tribochemistry in lubricated steel/steel pure sliding contacts. *Tribology International*. 2012;56:47-57.
45. Dave Webb, Needelman B. Preventing Water Contamination Problems. 2006.
46. Yang S, Reddyhoff T, Spikes H. Influence of lubricant properties on temperature rise and transmission efficiency. *Tribology Transactions*. 2013;56(6):1119-36.
47. Berkani S, Dassenoy F, Minfray C, Martin J-M, Cardon H, Montagnac G. Structural changes in tribo-Stressed zinc polyphosphates. *Tribology Letters*. 2013;51(3):489-98.
48. Fitch J, Jaggernauth S. Moisture-The second most destructive lubricant contaminate and its effects on bearing life 1994.
49. RM Gresham. When oil and water do mix. *Tribology & lubrication technology*. March 2008.
50. Sander J. Management of water during the lubricant life cycle. *Lubrication Engineers*. 2009.
51. Needelman W, LaVallee G. Forms of water in oil and their control. *Noria Lubrication Excellence Conference, Columbus Ohio*; 2006.
52. Bauer C, Day M. Water contamination in hydraulic and lube systems. *Practicing Oil Analysis magazine*. 2007.
53. Lancaster JK. A review of the influence of environmental humidity and water on friction, lubrication and wear. *Tribology International*. 1990;23(6):371-89.
54. Goto H, Buckley D. The influence of water vapour in air on the friction behaviour of pure metals during fretting. *Tribology international*. 1985;18(4):237-45.
55. Schatzberg P, Felsen IM. Effects of water and oxygen during rolling contact lubrication. *Wear*. 1968;12(5):331-42.
56. Liu W, Dong D, Kimura Y, Okada K. Elastohydrodynamic lubrication with water-in-oil emulsions. *Wear*. 1994;179(1):17-21.
57. Ray D, Vincent L, Coquillet B, Guirandeq P, Chene J, Aucouturier M. Hydrogen embrittlement of a stainless ball bearing steel. *Wear*. 1980;65(1):103-11.
58. Neeraj T, Srinivasan R, Li J. Hydrogen embrittlement of ferritic steels: Observations on deformation microstructure, nanoscale dimples and failure by nanovoiding. *Acta Materialia*. 2012;60(13):5160-71.
59. Madhavan P, Werner NC. Contamination control for extending fluid service life. *Practicing Oil Analysis Magazine* March 2005.

60. Cen H. Effect of water on the performance of lubricants and related tribochemistry in boundary lubricated steel/steel contacts: University of Leeds; 2012.
61. Sheiretov T, Van Glabbeek W, Cusano C. The effect of dissolved water on the tribological properties of polyalkylene glycol and polyolester lubricants. *Lubrication engineering*. 1996;52(6):463-80.
62. Spikes H. The history and mechanisms of ZDDP. *Tribology Letters*. 2004;17(3):469-89.
63. Baldwin BA. Relationship between surface composition and wear: an X-ray photoelectron spectroscopic study of surfaces tested with organosulfur compounds. *ASLE TRANSACTIONS*. 1976;19(4):335-44.
64. Hallouis M, Belin M, Martin J. The role of sulphur in ZDDP-induced reaction films formed in the presence of ZDDP: Contribution of electron spectroscopic imaging technique. *Lubrication Science*. 1990;2(4):337-49.
65. Martin J, Belin M, Mansot J, Dexpert H, Lagarde P. Friction-induced amorphization with ZDDP—an EXAFS study. *ASLE transactions*. 1986;29(4):523-31.
66. Armstrong D, Ferrari E, Roberts K, Adams D. An examination of the reactivity of zinc di-alkyl-di-thiophosphate in relation to its use as an anti-wear and anti-corrosion additive in lubricating oils. *Wear*. 1998;217(2):276-87.
67. Burn A, Smith G. The structure of basic zinc OO-dialklyl phosphorodithioates. *Chemical Communications (London)*. 1965(17):394-6.
68. Barnes AM, Bartle KD, Thibon VRA. A review of zinc dialkyldithiophosphates (ZDDPS): characterisation and role in the lubricating oil. *Tribology International*. 2001;34(6):389-95.
69. Rudnick LR. *Lubricant additives: chemistry and applications*: CRC press; 2009.
70. Pawlak Z. *Tribochemistry of lubricating oils*: Elsevier; 2003.
71. Armstrong D, Ferrari E, Roberts K, Adams D. An investigation into the molecular stability of zinc di-alkyl-di-thiophosphates (ZDDPs) in relation to their use as anti-wear and anti-corrosion additives in lubricating oils. *Wear*. 1997;208(1):138-46.
72. Dacre B, Bovington C. The adsorption and desorption of zinc di-isopropyldithiophosphate on steel. *ASLE TRANSACTIONS*. 1982;25(4):546-54.
73. Piras FM, Rossi A, Spencer ND. Combined in situ (ATR FT-IR) and ex situ (XPS) study of the ZnDTP-iron surface interaction. *Tribology Letters*. 2003;15(3):181-91.
74. Fuller ML, Kasrai M, Bancroft GM, Fyfe K, Tan KH. Solution decomposition of zinc dialkyl dithiophosphate and its effect on antiwear and thermal film formation studied by X-ray absorption spectroscopy. *Tribology international*. 1998;31(10):627-44.
75. Fuller M, Yin Z, Kasrai M, Bancroft GM, Yamaguchi ES, Ryason PR, et al. Chemical characterization of tribochemical and thermal films generated from neutral and basic ZDDPs using X-ray absorption spectroscopy. *Tribology International*. 1997;30(4):305-15.

76. Loeser E, Wiquist R, Twiss S. Cam and tappet lubrication III—radioactive study of phosphorus in the EP film. *ASLE TRANSACTIONS*. 1958;1(2):329-35.
77. Fujita H, Spikes H. The formation of zinc dithiophosphate antiwear films. *Proceedings of the Institution of Mechanical Engineers, Part J: Journal of Engineering Tribology*. 2004;218(4):265-78.
78. Taylor L, Dratva A, Spikes H. Friction and wear behavior of zinc dialkyldithiophosphate additive. *Tribology transactions*. 2000;43(3):469-79.
79. Palacios J. Thickness and chemical composition of films formed by antimony dithiocarbamate and zinc dithiophosphate. *Tribology international*. 1986;19(1):35-9.
80. Fuller MS, Fernandez LR, Massoumi G, Lennard W, Kasrai M, Bancroft G. The use of X-ray absorption spectroscopy for monitoring the thickness of antiwear films from ZDDP. *Tribology Letters*. 2000;8(4):187-92.
81. Aktary M, McDermott MT, McAlpine GA. Morphology and nanomechanical properties of ZDDP antiwear films as a function of tribological contact time. *Tribology letters*. 2002;12(3):155-62.
82. Harrison PG, Kikabhai T. Proton and phosphorus-31 nuclear magnetic resonance study of zinc (II) O, O'-dialkyl dithiophosphates in solution. *Journal of the Chemical Society, Dalton Transactions*. 1987(4):807-14.
83. S. Bec, A. Tonck, J. M. Georges, R. C. Coy, Bell JC, Roper GW. Relationship between mechanical properties and structures of zinc dithiophosphate anti-wear films. *Proceedings of the Royal Society A: Mathematical, Physical and Engineering Science*. 1999;445(1992):4181-203.
84. Gabi Nehme RM, Pranesh B. Effect of contact load and lubricant volume on the properties of tribofilms formed under boundary lubrication in a fully formulated oil under extreme load conditions. *Wear*. 2010;268(9):1129-47.
85. Nicholls MA, Nortona PR, Bancroft GM, M. Kasrai, T. Dob, Frazerc BH, et al. Nanometer scale chemomechanical characterization of antiwear films. *Tribology Letters*. 2004;17(2):205-16.
86. Nicholls MA, Do T, Norton PR, Kasrai M, Bancroft GM. Review of the lubrication of metallic surfaces by zinc dialkyl-dithiophosphates. *Tribology international*. 2005;38(1):15-39.
87. Pereira AL, Nicholls MA, Kasrai MM, Norton PR, and De Stasio G. Chemical characterization and nanomechanical properties of antiwear films fabricated from ZDDP on a near hypereutectic Al-Si alloy. *Tribology Letters*. 2005;18(4):411-27.
88. Mourhatch PA. Tribological behavior and nature of tribofilms generated from fluorinated ZDDP in comparison to ZDDP under extreme pressure conditions—Part II: Morphology and nanoscale properties of tribofilms. *tribology international*. 2011;44(3):201-10.
89. N.J. Mosey, T.K. Woo, MM. Kasrai, P.R. Norton, Bancroft GM, Muser MH. Interpretation of experiments on ZDDP anti-wear films through pressure-induced cross-linking. *Tribology Letters*. 2006;24(2):105-14.

90. Demmou K, Bec S, Loubet J-L, Martin J-M. Temperature effects on mechanical properties of zinc dithiophosphate tribofilms. *Tribology international*. 2006;39(12):1558-63.
91. Vengudusamy B, Green JH, Lamb GD, Spikes HA. Tribological properties of tribofilms formed from ZDDP in DLC/DLC and DLC/steel contacts. *Tribology International*. 2011;44(2):165-74.
92. Vengudusamy B, Green JH, Lamb GD, Spikes HA. Durability of ZDDP tribofilms formed in DLC/DLC contacts. *Tribology Letters*. 2013;51(3):469-78.
93. Morina A, Neville A. Tribofilms: aspects of formation, stability and removal. *Journal of Physics D: Applied Physics*. 2007;40(18):54-76.
94. Lin Y, So H. Limitations on use of ZDDP as an antiwear additive in boundary lubrication. *Tribology International*. 2004;37(1):25-33.
95. Crobu M, Rossi A, Mangolini F, Spencer ND. Tribochemistry of bulk zinc metaphosphate glasses. *Tribology letters*. 2010;39(2):121-34.
96. Yin Z, Kasrai M, Fuller M, Bancroft GM, Tan KH. Application of soft X-ray absorption spectroscopy in chemical characterization of antiwear films generated by ZDDP Part I: the effects of physical parameters. *Wear*. 1997;202(2):172-91.
97. Martin JM, Grossiord C, Le Mogne T, Bec S, Tonck A. The two-layer structure of ZnDTP tribofilms: Part I: AES, XPS and XANES analyses. *Tribology international*. 2001;34(8):523-30.
98. Crobu M, Rossi A, Mangolini F, Spencer ND. Chain-length-identification strategy in zinc polyphosphate glasses by means of XPS and ToF-SIMS. *Analytical and bioanalytical chemistry*. 2012;403(5):1415-32.
99. Naveira-Suarez A, Tomala A, Pasaribu R, Larsson R, Gebeshuber IC. Evolution of ZDDP-derived reaction layer morphology with rubbing time. *Scanning*. 2010;32(5):294-303.
100. Suárez AN. The behaviour of antiwear additives in lubricated rolling-sliding contacts: Luleå University of Technology; 2011.
101. Gunsel S, Spikes HA, Aderin M. In-situ measurement of zddp films in concentrated contacts. *Tribology transactions*. 1993;36(2):276-82.
102. Taylor L, Spikes H. Friction-enhancing properties of ZDDP antiwear additive: part I—friction and morphology of ZDDP reaction films. *Tribology transactions*. 2003;46(3):303-9.
103. Z. Zhang, E.S. Yamaguchi, Kasrai M, Bancroft GM. Tribofilms generated from ZDDP and DDP on steel surfaces: Part 1, growth, wear and morphology. *Tribology Letters*. 2005;19(3):211-20.
104. Fujita H, Glovnea R, Spikes H. Study of zinc dialkyldithiophosphate antiwear film formation and removal processes, part I: Experimental. *Tribology transactions*. 2005;48(4):558-66.
105. Fujita H, Spikes HA. Study of zinc dialkyldithiophosphate antiwear film formation and removal processes, Part II: Kinetic Model. *Tribology transactions*. 2007;48(4):567-75.



106. Gosvami N, Bares J, Mangolini F, Konicek A, Yablon D, Carpick R. Mechanisms of antiwear tribofilm growth revealed in situ by single-asperity sliding contacts. *Science*. 2015;348(6230):102-6.
107. Ghanbarzadeh A, Wilson M, Morina A, Dowson D, Neville A. Development of a new mechano-chemical model in boundary lubrication. *Tribology International*. 2016;93:573-82.
108. McQueen JS, Gao H, Black ED, Gangopadhyay AK, Jensen RK. Friction and wear of tribofilms formed by zinc dialkyl dithiophosphate antiwear additive in low viscosity engine oils. *Tribology International*. 2005;38(3):289-97.
109. Ghanbarzadeh A, Parsaeian P, Morina A, Wilson MC, van Eijk MC, Nedelcu I, et al. A semi-deterministic wear model considering the effect of zinc dialkyl dithiophosphate tribofilm. *Tribology Letters*. 2016;61(1):1-15.
110. Parsaeian P, Ghanbarzadeh A, Wilson M, Van Eijk MC, Nedelcu I, Dowson D, et al. An experimental and analytical study of the effect of water and its tribochemistry on the tribocorrosive wear of boundary lubricated systems with ZDDP-containing oil. *Wear*. 2016;358:23-31.
111. Faut OD, Wheeler DR. On the mechanism of lubrication by tricresylphosphate (TCP)—the coefficient of friction as a function of temperature for TCP on M-50 steel. *ASLE TRANSACTIONS*. 1983;26(3):344-50.
112. Landolt D, Mischler S, Stemp M. Electrochemical methods in tribocorrosion: a critical appraisal. *Electrochimica Acta*. 2001;46(24):3913-29.
113. Wood RJ, Bahaj AS, Turnock SR, Wang L, Evans M. Tribological design constraints of marine renewable energy systems. *Philosophical Transactions of the Royal Society A: Mathematical, Physical and Engineering Sciences*. 2010;368(1929):4807-27.
114. Mathew M, Srinivasa Pai P, Pourzal R, Fischer A, Wimmer M. Significance of tribocorrosion in biomedical applications: overview and current status. *Advances in tribology*. 2010;2009.
115. Steigerwald JM, Murarka SP, Gutmann RJ. *Chemical mechanical planarization of microelectronic materials*: John Wiley & Sons; 2008.
116. Mischler S, Debaud S, Landolt D. Wear-accelerated corrosion of passive metals in tribocorrosion systems. *Journal of the Electrochemical Society*. 1998;145(3):750-8.
117. Wood RJ. Tribo-corrosion of coatings: a review. *Journal of Physics D: Applied Physics*. 2007;40(18):5502.
118. Pamfilov E, Prozorov YS. On the modeling of mechanochemical wear. *Journal of Friction and Wear*. 2012;33(3):224-32.
119. Diomidis N, Celis J-P, Ponthiaux P, Wenger F. Tribocorrosion of stainless steel in sulfuric acid: Identification of corrosion–wear components and effect of contact area. *Wear*. 2010;269(1):93-103.
120. Jiang J, Stack MM, Neville A. Modelling the tribo-corrosion interaction in aqueous sliding conditions. *Tribology International*. 2002;35(10):669-79.

121. Burstein G, Davenport A. The current-time relationship during anodic oxide film growth under high electric field. *Journal of the Electrochemical Society*. 1989;136(4):936-41.
122. Jemmely P, Mischler S, Landolt D. Electrochemical modeling of passivation phenomena in tribocorrosion. *Wear*. 2000;237(1):63-76.
123. Hawk JA. *Wear of Engineering Materials: Proceedings from Materials Week 97, 15-18 September 1997, Indianapolis, Indiana: CRC; 1998.*
124. Watson S, Friedersdorf F, Madsen B, Cramer S. Methods of measuring wear-corrosion synergism. *Wear*. 1995;181:476-84.
125. Williams J. *Engineering tribology: Cambridge University Press; 2005.*
126. Meng H, Ludema K. Wear models and predictive equations: their form and content. *Wear*. 1995;181:443-57.
127. Meng HC. *Wear modeling: evaluation and categorization of wear models. 1994.*
128. Suh NP. An overview of the delamination theory of wear. *Wear*. 1977;44(1):1-16.
129. Rabinowicz E. *Friction and wear of materials. 1965.*
130. Archard J. Contact and rubbing of flat surfaces. *Journal of applied physics*. 1953;24(8):981-8.
131. Holm R, Holm EA. *Electric contacts. 1967.*
132. Sullivan JL. Boundary lubrication and oxidative wear. *Journal of Physics D: Applied Physics*. 1986;19(10):1999.
133. H. Zhang LC. A micro-contact model for boundary lubrication with lubricant/surface physiochemistry. *Journal of tribology*. 2003;125(1):8-15.
134. Andersson J, Larsson R, Almqvist A, Grahnb M, Minami I. Semi-deterministic chemo-mechanical model of boundary lubrication. *faraday Discussions*. 2012;156(1):343-60.
135. Bosman R, Schipper DJ. Running-in of systems protected by additive-rich oils. *Tribology letters*. 2011;41(1):263-82.
136. Holm R, Holm E. *Electric contacts handbook: Springer; 1958.*
137. Stolarski T. A probabilistic approach to wear prediction. *Journal of Physics D: Applied Physics*. 1990;23(9):1143.
138. Rowe C. Some aspects of the heat of adsorption in the function of a boundary lubricant. *ASLE TRANSACTIONS*. 1966;9(1):101-11.
139. Kingsbury EP. Some aspects of the thermal desorption of a boundary lubricant. *journal of applied physics*. 1958;29(6):888-91.
140. Akbarzadeh S, Khonsari MM. Thermoelastohydrodynamic analysis of spur gears with consideration of surface roughness. *Tribology Letters*. 2008;32(2):129-41.
141. Johnson KL, Greenwood JA, Poon SY. A simple theory of asperity contact in elastohydro-dynamic lubrication. *Wear*. 1972;19(1):91-108.
142. Beheshti A, Khonsari MM. A thermodynamic approach for prediction of wear coefficient under unlubricated sliding condition. *Tribology letters*. 2010;38(3):347-54.

143. Bhattacharya B, Ellingwood B. Continuum damage mechanics analysis of fatigue crack initiation. *International Journal of Fatigue*. 1998;20(9):631-9.
144. Hamrock BJ, Schmid SR, Jacobson BO. *Fundamentals of fluid film lubrication*: CRC press; 2004.
145. Kogut L, Etsion I. A finite element based elastic-plastic model for the contact of rough surfaces. *Tribology Transactions*. 2003;46(3):383-90.
146. Bush AW, Gibson RD, Keogh GP. The limit of elastic deformation in the contact of rough surfaces. *Mechanics Research Communications*. 1976;3(3):169-74.
147. McCool JJ. Relating profile instrument measurements to the functional performance of rough surfaces. *Journal of Tribology*. 1987;109(2):264-70.
148. Wu S, Cheng H. A sliding wear model for partial-EHL contacts. *Journal of Tribology*. 1991;113(1):134-41.
149. Almqvist A, Sahlin F, Larsson R, Glavatskih S. On the dry elasto-plastic contact of nominally flat surfaces. *Tribology International*. 2007;40(4):574-9.
150. Thompson RA, Bocchi W. A model for asperity load sharing in lubricated contacts. *ASLE TRANSACTIONS*. 1972;15(1):67-79.
151. Bhushan B. Contact mechanics of rough surfaces in tribology: multiple asperity contact. *Tribology letters*. 1998;4(1):1-35.
152. Borri-Brunetto M, Chiaia B, Ciavarella M. Incipient sliding of rough surfaces in contact: a multiscale numerical analysis. *Computer methods in applied mechanics and engineering*. 2001;190(46):6053-73.
153. Sahlin F, Larsson R, Almqvist A, Lugt P, Marklund P. A mixed lubrication model incorporating measured surface topography. Part 1: theory of flow factors. *Proceedings of the Institution of Mechanical Engineers, Part J: Journal of Engineering Tribology*. 2010;224(4):335-51.
154. Ilincic S, Vorlaufer G, Fotiu P, Vernes A, Franek F. Combined finite element-boundary element method modelling of elastic multi-asperity contacts. *Proceedings of the Institution of Mechanical Engineers, Part J: Journal of Engineering Tribology*. 2009;223(5):767-76.
155. Ren N, Lee SC. Contact simulation of three-dimensional rough surfaces using moving grid method. *Journal of tribology*. 1993;115(4):597-601.
156. Ghanbarzadeh A. *Mechano-chemical modelling of boundary lubrication*: University of Leeds; 2016.
157. Tian X, Bhushan B. A numerical three-dimensional model for the contact of rough surfaces by variational principle. *Journal of tribology*. 1996;118(1):33-42.
158. Aghdam A, Khonsari M. On the correlation between wear and entropy in dry sliding contact. *Wear*. 2011;270(11):781-90.
159. Gershman I, Bushe N. Elements of thermodynamics and self-organization during friction. *MATERIALS ENGINEERING-NEW YORK-*. 2007;31:13.
160. Nosonovsky M. Entropy in Tribology: in the Search for Applications. *Entropy*. 2010;12(6):1345-90.
161. Andersson J, Larsson R, Almqvist A, Grahn M, Minami I s. Semi-deterministic chemo-mechanical model of boundary lubrication. *Faraday discussions*. 2012;156(1):343-60.

162. So H, Lin Y. The theory of antiwear for ZDDP at elevated temperature in boundary lubrication condition. *Wear*. 1994;177(2):105-15.
163. Bulgarevich S, Boiko M, Kolesnikov V, Korets K. Population of transition states of triboactivated chemical processes. *Journal of Friction and Wear*. 2010;31(4):288-93.
164. Bulgarevich S, Boiko M, Kolesnikov V, Feizova V. Thermodynamic and kinetic analyses of probable chemical reactions in the tribocontact zone and the effect of heavy pressure on evolution of adsorption processes. *Journal of Friction and Wear*. 2011;32(4):301-9.
165. Ghanbarzadeh A, Wilson M, Morina A, Dowson D, Neville A. Development of a new mechano-chemical model in boundary lubrication. *Tribology International*. 2014.
166. Zhang Z, Yamaguchi E, Kasrai M, Bancroft G. Tribofilms generated from ZDDP and DDP on steel surfaces: Part 1, growth, wear and morphology. *Tribology Letters*. 2005;19(3):211-20.
167. Bosman R. Mild wear prediction of boundary-lubricated contacts. *Tribology letters*. 2011;42(2):169-78.
168. Minfray C, Martin J, De Barros M, Le Mogne T, Kersting R, Hagenhoff B. Chemistry of zddp tribofilm by tof-sims. *Tribology Letters*. 2004;17(3):351-7.
169. Benedet J, Green JH, Lamb GD, Spikes HA. Spurious mild wear measurement using white light interference microscopy in the presence of antiwear films. *Tribology Transactions*. 2009;52(6):841-6.
170. Spikes H, Cann P. The development and application of the spacer layer imaging method for measuring lubricant film thickness. *Proceedings of the Institution of Mechanical Engineers, Part J: Journal of Engineering Tribology*. 2001;215(3):261-77.
171. Fitch J, Jaggernauth S. MOISTURE--The Second Most Destructive Lubricant Contaminate, and its Effects on Bearing Life. *P/PM Technology*. 1994;12:1-4.
172. Gresham RM. When oil and water do mix. *Tribology & Lubrication Technology*. 2008;64(3):22.
173. Cen H, Morina A, Neville A, Pasaribu R, Nedelcu I. Effect of water on ZDDP anti-wear performance and related tribochemistry in lubricated steel/steel pure sliding contacts. *Tribology International*. 2012;56:47-57.
174. Nedelcu I, Piras E, Rossi A, Pasaribu H. XPS analysis on the influence of water on the evolution of zinc dialkyldithiophosphate-derived reaction layer in lubricated rolling contacts. *Surface and Interface Analysis*. 2012;44(8):1219-24.
175. Morina A, Neville A, Priest M, Green JH. ZDDP and MoDTC interactions in boundary lubrication—The effect of temperature and ZDDP/MoDTC ratio. *Tribology International*. 2006;39(12):1545-57.
176. Brückner R, Chun H-U, Goretzki H, Sammet M. XPS measurements and structural aspects of silicate and phosphate glasses. *Journal of Non-Crystalline Solids*. 1980;42(1):49-60.
177. Brow RK. An XPS study of oxygen bonding in zinc phosphate and zinc borophosphate glasses. *Journal of non-crystalline solids*. 1996;194(3):267-73.

178. Onyiriuka E. Zinc phosphate glass surfaces studied by XPS. *Journal of non-crystalline solids*. 1993;163(3):268-73.
179. Smets BM, Krol D. Group III ions in sodium silicate glass. Part. 1. X-Ray Photoelectron spectroscopy study. *Physics and chemistry of glasses*. 1984;25(5):113-8.
180. Liu H, Chin T, Yung S. FTIR and XPS studies of low-melting PbO-ZnO-P<sub>2</sub>O<sub>5</sub> glasses. *Materials chemistry and physics*. 1997;50(1):1-10.
181. Shih P, Yung S, Chin T. FTIR and XPS studies of P<sub>2</sub>O<sub>5</sub>-Na<sub>2</sub>O-CuO glasses. *Journal of non-crystalline solids*. 1999;244(2):211-22.
182. Khawaja E, Durrani S, Al-Adel F, Salim M, Hussain MS. X-ray photoelectron spectroscopy and Fourier transform-infrared studies of transition metal phosphate glasses. *Journal of materials science*. 1995;30(1):225-34.
183. Salim M, Khattak G, Fodor P, Wenger L. X-ray photoelectron spectroscopy (XPS) and magnetization studies of iron-vanadium phosphate glasses. *Journal of non-crystalline solids*. 2001;289(1):185-95.
184. Flambard A, Videau J-J, Delevoye L, Cardinal T, Labrugère C, Rivero C, et al. Structure and nonlinear optical properties of sodium-niobium phosphate glasses. *Journal of Non-Crystalline Solids*. 2008;354(30):3540-7.
185. Cai Z, Zhou Y, Qu J. Effect of oil temperature on tribological behavior of a lubricated steel-steel contact. *Wear*. 2015;332:1158-63.
186. Tonder Y. Simulation of 3-D random rough surface by 2-D digital filter and Fourier analysis. *International journal of machine tools and manufacture*. 1992;32(1):83-90.
187. Schipper D, Bosman R. Mild wear prediction of boundary-lubricated contacts. *Tribology Letters*. 2011;42(2):169-78.
188. Martin JM, Minfray C. The origin of anti-wear chemistry of ZDDP. *Faraday Discussions*. 2012;156(1):311-23.
189. Sheasby J, Caughlin T, Mackwood W. The effect of steel hardness on the performance of antiwear additives. *Wear*. 1996;201(1):209-16.
190. Bancroft G, Kasrai M, Fuller M, Yin Z, Fyfe K, Tan KH. Mechanisms of tribochemical film formation: stability of tribo- and thermally-generated ZDDP films. *Tribology Letters*. 1997;3(1):47-51.
191. Jahanmir S. Wear reduction and surface layer formation by a ZDDP additive. *Journal of tribology*. 1987;109(4):577-86.
192. Bosman R, Schipper DJ. Mild wear maps for boundary lubricated contacts. *Wear*. 2012;280:54-62.
193. Ghanbarzadeh A. Mechano-chemical modelling of boundary lubrication. UK: University of Leeds; 2016.
194. Canning G, Fuller MS, Bancroft G, Kasrai M, Cutler J, De Stasio G. Spectromicroscopy of tribological films from engine oil additives. Part I. Films from ZDDP's. *Tribology letters*. 1999;6(3-4):159-69.
195. Graham JF, McCague C, Norton PR. Topography and nanomechanical properties of tribochemical films derived from zinc dialkyl and diaryl dithiophosphates. *Tribology Letters*. 1999;6(3-4):149-57.

196. Morina A, Neville A, Priest M, Green JH. ZDDP and MoDTC interactions in boundary lubrication The effect of temperature and ZDDP MoDTC ratio. *Tribology international*. 2006;39(12):1545-57.
197. Landauer AK, Barnhill WC, Qu J. Correlating mechanical properties and anti-wear performance of tribofilms formed by ionic liquids, ZDDP and their combinations. *Wear*. 2016;354:78-82.
198. Kennedy F. Frictional heating and contact temperatures. *Modern tribology handbook*. 2001;1:235-59.
199. Blok H. The flash temperature concept. *Wear*. 1963;6(6):483-94.
200. Cen H, Morina A, Neville A, Pasaribu R, Nedelcu I. Effect of water on ZDDP anti-wear performance and related tribochemistry in lubricated steel/steel pure sliding contacts. *Tribology international*. 2012;56:47-57.
201. Schipper DJ, Bosman R. Mild Wear Prediction of Boundary-Lubricated Contacts: Part II. *Wear*. 2012;280:54-62.
202. Parsaeian P, Van Eijk MCP, Nedelcu I, Morina A, Neville A, Study of the Interfacial Mechanism of ZDDP Tribofilm in Humid Environment and its Effect on Tribochemical Wear; Part I: Experimental. *Tribology International*. Volume 107, March 2017, Pages 135–143.
203. Parsaeian P, Van Eijk MCP, Nedelcu I, Morina A, Neville A, Study of the Interfacial Mechanism of ZDDP Tribofilm in Humid Environment and its Effect on Tribochemical Wear; Part II: Numerical. *Tribology International*. Volume 107, March 2017, Pages 33–38.
204. Parsaeian P, Van Eijk MCP, Nedelcu I, Morina A, Neville A, A new insight into the interfacial mechanisms of the tribofilm formed by zinc dialkyl Dithiophosphate *Journal of Applied Surface Science*. *Applied Surface Science* 403, 472-486. 2016.